VULNERABILITY MODEL. A SIMULATION SYSTEM FOR ASSESSING DAMAGE RESULTING FROM MARINE SPILLS

ENVIRO CONTROL, INCORPORATED

PREPARED FOR

COAST GUARD

JUNE 1975

DISCLAIMER NOTICE

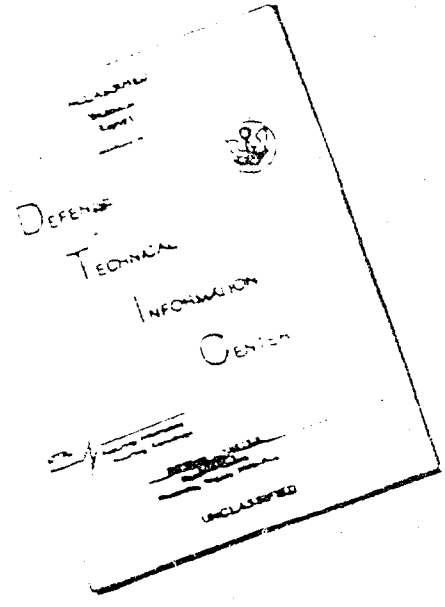

THIS DOCUMENT IS BEST QUALITY AVAILABLE. THE COPY FURNISHED TO DTIC CONTAINED A SIGNIFICANT NUMBER OF PAGES WHICH DO NOT REPRODUCE LEGIBLY.

Report No. CG-D-137-75

VULNERABILITY MODEL

A Simulation System for Assessing Damage Resulting from Marine Spills

June 1975

FINAL REPORT

Prepared for

DEPARTMENT OF TRANSPORTATION
UNITED STATES COAST GUARD
Office of Research and Development
Washington, D.C. 20590

Technical Report Documentation Page

1. Report No.	2. Government Accession No.	3. Recipient's Catalog No.
CG-D-136-75		

4. Title and Subtitle	5. Report Date
VULNERABILITY MODEL: A Simulation System for Assessing Damage Resulting from Marine Spills	June 1975
	6. Performing Organization Code
	8. Performing Organization Report No.
7. Author(s) Norman A. Eisenberg; Cornelius J. Lynch; Roger J. Breeding	
9. Performing Organization Name and Address	10. Work Unit No. (TRAIS)
Enviro Control, Inc. 1530 East Jefferson Street Rockville, MD 20852	DOT-CG-33,377-A
	11. Contract or Grant No.
	13. Type of Report and Period Covered
12. Sponsoring Agency Name and Address	Final Report
U. S. Coast Guard Office of Research and Development Washington, DC 20590	14. Sponsoring Agency Code

15. Supplementary Notes

16. Abstract

The Vulnerability Model (VM) is a computerized simulation system for assessing damage that results from marine spills of hazardous materials; the final report, summarized here, describes the research background, computational techniques, and preliminary test results associated with the first stage of development of the VM. This first stage of model development consisted of the design and implementation of an operational computer simulation, thereby demonstrating the feasibility of the philosophy, concepts, and approaches pertaining to the VM. Certain aspects of the modeling, as now operational, are subject to enhancement by augmentation, increase in precision, or both. Ultimately, the model is intended to be a comprehensive tool for assessing damage resulting from marine spills.

17. Key Words	18. Distribution Statement
Vulnerability Model Damage assessment Marine Spills	Document is available to the public through the National Technical Information Service, Springfield, VA 22161

19. Security Classif. (of this report)	20. Security Classif. (of this page)	21. No. of Pages	22. Price
Unclassified	Unclassified		

EXECUTIVE SUMMARY

The Vulnerability Model (VM) is a computerized simulation system for assessing damage that results from marine spills of hazardous materials; the final report, summarized here, describes the research background, computational techniques, and preliminary test results associated with the first stage of development of the VM. This first stage of model development consisted of the design and implementation of an operational computer simulation, thereby demonstrating the feasibility of the philosophy, concepts, and approaches pertaining to the VM. Certain aspects of the modeling, as now operational, are subject to enhancement by augmentation, increase in precision, or both. Ultimately, the model is intended to be a comprehensive tool for assessing damage resulting from marine spills. The research and development effort reported here was performed under Department of Transportation United States Coast Guard Contract number DOT-CG-33377-A. The entire documentation for the effort has five levels of reporting detail: (1) this executive summary presents a nontechnical overview of the VM purpose, structure, and operation, briefly describes methods of damage assessment, indicates the research background supporting the VM, and summarizes preliminary test results; (2) the main body of the final report provides the technical aspects of the VM structure, development, and use; (3) to allow a smooth flow to the presentation in the main report, more detailed information, such as involved mathematical derivations, complex flow charts, and case-history details, is relegated to the several appendixes; (4) a user's guide is provided as a separate document giving the details of the computer programming and the operation of the VM; (5) finally the Coast Guard has been issued the computer tapes and card decks required to set up and run the VM.

In recent years, industrial expansion, new technologies, and a centralization of chemical production have led to increased bulk transport of hazardous chemicals on U. S. waters. Steadily increasing transport of fuels, both conventional and nuclear, is required to meet the demands of the current energy crisis. An increase in the quantity and variety of hazardous chemicals transported in bulk is required to meet the demands of a U. S. chemical industry that is expanding at a rate many times that of population growth [S1].

To address the problems posed by the increase in transport of hazardous materials, the U. S. Congress has passed the Ports and Waterways Safety Act of 1972 that charges the U. S. Coast Guard with providing for the safety of "ports, harbors, waterfront areas, and navigable waterways of the United States." To discharge these duties related to safety, the U. S. Coast

---

[S1] Luckritz, R.T. Hazardous materials spill prevention in the bulk marine carriage of dangerous cargoes, pp. 18-24. In Control of Hazardous Material Spills, Proceedings of the 1974 National Conference on Control of Hazardous Material Spills. Am. Inst. Chem. Eng., New York, 1974.

Guard engages in such facets of spill control as prevention, containment operations, cleanup, and restoration. Although the response activities, such as containment, receive such publicity, the most productive spill control measure appears to be prevention, since spills of hazardous materials are difficult to detect, contain, control, or mitigate, and the damage caused by such spills is difficult to reverse. In order to assure the safety of marine transport by spill prevention, the Coast Guard is authorized to regulate the movement of bulk cargoes and the design and operation of vessels carrying them. The prevention of all accidental spills, however, appears unrealistic, because the only known way to preclude accidents entirely is to abstain from the activity giving rise to them.

Since cessation of marine transportation is impractical, some risk is unavoidable due to the threats posed by mechanical failure, by unusual environmental conditions (severe storm, tidal wave), and by human fallibility. Although the risk cannot be completely eliminated, appropriate regulations can reduce risk. However, substantial increases in safety rarely come cheaply. The reduction in risk attributable to any regulation must be weighed against the increased operation costs or capital expenditures such regulation requires. The need to perform cost-benefit analyses of Coast Guard actions has led to a research and development program to establish a Risk Management System. The VM is an important component of this system.

Background of Risk Management System [S2]

Development of the Risk Management System began in the spring of 1971. It involves analytic development in three separate fields:

- Spill-Risk Analysis (Spill Analysis) - assessment of risks that a vessel or facility spill will occur and assessment of the effectiveness of spill prevention regulations

- Vulnerability Analysis (Public Damage Assessment) - assessment of the threats to people, property, and the environment due to spills from a vessel or marine facility

- System Cost Analysis (Economic Impact) - assessment of the cost impacts on the government and consumers of implementing alternative regulatory actions for spill prevention

Figure S.1 depicts a systems approach to risk management which is the goal of the Risk Management System. When fully developed, this methodology will be applicable, both to nationwide regulation and to special circumstances within local port or waterway areas, for assessing the costs and benefits expected from regulatory changes within those areas.

[S2] Dunn, W.A., and P.M. Tullier. Spill Risk Analysis Program. Phase II. Methodology Development and Demonstration. Operations Research, Inc., Silver Spring, Md., August 1974. USCG Report No. CG-D-15-75 (NTIS AD 785026).

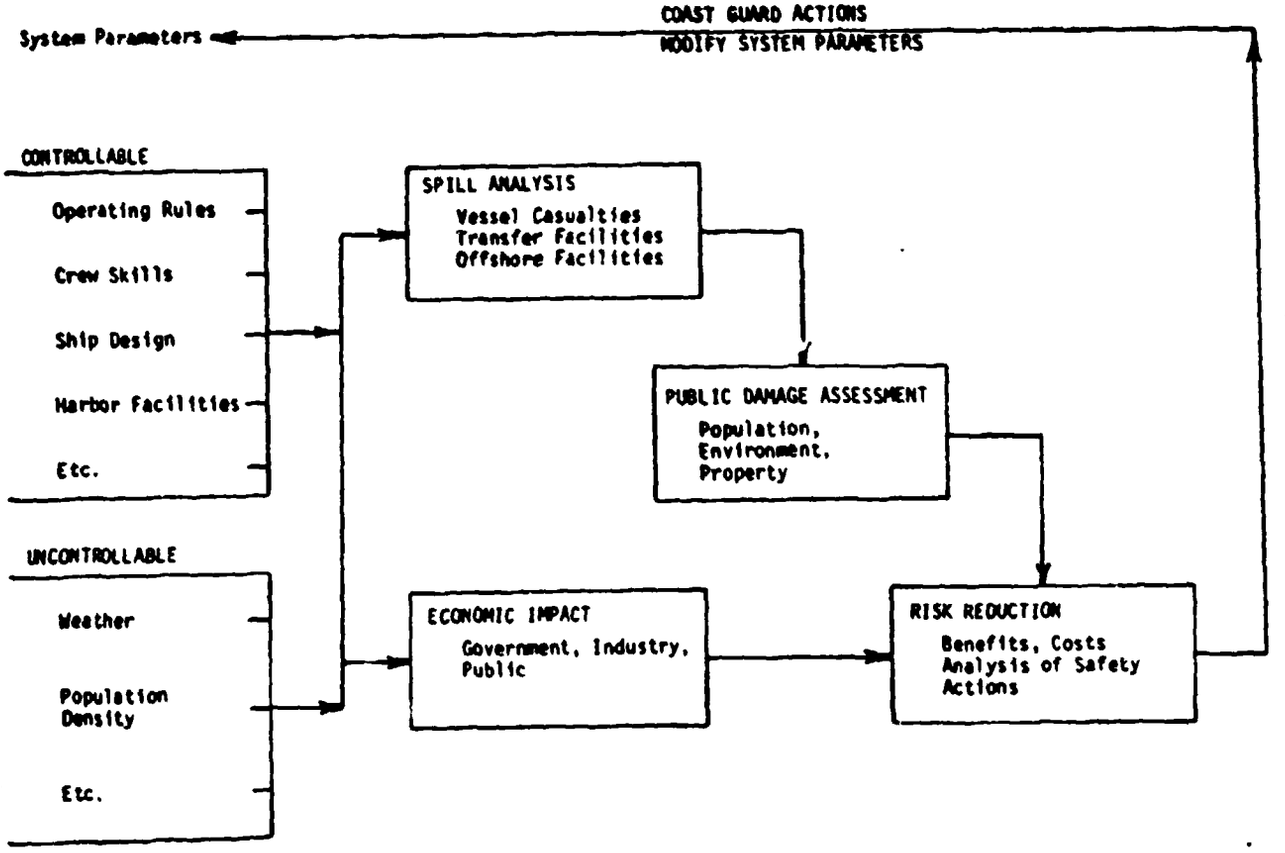

FIGURE 5.1. RISK MANAGEMENT - THE SYSTEMS APPROACH

Goal of This Effort

The use of deterministic models for assessing damage to vulnerable resources is not a new idea. Such modeling efforts have been used extensively for many years in the areas of civil defense (especially nuclear weapon attack assessments) and war gaming. What is new, however, is the use of these techniques to assess damages resulting from spills of cargoes carried in marine transport. Such modeling efforts can provide the Coast Guard with valuable information on which it can base its regulatory decisions. Thus, this research represents an effort to develop and to demonstrate the utility of techniques specifically designed to support regulatory decision-making.

A secondary use of considerable import is to assist in the planning and selection of response actions. A further benefit in obtaining a workable model at this stage of development is in identifying those areas of modeling most critical in obtaining accurate hazard assessments.

Limitations on the Scope of This Effort

A main consideration in developing a damage assessment tool has been to establish a workable model within a framework flexible enough to allow for future model enhancements. The approach taken was to simulate the spill through a series of separate submodels, many of which had previously been developed for the Coast Guard. In modeling complex physical processes, it has been necessary to make simplifying assumptions. A conservative design philosophy guided the development of models used in the VM; consequently, whenever alternate approximations were available, the approximations were chosen so that the VM does not underestimate damage. The approximations made in model development are recognized, but the modularized structure of the VM facilitates the insertion of additional and improved models as they become available.

In order to obtain a complete working damage assessment model within the time and resources allocated and to make maximum possible use of previous model development work, the scope of this effort was limited. Some of the more important limitations are as follows.

- The portion of the population indoors is considered to be sheltered; no damage is assessed to the indoor populace. Further, it was assumed that fifty percent of the subject population was indoors.*
- Census data were used to determine the location of the vulnerable population; since census data primarily deal with the location of the residence of people, no modeling was effected to deal with the movement of people from home to work, to school, to recreational areas, or to other nonresidential locations.
- Most of the physicochemical models consider that only a single process occurs at one time, so that separate physical events occurring simultaneously are modeled as a sequence of separate events; for example, the VM models spilling, spreading, and burning as separate events, each terminating before the next can begin, even though these events can and do occur simultaneously.

* Actually, 80-85 % of the population is normally indoors, but damage to the indoor population is not modeled in this first stage of the VM.

- Explosion of an unconfined vapor cloud is partially determined by a user input option and pa.tially determined by the simulated characteristics of the vapor cloud; since the decision to simulate an explosion is not entirely based on physical principles, it may properly be argued that the VM will simulate an explosion when, in fact, none could occur.

- Damage to the environment is not currently assessed; however the concentration of hazardous material in air and water is computed, so that the user may estimate environmental consequences at his option.

- Test runs were performed only for five cargoes.

- Only inhalation toxicity was treated; injury by ingestion of toxic materials was not assessed.

- Secondary damage mechanisms, such as ignition of expecially hazardous establishments (e.g., refineries), were not treated; only the direct consequences of the spill were simulated.

- Response actions (e.g., spill containment, population evacuation, and fire fighting) were not considered.

- Spills of solids and reacting chemicals were not considered.

- Underwater releases were not considered.

- Explosion damage to structures is assessed on the assumption that the structures affected are framed with wood members.

This listing of constraints on the development of the VM to its current state is not intended to discredit the VM. Rather this information is provided to help define just what type of results might reasonably be expected from the VM at this time. Although the VM has several important limitations, it is believed that, as it now stands, the VM is a useful tool for the risk analysis of marine spills; with further development and improvement, the VM should be able to provide even more utility and insight to the considerations of this important problem.

Major Accomplishment

The major accomplishment of this effort has been the demonstration that the concept of the VM is suitable for implementation as a functioning tool for use in risk analysis. It has been demonstrated that all of the building blocks required for a vulnerability analysis, viz., the data bases describing the vulnerable resources and physical setting of the spill, the predictive models describing spill development, and the predictive models describing damage to the vulnerable resources, are either currently available or can be obtained. Exercise of the VM for five hazardous cargoes of particular interest, for a variety of spill sizes, and for various environmental

conditions has yielded damage estimates that are judgementally credible within the input assumptions and apparently consistent with observations of actual accidental spills. (However, the amount of available quantitative information concerned with damage resulting from accidental spills of hazardous materials is small.)

Application of the VM

The VM is a damage assessment tool. Given a spill scenario by the user, that is, given the characteristics of the spill and the physical setting in which the spill occurs, the VM simulates the physicochemical transformations of the spilled material and estimates the damages inflicted on vulnerable resources by these processes. The VM addresses such questions as: If X tons of substance Y were spilled at location Z with the wind blowing due north, etc., how many people might be killed or injured? How many structures will be damaged? How much water and air pollution will occur and where? The VM is a deterministic model; that is, the probability of occurrence of the various events comprising the spill scenario is not considered. Instead the scenario specified by the user leads invariably to a particular spill development and damage estimate. Other ongoing elements of the USCG Risk Analysis Research Program are concerned with the definition of changes in the probabilities of events comprising the spill scenario as a function of changes in regulatory and operational controls. The probability changes, combined with VM damage estimates, will be used to determine the risk reduction benefit of certain types of Coast Guard safety actions.

Limitations on Use of the Results Derived from the VM

There is a danger that the preliminary results obtained from the VM might be misinterpreted, so care must be exercised in considerations of these results. One point that must always be borne in mind is that the VM is entirely deterministic.

The damage assessed by the model is predicated on a set of circumstances (input conditions) chosen by the user. The probability that such a set of conditions exists is not considered by the VM. The likelihood of a spill is small; this small probability combined with the probabilities of all of the other conditions yields a small overall probability that any given scenario actually occurs. Thus, although the consequences of some simulations are quite dire, the risk (the mathematical expectation) is small; large losses from rare events do not necessarily indicate a high risk activity.

Because the VM is completely deterministic and because no assessment is made of the likelihood of a user-chosen scenario, considerable judgment and experience are required to avoid unreasonable (even impossible) input conditions. For example, it is possible to simulate very large spills, even though no vessel in existence is large enough to carry that much cargo.

Another illustration of possible misuse of the VM is that the user may specify a large spill at a given site, even though ships capable of carrying that large a cargo as a single load cannot navigate the waters required to reach that spill site. It must also be acknowledged, when interpreting results, that the VM is in its first stage of development. Spills have been simulated for only five liquids. Solids, reacting substances, secondary damage mechanisms, damage to indoor (sheltered) populations, etc., have not

been modeled. Although such omissions do not automatically mean the results are incorrect, evaluation of results in a general context is not possible without further model development. Finally, interpretation of the results should be tempered with the knowledge that the VM alone cannot determine the risk of marine transport in comparison to other forms of bulk transport or even other human activity involving risk.

Overview of the VM

1. Scope

The VM is a computer simulation designed to provide quantitative measures of the consequences of marine spills of hazardous materials. The simulation starts with a description of the nature of the spill itself, continues through the dispersion of the hazardous material, and ultimately includes assessment of the immediate effects of the spill on surrounding vulnerable resources, namely, people, property, and the environment.

The model is designed so that it may ultimately treat any type of material carried in bulk quantities in marine transportation. These materials may exist in gas, liquid, or solid phase as cargoes and may change phase upon release into the air or water environment. The materials may react, dissolve, or otherwise be admixed with surrounding air and water. Where appropriate, the model treats the mass transfer from a material spilled in or on the water to the air. The logical sequencing in the VM has been designed so that the VM can treat virtually all of the large class of materials carried in bulk in marine transport; however, the computational submodels are not available now to describe the behavior of all of these materials when spilled. With the submodels that are operational, the VM is able to treat spills of many liquids and gases carried in bulk quantities. Many cargoes of particular hazard are carried as bulk liquids which can currently be treated by the VM at this first stage of development. At present, the VM has been exercised for only five cargoes.

2. Simulation Scenario

The simulation requires three types of descriptive data that define: (1) the spill, (2) the physical setting in which the spill occurs, and (3) the vulnerable resources that are subject to the effects of the spill. The spill is described in terms of its location and spill rate, the physical and chemical properties of the spilled material, and the quantity of the spill. The physical setting is described in terms of the geometric configuration of the shoreline(s), hydrologic/oceanographic properties, and meteorological data. Vulnerable resources are described in terms of demographic distribution, property distribution, and land/water use. The geographic area of concern may represent any user-defined location, a rectangular area measuring ten miles in length and five miles in width being typical of anticipated applications. The physical setting and the distribution of vulnerable resources are described in terms of mutually exclusive geographic cells that cover the entire area of concern.

3. Submodels

The VM consists of submodels interconnected by an executive routine, with built-in logic dictating the sequence of submodel processing as a function of the spill development. Among these submodels are simulations of surface spreading, water mixing, air dispersion, conflagration and explosion, and submodels for assessing the effects from the dissemination of the hazardous material on vulnerable resources. Some of the submodels had been designed previously under U. S. Coast Guard sponsorship as part of the CHRIS (Chemical Hazard Response Information System) [S3] model development. Others were designed specifically for the VM. A generalized flow diagram of the model is presented in Figure S.2 and a more detailed description follows.

4. Operational Phases

The VM operates in two phases. Phase I simulates the spill itself, the physical and chemical transformations of the spilled substance and its dissemination in space. This phase covers the time period from the initiation of the spill until a user-specified time has elapsed. The time interval between simulation calculations is specified by the user but may be overridden by certain submodels (such as the explosion submodel). A time-history file of the spill sequence simulated during the first phase is retained in some form of computer storage such as magnetic tape or disc.

In Phase II, the computer first superimposes this time-history file upon the vulnerable resources map and then assesses the effects of toxicity, explosion, and/or fire on the vulnerable resources as a function of time. Estimates of deaths and nonlethal injuries to people and of damage to property are presented in tables.

5. Current Status of Development

At present the VM is in a first stage of development. It has been demonstrated that an actual working model is capable of carrying on a simulation from the specification of cargo and spill conditions through to the assessment of damages to vulnerable resources. The quantitative results of the simulation appear to correlate with the picture of events given both by expert judgment and by historical records of accidental spills. This correlation is obtained even though it is recognized that some of the modeling, by necessity, is not at the highest level of sophistication. Furthermore, the cost of a given simulation has been kept within reasonable bounds. Likewise the cost of data preparation required by the VM is not excessive. Interpretation of output requires a knowledge of the basis (not the technical details) of the modeling methods used and the ability to judge the suitability of arbitrary user inputs. Once the proper use

---

[S3] Raj, P.P.K., and A.S. Kalelkar. Assessment Models in Support of the Hazard Assessment Handbook. Arthur D. Little, Inc., Cambridge, Mass., January 1974. USCG Report No. CG-D-65-74 (NTIS AD 776617).

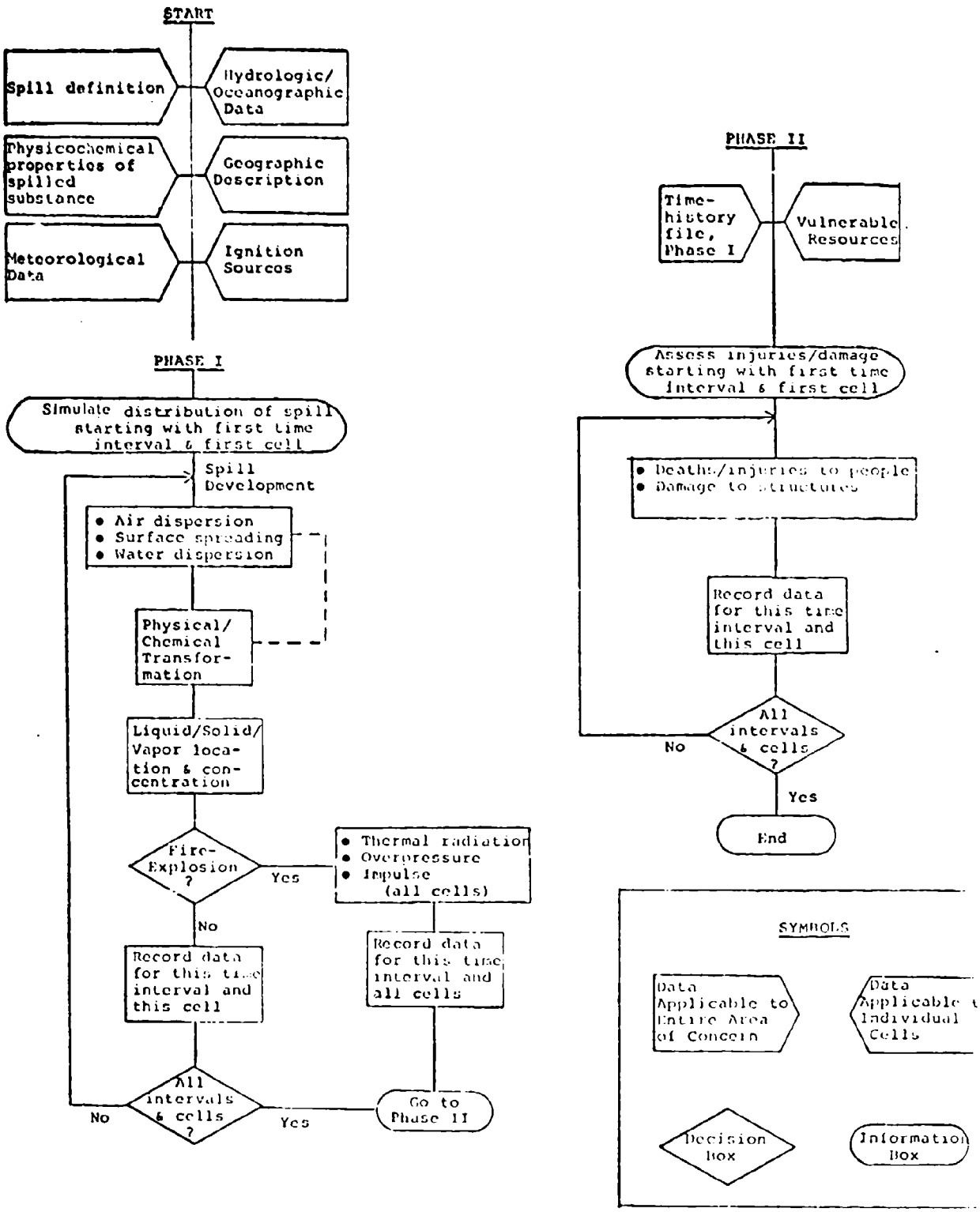

FIGURE S.2. GENERALIZED FLOW DIAGRAM OF THE VULNERABILITY MODEL

of the VM is learned, there is virtually no cost involved in output interpretation, since the computer results are presented in an easy-to-understand, user-oriented way.

Phase I Submodels

This section describes those submodels that are presently included in Phase I of the VM. Because the air dispersion submodel which was originally part of HACS* [S4] has been extensively revised, and because the fire and explosion submodels were developed almost entirely in this program, these submodels are discussed in greater detail than other Phase I submodels. Some of these other Phase I submodels, which were developed previously under USCG sponsorship, were modified somewhat for inclusion in the VM.

The submodels used in the VM treat the physicochemical processes affecting the spilled hazardous material; at the present time, the processes simulated by the VM may be classified as follows:

1. Cargo venting
2. Spill development
3. Air dispersion
4. Combustion (fire and explosion)

For certain of these processes different submodels are used, depending upon the nature of the spilled substance. Other processes, such as fire and explosion, consist of a sequence of dissimilar events, so the computer simulation consists of a sequence of submodels. The operational sequence of these various submodels is shown in Figure S.3.

The Phase I submodels for various physical and chemical processes treated by the VM are connected by an executive and storage routine. The sequence of processing depends upon the cargo and the development of the situation. The first submodel used is always the tank venting submodel, which calculates the rate of escape of the cargo in both gas and liquid phases as a function of initial tank conditions and the size and location of the vent or rupture. If only gas is vented, the simulation will pass directly to the air dispersion submodel from the venting submodel. If the cargo is vented as a liquid, it may remain in that phase or it may change to gas phase. If the cargo does change to a gas, some of it may flash directly to a gas when the tank pressure is released, but in most cases the bulk of the gas will be released more slowly by evaporation or boiling.

For many liquid spills, a pool of the cargo will form on the surface of the water, but a cargo with a liquid-phase density greater than that of

---

* Hazard Assessment Computer System

[S4] Hazard Assessment Computer System (HACS) User Manual. Arthur D. Little, Inc., Cambridge, Mass., December 1974.

FIGURE S.3. OVERALL FLOW DIAGRAM FOR THE VM.

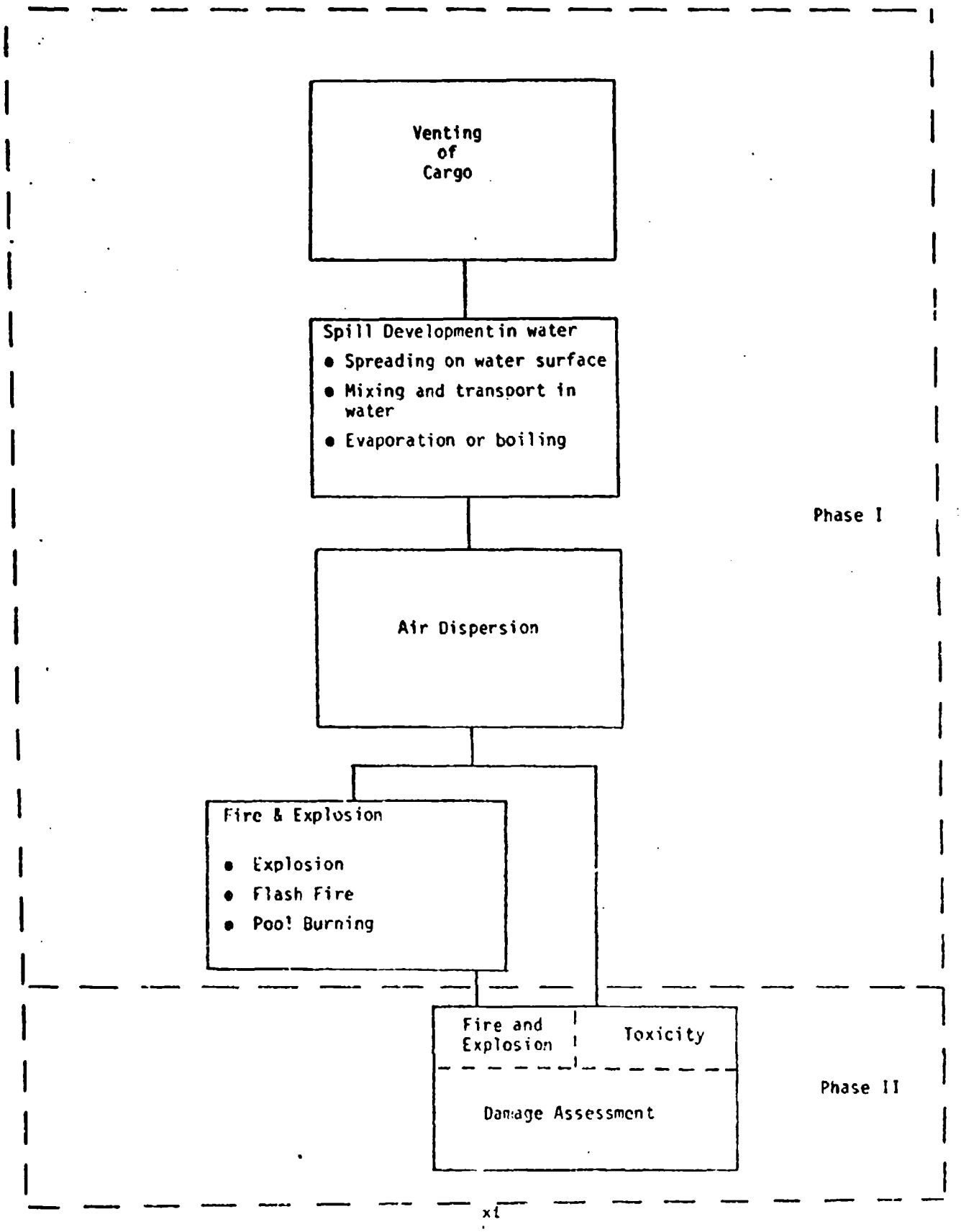

water will sink at once. At present there are five submodels for treating a spilled liquid:

1. Spreading and evaporation of an immiscible, floating, cryogenic liquid

2. Spreading and evaporation of an immiscible, floating liquid with high vapor pressure

3. Sinking and boiling of an immiscible liquid

4. Mixing, advection, and dilution of a miscible liquid in a tidal river, nontidal river, or still water

5. Mixing, dilution, and evaporation of a miscible liquid with high vapor pressure

Of course there are possibilities other than these five, but these five do cover a large number of hazardous cargoes frequently carried in bulk quantities. Liquefied natural gas, for example, is treated by the first submodel, gasoline by the second, and liquid chlorine by the third. The fourth submodel does not give an escape of gas to the atmosphere, so the simulation may stop with the calculation of the cargo concentration in the water or the simulation may proceed to calculate evaporation. The other submodels give a rate and duration for the gas evolution, and the simulation proceeds to the air dispersion model.

Air Dispersion

This submodel calculates the concentration of the cargo in gas phase in the air from the time the gas is released into the atmosphere until a fire or explosion occurs or until the maximum time stipulated for the simulation is reached.

The submodel is based on the Gaussian distribution, which is a theoretical solution to the partial differential equation governing diffusion. The dispersion coefficients used in the Gaussian distribution are obtained from the analysis of many observations of plumes from tall stacks and of puffs of smoke or some other tracer. Plumes result from continuous releases, whereas puffs result from instantaneous releases. Puffs are three-dimensional Gaussian distributions in which the dispersion coefficients depend upon the distance traveled by the puff center-of-mass. The plume is a two-dimensional Gaussian distribution in which the dispersion coefficients depend upon the distance downwind from the source to the observation point. The values of dispersion coefficients obtained from experimental observations are parameterized on the basis of the atmospheric stability or the turbulence class.

At present, the submodel will select the plume (continuous source Gaussian distribution) if the release time of the spilled material into the air is relatively long; for short release times, the puff (instantaneous source Gaussian distribution) is selected. Since there is no model extant that adequately treats spills with intermediate release times, either a puff or plume model is used until more adequate models are available. Because

the Gaussian models were based on data gathered from dilute plumes and puffs, their use for very concentrated cases, as in the VM, is an extrapolation. When the puff model is used close to a very large spill of material which vaporizes quickly, the standard Gaussian model gives concentrations which are higher than the density of pure cargo vapor at ambient atmospheric temperature and pressure. The puff model has been modified to preclude this by allowing a region of pure cargo vapor surrounded by a region where the concentration decreases in the Gaussian fashion. The pure cargo vapor concentration is at the proper density for ambient conditions. This modified distribution is used only when the regular puff model would give unrealistically high concentrations.

Fire and Explosion

This group of submodels determines whether a flammable cargo will be ignited and then determines the physical characteristics of the resulting combustion (fire, explosion, or both). Four types of fire and explosion phenomena are modeled in this section of the VM; they are:

1. Ignition
2. Explosion
3. Flash fire
4. Pool burning

The modeling of the phenomena of fire and explosion proceeds in three temporal phases. First the decision of whether, when, and where ignition occurs is made. Subsequent to ignition either an explosion or a flash fire is modeled. Following either of these events, the burning of flammable liquid on the water surface, if any liquid remains, is modeled; currently, burning from a vessel venting flammable fuel is not modeled.

The ignition submodel determines whether ignition occurs, which ignition source originates the ignition, and at what time during the simulation the ignition takes place. All ignition sources are assumed to be located at the grid cell centers. The user predetermines whether a given ignition source will cause fire or explosion. The user also specifies the strength of the ignition source. Since combustion will occur only over a certain range of fuel-air ratios, the decision that combustion occurs will be made only if the vapor concentration in a given cell is within the flammability limits for the substance under consideration and the given cell contains an ignition source of strength sufficient to ignite the spilled substance.

The explosion submodel calculates the peak overpressure and the dynamic impulse generated by the explosion of a flammable fuel-air (cargo-air) mixture. In addition to these variables that are required for damage assessment, the explosive yield and TNT equivalent are also determined. The well-known scaling laws for condensed phase explosions are assumed to hold. Only that portion of the fuel-air mixture with a concentration between the explosive limits is permitted to contribute to the explosive yield. For that part of the fuel-air mixture richer than stoichiometric, but leaner than the upper-explosive-limit concentration, only that fraction of fuel for which there is sufficient oxygen for complete burning contributes to the explosive yield.

The flash fire submodel calculates the effective radiation intensity level and the effective radiation duration resulting from the flash fire. The flash fire is considered to be the rapid combustion without detonation of the premixed fuel-air layer within the flammable concentration limits. The heat generated essentially instantaneously by combustion is assumed to be lost from the combustion layer entirely by radiation; thus the radiation loss as a function of time may be calculated. The time varying radiation level is represented by a fixed radiation level (the effective radiation level) and an effective duration. This submodel assumes that only that portion of the fuel-air mixture within the flammable limits burns and then only to the extent permitted by the local oxygen concentration. The radiation from the flash fire is assumed to affect only those portions of space inside the burning layer.

The pool burning submodel calculates the duration and magnitude of thermal radiation emitted by a burning pool of flammable cargo; the radiation level is calculated for any desired point in space. This submodel is comprised of several other submodels:

1. Flame size
2. Thermal radiation from flames
3. Radiation view factor between an inclined cylindrical flame and an arbitrarily oriented surface in space
4. Burning time

The flame size submodel calculates the height, diameter, and angle of inclination of a flame from a burning pool; the wind blowing across the pool surface causes the flame to be inclined with respect to the normal to the pool surface. The formulas used to calculate flame height, diameter, and inclination angle are empirical expressions obtained by curve fitting experimental laboratory data and extrapolating to the larger scale occurrences possibly resulting from marine spills of hazardous materials.

The thermal radiation from flames submodel calculates the radiant heat flux incident on a receptor at some distance from a burning pool. The flame from the burning pool is modeled as a cylindrical radiator of uniform temperature; this constitutes the major assumption of this submodel. The cylindrical radiator is allowed to be inclined with respect to the vertical. The atmospheric transmissivity and flame emissivity are assumed to be one, i.e., the atmosphere is not allowed to absorb radiant energy and the flame is treated as an ideal black body radiator.

The radiation view factor between an inclined flame and an arbitrarily oriented surface in space submodel calculates, on a normalized basis, the view factor between a cylindrical, inclined flame and a receptor; the receptor is assumed to be oriented with respect to the flame so that it receives the maximum possible radiation flux. The view factor is a purely geometrical property of the spatial arrangement of the flame and receptor. Thus no physical assumptions, except those basic to radiant heat transfer, are required by this model.

The burning time submodel calculates the length of time the pool will continue to burn after it is ignited. It is assumed that the pool is

extinguished when all of the fuel remaining in the pool at the time of ignition is burned up. It is further assumed that fuel leaves the pool only by burning but not by evaporation or by water mixing. It is also assumed that spreading stops when ignition occurs; although spreading will not cease entirely after ignition, the spreading rate will certainly be reduced because mass is being lost by combustion.

After the spill development is simulated and the results are stored by grid cell and time interval, these data along with the information describing the vulnerable resources are used to assess the damage which may result.

Phase II - Damage Assessment

As it currently stands, the VM models damage to vulnerable resources from four physical events:

1. Air dispersion of a toxic gas
2. Explosion
3. Flash fire
4. Pool burning

Damage to vulnerable resources is conveniently discussed in terms of (1) toxic injury, (2) explosion damage, and (3) fire damage. The assessment algorithms for toxic damage are highly dependent on the type of substance spilled; whereas the assessment algorithms for fire and explosion are independent of the type of substance spilled, though the values of the variables used in the algorithm do depend on the type of substance spilled.

The vulnerable resource "people" may be affected by inhalation of toxic vapor, by thermal radiation from a flash fire, and by peak overpressure or impulse from an explosion or by some combination of these. The vulnerable resource "structures" may be affected by thermal radiation from a flash fire or burning pool and by peak overpressure or impulse from an explosion. The vulnerable resource "environment", defined as air and water for the purposes of the VM, may be affected by the spilled substance in its vapor or liquid phase or by a reaction product. In most cases, the percent of the vulnerable resources affected within a given grid cell is calculated and then applied to the numbers of vulnerable resources present, giving the total numbers of vulnerable resources affected (for a given time period and given grid cell). Figure S.4 shows the specific types of injury and damage assessed for toxic gases, fire, and explosion. The code name of the algorithm used for computing the portion of the resource affected is listed under the column heading "Function." The factor or factors calculated from the simulations of the physical events which are used by each algorithm to assess damage are shown in the adjacent column.

For most of the assessment functions, the damage or injury is related to the causative factor by means of probit equations, resulting in the

FIGURE S.4. PHASE II DAMAGE ASSESSMENT

Damage Causing Event	Vulnerable Resource	Type of Injury or Damage		Cause of Injury or Damage	Outdoors (Unsheltered)	
					Function	Factor(s)
TOXICITY	People	Death		Toxic vapor: concentration or cumulative dose	T1	Concentration and time
		Nonlethal injury			T2	
		Irritation			T3	Concentration
EXPLOSION	People	Death		Direct blast	E1	Peak overpressure
				Impact	E2	Impulse
		Nonlethal Injury	Eardrum rupture	Direct blast	E3	Peak overpressure
			Bone fracture	Impact	E4	Impulse
			Puncture wounds	Flying fragments	E5	Impulse
			Multiple injury	Two or more of the above	E6	Impulse or peak overpressure and impulse
	Structures	Structural damage		Direct blast	S1	Peak overpressure
		Glass breakage		Direct blast	S2	Peak overpressure
POOL BURNING	People	Death		Thermal radiation	B1*	Duration and magnitude of thermal radiation
		First degree burn			B2*	
	Structures	Ignition		Thermal radiation	B3	Duration and magnitude of thermal radiation
FLASH FIRE	People	Death		Thermal radiation	F1	Effective duration and effective magnitude of thermal radiation
		First degree burn			F2	
	Structures	Ignition		Thermal radiation	F3	Effective duration and effective magnitude of thermal radiation

* These functions are essentially the same as F1 and F2; however as indicated in the adjacent column, slightly different arguments are used. These functions have not yet been implemented as part of the computer program, although to do so will be very easy.

calculation of the fraction of the population in each cell which is affected. Four assessment procedures, however, use simple threshold criteria; they are: (1) B3 - ignition of structures from pool burning, (2) F3 - ignition of structures from flash fire, (3) F2 - nonlethal injury from a flash fire, and (4) T3 - irritation from inhalation of toxic gases.

Provisions have been made in the VM to prevent double counting in three different situations. Double counting is used in this context to mean the inclusion of an element of some vulnerable resource (e.g., a person or a building) in more than one category of damage or injury. Three situations arise in which double counting will occur unless provisions are made to prevent it. The situations are as follows.

1. A single damage mechanism from one event simultaneously causes injuries of differing severity (e.g., inhalation of toxic gas may cause death, nonlethal injury, or irritation).

2. Two or more damage mechanisms from one event simultaneously cause injuries of the same severity (e.g., an explosion can kill people either by direct blast effects or by impact).

3. Different events at different times cause damage to the same resource, but the first event so severely damages some portion of the resource that further damage is irrelevant (e.g., persons killed by toxic gas cannot be further injured by a subsequent explosion).

1. Toxic Injury

Toxic injury is assessed only for the vulnerable resource "people." The toxic damage caused by irritant gases can in general be classed into three categories:

a. Death

b. Nonlethal injury

c. Irritation

The category of injury sustained by exposed resources depends, in general, upon both the duration of exposure and the concentration level experienced. This dependence is nonlinear; dose, the product of concentration level and duration, is not the appropriate variable to assess response to irritant gases. For example, for concentrations over the lethality threshold, doubling the concentration level does not halve the time required to produce the same death rate; instead, as the concentration level increases, the time to produce a given injury level decreases at a disproportionately rapid rate. Toxic damages to the vulnerable resource "environment" is not assessed in the VM at this time. The VM predicts the concentration of a toxic substance in the air and water. Comparison of these predicted concentrations to air and water quality standards would appear to be an attractive method for assessing damage to the environment, but such an

approach has many pitfalls, among which are: (1) difficulty of implementation; (2) multiple standards for the same substance; (3) chronic, instead of acute, exposure standards; (4) statement of quality standards in a form other than levels not to be exceeded. Because of these problems, the condition of exceeding air or water quality standards has not been adopted as a viable procedure for assessment of environment damage in the VM. It was determined that an assessment of damage to people and property would be considered as the original tasks of the VM. It is anticipated that environmental damage will be considered at a later date.

2. Explosion Damage

Explosion damage is assessed to the vulnerable resources "people" and "structures." Personnel experience explosion damage in two categories, (a) death and (b) nonlethal injury. It is customary to categorize explosion damage to personnel in three categories, depending in the causative mechanism of damage; thus:

a. primary damage - direct blast effects (interaction between the blast wave and personnel only, with no other intervening or associated factors)

b. secondary damage - damage from missiles and fragments

c. tertiary damage - damage from translation and subsequent collision with an obstacle; i.e., impact

In the VM, death is assessed for primary damage manifested as lung hemmorhage or for tertiary damage manifested as skull and body bone fractures. Nonlethal injuries are assessed for all three damage categories, including the secondary damage of puncture wounds from missile penetration. In addition, injury resulting from two or more damage mechanisms is assessed in a separate category, multiple injury. Structures experience explosion damage in two categories: (a) serious structural damage and (b) window glass breakage. The physical variable that determines the extent of explosion damage in the VM is the peak overpressure.

3. Fire Damage

Damages from fire are assessed to the vulnerable resources, "people" and "structures." The damage assessed to structures is ignition. The damages assessed to personnel are: (a) death and (b) nonlethal burns. For all types of damages, two parameters have been found to be significant: (a) level of thermal radiation and (b) duration of the thermal radiation; therefore a variable combining these two parameters is used for assessment purposes. The assessment of deaths from flash fire is based on data obtained primarily from studies of the effects of nuclear weapons. The radiation from a flash fire is time varying. To be compatible with the damage assessment procedure, this time varying radiation is parameterized by calculating an effective pulse intensity and an effective pulse duration. Because of the uncertainty in determining the degree of the burns and the effects of clothing and shielding, the VM does not make a quantitative assessment of nonlethal burn injuries. Instead, it informs the user that the threshold for causing first degree burns to exposed skin has been exceeded.

The assessment of fire damage to structures is based on studies of the ignition of wood. Factors influencing wood ignition are: (a) radiation intensity level, (b) duration of radiation exposure, (c) wood type, and (d) the presence or absence of a pilot flame near the irradiated wood. Duration and level of radiation intensity are factors computed by Phase I submodels. Wood type is not treated explicitly; average values are used. For flash fire the presence of a pilot flame is assumed; for pool burning pilot flames are assumed to be absent.

Input/Output

Four types of input data are required to run the VM:

1. The physical and chemical properties of the cargo, which are stored in a library file; also a library file of default values for missing property values or missing user-supplied data

2. Demographic and other local information for the region of interest, also stored in a library file

3. Data defining the spill and the air and water conditions at the time and location of the spill, and locations and strengths of ignition sources

4. Operating parameters and override values

The physical and chemical properties of the cargo are stored in the chemical properties file; this file, designed for use with HACS [S4], has been adopted for use with the VM. In addition to obvious information about each material such as molecular weight and density at standard temperature and pressure, the properties file contains some information about flammability, toxicity, flame temperature, and other properties of the material. For properties such as vapor pressure, viscosity, and thermal conductivity which vary with the temperature, the constants in the equations that give these quantities as functions of temperature are stored in the properties file.

The information about the distribution of population and buildings was taken from census data, and, at present, each census tract constitutes a cell. Those census tracts that included any navigable water were divided into the land portion and the water portion. Each cell is identified by a number and represented by a grid point. For regularly shaped tracts with a uniform housing density, the grid point was chosen to be approximately the center of the tract. For irregularly shaped tracts, or those which included a significant amount of uninhabited area, a point representative of the settled area was chosen to represent the census tract.

The third category of input information required is that which defines the spill and the air and water environment in which it occurs. These data include the location of the spill, the substance in the tank, the tank temperature, pressure and dimensions, and the size and location of the rupture or vent. To define the environmental conditions, such items as air temperature, pressure, humidity, wind velocity, and stability class are needed, in addition to water temperature, salinity, pH, and current or tidal conditions.

The fourth category of data includes information which the user provides for each simulation and which does not fit in the previous category. For example, the user must specify what portion of the available grid is to be used for this simulation. The user may wish to override the default value for an internal parameter such as the time step used in the air dispersion submodel. Or, if chemical properties of the spilled cargo are known to the user but have not yet been placed in the properties file, the user may specify the values of these properties in order to override the default values which would otherwise be used.

The transfer from the simulation of physical events to the damage assessment portion of the VM is by means of files which store the values of physical quantities. The largest files are those which store the concentration of the cargo in the air and in the water as functions of time and grid point. For "one-time" events such as fires or explosions, only one value of each physical quantity used in damage assessment need be stored for each grid point. For explosions, the values of the peak overpressure and the dynamic impulse are given. For a flash fire, the effective radiation intensity and duration are given, and for pool burning the radiation intensity and burning time are given. The effects of toxic gases are assessed directly from the variation of concentration with time. After the spill development is simulated and the results are stored by grid cell and time interval, these data along with the information describing the vulnerable resources are used to assess the damage which may result.

After the Phase I simulation results have been processed in Phase II to give damage assessments, key features of the Phase I simulation, as well as the results of the Phase II damage assessment, are printed out in a user-oriented, easily interpreted format. Both in the cell-by-cell printout and in the summary printout, damage is separated into classes by receptor (i.e., people or structures) and by causes (i.e., toxicity, explosion or fire).

Because the final damage assessment is presented in an easy to understand, user-oriented manner, further processing of the data or lengthy analysis is obviated. Of course, it is assumed that the user is knowledgeable about the cargo type, the geographical area, and the modeling assumptions to the extent that the results will not be misinterpreted.

Test Results

Test runs of the VM were made for the five cargoes considered under a variety of spill and environmental conditions; these test runs were performed in order to:

- Show the feasibility of the VM concept
- Test the computerized logic deciding the sequence of submodel execution
- Demonstrate the plausibility of the damage assessment compiled
- Test the sensitivity of the computed results to various input parameters

Sizes of spills simulated ranged from 0.6 m^3 (160 gallons) to 50,000 m^3 (13 million gallons). Wind direction, wind speed, spill size, cargo type, ignition source type, and atmospheric stability class were the input parameters varied in the course of the testing.

The test results gave spill development behavior and damage estimates which are not inconsistent with the small number of observed accidental spills. In general, spills of the toxic irritant gases produced simulated injuries and deaths that were an order of magnitude larger than the damages to people resulting from the explosion of an equal amount of spilled flammable material. Injury and death from deflagration (flash fire) of a flammable spilled material were considerably less than the injury and death produced by the detonation (explosion) of the same amount of flammable spilled material.

Uses of the VM and Suggested Improvements

At present, the VM is in its first stage of development; even in this developmental stage the VM is a useful tool. Among the uses of the VM are:

- Demonstration of the feasibility of implementing a simulation system for assessing damage resulting from spills of hazardous materials
- Aid in planning future R&D efforts by pinpointing areas where modeling needs improvement
- Aid in planning regulatory actions
- Aid in planning programs for response measures

Although it is useful in its present state of development, the VM requires further improvement before it will be able to realize its full potential for utility as a risk analysis tool. Improvements to the VM can be divided into two classes:

1. Improvements to specific submodels or the addition of submodels to account for additional phenomena
2. Improvements to the overall VM structure

Work should be undertaken to expand and improve the spill development (Phase I) modeling. The VM should be expanded to include new submodels developed for the Coast Guard; seven additional submodels have been developed that are suitable for inclusion in the VM. These are:

1. Release and migration of heavy insolubles on river beds
2. Heating, rupture of the container, and release of pressurized cargo in a fire
3. The release of three specific reactive chemicals
4. Release, spread, dispersion, and fire hazard due to a continuous release of cold, liquefied gases
5. Water dispersion of chemicals with finite solubility

6. Heating and rupture of tanks on sunken barges carrying cryogenic materials

7. Release of cold and soluble chemicals underwater

The VM should be exercised for various additional cargoes, especially chemicals of the type to which these new submodels apply. Two areas of fire and explosion modeling currently in the VM should be improved. A more sophisticated treatment of the flash fire phenomena should be achieved. At present, the radiation characteristics at the site of combustion are calculated, but radiation levels at points distant from the site of combustion are not calculated. Consequently, no damage is assessed, except in those cells containing burning fuel at the cell center. An improved flash fire submodel should permit assessment of damage at points distant from the site of combustion. This improved calculation of radiation levels will continue to treat the variation of radiation with time but will improve the treatment of radiation variation in space. Another area of fire and explosion modeling that requires improvement is the treatment of ignition sources. The present model classifies ignition sources on the basis of strength by using the concept of flash point in a rather unconventional manner. Also the decision as to whether conflagration or detonation results if an ignition occurs is made a priori by the user, rather than being a computed decision in the simulation. At this time, it is doubtful that a model can be formulated to make the choice between conflagration and detonation except at a disproportionately high effort and cost.

On the other hand, other aspects of the modeling of ignition phenomena could be improved. A treatment is desired which would consider ignition potential as a true function of area, rather than the current treatment which considers ignition sources to be concentrated at the center of a grid cell. By describing ignition sources in a manner other than locating the sources at discrete sites (the cell centers), a more realistic assessment of time to ignition and distance between ignition point and spill may be obtained. The ability to grade ignition sources according to strength is a desirable property of the VM. However, a gradation system that is based on flashpoint, although useful, lacks rigor in the correspondence between the physical phenomena modeled and the mathematical description used in the VM. However, no solution may exist to the ignition gradation problem, which is both physically more realistic and manageable in terms of computation and data preparation; therefore, the problem of ignition source gradation may be researched, but a modification to this portion of the VM may not be advisable unless a tractable solution is found.

Certain aspects of current damage assessment procedures should be improved. The VM should be modified to assess deaths and injuries suffered by indoor sheltered populations due to all relevant damage mechanisms. Consideration should be given to the varying degrees of shelter afforded by different types of structures. For injury caused by inhalation of toxic gases, assessment of injury to the indoor population will involve considerations of seepage of the toxic substance into structures. The assessment techniques for damage caused by inhalation of toxic gases evolved during the first stage of development of the VM require that the time history of

concentration of the gas be known. For injury caused by explosion, assessment of injury to the indoor population will involve the degree of shelter afforded by the placement of the people in the building. For example, persons in front of glass walls or large windows facing the blast will have a much greater chance of injury from flying fragments than persons not so located. Buildings with fewer and smaller windows will not present this hazard but may cause high velocity jets to issue from those windows facing the blast, and these high velocity jets of air may cause serious translation damage. Injury to persons inside buildings as a result of flash fire or pool burning is much less likely to occur as a primary damage mechanism than injury to sheltered populations from explosion or toxic substances. Whether a person inside a building is harmed directly by burning of the spilled material depends mainly on whether that person is in front of a large window or is otherwise in the building but "unsheltered" by the building.

The data file of vulnerable resources should be expanded to account for those portions of the population that are found in the different classifications of structures for different times of the day and different days of the week. It may be desirable to categorize the population into three location classes: (1) at home, (2) at work, and (3) in transit. A fourth, and possibly highly significant class, may be "at a recreation facility," e.g., at a stadium, playground, beach, or fairground. Movement of the population, especially regarding recreational location, will also depend on the time of year. The "at work" location of the younger segment of the population will normally be at schools; in most parts of the country, schools are closed or only partially utilized in the summer.

A better treatment of the ignition of structures should be brought about. A more precise method to account for shielding from thermal radiation is to be devised. The current criterion that 25% of the structures are ignited in a cell subject to radiation sufficient to cause ignition is to be replaced by a criterion that has a variable percentage ignited and the percentage ignited is to be calculated on the basis of physical principles.

The damage assessment procedures in the VM should be expanded to account for damage mechanisms not currently modeled. Among the additional damage mechanisms that should be accounted for in the VM are the following:

1. The spread of fires initiated by the burning of the spilled cargo should be considered. This will involve both fire spread from building to building and the ignition of new sources of fuels, as might be found in a nearby refinery.

2. The inhalation of toxic combustion products should be examined.

3. The ingestion of water containing toxic concentrations of pollutant should be considered. A specific level of injury or percent of population injured is not possible since the quantity and rate of ingestion are highly variable and unpredictable. What is required is some indication of the toxic hazard presented by a given concentration of spilled substance.

4. The phenomenon of a rolling fireball should be examined, and modeled if it is to be a significant damage mechanism. The rolling fireball is distinguished from the flash fire by: (1) combustion in the

flash fire is rapid compared to combustion in the fireball; (2) the burning mixture in the fireball is rich and is supported by turbulent diffusion, whereas the burning mixture in the flash fire is premixed to within the flammable limits.

5. Injury by asphyxiation should be addressed.

6. Further consideration should be given to the significant ways in which diffuse explosions differ from conventional explosions, both in physical characteristics and in damage phenomena; the possibility that a deflagration may "shock up" to produce a significant blast overpressure should be considered.

Methods to make the VM more accurate and efficient by modifying the present grid cell structure should be examined. One possible approach is to compute the precise region of damage from a spill-based coordinate system and then to process only those demographic data pertinent to the impacted area. Such an approach may also permit the plotting of isodamage contours. To restructure the VM in this manner will require that the computation of physical phenomena at cell centers be abandoned; consequently, the Phase I subroutines may require revision to compute the locus of a constant value of a physical parameter (say overpressure) rather than to compute the value of a parameter at a given point.

Conclusion

The listing of such a large number of recommendations was intended to point the way toward areas related to the VM for which additional effort is believed to have the greatest potential for benefit. This list of recommendations is not, nor is it intended to be, an indictment of the VM. To the contrary, the VM, in this its first stage of development albeit crude in certain aspects, is believed to be a useful, practical tool for use in the risk analysis of marine spills. Further development of the VM will make this already functional tool more useful, more precise, and more widely applicable.

REFERENCES

[S1] Luckritz, R.T. Hazardous materials spill prevention in the bulk marine carriage of dangerous cargoes, pp. 18-24. In Control of Hazardous Material Spills, Proceedings of the 1974 National Conference on Control of Hazardous Material Spills. Am. Inst. Chem. Eng., N.Y., 1974.

[S2] Dunn, W.A., and P.M. Tullier. Spill Risk Analysis Program. Phase II. Methodology Development and Demonstration. Operations Research, Inc., Silver Spring, MD, August 1974. USCG Report No. CG-D-15-75 (NTIS AD 785026).

[S3] Raj, P.P.K. and A.S. Kalelkar. Assessment Models in Support of the Hazard Assessment Handbook. Arthur D. Little, Inc., Cambridge, Mass., January 1974. USCG Report No. CG-D-65-74 (NTIS AD 776617).

[S4] Hazard Assessment Computer System (HACS) User Manual. Arthur D. Little, Inc., Cambridge, Mass., December 1974.

ACKNOWLEDGMENTS

The authors wish to acknowledge the contributions made to the development of the Vulnerability Model by other members of the ECI staff. John Morton provided toxicological expertise and is primarily responsible for Appendix E. Dr. A. Hadermann, Dr. Timothy Kao, Mr. J. Horowitz, Mr. I. Takacs, and Mr. R. M. Rowley provided assistance in their areas of particular expertise, which are, respectively, physical chemistry, transport phenomena and flow chart development, water quality, air quality, and computer systems.

Dr. John A. Brown, of John Brown Associates, Inc., performed the historical survey reported in Chapter 9 and Appendix F. Most of the computer programming was done by Mr. J. Weirman, Operations Research, Inc.

The authors gratefully acknowledge the assistance provided them by Mr. Neal FitzSimons of the Defense Civil Preparedness Agency.

The program was performed for the Office of Research and Development, U. S. Coast Guard, under the supervision of Mr. John Dwyer. The guidance and insights provided by Mr. Dwyer were most helpful in the successful completion of this work; the comments and advice of other USCG staff members, particularly Dr. John Gardenier, Dr. John Cece, and Lt. Michael Taylor, are greatly appreciated. The direction provided by the members of the Risk Analysis Advisory Board is sincerely acknowledged.

TABLE OF CONTENTS

APPENDIXES, continued

APPENDIXES, continued

LIST OF TABLES

CHAPTER 7, continued

LIST OF ILLUSTRATIONS

INTRODUCTION

This report describes the development of a computerized simulation model designed to estimate the consequences of a marine spill of a hazardous chemical. This Vulnerability Model (VM) has been developed for the U. S. Coast Guard under contract DOT-CG-33377-A. The model simulates the physical phenomena associated with spills and the responses of vulnerable resources to the various damage-inducing mechanisms resulting from the spill. The VM produces estimates of the total losses incurred in terms of deaths, injuries and value of property damage. It also identifies the time and location of the losses and the damage mechanism which caused them.

In recent years, new technologies and an expanding search for energy sources have led to increased bulk transport of hazardous chemicals on U. S. waters. The Ports and Waterways Safety Act of 1972 charges the Coast Guard with providing for the safety of "ports, harbors, waterfront areas and navigable waterways of the United States." To meet this responsibility, the Coast Guard is authorized to regulate the movement of bulk cargoes and the design and operation of vessels carrying them. Substantial increases in safety rarely come cheaply. The reduction in risk attributable to any regulation must be weighed against the increased operating costs of capital expenditures such regulation requires. The need to perform cost-benefit analyses of Coast Guard actions has led to a research and development program to establish a Risk Management System. The VM is an important component of this system.

The Risk Management System (Figure I-1, [1]) consists of three submodels linked together to relate various system parameters to the risks and costs of operating the system. The first submodel is spill analysis, which estimates the change in the likelihood of spill accidents induced by regulating the values of some system parameters. Next is the damage assessment phase in which the VM estimates the consequences of a spill occurring for a given set of conditions. When the consequences of an accident are combined with the likelihood of the accident occurring, a measure of the system risk is produced. It then remains to measure the economic impact of the regulation by varying the inputs to the cost submodel. The merit of the regulation can then be evaluated by comparing the reduction in risks to the increase in costs.

The main objective in developing a damage assessment tool has been to establish a workable model within a framework flexible enough to allow for future model enhancements. The approach taken was to simulate the spill through a series of separate submodels. Many of these submodels had previously been developed for the Coast Guard. In modeling complex physical processes, it has been necessary to make simplifying assumptions. A conservative design philosophy guided the development of models used in

---

[1] Dunn, W. A., and P. M. Tullier. Spill Risk Analysis Program. Phase II. Methodology Development and Demonstration. Operations Research, Inc., Silver Spring, Md., August 1974. USCG Report No. CG-D-15-75 (NTIS AD 785026).

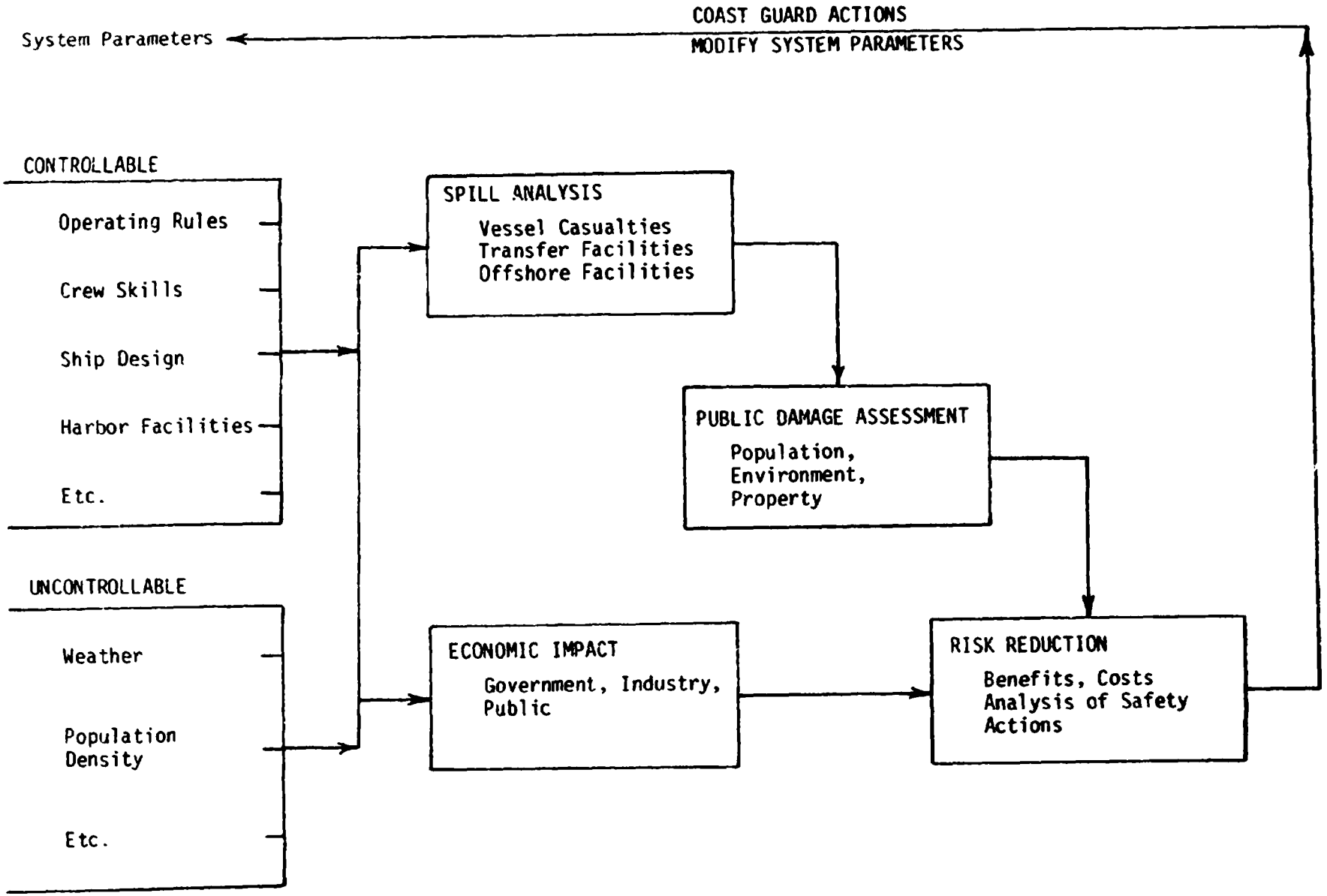

FIGURE I-1. RISK MANAGEMENT - THE SYSTEMS APPROACH

the VM; consequently, whenever alternate approximations were available, the approximations were chosen so that the VM does not underestimate damage. The approximations made in model development are recognized, but the modularized structure of the VM facilitates the insertion of additional and improved models as they become available. A subsidiary objective in developing the VM is to aid in the assessment of the effectiveness of response measures (e.g., evacuation, chemical neutralization or adsorption, and firefighting). The effectiveness of various response measures is determined by simulating a spill and appropriately manipulating those parameters of the model affected by the postulated response. Use of the VM for evaluating response measures is deferred pending further model development.

There is a danger that the results of the VM may be misinterpreted, so caution and care must be exercised when considering the results. One point that must always be borne in mind is that the VM is entirely deterministic. The damages assessed by the model are predicated on a set of circumstances (input conditions) chosen by the user. The probability that such a set of conditions exists is not considered by the VM. The likelihood of a spill is small; this small probability combined with the probabilities of all of the other conditions yields a small overall probability that any given scenario actually occurs. Thus, although the consequences of some simulations are quite dire, the risk (the expected value) is small; large losses from rare events do not necessarily indicate a high risk activity. Because the VM is completely deterministic and because no assessment is made of the likelihood of a user-chosen scenario, considerable judgment and experience are required to avoid unreasonable (even impossible) input conditions. For example, it is possible to simulate a very large spill, even though no vessel in existence is large enough to carry that much cargo. Another instance of the possible simulation of an unrealistic scenario is the specification of a certain size spill at a location unreachable by a cargo ship large enough to carry the quantity of material specified as spilled. A further example is that the user may specify an explosion-generating ignition source, thereby causing an explosion to be simulated, for a situation in which the chemical properties of the spilled substance or the conditions at the time of ignition make the likelihood of explosion extremely small. It must also be acknowledged, when interpreting results, that the VM is in its first stage of development. Spills have been simulated for only five liquids. Solids, reacting substances, secondary damage mechanisms, damage to indoor (sheltered) populations, etc., have not been modeled. Although such omissions do not invalidate the results, comparison of results in a general context (for different chemicals, different locations, etc.) should be made with caution until further development improves the accuracy and confidence level of the model. Finally, interpretation of the results should be tempered with the knowledge that the VM alone cannot determine the risk of marine transport in comparison with other forms of bulk transport or even with other human activity involving risk.

In spite of some current limitations, the VM can perform many useful functions. By using it, the relative potential consequences of transporting different commodities can be assessed in a physically based, consistent, quantitative manner. Damage estimates resulting from a simulated spill of one cargo may have a different degree of accuracy from the results of

another cargo, since a different set of submodels, each with its own precision, is used to obtain the result. Nevertheless, the relative potential consequences of transporting different cargoes are given. The sensitivity of the damage estimates to the location of the spill can also be shown with the present model. Damage estimates for locations with greatly different topographic features may possess different degrees of accuracy, since some submodels give more accurate simulations for one type of topography than another. Regardless, the relative potential consequences at different locations can be demonstrated. This type of information should be very useful in determining where facilities to load and unload vessels should be optimally located.

This final report marks the end of the first phase in the development of the VM. This model is but one of several elements in a continuing search for better methods to identify, assess, and control risks and to improve safety associated with the transport of hazardous materials. It is recognized that the subject matter of this report is emotionally sensitive and that the interim findings presented are subject to misinterpretation or misuse. However, it is concluded that the potential benefits to be derived from presenting these findings far outweigh the possible harm that could occur if the results are misinterpreted, misused, or misrepresented by persons with differing motives. Constructive interest, suggestions, and criticisms of this research effort, the methods used, and the interpretation of results are solicited.

The repetitive statement of so many cautionary notes is not, nor is it intended to be, an indictment of the VM. To the contrary, the VM, in this its first stage of development, is believed to be a useful, practical tool for use in the risk analysis of marine spills. Further development of the VM will make this already functional tool more useful, more precise, and more widely applicable.

Chapter 1 of this report presents an overview of the VM design. Chapter 2 consists of a summary of the several submodels used in the VM, some of which had been developed previously under USCG sponsorship; other submodels were developed as part of this current project. Chapter 3 describes air dispersion modeling, and Chapter 4 describes fire and explosion modeling; both of these areas of modeling have received considerable attention during this effort and are, therefore, given detailed description. The VM operates in two stages, referred to as Phase I and Phase II. Phase I simulates the spill itself and the distribution of the spilled substance in space, whereas Phase II uses data from Phase I to assess injuries/damage to vulnerable resources. Chapter 5 summarizes the type of input and output data associated with Phase I, and Chapter 6 summarizes the assessment procedures used in Phase II, including flow diagrams. Chapter 7 describes test computer runs of the VM . Chapter 8 presents a sensitivity analysis of the VM for input variable changes. Chapter 9 summarizes the conclusions of a historical survey performed in this effort to help validate the VM. Chapter 10 gives conclusions and recommendations. Appendix A contains flow diagrams and a related description of Phase I. Appendix B gives details of the air dispersion modeling. Appendixes C and D give details of the fire/explosion submodels and their damage assessment procedures, respectively. Appendix E describes the approach taken in deriving the toxicity damage assessment procedures. Appendix F is a set of case studies

compiled in the historical survey subtask. Appendix G details procedures to avoid double counting in damage assessment. Instructions on data preparation and model execution are found in a separate document, the "Vulnerability Model User's Manual."

CHAPTER 1

GENERAL DESCRIPTION OF THE VULNERABILITY MODEL

Introduction

This chapter presents a general overview of the Vulnerability Model (VM) and lists some of the constraints necessarily imposed upon model design and development in order to produce an operational package within the resources available. Details of what is summarized here are presented in the following chapters and in the appendixes.

Vulnerability Model

1. Scope

The VM is a computer simulation designed to provide quantitative measures of the consequences of marine spills of hazardous materials. The simulation starts with a description of the nature of the spill itself, continues through the dispersion of the hazardous material, and ultimately includes an assessment of the immediate effects of the spill on surrounding vulnerable resources, namely, people, property, and the environment.

The VM was originally conceived to be, and is ultimately intended to be, a damage assessment tool capable of treating spills of virtually all cargoes carried in marine bulk transport. However, in order to obtain a complete, functional simulation system within the resources allocated, the version of the VM operational at present was developed with fewer capabilities and less completeness than the comprehensive model originally envisioned. A comprehensive version of the VM should treat all cargoes whether in solid, liquid, or gas phase. The model should also treat other physicochemical processes affecting cargoes, including change of phase upon release into air or water, reaction, dissolution, admixture, and mass transfer between water and air. The version of the VM operational at present treats only fluid cargoes and is able to simulate only some of the physicochemical processes that a more complete model could simulate. Currently, the VM has been exercised for only five cargoes: anhydrous ammonia, chlorine, gasoline, liquefied natural gas, and methanol.

A main consideration in developing a damage assessment tool has been to establish a workable model within a framework flexible enough to allow for future model enhancements. The approach taken was to simulate the spill through a series of separate submodels, many of which had previously been developed for the Coast Guard. In modeling complex physical processes, it has been necessary to make simplifying assumptions. A conservative design philosophy guided the development of models used in the VM; consequently, whenever alternate approximations were available, the approximations were chosen so that the VM does not underestimate damage. The approximations made in model development are recognized, but the modularized structure of the VM facilitates the insertion of additional and improved

models as they become available. However, because the ultimate goal of the VM is a general use damage assessment tool, the use of chemical-specific models has been avoided.

2. Simulation Scenario

The simulation requires three types of descriptive data that define: (1) the spill, (2) the physical setting in which the spill occurs, and (3) the vulnerable resources that are subject to the effects of the spill. The spill is described in terms of its location and spill rate, the physical and chemical properties of the spilled material, and the quantity of the spill. The physical setting is described in terms of the geometric configuration of the shoreline(s), hydrologic/oceanographic properties, and meteorological data. Vulnerable resources are described in terms of demographic distribution, property distribution, and land/water use. The geographic area of concern may represent any user-defined location, a rectangular area measuring 10 miles in length and 5 miles in width being typical of anticipated applications. The physical setting and the distribution of vulnerable resources are described in terms of mutually exclusive geographic cells that cover the entire area of concern.

3. Submodels

The VM consists of submodels interconnected by an executive routine, with built-in logic dictating the sequence of submodel processing as a function of the spill development. Among these submodels are simulations of surface spreading, water mixing, air dispersion, conflagration and explosion and submodels for assessing the effects from the dissemination of the hazardous material on vulnerable resources. Some of the submodels had been designed previously under U. S. Coast Guard sponsorship as part of the CHRIS (Chemical Hazard Response Information System) [2] project development. CHRIS is a chemical hazard response information system embodied in a set of field manuals; the models in CHRIS are presented in a format for hand calculation of spill development. Some of these same models have also been incorporated into HACS (Hazard Assessment Computer System) [3], which is designed for headquarters use. The models in HACS are presented in a format for computer calculation of spill development. Several of the submodels in the VM, including all of the damage assessment procedures, were designed specifically for the VM. A generalized flow diagram of the model is presented in Figure 1-1.

---

[2] Raj, R. R. K., and A. S. Kalelkar. Assessment Models in Support of the Hazard Assessment Handbook. Arthur D. Little, Inc., Cambridge, Mass., January 1974. USCG Report No. CG-D-65-74 (NTIS AD 776617).

[3] Hazard Assessment Computer System (HACS) User Manual. Arthur D. Little, Inc., Cambridge, Mass., December 1974.

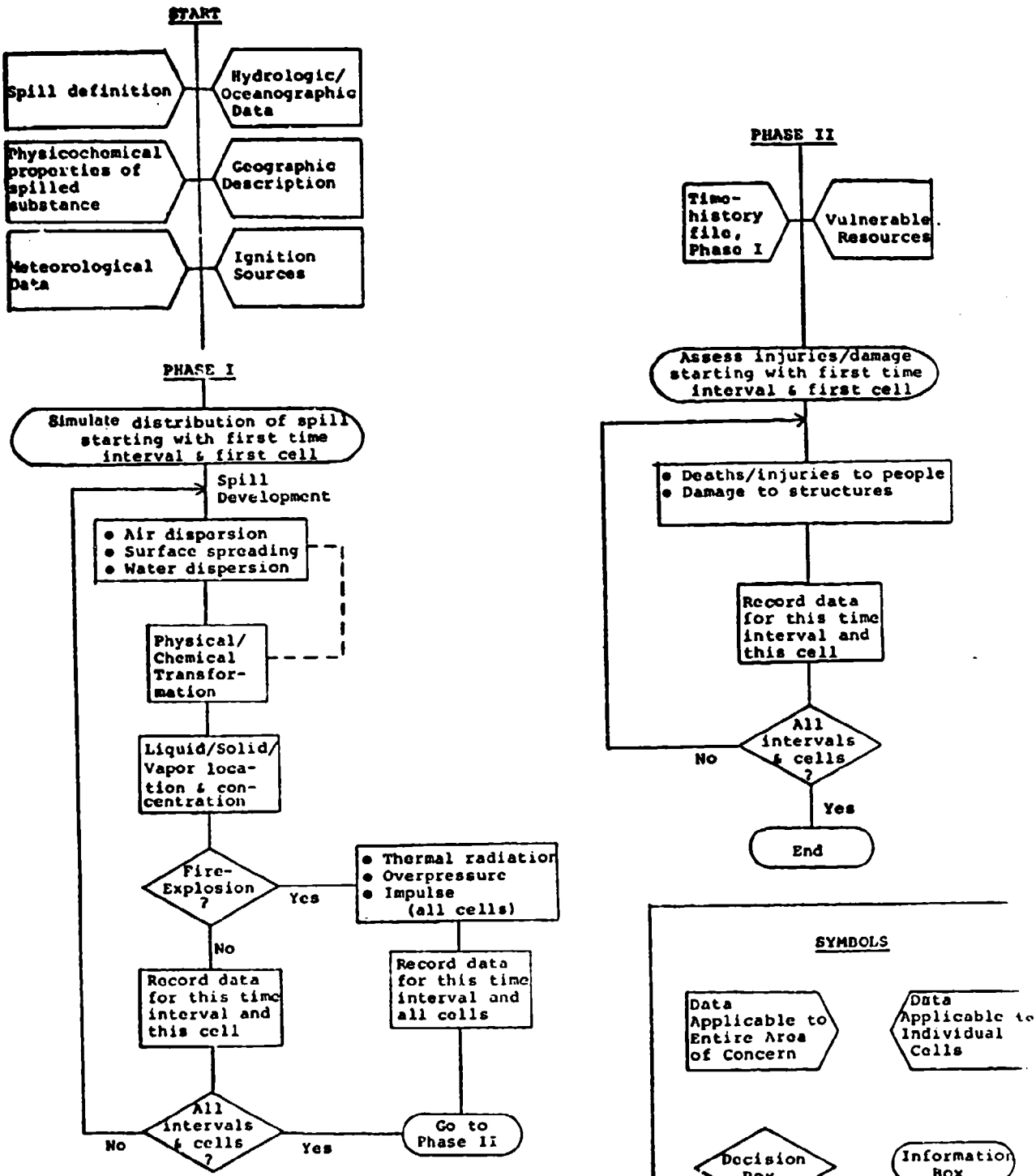

FIGURE 1-1. GENERALIZED FLOW DIAGRAM OF THE VULNERABILITY MODEL

4. Operational Phases

The VM operates in two phases. Phase I simulates the spill itself, the physical and chemical transformations of the spilled substance and its dissemination in space. This phase covers the time period from the initiation of the spill until a user-specified time has elapsed. The time interval between simulation calculations is specified by the user but may be overridden by certain submodels (such as the explosion submodel). A time-history file of the spill sequence simulated during the first phase is retained on magnetic tape, disk, or other semipermanent computer storage media.

In Phase II, the computer first superimposes this time-history file upon the vulnerable resources map and then assesses the effects of toxicity, explosion and/or fire on the vulnerable resources as a function of time. Estimates of deaths and nonlethal injuri s to people and of damage to property are provided in tables.

A schematic of the types of submodels currently implemented in Phase I and Phase II is given in Figure 1-2. Details of the Phase I submodels as implemented currently are given in Chapters 2, 3, and 4 and Appendixes B and C. Details of the Phase II submodels as implemented currently are given in Chapter 6 and Appendixes D, E, and G. Generalized flow diagrams of Phase I submodels for a comprehensive version of the VM, i.e., flow diagrams showing spill development for virtually all marine cargoes, are presented with an explanatory narrative in Appendix A. These flow diagrams and discussion are presented to guide the development of new models and to indicate the planned structure of a comprehensive VM; the material presented in Appendix A should not be interpreted as representing the current state of development of the VM.

5. Constraints

This section lists some of those constraints to model development and application required to produce an operational model within the resources available. It should be noted that some of the limitations listed here may be relaxed or removed in the event of further model development.

(a) Several submodels applicable to marine spills of hazardous chemicals have been developed under contract to the USCG and are described in the CHRIS documentation [2]. Some of these have been programmed in FORTRAN and are currently integrated into HACS [3], also under contract to the USCG. Concurrent with development of the VM, the CHRIS and HACS documentation has been reviewed with the intent of using as many available submodel designs and computer routines as feasible in order to avoid duplicating research, development and computer programming. Some of these submodels are being used in the VM with little or no modification.

(b) Secondary damage mechanisms, such as ignition of specially hazardous establishments (e.g., refineries), were not treated; only the direct consequences of the spill were simulated. Treatment of secondary effects, such as fire storms, additional spills caused by the primary spill, hazards from damage to key facilities (such a gas distribution on water supply system), was deferred for future development.

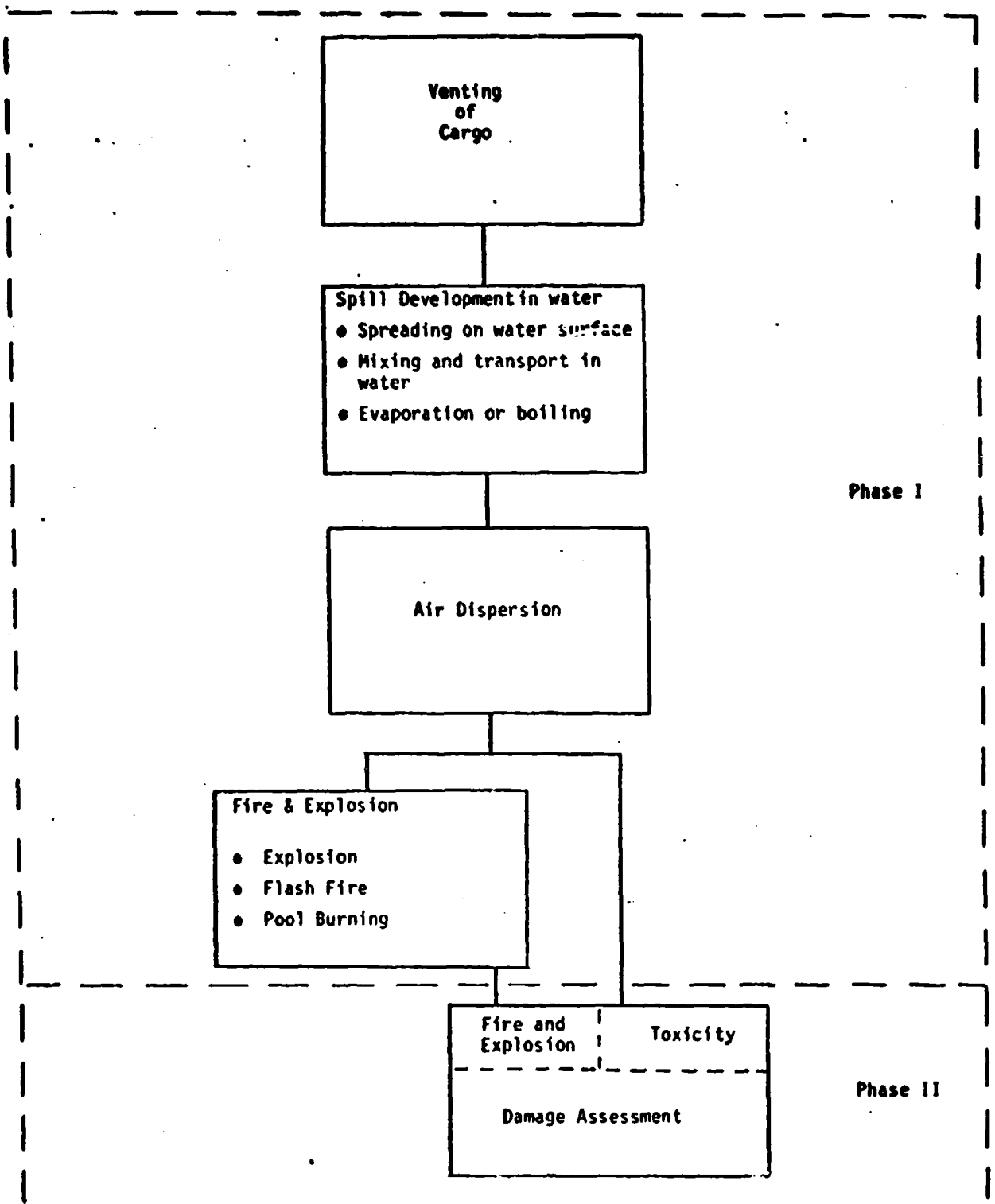

FIGURE 1-2. TYPES OF SUBMODELS CURRENTLY IMPLEMENTED IN PHASE I AND PHASE II

(c) The portion of the population indoors was considered to be sheltered, and no damage was assessed to this group. Further, it was assumed that fifty percent of the subject population was indoors.

(d) Explosion damage to structures was assessed on the assumption that the structures affected are framed with wood members; treatment of explosion damage to more substantial structures was deferred for future development.

(e) Only inhalation toxicity was treated; injury by ingestion of toxic materials was not assessed.

(f) Micrometeorological effects (e.g., airflow patterns around buildings) were not modeled because to do so would necessitate so fine a degree of resolution in the model that input preparation and computer run time would become prohibitively expensive. Consequently, modeling to account for the net effects of micrometeorology has been developed and is described in Chapter 3; however, the computer programming for this modeling has not been implemented. In addition, a uniform wind velocity was assumed to prevail over the entire area of concern.

(g) Certain aspects of underwater modeling of chemicals were beyond the scope of this stage in the development of the VM. Initially, vessel spills were to be modeled only for hull ruptures at or above the waterline. Underwater releases were not considered.

(h) Hazardous spills occurring on land that remain on land would require substantial modification of the model. Spills occurring on land but reaching the water could be treated as special cases of spills on water during subsequent development of the VM.

(i) Of the various hazards resulting from spills, air and water pollution received lowest priority in order to avoid duplicating work now in progress at EPA. Damage to the environment was not assessed; however, the concentration of hazardous material in air and water was computed, so that the user may estimate environmental consequences at his option.

(j) Explosions of nonchemical origin, such as those that can occur when cryogens are released on water, were not considered in this model.

(k) The model was designed primarily to assess risk to the public rather than to those persons experiencing prolonged or unusual levels of exposure to hazards (such as emergency personnel).

(l) Explosion of an unconfined vapor cloud is partially determined by a user input option and partially determined by the simulated characteristics of the vapor cloud; since the decision to simulate an explosion is not entirely based on physical principles, it may properly be argued that the VM will simulate an explosion when, in fact, none could occur.

(m) Test runs were performed only for five cargoes: anhydrous ammonia, LNG (liquefied natural gas), chlorine, methanol (wood alcohol), and gasoline; an analysis of inhalation toxicology was performed only for ammonia and chlorine.

(n) Response actions (e.g., spill containment, population evacuation, and fire fighting) were not considered.

(o) Spills of solids and reacting chemicals were not considered.

(p) Census data were used to determine the location of the vulnerable population; since census data primarily deal with the location of the residence of people, no modeling was effected to deal with the movement of people from home to work, to school, to recreational areas, or to other nonresidential locations.

(q) Most of the physicochemical models consider that only a single process occurs at one time, so that separate physical events occurring simultaneously are modeled as a sequence of separate events; for example, the VM models spilling, spreading, and burning as separate events, each terminating before the next can begin, even though these events can and do occur simultaneously.

6. Current Status of Development

At present, the VM is in a first stage of development. It has been demonstrated that an actual working model is capable of carrying on a simulation from the specification of cargo and spill conditions through to the assessment of damages to vulnerable resources. The quantitative results of the simulation appear to correlate with the picture of events given both by expert judgment and by historical records of accidental spills. This correlation is obtained even though it is recognized that some of the modeling, by necessity, is not at the highest level of sophistication. Furthermore, the cost of a given simulation has been kept within reasonable bounds. Likewise the cost of data preparation required by the VM is not excessive. There is virtually no cost involved in output interpretation, since the computer results are presented in an easy-to-understand, user-oriented way.

Although the results are presented in what is thought to be a clear, forthright manner, there does exist a danger that the results of a given simulation may be misinterpreted. The VM is a deterministic model. It predicts, with what is thought to be a reasonable degree of realism, the consequences of a situation specified by the user's set of input variables. It certainly does not predict what are the absolutely certain, not even the probable, outcomes of certain activities of marine transportation; this is because the VM is a tool for damage assessment, which is only a part of the larger problem of risk analysis. At least five other considerations, not within the current scope of the VM, are required to perform risk analysis.

(1) The probability of the various events (the spill, the wind direction, the material spilled, etc.) predicating a given spill scenario must be considered; the likelihood, perhaps even the possibility, of certain events simulated cannot be determined without further research.

(2) The risk of damage to vulnerable resources presented by some facet of marine transport should be judged relative to risks presented by other endeavors. For example, the risk associated with a particular maritime activity may be relatively acceptable if it is less than the risk associated with some other form of bulk transport, such as rail, truck, or pipeline transport.

(3) The VM is not providing a cost/benefit analysis of the regulatory control of marine transport activities; neither is it determining risks, including economic risk, engendered by discontinuance of these maritime activities. For example, to discontinue shipment of chlorine could result in a serious water quality crisis; to stop the importation of LNG could worsen the energy crisis.

(4) In modeling complex physical processes, it has been necessary to make simplifying assumptions. A conservative design philosophy guided the development of models used in the VM; consequently, whenever alternate approximations were available, the approximations were chosen so that the VM does not underestimate damage. This conservative model design philosophy has a tendency to yield high estimates of damage; thus, if a spill scenario were actually repeated many times, it is likely that only a few occurrences of such a scenario, if any, would yield damage as large as that predicted by the VM simulation. On the other hand, it has not been deemed feasible or appropriate at this stage of VM development to define quantitatively the "worst case" of a spill and its consequences.

(5) The levels of risk acceptable to our dynamic society are not well defined, are changing, and are not truly within the province of the VM; judgments regarding these levels of risk are to be determined by the policy makers and public.

The preceding strong caveat is an attempt to prevent misinterpretation of the results of VM simulations. By no means is it intended to discredit the VM. It is believed that, as it now stands, the VM is a useful tool for the risk analysis of marine spills; with further development and improvement the VM should be able to provide even more utility and insight into considerations of this important problem.

CHAPTER 2

DESCRIPTION OF SUBMODELS USED IN PHASE I OF THE VULNERABILITY MODEL

Introduction

This chapter describes those submodels that are presently included in Phase I of the VM. Because the air dispersion submodel which was originally part of HACS has been extensively revised, and because the fire and explosion submodels were developed almost entirely in this program, these submodels are discussed in some detail in Chapters 3 and 4, respectively. The other Phase I submodels were developed previously under USCG sponsorship. Some of these submodels were modified somewhat for inclusion in the VM. Detailed descriptions of these submodels are contained in the CHRIS documentation. The Phase II submodels (damage assessment) are treated in Chapter 6 and associated appendixes.

The submodels used in the VM treat the physicochemical processes affecting the spilled hazardous material; at the present time, the processes simulated by the VM may be classified as follows:

1. cargo venting
2. spill development in water
   - A. surface spreading
   - B. water mixing
   - C. sinking and boiling
3. air dispersion
4. fire and explosion

For certain of these processes different submodels are used, depending upon the nature of the spilled substance. Other processes, such as fire and explosion, consist of a sequence of dissimilar events so that the computer simulation consists of a sequence of submodels.

The selection of submodels, the flow of data, and the sequencing of submodel execution are controlled by internal logic embodied in the Phase I executive subprogram. The decisions made by the Phase I executive are based on properties of the cargo, user inputs, results computed by Phase I subprograms, or some combination of these. A flow chart indicating the sequence of subprogram execution and the important decisions determining branching is given in Figures 2-1a and 2-1b. This flow chart represents the structure of Phase I as it is currently programmed in the operational VM; the analogous flow chart for a comprehensive version of the VM, which version would be the ultimate product of further development, is presented

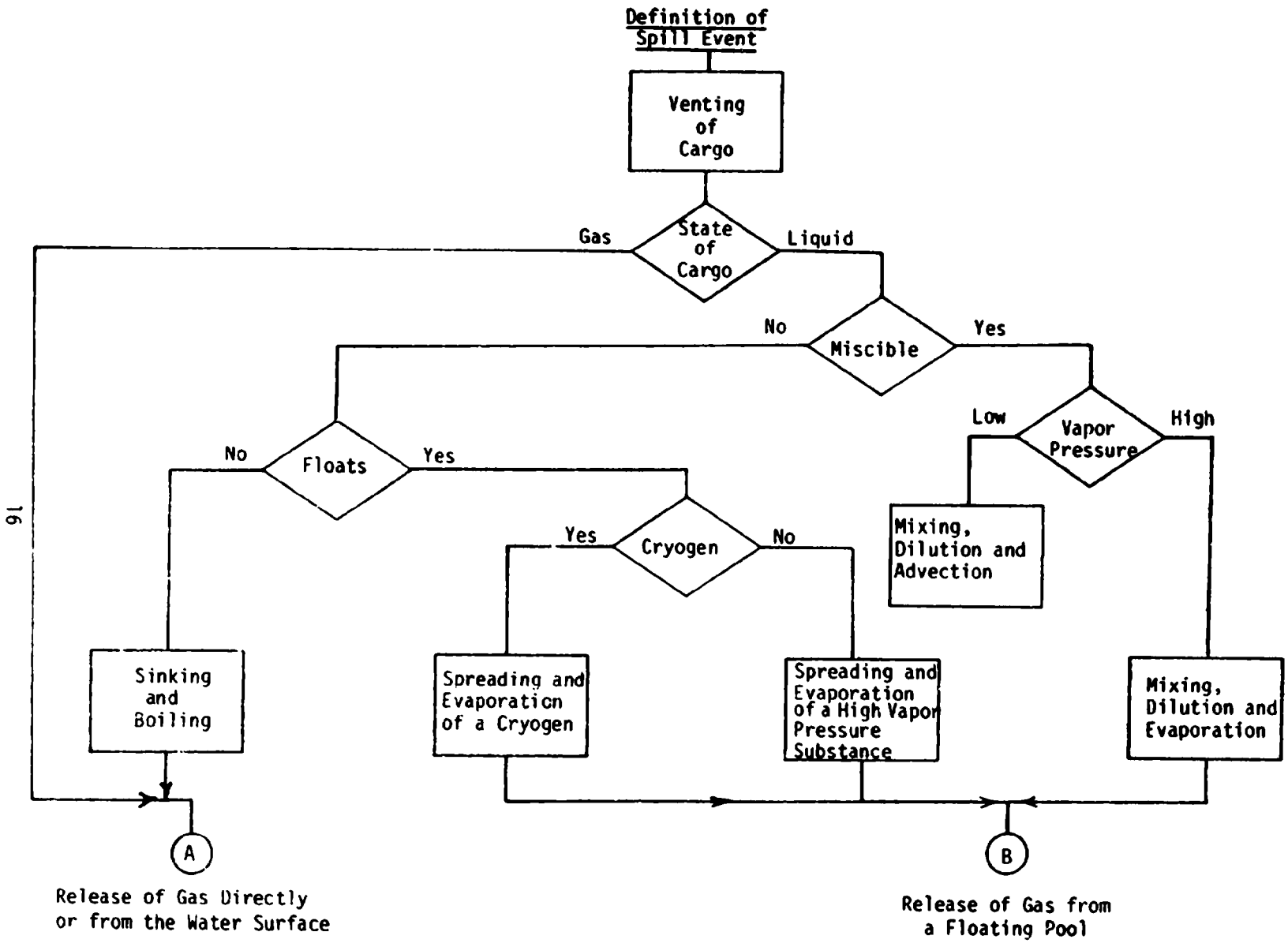

FIGURE 2-1a. FLOW CHART FOR PHASE I DETAILING SUBPROGRAM SEQUENCING AND BRANCHING DECISIONS FOR CARGO VENTING AND SPILL DEVELOPMENT IN WATER

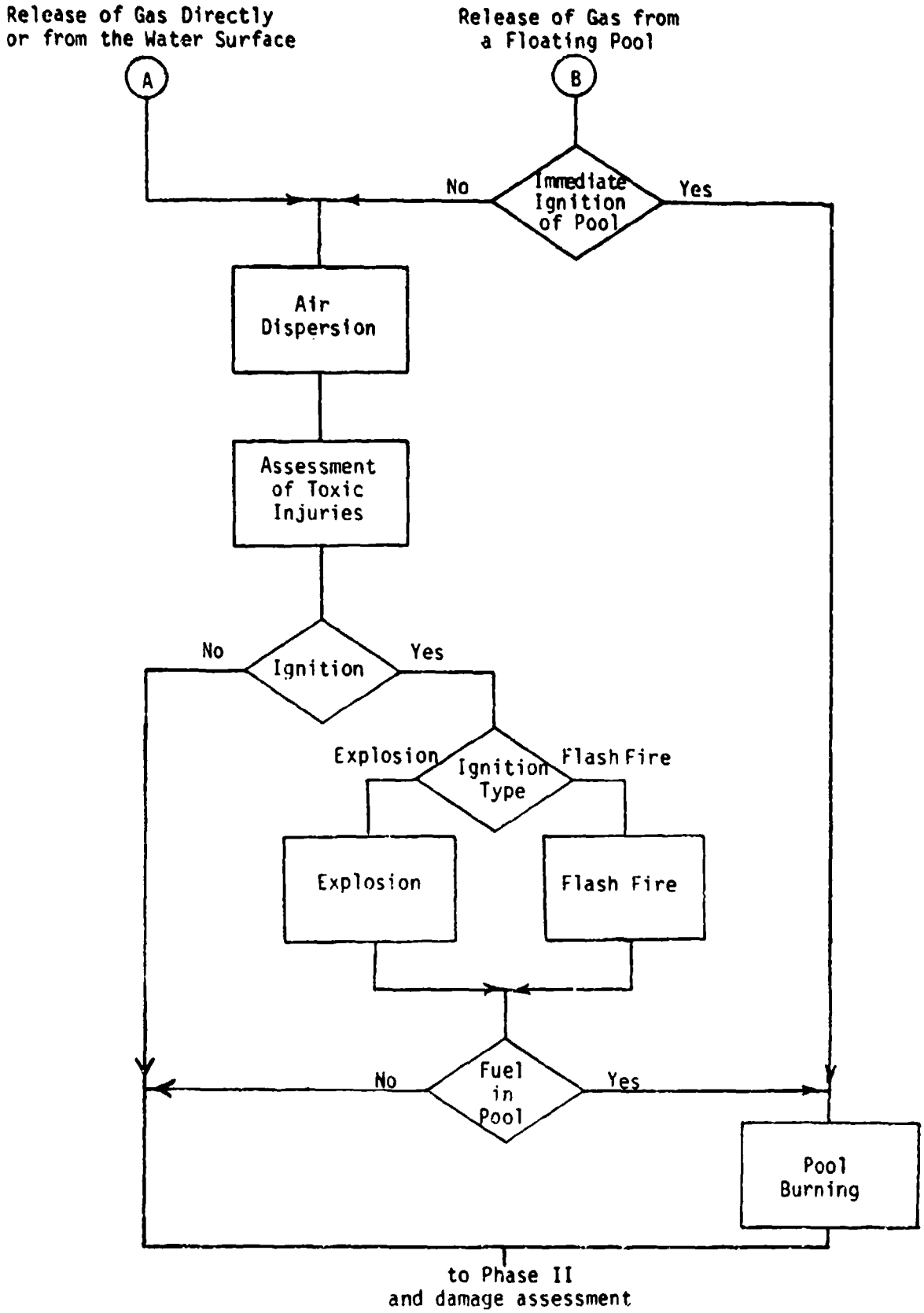

FIGURE 2-1b. FLOW CHART FOR PHASE I DETAILING SUBPROGRAM SEQUENCING AND BRANCHING DECISIONS FOR AIR DISPERSION AND FIRE AND EXPLOSION

with an explanatory narrative in Appendix A. The following consists of brief discussions of the computational submodels used in Phase I.

1. Rate of Escape of Fluid Cargo [2, Ch. 2]

This submodel provides a time history of tank conditions and venting rates of gas or liquid subsequent to a rupture in the tank wall. The venting of fluids is described by equations applicable to ideal fluid flow; i.e., the flow is assumed to be inviscid. Low flow rates (caused by small vent holes, low driving pressures, or high fluid density) and high cargo viscosity are two factors that will tend to make the inviscid assumption invalid. Since viscous effects reduce the venting rate, this assumption will tend to cause venting rate, and therefore combustion and toxic damage, to be moderately overestimated. For gas venting it is assumed that the perfect gas law holds; although this is a rather standard engineering assumption, the fact that many cargoes of interest experience wide swings in pressure and temperature during venting may introduce considerable divergence from the perfect gas law, especially for certain cargoes. Departure from the perfect gas law is expected to influence damage estimates only slightly; whether damage is overestimated or underestimated by use of this approximation is not clear at this time and may well depend upon the cargo, tank pressure, and tank temperature. Equilibrium thermodynamic relationships are assumed to be valid descriptors of the non-equilibrium venting processes; this assumption, however, is virtually universally in engineering and is not expected to produce any significant error. It is assumed that all of the liquid and gas inside the tank is at a uniform temperature during each step of the venting process; this assumption is difficult to justify, but at this time it has not been determined to what extent accuracy is compromised by the errors arising from this assumption. Rapid venting will tend to prevent the attainment of thermal equilibrium inside the tank. The thermodynamic process experienced by the fluid in the tank is assumed to be either adiabatic or isothermal. This common engineering assumption represents the limiting cases for polytropic processes; however, the actual thermodynamic process experienced in venting may be some other polytropic process or may not even be describable as a polytropic process. These assumptions about the thermodynamic process may yield considerable error in the estimate of venting time and total mass vented; however, further study is required to quantify the extent of the error. In any event, assumptions that underestimate venting rate or total mass vented will tend to underestimate damage. Evidently, the more mass of hazardous substance escaping from the vessel, the more damage it is capable of producing. Damage will be greater for higher venting rates because less time is then available to reduce the concentration of the hazardous substance to acceptable levels. This is true regardless of whether these levels are related to toxic damage or flammability limits.

Required input data are:

- initial tank conditions (temperature, pressure), tank volume (and approximate geometry), and initial mass content;
- physical and chemical properties of the spilled substance;
- size and location of the rupture.

If the tank contains only gas or if the rupture is above the liquid-vapor interface, only gas is vented. If the rupture is below the liquid-vapor interface, only liquid is vented; however, there is a provision for changing from the venting of liquid cargo to the venting of gaseous cargo, if and when the liquid level falls below the level of the vent.

This is an acknowledged deficiency in modeling that may underestimate damage for releases of high vapor pressure cargoes (such as LNG and chlorine), when the vent hole is placed near the top of the tank, but below the initial liquid level in the tank.

For vented gas, the flow may be choked. When the pressure inside the tank is sufficiently large with respect to atmospheric pressure (as a function of the specific heat ratio for the gas), the flow that will occur at the hole is said to be choked flow. The functional dependence of flow rate on tank pressure depends upon whether the flow is choked or not.

This submodel is employed in the first calculation block on the main flow chart presented in Appendix A. This submodel should be accurate for many fluid cargoes, except highly viscous cargoes carried in containers with internal pressures near atmospheric pressure. (The model is not valid if the Reynolds number is too small). This model is also less valid for very high flow rates, when the mechanical dynamics as well as the thermodynamics of the fluid in and exiting from the container become important. The degree of error involved by neglecting these dynamic effects has not yet been quantified, but neglect of dynamic effects probably tends to underestimate damage.

2. Spill Development in Water

Submodels simulating the physical processes affecting the hazardous material spilled in the water are classified in the categories of (A) surface spreading, (B) water mixing, and (C) sinking and boiling.

A. Surface Spreading

The surface spreading submodel treats two cases of an immiscible liquid on the water surface: (1) simultaneous spreading and evaporation of a cryogenic liquid on water and (2) simultaneous spreading and cooling of a high vapor pressure chemical.

(1) Simultaneous Spreading and Evaporation of a Cryogenic Liquid on Water [2, Ch. 9]

This submodel estimates the spread rate, time required for complete evaporation, and the maximum extent of spread of a cryogenic liquid floating on the water surface. It is assumed that the spill occurs instantaneously, the spread area is continuous at every instant, and the heat for evaporation comes primarily from water. It is further assumed that the properties of the spilled liquid do not change during the spread. The input data required include the properties of the liquid and the heat transfer coefficient between the liquid and water. Since the heat necessary to evaporate the cryogen comes from water, the water may freeze and an ice sheet may be formed under the spreading liquid. The submodel treats this possibility.

The assumptions that the spill is instantaneous and that the spreading is continuous are made for model development purposes only and do not reflect what might be realistically expected to occur in an actual spill. The violent agitation of the interface between the water and the spilled cryogenic liquid due to the rapid boiling of the cargo at this point may keep a solid ice sheet from forming under the spill and may make the spill pool break up into many small pools. The assumptions that the spill is instantaneous and that the spreading is continuous tend to underestimate the extent of spreading and the amount of the cryogen evaporated; thus the damage caused by the spill may be moderately underestimated.

This submodel was developed primarily for liquid natural gas but will adequately treat spills of other liquefied hydrocarbons. Although some ammonia may go into solution in the water, this submodel is being used in the case of a liquid ammonia spill at this time. Liquid anhydrous ammonia is not normally carried in refrigerated containers; treating it as a cryogen is thus decidely unconventional. However, the processes of venting and evaporation will tend to cool the ammonia, so that its spill development in water will be similar to that of a cryogen. When the development of the VM was undertaken, no submodel was available in HACS which considered the spread, dissolution, and evaporation of a liquid of finite solubility such as anhydrous ammonia. Furthermore the dissolution model in HACS does not consider evaporation. The analysis performed in the A. D. Little study [4] considered the dissolution of liquid NH_3 in a highly idealized context with no surface spreading. This analysis was thermodynamically based and is not easy to incorporate into a model that considers the diffusion of the ammonia into the water and the transport by currents. Furthermore, the philosophy in the VM is to avoid chemically specific submodels. Therefore, the submodel for an insoluble cryogen was used. Although use of this submodel for a spill of liquid ammonia is not altogether appropriate, it is the best choice at this time.

(2) Simultaneous Spreading and Cooling of a High Vapor Pressure Chemical [2, Ch. 10]

This submodel is used to estimate the extent of spread and the evaporation rate of a high vapor pressure, lighter-than-water liquid spilled on water. In order to construct a mathematically tractable submodel, spreading and evaporation are estimated independently. The submodel utilizes basic concepts of spread and evaporation caused by a vapor pressure difference between the liquid surface and the atmosphere.

The following assumptions are made.

(i) All of the liquid is spilled instantaneously.

(ii) The spreading is independent of evaporation.

(iii) Entire liquid mass is at a single temperature (mixed mean temperature) at every instant of time; that is, there are no thermal gradients in the liquid mass itself.

---

[4] Raj, P. P. K., J. Hagopian, and A. S. Kalelkar. Prediction of Hazards of Spills of Anhydrous Ammonia on Water. Arthur D. Little, Inc., Cambridge, Mass., Jan. 1974. D.O.T. Report No. CG-D-74-74 (NTIS AD 779400).

(iv) Liquid and water properties are constant.

(v) The mass-transfer coefficient is constant.

(vi) The vapor concentration of the cargo in the distant atmosphere is zero.

(vii) The temperature of the liquid when first spilled is the same as that of the water temperature.

Assumptions (iv) and (vi) appear to be valid and do not seem to induce any significant errors. Assumption (vii) may not be correct at all times but probably has a small effect on damage compared to other assumptions. Assumptions (ii) and (iii) may introduce significant errors in damage assessment, but the error will in general overestimate damage. The effect of assumptions (i) and (v) may be to underestimate damage in some cases.

Input data required to run the submodel include the physical and thermal properties of the spilled substance and the saturated vapor pressure-temperature relationship for the substance.

This model was developed with extremely high vapor pressure substances such as diethyl ether and ethyl acetate in mind, but it should also serve for propylamine, pentane, ethyl bromide, and other petroleum derivatives. The VM also uses this submodel for gasoline.

B. Water Mixing

Two submodels for the mixing of a miscible liquid with water have been selected for initial inclusion in the VM: (1) mixing of a neutrally buoyant liquid and (2) mixing of a highly soluble, high vapor pressure liquid.

(1) Mixing and Dilution of a Water-Miscible Liquid [2, Ch. 4]

This submodel estimates the concentration, over time, of a water-miscible chemical spilled on water. Classical diffusion equations are used, strictly applicable to neutrally buoyant solutes (liquids and solids that dissolve in water). Both instantaneous and continuous spills are considered. Calculations are dependent upon the state of the water surface -- calm water, tidal river, or nontidal river.

It is assumed that there is no rapid settling of the liquid due to high density of the spilled chemical, and it is assumed that no heat transfer, chemical reaction, or phase changes take place (i.e., it is assumed that the total mass of the liquid which is mixing with water remains a constant). As long as these constraints on the nature of the spilled cargo are adhered to, this submodel should yield reasonably realistic results; however, spills of cargoes that are not neutrally buoyant may behave in a manner significantly different from that predicted by this submodel. The geometry of the water region, stream and tidal velocities, total mass of liquid spilled, and the location of the spill are required input.

This submodel is very detailed in its treatment of the currents and density gradients in the water but does not consider evaporation. It is used in the VM to calculate the concentration of methyl alcohol in the river.

(2) Mixing and Dilution of a High Vapor Pressure, Highly Soluble Chemical [2, Ch. 11]

This submodel estimates the vaporization rate as well as the area and duration over which the evaporation takes place for the spill of a high vapor pressure, highly soluble liquid on water. The submodel is basically that of mixing and dilution in a river of uniform velocity over a cross section. For the navigable rivers of primary interest in the VM, the assumption of a uniform velocity profile is quite reasonable since the boundary layers on the channel sides and bottom are small compared to the stream dimensions. The effect of the approximation on damage assessment is difficult to determine without further study. It is first assumed that the entire liquid spilled goes into solution in water and the concentration is then estimated. The vapor pressure (on the water surface) is then calculated and the vaporization rate is estimated.

The basic assumptions are as follows.

(i) The air is saturated with vapor just above the water surface.

(ii) The chemical spilled reaches the temperature of the water instantly.

(iii) To estimate the water dispersion (and hence surface concentration), it is assumed that the entire mass of the liquid spill initially goes into solution with water.

(iv) An instantaneous spill at a point is assumed for calculating the water dispersion.

Of these assumptions, the last (iv) is least justifiable and most likely to produce error in the damage assessment; for the case of relatively long spill release times, the model may tend to underestimate the evaporation rate and thereby underestimate the damage caused by the dispersed vapor. The other assumptions, (i), (ii), and (iii), seem to be suitable for the level of accuracy required.

Required inputs include the mass of liquid spilled, saturated vapor pressure relationship (at water temperature), characteristics of the river, and the mass-transfer coefficient for surface evaporation.

This submodel is an extension of the previously described submodel to include the calculation of evaporation rates. In order to concentrate on this, only simple water conditions are considered. This submodel is appropriate for spills of methyl alcohol, diethylamine, or trimethylamine.

C. Boiling of Heavy Liquids with Boiling Temperatures Less than Ambient [2, Ch. 12]

This submodel estimates the rate of boiling for immiscible liquids having densities greater than that of water and having boiling points below ambient water temperature. Boiling and sinking occur at the same time.

The basic assumptions are as follows.

(i) The liquid spilled breaks up into small drops instantaneously, and these drops attain terminal velocities in a very short time with very little evaporation.

(ii) All of the drops formed are of the same size.

(iii) The drop cluster formed has high porosity; that is, the inter-drop distances are large enough so that, as a first approximation, the effect of other drops on the motion of any single drop in the cluster can be neglected. In short, it is assumed that the motion of each drop is independent from all others.

(iv) The critical Weber number is 8; that is, any drop moving at a velocity greater than that for which the Weber number is 8 breaks up into smaller drops

(v) Forced convection heat and mass transfer results are assumed to apply

The last assumption, (v), seems quite acceptable. Assumption (iv) may not be quite true since boiling simultaneous with sinking is liable to affect the stability of the droplets, thereby changing the critical Weber number; however, the error introduced into the damage assessment by this slightly to moderately inappropriate assumption is expected to be small. Assumptions (i), (ii), and (iii) are all subject to challenge. The spilled liquid may tend to stay together, rather than break up into widely dispersed, uniform droplets as assumed. Nevertheless, these assumptions will all tend to produce a rate of vapor evolution higher than that which will actually occur. Consequently, the damages caused by the air dispersion of the evolved vapor are liable to be overestimated.

The density and surface tension of the spilled liquid, its boiling temperature at atmospheric pressure, the latent heat of vaporization, and the temperature, density, specific heat, and viscosity of the water are needed for these calculations.

This submodel is appropriate for Freon 114 and some other halogenated-hydrocarbons. It may be used for liquid chlorine spills; however, since chlorine is slightly soluble in water, some chlorine will be lost by going into solution.

3. Atmospheric Dispersion

This submodel calculates the concentration of the cargo in gas phase in the air from the time the gas is released into the atmosphere until a fire or explosion occurs, or until the maximum time stipulated for the simulation is reached. If the cargo vents as a gas, or the gas is generated by a liquid cargo which is denser than water and which has a boiling point higher than the ambient water temperature, the source of the vapor is taken to be a point source. If the gas is liberated by evaporation from a pool of liquid cargo on the water surface, the point source is removed to a virtual position five pool diameters upwind.

The submodel is based on the Gaussian distribution, which is a theoretical solution to the partial differential equation governing diffusion problems. The dispersion coefficients used in the Gaussian distribution are obtained from the analysis of many observations of plumes from tall stacks and of puffs of smoke or some other tracer. Plumes result from continuous releases, whereas puffs result from instantaneous releases. Puffs are three-dimensional Gaussian distributions in which the dispersion coefficients depend upon the distance traveled by the puff center-of-mass. The plume is a two-dimensional Gaussian distribution in which the dispersion coefficients depend upon the distance downwind from the source to the observation point. The values for dispersion coefficients that have been compiled are based on data in which the distances (distance travelled for the puff - distance downwind for the plume) range from approximately 100 meters to several kilometers; for calculations involving short or long distances extending beyond the range covered by experiment, the VM uses values for the dispersion coefficients extrapolated from the empirical values. Extrapolation far back from 100 meters toward zero may yield inaccurate concentration values; a model, other than the Gaussian plume model, is probably more appropriate for small distances ($\sim$10 meters).

The dispersion coefficients are parameterized on the basis of the atmospheric stability or the turbulence class. The atmospheric stability is related to the amount of mixing in the lowest several hundred meters of the atmosphere, which is strongly dependent upon the variation of the temperature and wind velocity as functions of height and, near the ground, upon the surface roughness. The temperature structure is, in turn, dependent on the amount of heat from the sun reaching the ground and on the absorption properties of the ground. Criteria for determining the stability class based on these factors are given in standard references (see for example, Slade [5] as explained in Chapter 3).

At present, the submodel will select the plume (continuous source Gaussian distribution) if the total release time is longer than five time steps, although the user may specify that the puff (instantaneous source) Gaussian distribution be used regardless of the release time. It is presumed that the time steps are chosen to be related to certain advection times as explained elsewhere. Furthermore, the plume model is not used for wind speeds of less than 2 meters per second, because it is not valid for light winds. The plume model does not allow for diffusion in the direction of the wind, so the discontinuous changes in concentration at the upstream and downstream ends of the modeled plume are more abrupt than in reality. The puff model has the puff center leaving the source position when the gas liberation begins, but the total mass in the puff increases as the mass of gas liberated increases. Neither of these aspects of the model is wholly satisfactory, but no analytic models for short plumes or long puffs are currently available.

---

[5] Slade, D. H. (ed.). Meteorology and Atomic Energy 1968. U. S. Atomic Energy Commission, Oak Ridge, Tenn., July 1968. (NTIS TID-24190)

Implicit in the Gaussian models is the assumption that the wind velocity is not a function of time or position. For the plume model, the effects of surface roughness and the meandering of the plume with time may be approximated by adjustments to the dispersion coefficients. However, one value of the surface roughness must be taken for the entire area of interest. The meandering adjustment changes the time-average concentration but does not attempt to model the statistical fluctuations of the concentration within that averaging period. Buoyancy effects are not considered in either the plume or the puff model.

Because the Gaussian models were based on data gathered from dilute plumes and puffs, their use for very concentrated cases, as in the VM, is an extrapolation. When the puff model was used close to a very large spill of material which vaporizes quickly, the model originally gave concentrations which were higher than the density of the cargo vapor at ambient atmospheric temperature and pressure. The puff model has been modified to preclude this by allowing a region of pure cargo vapor surrounded by a region in which the concentration decreases in the Gaussian fashion. The pure cargo vapor concentration is at the proper density for ambient conditions. This modified distribution is used only when the regular puff model would give unrealistically high concentrations.

The air dispersion submodel is presently being used only for the case of cargo vapors in the air, even though this submodel is also applicable to cases in which the cargo material is suspended in very fine solid or liquid particles. Currently, loss mechanisms are not included, nor are reactions taken into account. The possibility of the formation of a fog by the cargo droplets or by the cooling of the air to form water droplets is not considered. The effects of precipitation upon the concentration are not considered, except insofar as the precipitation may affect the stability class.

The data inputs required for this submodel are: wind speed, stability class, spill location, pool diameter, and the rate of cargo vapor liberation. A flag may specify if the puff model is to be used regardless of the gas escape rate. This submodel is discussed in more detail in Chapter 3 and Appendix B.

4. Fire and Explosion

This group of submodels determines whether a flammable cargo will be ignited and then determines the physical characteristics of the resulting combustion (fire, explosion, or both). Four types of fire and explosion phenomena are modeled in this section of the VM; they are: (A) ignition, (B) explosion, (C) flash fire, and (D) pool burning. The modeling of the phenomena of fire and explosion proceeds in three temporal phases. First the decision of whether, when, and where ignition occurs is made by the internal computer logic based on user inputs, results computed by submodels, and the properties of the cargo. Subsequent to ignition, either an explosion or a flash fire is modeled, depending on the type of ignition source specified by the user, as explained below. Following either of these events, the burning of flammable liquid on the water surface, if any liquid remains, is modeled; currently, burning from a vessel venting flammable fuel is not modeled. In addition, the user may specify that ignition

occurs at the spill site so that only pool burning results. The treatment of (A) ignition, (B) explosion, and (C) flash fire is presented in greater detail in Chapter 4; a more complete evaluation of the acceptability of the assumptions used to develop these models is given there.

A. Ignition

This submodel determines whether ignition occurs, which ignition source originates the ignition, and at what time during the simulation the ignition takes place. All ignition sources are assumed to be located at the grid cell centers. This assumption is not realistic, especially in an urban area, but is an expendient measure used to avoid a detailed and costly specification of the boundaries of each grid cell. In some cases, this assumption will cause explosion and fire damage to be overestimated, since the size and travel of the flammable cloud will be greater for delayed ignition at the cell center than for ignition at a cell boundary. In other cases, however, ignition will not be simulated when, in fact, it would occur, because the concentration of the vapor at the cell center is below flammable limits, even though the concentration is within flammable limits elsewhere in the cell. The user predetermines whether a given ignition source will cause fire or explosion. This a priori determination of the nature of combustion may produce the simulation of an explosion when, in fact, an explosion is unlikely or even impossible. This expediency is justified by the lack of a general theory to predict the combustion behavior of unconfined flammable vapor clouds. In addition to lack of agreement about the conditions under which unconfined vapor clouds ignite, a technical determination of combustion behavior is further inhibited by the difficulty in specifying certain parameters known to influence combustion behavior. For example, an initiating detonation of sufficient strength may induce the detonation of a contiguous unconfined vapor cloud; however, the strength, time, and location of an initiating detonation that arises, say, from the seepage of the flammable vapor into a confined space (such as a building enclosing electrical equipment) are very difficult parameters to compute or even estimate. The user also specifies the strength of the ignition source. The classification of ignition sources according to potency is based on the NFPA classification of flammable liquids [6]. Flammable liquids are classified according to ease of ignition by flashpoint; the higher the flashpoint of a liquid the more difficult that liquid is to ignite. As discussed in more detail in Chapter 4, the use of the concept of flashpoint to grade ignition sources is a rather unconventional technique, adopted in the VM so that the user has the option of changing a simulation by only type of flammable substance spilled, yet obtaining combustion in one case and not in the other. Ignition sources are so designated that the NFPA class of liquids they can ignite is known; of course, all liquids more flammable than the designated class are also assumed to be ignited by that same ignition source.

This submodel uses basic physicochemical principles to determine the ignition event. There are three requirements for combustion: (1) fuel, (2) oxidizing agent, and (3) ignition source. The user will specify whether a given grid cell contains an ignition source. The fuel is provided

---

[6] Tyron, G. H. (ed.). Fire Protection Handbook, 13th ed. National Fire Protection Association, Boston, 1969.

by the dispersed flammable vapor, whereas the oxidizing agent is provided by the oxygen in the air. Since combustion will occur only over a certain range of fuel-air ratios, the decision that combustion occurs will be made only if the vapor concentration in a given cell is within the flammability limits for the substance under consideration and the given cell contains an ignition source of strength sufficient to ignite the spilled cargo. The user must use judgment in specifying an ignition source and its strength at a given location. Rural areas should have fewer ignition sources per unit area, whereas urban areas should have a greater concentration of ignition sources. Ignition sources specified for residential and recreational areas should be less potent than those specified for heavy industrial areas containing facilities, such as welding shops and smelters, that are very powerful sources of ignition.

The input data required for this submodel are:

- type (fire or explosion) of ignition source for each grid cell;
- potency class of each ignition source;
- flashpoint of the spilled substance;
- upper and lower flammability limits of the spilled substance;
- concentration of the air-dispersed cargo for the time and grid cell location under consideration.

B. Explosion

This submodel calculates the peak overpressure and the dynamic impulse generated by the explosion of a flammable cargo-air mixture. In addition to these variables required for damage assessment in Phase II, the explosive yield and TNT equivalent are also determined.

This submodel assumes the following.

- The exploding mass acts like a condensed phase explosive (high explosive) located on the water or land surface.
- The explosive yield is given by the product of the heat of combustion per unit mass an_ the total mass of fuel participating in the explosion.
- Only that portion of the fuel-air mixture with a concentration between the explosive limits can contribute to the explosive yield. For that part of the fuel-air mixture richer than stoichiometric, but leaner than the upper-explosive-limit concentration, only that fraction of fuel for which there is sufficient oxygen for complete burning contributes to the explosive yield.
- The well-known scaling laws for explosions are assumed to hold.

This model requires as input the time of ignition, the parametric values determining the concentration in space at the time of ignition, the heat of combustion of the fuel (cargo), the location of the explosion epicenter, and the atmospheric temperature and pressure.

C. Flash Fire

This submodel calculates the effective radiation intensity level and the effective radiation duration resulting from the flash fire. The flash fire is considered to be the rapid combustion without detonation of the fuel-air layer premixed within the flammable concentration limits. The heat generated essentially instantaneously by combustion is assumed to be lost from the combustion layer entirely by radiation; thus the radiation loss as a function of time may be calculated. In order to fit in with the computational procedure in Phase II, this time-varying radiation level is represented by a fixed radiation level (the effective radiation level) and an effective duration.

This submodel assumes the following.

- Only that portion of the fuel-air mixture within the flammable limits burns and then only to the extent permitted by the local oxygen concentration.
- The energy released by combustion is mixed uniformly throughout the combustion layer.
- The heated combustion layer loses energy entirely by radiation.
- The emissivity of the layer is taken to be unity.
- The effective duration is three times the time required to reach the temperature given by the average of peak temperature and ambient temperature.
- The radiation intensity is that level emitted by the layer when its temperature is the average of the peak temperature and ambient temperature.
- The radiation from the flash fire is allowed to affect only those portions of space inside the burning layer.

The input data required for this submodel include the time of ignition, the parametric values determining the spatial concentration at the time of ignition, the heat of combustion of the fuel (cargo), and the ambient temperature.

D. Pool Burning

This submodel calculates the duration and magnitude of thermal radiation emitted by a burning pool of flammable cargo; the radiation level is calculated for any desired point in space. This submodel is comprised of the following submodels:

(1) flame size;

(2) thermal radiation from flames;

(3) radiation view factor between an inclined flame and an arbitrarily oriented surface in space;

(4) burning time.

The pool burning submodel calls submodels (1), (2), and (4) above once for the entire grid structure; submodel (3) is called for each grid point. The burning time [submodel (4)] is the same for all grid cells. The flame size calculation (1) is used as input to the thermal radiation calculation (2) which in turn is used with the view factor calculation (3) to give the radiation intensity at the selected spatial location. In the following discussion, these four submodels, comprising the pool burning submodel, are described in more detail.

(1) Flame Size

This submodel calculates the height, diameter, and angle of inclination of the flame from a burning pool; the wind blowing across the pool surface causes the flame to be inclined with respect to the normal to the pool surface. The details of this submodel are given in the CHRIS documentation [2, Ch. 6].

The formulas used to calculate flame height, diameter, and inclination angle are empirical expressions obtained by curve-fitting experimental data. The major assumption for these models then is that relationships obtained under laboratory conditions may be extended to larger scale occurrences in the field. Although large-scale events will probably behave very much like small-scale laboratory experiments, provided all experimental conditions other than size are duplicated, the fact is that the conditions in the field are different from those in the laboratory. Perhaps the most significant difference is that in the laboratory an effort is made to keep wind velocity constant, whereas in the field the wind gusts, changing both speed and direction. At this time, the effect of these discrepancies on damage assessment is not known.

The data required for this submodel are:

- liquid burning rate
- pool diameter
- wind velocity

(2) Thermal Radiation From Flame

This submodel calculates the radiant heat flux incident on a receptor at some distance from a burning pool. A detailed discussion of this submodel is given in the CHRIS documentation [2, Ch. 7].

The flame from the burning pool is modeled as a cylindrical radiator of uniform temperature; this constitutes the major assumption of this submodel. The cylindrical radiator is allowed to be inclined with respect to the vertical. The atmospheric transmissivity and flame emissivity are assumed to be one, i.e. the atmosphere is not allowed to absorb radiant energy and the flame is treated as an ideal black body radiator. These assumptions about atmospheric transmissivity and flame emissivity are not correct; however the degree of error induced in the damage assessment by the use of these assumptions is unknown. The assumption that the flame is a cylindrical radiator of uniform temperature is more realistic and probably has a negligible effect on the estimation of damage.

The input data required by this submodel are:

- flame height, diameter, and inclination angle;
- location of the receptor with respect to the burning pool;
- the adiabatic flame temperature.

(3) Radiation View Factor Between an Inclined Flame and an Arbitrarily Oriented Surface in Space

This submodel calculates on a normalized basis, the view factor between a cylindrical, inclined flame and a receptor; the receptor is assumed to be oriented with respect to the flame so that it receives the maximum possible radiation flux. As discussed in many standard texts on heat transfer, for example Eckert and Drake [7], the view factor is a purely geometrical property of the spatial arrangement of the flame and receptor. Thus no physical assumptions, except those basic to radiant heat transfer, are required by this model.

The input data required by this submodel are the same as for (2) above, namely:

- flame height, diameter, and inclination angle;
- the location of the receptor.

(4) Burning Time

This submodel calculates the length of time the pool will continue to burn after it is ignited.

It is assumed that the pool is extinguished when all of the fuel remaining in the pool at the time of ignition is burned up. It is further assumed that fuel leaves the pool not by evaporation or water mixing, but only by burning. The burning time is calculated by the following:

$$t_b = \frac{V_p}{A_p r_b}$$

where

t_b = pool burning time (s);

V_p = volume of fuel remaining in the pool at the time of ignition (m^3);

A_p = area of the pool at the time of ignition (m^2);

r_b = burning rate of the fuel (m/s).

---

[7] Eckert, E. R. G., and R. M. Drake. Heat and Mass Transfer. McGraw-Hill, New York, 1959.

The assumption, implicit in the above, that spreading stops after ignition, is subject to dispute. However, at the present time, no analysis is extant which treats the spread of a burning pool of spilled cargo. Certainly spreading rate will be reduced after ignition, because mass is being reduced by combustion.

The data required for this submodel are the volume of cargo remaining in the pool at the time of ignition, the area of the pool at ignition time, and the burning rate of the cargo.

CHAPTER 3

AIR DISPERSION

In order to affect the vulnerable resources, the spilled material must be transported away from the spill site and dispersed in the air and water in the vicinity of the spill. This dispersion is the result of a number of natural phenomena. The most important of these phenomena, however, are the convection of the material with existing currents in the air and water and the diffusion of the material from a small volume of high concentration to form a larger volume of low concentration. These mechaniams, over which man has very little control, seriously increase the hazard from the spill and hinder the cleanup efforts.

Although there is no intention to undervalue the serious consequences of the cargo's dispersion in the water, the effects of the hazardous material in the water are neither immediate nor violent in most cases. There may be sufficient time to shut down the water intakes to water supply systems, close shellfish beds to harvesting, or warn the populace against eating fish caught from a certain section of the river. But the effects of the dispersion of the cargo in the air may be of immediate significance. A fire or explosion may devastate part of a city or town, perhaps killing many people, or toxic vapors could cause numerous casualties in a matter of minutes or hours. Thus the air dispersion submodel is of particular importance, because air dispersion is much faster than water dispersion, combustion can take place in air but not in water, and people can be injured very rapidly by inhalation of toxic gases or by asphyxia.

The air dispersion submodel calculates the location and concentration of the cargo in the air from the time that is escapes until the time that there is no further interest in its dispersion. At this time, the dispersion of the cargo in the air is treated only if the cargo is in the gas phase. The air dispersion of particulates and aerosols is not currently treated, although the same Gaussian models may be applied, as is or modified to include loss mechanisms and reactions. The escape of the gas may be by direct venting from a tank or by means of evaporation or boiling from a pool of spilled liquid cargo. The case of a liquid cargo which is denser than water and has a boiling point lower than the ambient water temperature is also considered. In this case, the gas is liberated at the water surface. Mechanisms which might be investigated for future inclusion include loss by chemical reactions, scavenging by aerosols, rainout (loss of the vapor by going into solution in the raindrops), and impingement upon vegetation.

Basis of the Submodel - Gaussian Distribution

Almost every model of atmospheric dispersion employs one of two approaches, or, occasionally, some combination of the two. These approaches are the Gaussian distribution and the finite-difference model. These approaches are quite different in use and in their basic assumptions. The Gaussian models are semi-empirical and are dependent upon the determination of certain parameters from experiments. The finite-difference models operate from basic laws of fluid dynamics. CHRIS and HACS have chosen to utilize Gaussian models, and the VM is currently using Gaussian models.

The finite-difference models operate by the repetitious application of basic equations at many points in space for a number of time steps. There are no analytic means by which the concentration at the 30th time step can be calculated - the program must proceed through the first 29 time steps first. Other drawbacks of the finite-difference models are that they require a regular grid and that special precautions must be taken at the edges of the grid to ensure that the presence of the edges does not affect the results. The accuracy of the results is primarily dependent upon the fineness of the mesh.

Once the grid network is set up and the data storage and manipulation problems are solved, the finite-difference model is very flexible insofar as physical phenomena are concerned. The statements of the basic equations occupy only a small part of the program, and features such as buoyancy and the change of wind velocity with time or position may be easily incorporated. The case in which the wind speed is zero or very close to zero causes no special problems. Removal and generation terms may also be added to the equations in a fairly straightforward manner. But the finite-difference models occupy more storage space and take much more computer time than the Gaussian models.

CHRIS and HACS use Gaussian air dispersion models. Although Raj and Kalelkar [2] discuss both the plume (continuous source) model and the puff (instantaneous source) model, only the puff model was programmed for HACS at the time HACS was received. Because of the use of Gaussian models by CHRIS and HACS and because of attempts to economize on both computer storage and running time, Gaussian models are used in the VM as well.

Since the Gaussian models are largely empirical, one must always be careful that they are not used to simulate conditions which are widely different from those under which they are validated. Specifically, the diffusion coefficients have been obtained for plumes and puffs which are diffuse and for which the tracer gas or smoke has a density close to the density of air. For the case of a vapor which has a density quite different from that of air, or for the case in which the vapor is very concentrated, say, more than several percent, the Gaussian models would have to be applied with caution. Since the model does not operate directly from basic physical principles, the modification of the model to account for effects such as buoyancy is not straightforward and may require experimental validation.

In addition to speed of operation, the Gaussian models have two advantages in being analytic expressions. First, the time step can be chosen on the basis of the times at which an output is desired, and it is not necessary to evaluate the expression at intermediate times to obtain a concentration at a desired time. Second, the concentration can be calculated for any arbitrary location and only for that location. The finite-difference model requires that the concentration at all grid points be calculated at each time step. The concentration in a Gaussian model may be found for any point at any time without calculating that for other points and times. And the Gaussian models do not require any regular grid system. This feature is quite valuable in the VM where to facilitate model testing the present grid system is based on census tracts, which are irregular in density and distribution.

Description of the Submodels

The basic mathematics for both the puff and the plume is contained in Chapter 5 of [2]. The concentration at some point (x, y, z) at time t is given for the puff model by

$$C_I(x,y,z,t) = \frac{2M}{(2\pi)^{3/2}\sigma_x\sigma_y\sigma_z} \exp\left[-\frac{(x-Ut)^2}{2\sigma_x^2} - \frac{y^2}{2\sigma_y^2} - \frac{z^2}{2\sigma_z^2}\right] \quad (3\text{-}1)$$

and for the plume model by

$$C_c(x,y,z,t) = \frac{2Q}{(2\pi)U\sigma_y\sigma_z} \exp\left[-\frac{y^2}{2\sigma_y^2} - \frac{z^2}{2\sigma_z^2}\right] \quad (3\text{-}2)$$

The following nomenclature is used:

σ_x, σ_y, σ_z = diffusion coefficients (m)
C_I = concentration for an instantaneous release, i.e., puff (kg/m^3)
C_c = concentration for a continuous release, i.e., plume (kg/m^3)
M = mass of vapor liberated (kg)
U = wind speed (m/s)
Q = rate of vapor liberation (kg/s)
x, y, z = Cartesian coordinates with the origin at the source of the air dispersion material. The wind is taken to blow toward the positive x-direction. The vertical coordinate is z. The cross-wind coordinate is y.

Note that, as explained in the following discussion, the σ's in equation (3-1), which depend on the distance travelled by the center of the puff, are different from the σ's in equation (3-2), which depend on the distance (x) downwind from the source.

For the venting of the cargo in the gaseous state, the coordinate system has the origin at the spill location. For the release of vapor by evaporation from a pool of liquid cargo on the water surface, the coordinate system has the origin five pool diameters upwind of the pool center. The positive x axis is oriented in the direction toward which the wind is blowing. The z = 0 plane is the water surface, and for venting gas it is assumed that the vent is at the water surface. Unless specifically directed otherwise, the VM evaluates the concentration at z = 1 m. At present, the rate of vapor liberation, Q, is the average release rate. It is a simple modification to incorporate a variable release rate by evaluating Q at time t_e, where $t_e = t - x/U$; t_e is the time at which the vapor observed at the point, (x, y, z), at the time, t, was released. This has not been done because of the difficulty of calculating the amount of vapor which burns or explodes when the release rate is variable. Modification of this part of the model to allow for variable release rates would be valuable, if priorities in further work permit.

Diffusion Coefficients

The diffusion coefficients in (3-1) and (3-2) are parameters which have been determined by experiments. They are strong functions of the stability of the atmosphere - the amount of turbulence present and the variation of the temperature with height. Different experimenters have classified the stability of the atmosphere in different manners, so that direct comparison of one parameterization of the diffusion coefficients with another is not always possible. For the plume model, the set of coefficients derived by Pasquill [8], [9] has found wide acceptance. Figures 3-1 and 3-2 show these curves. The figures have been taken from Chapter 3 of Meteorology and Atomic Energy [5], and the reader is referred to this chapter for a discussion of atmospheric stability. These curves have been numerically approximated in HACS subroutine JHHDC. The values of the diffusion coefficients used for the puff model have been taken from Chapter 4 of Meteorology and Atmomic Energy [5] and are shown in Table 3-1. There has been much less work on puffs than there has been on plumes, so the coefficients for the puff model are not as widely used as the plume coefficients.

A summary of the stability classes is shown in Table 3-2. These are the classes used in the parameterization of the dispersion coefficients for the plume model. The parameterization for the puff coefficients is only for three classes of stability. The program is set up to allow for six stability classes in case the plume model is used, but, if the puff model is used, designation of classes A, B, or C will result in the unstable parameterization being used, classes D and E will use the neutral figures, and class F refers to the very stable curve.

---

[8] Pasquill, F. The estimation of the dispersion of windborne material. Meteorology Mag. 90:33-49, 1961.

[9] Pasquill, F. Atmospheric Diffusion. Van Nostrand, London, 1962.

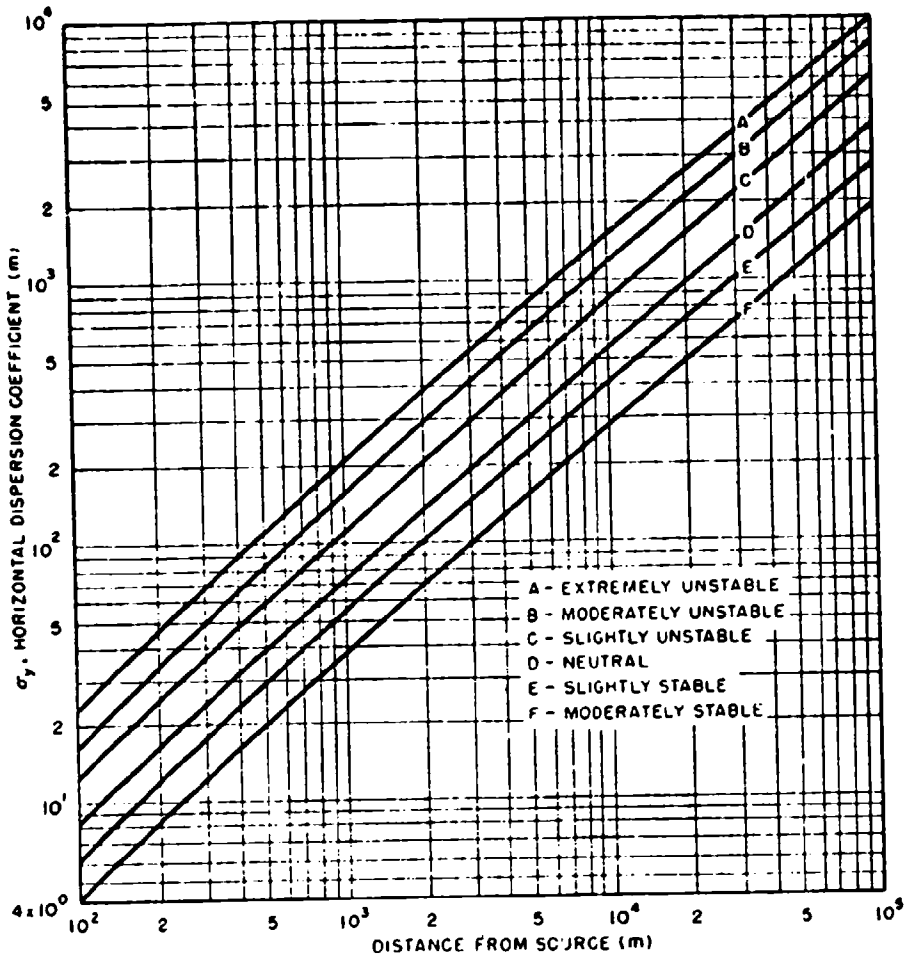

FIGURE 3-1

HORIZONTAL DISPERSION COEFFICIENT, σ_y, VS. DOWNWIND DISTANCE FROM SOURCE FOR PASQUILL'S TURBULENCE TYPES USED FOR THE PLUME MODEL

(From page 102 of [5])

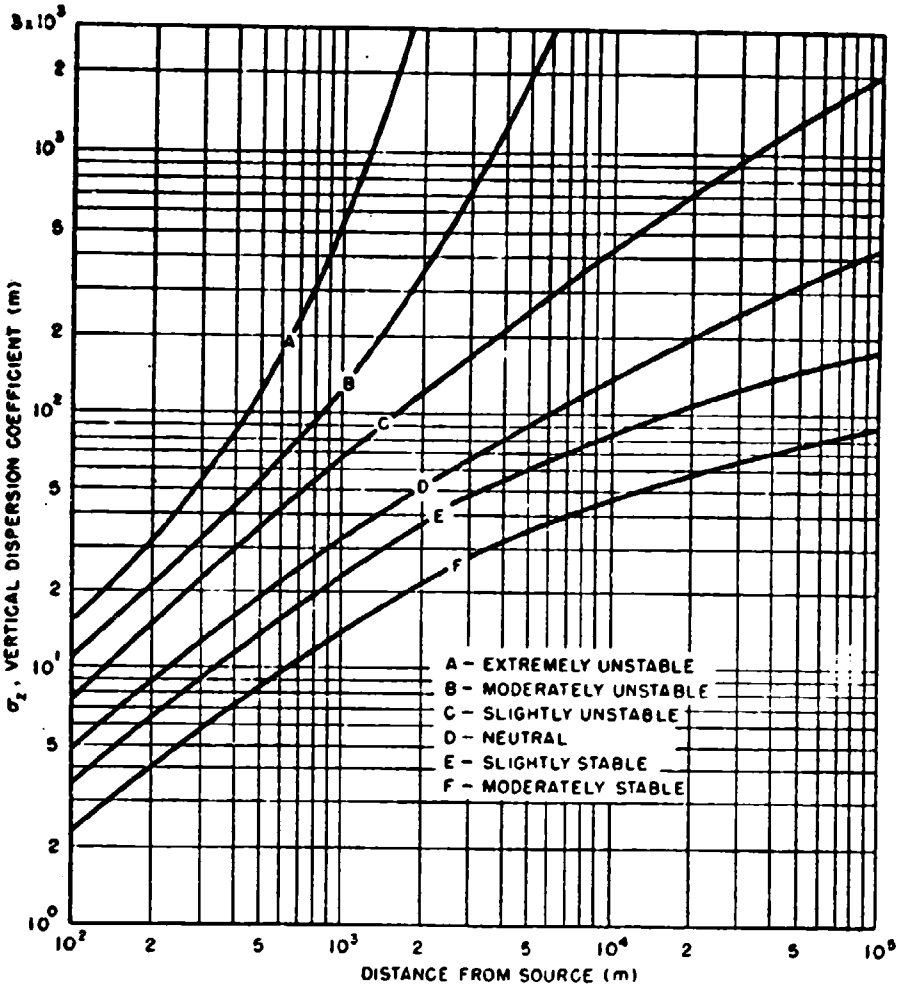

FIGURE 3-2

VERTICAL DISPERSION COEFFICIENT, σ_z, VS. DOWNWIND DISTANCE FROM SOURCE FOR PASQUILL'S TURBULENCE TYPES USED FOR THE PLUME MODEL

(From page 103 of [5])

Parameter	Conditions	100 m	4000 m	Approximate power function
σ_y (m)	Unstable	10.0	300	$0.14(x)^{0.92}$
	Neutral	4.0	120	$0.06(x)^{0.92}$
	Very stable	1.3	35.0	$0.02(x)^{0.89}$
σ_z (m)	Unstable	15.0	220	$0.53(x)^{0.73}$
	Neutral	3.8	50.0	$0.15(x)^{0.70}$
	Very stable	0.75	7.0	$0.05(x)^{0.61}$

TABLE 3-1

SUGGESTED ESTIMATES FOR σ_y, σ_z (From page 175 of [5])

The values for σ given in the columns headed 100 m and 4000 m are observed values. The approximate power function given in the last column relates the value of σ to distance travelled by the puff center (x) for the cases indicated; these functions are obtained by curve fitting the observed data.

A— Extremely unstable conditions
B— Moderately unstable conditions
C— Slightly unstable conditions
D— Neutral conditions*
E— Slightly stable conditions
F— Moderately stable conditions

Surface wind speed, m/sec	Daytime insolation			Nighttime conditions	
	Strong	Moderate	Slight	Thin overcast or ≥ 4/8 cloudiness†	≤ 3/8 cloudiness
<2	A	A-B	B		
2	A-B	B	C	E	F
4	B	B-C	C	D	E
6	C	C-D	D	D	D
>6	C	D	D	D	D

*Applicable to heavy overcast, day or night.
†The degree of cloudiness is defined as that fraction of the sky above the local apparent horizon which is covered by clouds.

TABLE 3-2

RELATION OF TURBULENCE TYPES TO WEATHER CONDITIONS

(From page 101 of [5])

In Figures 3-1 and 3-2, we note that the abscissa extends from 100 m to 100 km, but this does not mean that the curves for the diffusion parameters are valid over that entire distance. These curves were derived from data obtained from about 100 m downwind of the source to several kilometers. In a few cases, data were obtained between 5 and 20 kilometers. Although the figures do not imply anything about use of these curves for distances shorter than 100 m, it might be inferred from Figures 3-1 and 3-2 that these curves are to be used for distances up to 100 km. This inference is not correct. For example, for stability class A at 20 km, σ_z = 3000 m. This length is greater than the height of the inversion base on all days, except the hottest sunny summer days. Thus, even for distances as short as 20 km, the Gaussian model must be used with care for certain stability classes.

On days for which unstable atmospheric conditions prevail, at distances sufficiently far from the source the value of σ_z will predict mixing above the inversion base, which in fact will not occur. For stable regimes, the detailed layer structure sometimes has to be taken into account. Fortunately, the VM is usually not concerned with distances greater than 10 km, and the curves for the dispersion coefficients are trustworthy for all stability classes up to 10 km. For short distances, the curves may safely be extrapolated to 50 m, but their use for distances of less than 50 m is questionable. Certainly their extrapolation to 10 m is unwarranted.

The same caveats on use apply to the puff dispersion coefficients in Table 3-1. The values of σ_y and σ_z are given for 100 m and 4000 m, because these are the limits of the range over which the given power function approximation is strictly accurate. The VM uses these power functions for the range from 50 m to 10 km, when necessary.

Choice Between Puff Model or Plume Model

As stated above the plume model is strictly applicable only to continuous releases, whereas the puff model is strictly applicable only to instantaneous releases. The spills to be simulated in the VM will generally release material into the air over some finite time; i.e., the release time will be neither infinite, as required for the plume, nor infinitesimal, as required for the puff. Since no model was readily available for use in the VM to treat the realistic case of a finite release time, it was decided that the puff model would be used for those cases in which the release time is short, whereas the plume model would be used for those cases in which the release time is long. To accomplish this, however, a precise, quantitative definition of "short" and "long" release times must be made.

For "long" release times, the prevailing wind will disseminate the airborne material in a cone-shaped plume: subsequent to the end of the release, the entire plume will be translated in the windward direction with minimal change in length measured along the wind axis. For a plume, the main cause for dissemination of material in the direction of the wind is advection by the wind. For "short" release times the wind does not have sufficient time to disseminate the airborne material, so a puff, expanding as it travels, is formed. Although the wind transports the puff as a whole in the windward direction, the wind does not spread the material to any great extent. However, turbulent diffusion will cause the puff to spread in the windward direction. Evidently then the key to choosing

between the puff and the plume is whether advection or diffusion is the predominant mechanism for spreading the material in the windward direction.

The plume model will be preferable to the puff model if the diffusion in the x direction (the windward direction) is small with respect to the length of the plume. The length of the plume will be Ut_e, where U is the wind speed and t_e is the time it takes for complete evaporation of the gas. Thus, when the last bit of gas is released at time t_e, the first bit, released at t = 0, will be at $x = Ut_e$. The scale of the diffusion in the x direction is given by σ_x, where the puff data are used to evaluate σ_x as a function of distance. Evaluating σ_x at $Ut_e/2$, we compare σ_x and Ut_e. If Ut_e is greater than $5\sigma_x$, then the plume is long with respect to the diffusion in the x direction which will occur at each end, and the plume model is preferable. If Ut_e is smaller than $2\sigma_x$, then the diffusion in the x direction should not be ignored and the puff model should be used. If Ut_e is between $2\sigma_x$ and $5\sigma_x$, then neither model is entirely appropriate, and either may be used at the discretion of the person using the VM. Since the plume model equation is undefined for zero wind speed and is inaccurate for low wind speeds, the use of the plume model is not recommended when U is less than 2 m/s.

Choice of Time Step

The choice of an appropriate duration for the time step is also related to the wind transport time H/U. H is the scale of the region of interest and might range from 0.5 km for a small spill to 5 km or more for a large spill. In order to get some detail from the VM, the time step should be a fraction of H/U, say,(H/U)/10 to (H/U)/5. Further, no matter what values H and U have, the time step chosen should not be so large that the puff may completely pass by a grid cell during the time step. For the puff distribution to be evaluated at a point within $0.5\sigma_x$ of the peak value, the time step, Δt, must be less than σ_x/U, since it will take σ_x/U to move the puff a distance σ_x. As σ_x will vary with the time that the puff has been traveling from the source, a typical value of σ_x for the chosen stability class should be selected. For wind speed of about 5 m/s or less, time steps between 0.5 and 2 min are generally appropriate.

As presently implemented, the plume model uses the average escape rate for the duration of the vapor release, so the concentration at any point will be constant for a time equal to the release time. Thus the selection of a time step, Δt, is not quite as crucial as it is in the puff model, where a concentration close to the maximum concentration may be missed entirely if Δt is too long. If the plume model is appropriate and the time step is less than (H/U)/5, then the release of the gas should extend over several Δt or longer. The choice of time step and the decision of whether or not the plume model is appropriate are discussed in greater detail in Appendix B3.

Modification of the Puff Model

The dispersion coefficients for the puff model were derived for dilute concentrations; therefore, when the puff model is applied close to a large spill, it may calculate a concentration of the cargo gas which is greater than the density of pure cargo gas at ambient atmospheric temperature and pressure. This is unrealistic, of course, and the Gaussian puff dispersion model has been modified to preclude this event. If the

regular puff equation would give a concentration at the puff center which exceeds the density of pure gas at ambient conditions, a modified distribution is used. This distribution has a hemisphere of pure cargo gas centered about the puff center, and from the surface of the hemisphere the concentration decreases in Gaussian fashion, with dispersion coefficients appropriate to the distance the puff has traveled from the spill. The radius of the hemisphere is determined by the necessity of conserving mass. As the puff is translated downwind, the radius of the hemisphere of pure vapor will shrink to zero, whereupon we have the regular Gaussian puff distribution. The details of this modification are contained in Appendix B1.

Effects of Surface Roughness

The dispersion coefficients have been derived, for the most part, from experiments conducted over flat grasslands. The effects of buildings in urban and suburban areas are to enhance the mixing processes, mostly by the greater mechanical turbulence induced but partially from the different thermal characteristics of manmade surfaces such as cement and asphalt. The plume model may be adjusted to account for these surface effects, but at present there is no way to adjust for a change in surface roughness. Thus one class of surface roughness which typifies the entire region over which the plume travels is required.

In a paper to be published in the Journal of the Air Pollution Control Association (kindly made available to us in advance by the author), N. E. Bowne suggests modifications of the standard diffusion parameters which will more accurately depict the spread of a plume over urban and suburban areas. Selected values of σ_y are presented in Table 3-3 to show that the dispersion over built-up terrain may be several times greater than it is over rural areas. These corrections for surface effects have not yet been implemented in the computer simulation.

Meandering of the Plume

The assumption that the wind is a constant with respect to time, location, and height does not mean that the random or statistical fluctuation of the wind direction about a mean value has to be omitted entirely. This is also known as meandering of the plume, and changes in the wind direction which have time periods shorter than the observation or averaging period may be treated in a statistical manner. Thus synoptic changes which typically have time scales on the order of one to several hours are excluded. But fluctuations with periods of seconds and minutes are amenable to statistical treatments. These short-period variations are of interest because they will spread the plume from the spill over a wider area than will the theoretical, but never observed, constant wind. The amount of cross-plume dispersion (the spread in the direction perpendicular to the mean wind direction) in the Gaussian model is controlled by the value of the parameter σ_y. The longer the measuring period, the larger σ_y should be to account for increased spreading of the effluents by random changes in the wind direction during this period. The values for σ_y and σ_z given in Slade [5] and used by Raj and Kalelkar [2] are the values originally published by Pasquill from measurements having a duration of roughly 10 minutes. For this reason, the concentrations calculated using these diffusion coefficients will likewise be the average concentration for a 10-minute duration. For time averages other than 10 minutes, the value of the diffusion coefficient, σ_y, changes because of ever present random fluctuations in wind direction.

		Dispersion Coefficients, m			
		Distance Downwind, km			
	Stability Category	0.1	1	10	100
Sigma y, rural	A	30	200	1500	11000
	B	22	160	1200	8000
	C	14	110	800	6000
	D	9	70	550	4100
	E	7	55	400	3000
	F	5	32	270	2000
Sigma y, urban	A	58	310	1900	11000
	B	45	230	1500	8000
	C	38	190	1100	6000
	D	32	150	780	4000
	E	26	110	500	2500
	F	21	75	390	1900
Sigma z, rural	A	14	400	3000	3000
	B	10	100	1400	2300
	C	7	63	500	1600
	D	5	31	130	500
	E	3	20	78	200
	F	2	14	48	100
Sigma z, suburban	A	15	400	2900	3000
	B	12	100	1300	2400
	C	10	62	490	1600
	D	8	39	250	800
	E	7	26	140	440
	F	6	20	80	180
Sigma z, urban	A	26	700	3000	3000
	B	20	280	2500	2500
	C	17	150	1500	1700
	D	15	90	700	1200
	E	13	45	200	500
	F	12	31	100	220

TABLE 3-3 (from N. E. Bowne)

SELECTED VALUES OF σ_y

Dispersion coefficients for three types of regions showing the influence of surface roughness and other gross measures of micrometeorological factors

For very short durations (seconds), the wind direction will change very little, so the average concentration for this period will be a maximum. For periods on the order of an hour or two, the fluctuating wind direction will move the plume about, and the average concentration over an hour or more will be much lower. The corrections to σ_y to account for the averaging time have been given by Turner [10], who summarized the work of Stewart, Gale, and Crooks [11] and Cramer [12], and found that concentrations decrease with sampling times of from 3 seconds to 30 minutes according to a one-fifth power law function ($C \propto t^{-.2}$). Nonhebel [13] reported correction coefficients for σ_y for periods of as long as 24 hours.

The $t^{-.2}$ power correction factor is plotted in Figure 3-3. Extrapolation of this curve for periods of less than 10 seconds and longer than 1 hour must be used cautiously, as the power law was designed to fit the data in the range from about 1 minute to about thirty minutes. The correction factor from Figure 3-3 may be used to adjust the plume concentration on axis by multiplying the concentration calculated for 10 minutes by the correction factor. For concentrations off the axis, the value of σ_y for 10 minutes must be divided by the correction factor, and the plume concentration calculated as usual with the adjusted σ_y.

Although the correction of one calculated concentration is no problem, the situation is more complicated for a number of sequential calculations. Let us compare 10 sequential calculations for a period of 1 minute with a single calculation for 10 minutes. Figure 3-3 shows that the value on axis calculated for a 1-minute averaging period will be 1.6 times the value for the 10-minute averaging period. If the wind direction does not change, the average for the ten 1-minute periods will be the same as for any individual 1-minute period and will be 1.6 times the average for one 10-minute period. This is incorrect, of course, and is due to the fact that the wind did not vary in direction from one 1-minute period to the next as it would in the physical world. For sequential applications of the Gaussian plume equation, then, if the correction factor is to be applied to σ_y to account for the length of the time step, then the wind direction must also be changed in a random manner about an average direction. Modification of the air dispersion submodel to account for the duration of the averaging period and the statistical fluctuations of the wind direction was felt to be inappropriate at this stage in the development of the VM, since departures from accurate simulation of the physical world in other ways were considered more serious.

---

[10] Turner, D. Workbook of Atmospheric Dispersion Estimates. Environmental Protection Agency, Washington, D.C., Revised 1970. Publication No. AP-26.

[11] Stewart, N. C., H. J. Gale, and R. N. Crooks. The atmospheric diffusion of gases discharged from the chimney of the Harwell Reactor BEPO. Int. J. Air. Pollution 1:87-102, 1958.

[12] Cramer, H. E. Engineering estimates of atmospheric dispersal capacity. Amer. Ind. Hyg. Assoc. J. 20:183-189, 1959.

[13] Nonhebel, G. Recommendations on heights for new industrial chimneys. J. Inst. Fuel 33:479-513, 1960.

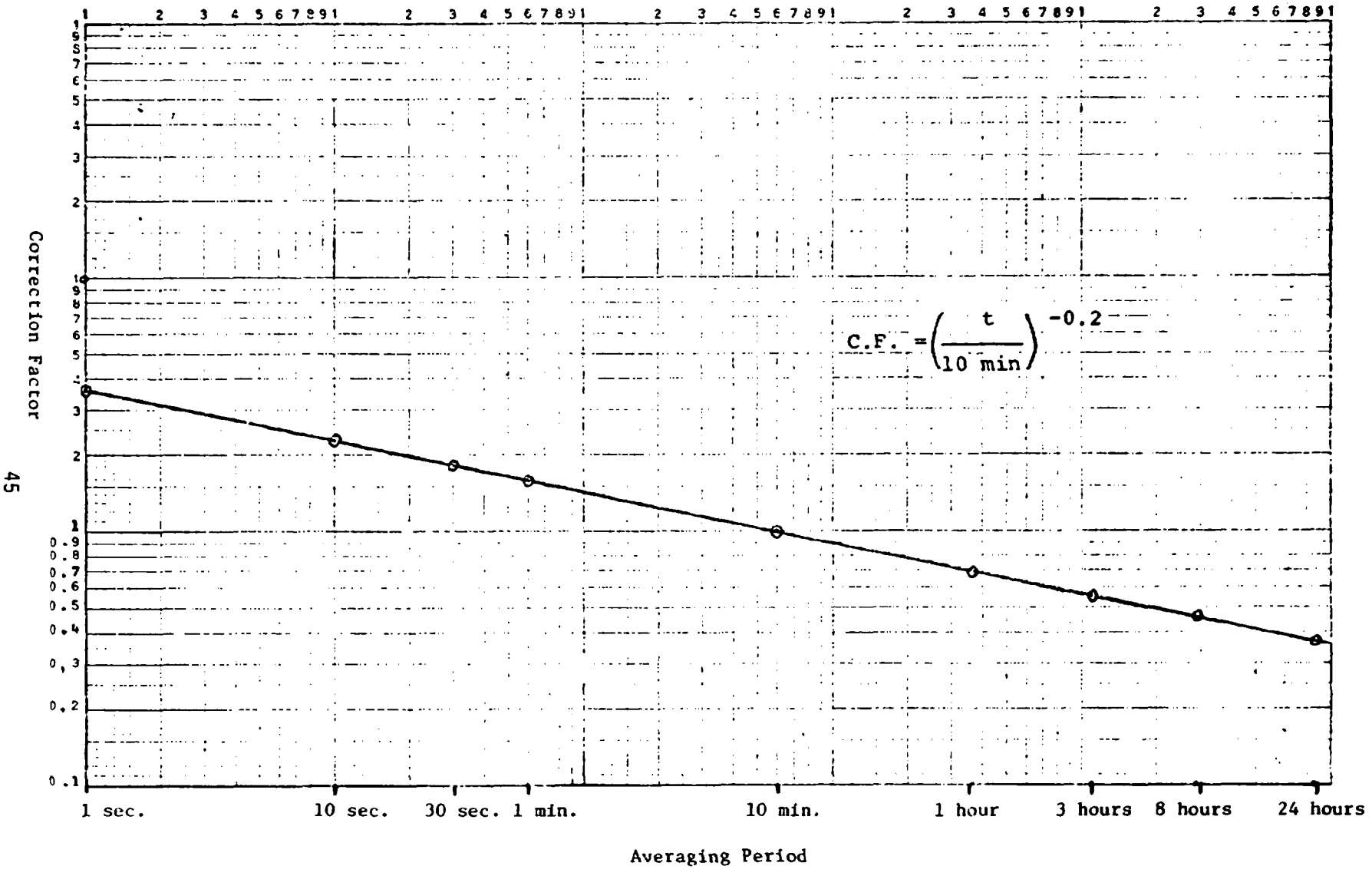

FIGURE 3-3

CORRECTION FACTOR FOR MEANDER OF WIND

Peak Concentration vs. Average Concentration

This meandering of the plume with time will result in an average concentration which is lower than the maximum values obtained instantaneously during the averaging period. In the assessment of toxic effects, the nonlinearity of the concentration-response curve is not so great that this is a serious matter. For flammable vapor clouds, on the other hand, the variation of the instantaneous concentration from the average may mean that vapor cloud would ignite, even though its average concentration was outside the range of flammable concentrations. If the development of the VM continues, it is urged that consideration be given to allowing ignition to occur when the average concentration is outside the flammable concentration range but close to the limiting concentration. Once an appropriate peak-to-mean ratio for the dispersion process is decided upon, the mathematics for determining the new ignition range and the modification of the computer program are straightforward.

Buoyancy

Fluid cargoes which have boiling points below 5°C at atmospheric pressure are usually transported in liquid form, with either pressure or refrigeration or both being employed to keep the cargo in the liquid state. If such a cargo is spilled, the evolved vapor and the air immediately surrounding it will be near the boiling point of the cargo whether or not the cargo was refrigerated. This is because the vapor is given off at the boiling point temperature and brings the surrounding air close to that temperature by bulk mixing.

The low temperature of the recently evolved vapor may have a considerable effect upon the density of the cargo gas, and, if this is the case, the dispersion of the vapor will be significantly different from that of a neutrally buoyant gas. The Gaussian dispersion models, of course, were derived for the neutrally buoyant case, so the present air dispersion submodel will not be particularly accurate when the vapor cloud is very cold. The actual cloud will occupy a greater area close to the ground or water surface and will not extend as high as the calculated cloud. Negative buoyancy will also be a significant factor for very dense gases, such as radon and sulfur dioxide, even if transported and vented as gases at ambient temperature.

Positive buoyancy may be a significant factor in the air dispersion of certain materials vented as gases that are lighter than air, such as hydrogen and methane. Some materials carried as cryogenic liquids, such as LNG, may be negatively buoyant soon after release because of cooling, but upon heating by contact and admixture with the atmospher they may become positively buoyant. The transition from negative to positive buoyancy poses formidable problems of analysis.

The means to incorporate the effects of buoyancy into the Gaussian plume and puff models now used in the VM are neither straightforward nor clearly available. Although the Gaussian models are based on a theoretical solution to a diffusion equation, the values for the dispersion coefficients are obtained from experimental measurements. Thus there is no simple, easily justified adjustment that can be made to the model without some experimental verification. The adoption of unvalidated schemes for use in the VM was deemed inappropriate at this time.

One possible approach to the consideration of buoyancy effects is that correction factors for the neutrally buoyant σ_y and σ_z could be derived from comparison of data from actual spills with concentrations calculated for neutral buoyancy. These correction factors could be parameterized functions of time and stability class to take into account the change in buoyancy with time caused by admixture, warming, or both. Another possibility is the use of one of the empirical air dispersion models developed specifically for spills of this kind [4], [14], [15], although a design guide for the VM has been to avoid the use of chemically specific models. Whatever correction method might be used, it should certainly have the feature that as the cargo becomes close to neutral buoyancy by dilution with air or by warming, then the description of the dispersion should reduce to one of the standard conventional forms of the Gaussian model.

---

[14] Fay, J. A. Unusual fire hazard of LNG tanker spills. Combustion Sci. Technol. 1:47, 1973.

[15] Feldbauer, G. W., et al. Spills of LNG on Water - Vaporization and Downwind Drift of Combustible Mixtures. Esso Research & Engineering Company, March 1973. Report No. EE61E-72 (Released by the American Petroleum Institute, Re 6Z32).

CHAPTER 4

FIRE AND EXPLOSION SUBMODELS

The purpose of the fire and explosion submodels is to calculate those physical quantities required by the Phase II damage assessment models to estimate the consequences of explosion, fire, or both. This set of submodels determines the type of event (fire or explosion), where it occurs, and when it occurs and what physical consequences of import to the VM occur.

The processes of fire and explosion will in general occur in two phases. First, an extended vapor-air cloud will rapidly burn or explode. Following either of these forms of rapid combustion, relatively slow burning from the surface of the spill will take place. The rapid combustion occurs because the fuel and oxidant are premixed over a relatively large region of space. The slower burning from the surface of the spill is a typical diffusion flame in which combustion occurs in a narrow reaction zone into which both fuel and oxidant diffuse. Because the physical processes, and hence the damage mechanisms for personnel and material, are quite different in the cases of rapid and slow combustion, different models are required for each of the three processes involved: namely, explosion, flash fire, and burning from the surface of the spill.

The relationship of the four fire and explosion submodels used in the VM to model the various processes involved and their sequence are displayed in the flow chart shown in Figure 4-1. First the decision of whether or not ignition occurs is made; of course, if there is no ignition, no further processing of the fire and explosion submodels is performed. If there is ignition, a user option determines whether fire or explosion is to be modeled. In either event, a check is made, after the rapid combustion event is simulated, to determine whether any fuel remains in the pool of spilled material; if any fuel remains, then burning from the pool is modeled. In the following are presented details of the simulation of each of the four events modeled.

The Ignition Submodel

A primary decision to be made in the fire and explosion submodels is whether combustion (either conflagration or detonation) occurs. Three items are required for combustion to occur: (1) fuel, (2) oxidizing agent, and (3) an ignition source. The user will specify whether a given grid cell contains an ignition source. The fuel is provided by the dispersed flammable vapor, whereas the oxidizing agent is provided by the oxygen in the air. Since combustion will occur only over a certain range of fuel-air ratios, the decision in the VM that combustion does occur is made only if the vapor concentration in a given cell is within the flammability range for the substance under consideration and if the given cell contains an ignition source.

A refinement of the model is to specify whether the ignition source causes an explosion or just a fire (provided, of course, that the vapor-air mixture is in the ignitable range). There are several reasons for choosing the occurrence of fire or explosion on an a priori basis. These reasons all deter the formation of a deterministic model for this decision. One reason is that unconfined vapor-air mixtures are normally not considered to be

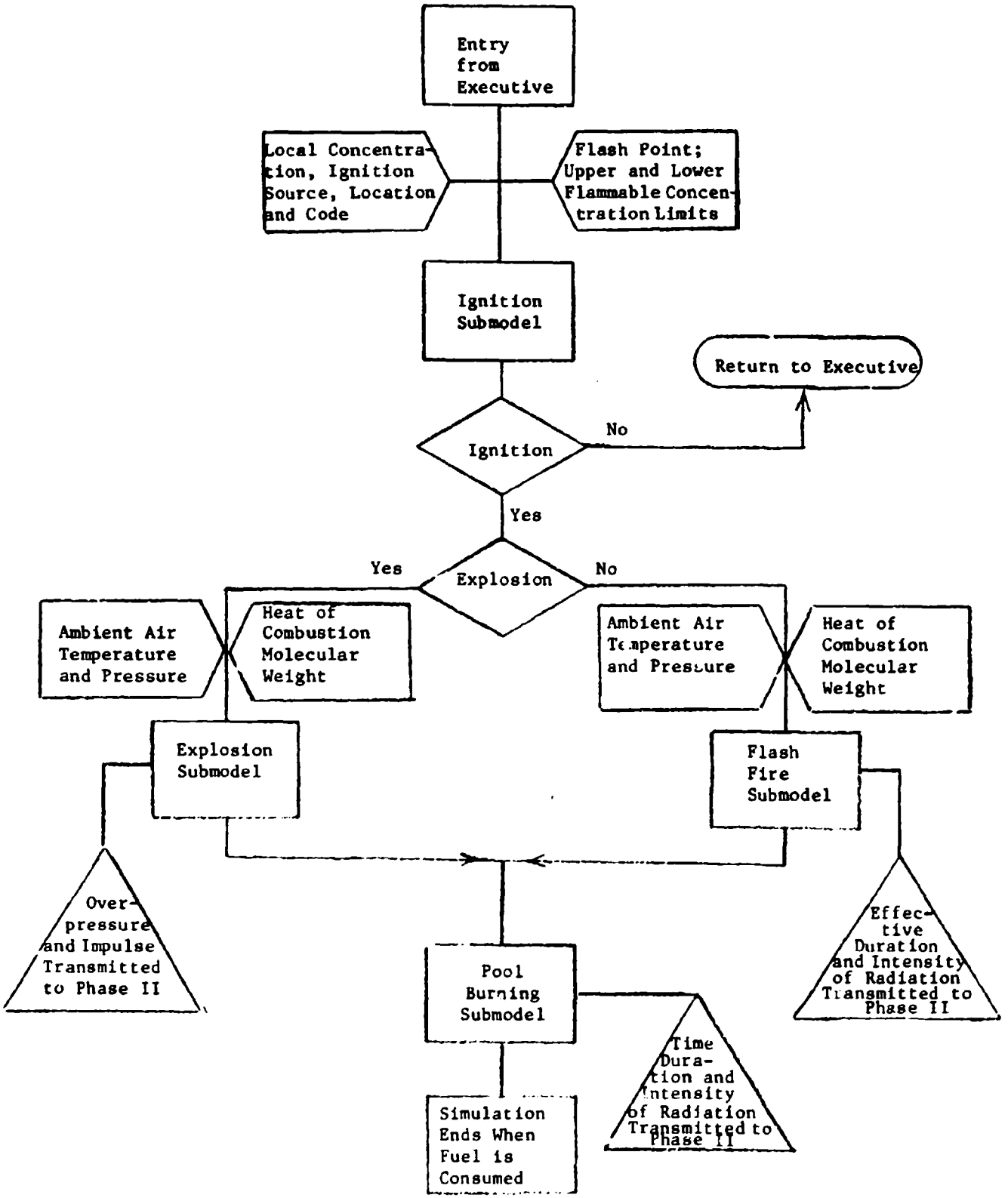

FIGURE 4-1

FLOW CHART OF FIRE AND EXPLOSION SUBMODELS

explosive. However, such unconfined vapor-air mixtures can and do explode if ignition is initiated by a detonation [16] [17]. In the context of accidental spills, such initiating detonations could originate from (1) the detonation of high explosive (say, as a result of a ship collision) or (2) the detonation of a vapor-air mixture which has seeped into an enclosed space (this source is much more likely to occur). In either case, the size and location of the initiating detonation are quite unpredictable, because of the large number of unspecified (and probably unspecifiable) variables that contribute to these properties of the explosion. Furthermore, the basic research to determine the detonatability of unconfined vapor-air mixtures as a function of the strength of the initiating detonation is not complete and in some cases is the subject of current or planned studies. Thus, even if the properties of the initiating explosion were known quantitatively, there is no method currently available that could be used to predict whether the vapor-air plume would explode.

Another refinement of the model is the gradations permitted in ignition source strength. The user is allowed to specify the ignition potential of a given source so that, for example, a single specification of a set of ignition sources will result in ignition for a highly flammable substance but will not simulate an ignition for a less flammable substance. The gradations used in the VM for ignition sources are based on the NFPA classification system [6, p. 4-8ff.] for flammable substances. The NFPA classification system is based on the concept of "flashpoint." A substance with low flashpoint is very flammable, whereas a substance with a high flashpoint is more difficult to ignite. In the VM, an ignition source is designated as belonging to a given classification based on the flashpoint of substances it is capable of igniting. Strong sources will ignite most combustible substances, those of both low and high flammability. Weaker sources are only able to ignite the most flammable materials. The gradation of ignition sources is discussed in more detail in Appendix C1. This rather unconventional application of the concept of flashpoint is primarily an attempt to allow the user to specify ignition sources of different strengths; thus two simulations having the same input data, except for the type of substance spilled, will yield ignition in one case but not in the other. As explained in Appendix C1, a complete treatment of ignition sources would require very complex models and massive quantities of input data to support them.

Amount of Material in Rapid Combustion

For both the explosion and flash fire submodels it is necessary to determine the amount of fuel that burns in the rapid combustion process. Because the flammable clouds have a spatial and temporal variation in concentration of fuel, calculation of the mass that burns is not an especially straightforward procedure. As discussed in Appendix C2, it seems

---

[16] Strehlow, R. A. Uncombined vapor-cloud explosions - an overview. In Proceedings of the International Symposium on Combustion, 1972.

[17] Brown, J. A. A Study of the Growing Danger of Detonation in Unconfined Gas Cloud Explosions. John Brown Associates, Inc., Berkeley Heights, N.J., December 1973.

appropriate to allow only that portion of the fuel-air mixture that has a concentration between flammable limits to contribute to the energy yield of the rapid burning phase of combustion. The fuel-air mixture that contributes to the energy yield may be divided into two parts: (1) the mixture with a concentration varying from the lower explosive limit to stoichiometric and (2) the mixture with a concentration varying from stoichiometric to the upper explosive limit. The portion (1) leaner than stoichiometric burns completely; the portion (2) richer than stoichiometric burns incompletely from lack of sufficient oxygen content. The amount (mass) of fuel that burns in the leaner portion is given by the volume integral of the concentration over that portion of the fuel-air cloud. The mass of fuel that burns in the richer portion is given by the volume integral of concentration over that space, with a multiplicative weighting factor inside the integral to account for the absence of sufficient oxygen to support complete combustion. Thus,

$$m_e = \int_{V_3} C(x,y,z,t)\,d\tau + \int_{V_4} F(C)C(x,y,z,t)\,d\tau \qquad (4\text{-}1)$$

where

m_e = mass of fuel burning

$C(x,y,z,t)$ = concentration of the flammable material (z is the vertical coordinate)

$F(C)$ = a weighting function, dependent on concentration, giving the fraction of fuel present that can burn

V_3 = the region in the half space $z \geq 0$ enclosed by the surfaces: $C(x,y,z,t) = K_L$ and $C(x,y,z,t) = K_S$ (where K_L is the lower explosive limit concentration K_S is the stoichiometric concentration)

V_4 = the region in the half space $z \geq 0$ enclosed by the surfaces: $C(x,y,z,t) = K_S$ and $C(x,y,z,t) = K_U$ (where K_U is the upper explosive limit concentration)

$d\tau$ = the element of volume

This formulation, including an evaluation of the weighting function, $F(C)$, is discussed in more detail in Appendix C2. The analytical forms for the participating mass, m_e, that are obtained by performing the integration indicated in equation (4-1) for specific choices of concentration distribution, $C(x,y,z,t)$, are given in Appendix C2 for a simple puff model and are given in Appendixes B1 and B2 for the modified puff and plume distributions of concentration, respectively.

One further detail in these calculations is the time at which the ignition occurs. Rather than use the preset computation interval, it seems more realistic to assume that an ignition occurs at that moment the concentration contour of the lower flammable limit first coincides with the coordinates of the ignition source. To calculate the time of this occurrence, one sets $C(x,y,z,t) = K_L$ and then solves for t. For the simple puff concentration distribution (see Chapter 3), this procedure yields

$$t_i = \frac{x_i - \sqrt{2}\sigma_x \left\{ \ln\left[\frac{2m}{(2\pi)^{3/2}\sigma_x\sigma_y\sigma_z K_L}\right] - \frac{y_i^2}{2\sigma_y^2} \right\}^{1/2}}{U} \qquad (4\text{-}2a)$$

where

t_i = time of ignition
x_i, y_i = grid coordinates of the ignition source

$\sigma_x, \sigma_y, \sigma_z$ = the standard deviations of the Gaussian concentration profile in the noted direction
U = the wind speed
m = the mass of gas in the puff

and for the plume concentration distribution the time of ignition is given by

$$t_i = \frac{x_i}{U} \qquad (4\text{-}2b)$$

In solving equation (4-2a), it must be borne in mind that σ_x, σ_y, and σ_z are functions of time; consequently, an iterative procedure is required to find t_i. In practice the iteration is begun at time t_1, the time at which the concentration at some grid location with an ignition source first exceeds (or is exactly equal to) the lower flammable limit. The distance traveled by the puff at the time t_1 is given by

$$x_1 = Ut_1$$

This value of x_1 is substituted into the approximate power functions given in Table 3-1 to yield values for σ_y and σ_z (σ_x is assumed equal to σ_y). Substituting these values of σ and x_1 into equation (4-2a) gives a new value for time, t_2. The value of t_2 will, in general, be smaller than t_1, because the concentration at x_1, at t_1, will rarely exactly equal the lower flammable limit. The value, t_2, is used to find another set of σ's and the whole process is repeated until the differences between successive values of t_i are small compared to the value. For example, if

$$\frac{t_i - t_{i-1}}{t_i} < 0.001$$

then the iteration would be stopped, and t_i would be taken to be the time of explosion. Once t_i is determined, all of the σ's are known.

The Explosion Submodel

A fundamental quantity needed to characterize the explosion of a vapor-air plume is the energy yield. Kinney [18] points out that a good approximation to the energy yield of an explosion is the change in Helmholtz free energy caused by the chemical reaction producing the explosion. However, many authors [17] [19] analyzing the potential yield of a spill of combustible material calculate on the basis of enthalpy change produced by the chemical reaction. This apparent conflict was resolved by determining that, for vapor-air explosions, the difference between the change in the Helmholtz free energy and the change in enthalpy is negligible. The details of this analysis are presented in Appendix C3.

Therefore, the energy yield of a vapor-air mixture exploding is taken to be

$$W = (-\Delta H)\frac{m_e}{M} \qquad (4\text{-}3)$$

where

W = explosion yield (kcal)
ΔH = change in enthalpy with combustion (heat of combustion kcal/kg-mole)
m_e = mass of the exploding fuel (kg)
M = molecular weight of the fuel

Heats of combustion are determined by measuring the amount of heat liberated when a fuel reacts completely and forms definite reaction products. In an explosion (or flash fire), the chemical products formed by the reaction are not necessarily the same as those formed in the laboratory experiments because the elevated temperature causes the reaction products to dissociate. Nevertheless, the degree of accuracy inherent in equation (4-3) is consistent with the accuracy of the models used elsewhere in this program. It should be noted that the heat of combustion, $-\Delta H$, is for final products that include water vapor; most handbooks give $-\Delta H$ for final products that include liquid water. These values for $-\Delta H$ must be corrected for the heat of vaporization of water. In addition, it should be noted that heats of combustion are measured for the substance in the normal state at 25°C. If the reaction of interest is for a substance normally a liquid at 25°C, then, unless specified otherwise, the handbook value must be corrected to account for the heat of vaporization of the fuel. These corrections are detailed in Appendix C4.

---

[18] Kinney, G. F. Explosive Shocks in Air, p. 11. The MacMillan Co., New York, 1962.

[19] Strehlow, R. A. Equivalent Explosive Yield of the Explosion in the Alton and Southern Gateway Yard, East St. Louis, Illinois, January 22, 1972. Engineering Experiment Station, College of Engineering, University of Illinois, Urbana, June 1973. Report No. AAE TR 73-3, UILU-ENG-73 05-05.

Once the explosive yield is determined from equations (4-1), (4-2) and (4-3), the physical parameters of the explosion germane to damage assessment can be calculated from the scaling laws stated by Kinney [20]. The explosion scaling laws are based on the principle of geometrical similarity plus certain basic theoretical considerations and experimental observations. An explosion generates a peak overpressure in the surrounding medium which is dependent on the explosive energy per unit mass in the medium. For most explosions, some sort of spherical symmetry holds, so the volume of the medium affected by the explosion is proportional to d^3, where d is the distance traveled by the wave front. The mass of the medium affected is then proportional to ρd^3, where ρ is the density of the medium. Thus, in two geometrically similar explosions, the peak overpressure observed at some point will be the same when $W/\rho d^3$ is the same in both cases, where W is the energy yield of the explosion. Experiments have been performed on reference explosions in reference media (atmospheres) that correlate peak overpressure and other explosion parameters with distance from the site of the explosion. The observations in nonreference explosions can be determined by combining these tabulated results with the scaling laws. Further dimensional analysis will give scaling laws for quantities other than peak overpressure. These scaling laws are summarized by the following equations:

$$d_s = \frac{d_a (P/P_O)^{1/3}}{(W'/W_O)^{1/3} (T/T_O)^{1/3}} \qquad (4\text{-}4)$$

$$t_a = \frac{t_s (W'/W_O)^{1/3}}{(P/P_O)^{1/3} (T/T_O)^{1/6}} \qquad (4\text{-}5)$$

$$I_a = \frac{I_s (W'/W_O)^{1/3} (P/P_O)^{2/3}}{(T/T_O)^{1/6}} \qquad (4\text{-}6)$$

where

d_s = scaled distance from explosion center (m)

d_a = actual distance from explosion center (m)

P,T = pressure and temperature of the atmosphere in the actual case (bar, °K)

P_O, T_O = pressure and temperature of the atmosphere in the case of the reference explosion (P_O = 1 bar, T_O = 288.15°K)

---

[20] Kinney, G. F. Engineering Elements of Explosions. Naval Weapons Center, China Lake, Calif., November 1968. Report No. NWC TP-4654.

W' = effective energy yield of the actual explosion

W_o = energy yield of the reference explosion (1 kg of TNT yields 1.12×10^6 calories; thus $W_o = 1.12 \times 10^6$ calories)

t_a = actual time (s)

t_s = scaled time (s)

I_a = actual impulse ($N\text{-}S/m^2$)

I_s = scaled impulse ($N\text{-}S/m^2$)

These laws are simplified considerably if the actual explosion is assumed to occur in the same atmosphere as the reference explosion. Since ratios of absolute values for atmospheric pressure and temperature are raised to fractional powers, these factors are close to unity even when the reference and actual atmospheres are not identical. By assuming essentially identical atmospheres, one obtains

$$d_s = \frac{d_a}{\left(\frac{W'}{W_o}\right)^{1/3}} \tag{4-7}$$

$$t_a = t_s \left(\frac{W'}{W_o}\right)^{1/3} \tag{4-8}$$

$$I_a = I_s \left(\frac{W'}{W_o}\right)^{1/3} \tag{4-9}$$

To use these scaling laws, reference is made to Table 4-1 on the following page. The scaled distance is computed by equation (4-4) or (4-7) using the computed value of the energy yield. From the scaled distance the tables give overpressure and Mach number directly. The tables also give the scaled time and impulse from which the actual time and impulse may be computed by the use of equations (4-5) or (4-8) and (4-6) or (4-9). Thus, use of the scaling laws and the tabulated reference values will give, for any distance from the explosion center, the overpressure and impulse. These parameters are necessary to evaluate damage in Phase II.

In equations (4-4) through (4-9), the quantity W', the effective yield, is used. The data for the reference explosion tabulated in Table 4-1 are for a spherically symmetric explosion. For an explosion with a center on a rigid surface, the symmetry is hemispherical, i.e., the rigid surface reflects completely all explosive energy impinging

BASIS ONE KILOGRAM

SCALED DISTANCE (METERS)	SHOCK FRONT MACH NUMBER	SHOCK FRONT TRAVEL TIME (MS)	SHOCK FRONT AVERAGE TRAVEL SPEED (M/MS)	SIDE-ON PEAK OVERPRESSURE (BARS)	SIDE-ON IMPULSE (BAR-MS)	SIDE-ON PRESSURE DURATION (MS)	SIDE-ON DECAY PARAMETER	REFLECTED PEAK OVERPRESSURE RATIO	REFLECTED IMPULSE (BAR-MS)	REFLECTED VELOCITY DURATION (MS)
.94	3.405	.438	2.147	12.36	1.309	.634		72.	6.45	.724
.952	3.369	.448	2.124	12.04	1.292	.640	4.72	69.8	6.38	.725
.96	3.339	.455	2.110	11.84	1.282	.644	4.7	68.31	6.33	.723
.98	3.274	.473	2.074	11.34	1.257	.655	4.7	64.73	6.20	.726
1.00	3.210	.491	2.039	10.85	1.236	.666	4.6	61.30	6.06	.732
1.02	3.147	.509	2.004	10.39	1.217	.677	4.5	58.02	5.91	.742
1.04	3.086	.528	1.971	9.94	1.200	.687	4.4	54.88	5.75	.755
1.06	3.021	.547	1.938	9.48	1.206	.706	4.3	51.70	5.51	.797
1.08	2.957	.567	1.905	9.04	1.214	.725	4.1	48.63	5.28	.844
1.10	2.895	.587	1.874	8.61	1.224	.745	3.9	45.71	5.05	.893
1.12	2.835	.608	1.841	8.21	1.216	.758	3.8	43.04	4.92	.927
1.14	2.778	.630	1.810	7.84	1.205	.770	3.7	40.53	4.81	.957
1.16	2.723	.652	1.779	7.48	1.192	.781	3.6	38.18	4.73	.984
1.18	2.670	.674	1.751	7.15	1.176	.790	3.5	35.97	4.66	1.009
1.20	2.619	.697	1.723	6.83	1.158	.798	3.4	33.92	4.61	1.030
1.22	2.571	.718	1.698	6.54	1.140	.804	3.3	32.05	4.57	1.050
1.24	2.526	.739	1.678	6.28	1.127	.810	3.1	30.36	4.52	1.070
1.26	2.483	.760	1.658	6.02	1.114	.815	3.0	28.77	4.46	1.090
1.28	2.441	.781	1.638	5.78	1.102	.820	2.9	27.27	4.41	1.109
1.30	2.400	.803	1.619	5.55	1.090	.825	2.8	25.86	4.36	1.128
1.32	2.361	.825	1.600	5.34	1.078	.830	2.7	24.54	4.32	1.146
1.34	2.324	.848	1.581	5.13	1.066	.835	2.6	23.30	4.27	1.165
1.36	2.288	.870	1.563	4.94	1.055	.841	2.5	22.15	4.23	1.182
1.38	2.254	.894	1.544	4.76	1.044	.846	2.4	21.09	4.19	1.200
1.40	2.222	.917	1.526	4.59	1.033	.851	2.3	20.10	4.15	1.217
1.42	2.192	.941	1.509	4.44	1.022	.856	2.2	19.20	4.11	1.234
1.44	2.162	.966	1.490	4.29	1.012	.862	2.2	18.35	4.07	1.249
1.46	2.132	.995	1.469	4.14	1.003	.872	2.1	17.49	4.02	1.259
1.48	2.102	1.024	1.446	3.99	.994	.883	2.0	16.67	3.97	1.271

TABLE 4-1

SAMPLE OF TABULATED DATA FOR A REFERENCE EXPLOSION OF 1 kg of TNT [20]

upon it. To account for the additional energy imparted to the upper half plane by the reflective surface, the yield is taken to be twice the yield expected from a spherically symmetric explosion of the same size. Therefore, we take

$$W' = 2W \qquad (4\text{-}10)$$

where W is the yield computed according to equation (4-3).

The design of the explosion model is based on scaling laws strictly applicable to condensed phase explosions. However, explosions of fuel-air clouds, called diffuse explosions by one source [21], have significant differences from condensed phase explosions. The nature of exploding fuel-air clouds has been the subject of considerable recent research [22], [23], [24], [25]. Unfortunately, scientific research into the basic phenomena of diffuse explosions has not yet proceeded to the point where the results of the research can be incorporated into the VM, that is, no suitable theoretical or semiempirical models for diffuse explosions are extant. One problem area not yet treated satisfactorily is the propagation of combustion waves through regions of nonuniform fuel concentration; some very recent research [26] has begun to address this problem. Another problem to be addressed is "shocking up." Classical combustion wave theory (Chapman-Jouget theory) [27] predicts that the combustion wave in a fuel-air mixture will be either subsonic (deflagrative) or supersonic (detonative). From classical theory, explosions result only when a detonative combustion wave propagates; de-

---

[21] Kirk, P. L. Fire Investigation. John Wiley & Sons, Inc., New York, 1969.

[22] Hawkins, S. J., and J. A. Hicks. A New Explosives Technique for Synthesizing a Wide Range of Pressure Waveforms in Air. Part 1: Approximate Theory of Air Blast from Extended Explosive Charges. Ministry of Technology, Explosives Research and Development Establishment, Waltham Abbey, Essex, Oct. 2, 1968. Report No. ERDE 9/R/68.

[23] Woolfolk, R. W., and C. M. Ablow. Dependence of the blast wave from an explosion on the energy release rate. In Proceedings of the Fifteenth International Symposium on Combustion, August 1974.

[24] Strehlow, R. A., L. D. Savage, and G. M. Vance. On the measurement of energy release rates in vapor cloud explosions. Combustion Sci. Technol. 6:307-312, 1973.

[25] Strehlow, R. A., and A. A. Adamczyk. On the Nature of Non-Ideal Blast Waves. Engineering Experiment Station, College of Engineering, University of Illinois, Urbana, April 1974. Report No. AFOSR-TR-0834.

[26] Karim, G. A., and P. Tsang. Flame propagation through atmospheres involving concentration gradients formed by mass transfer phenomena. Presented at the ASME-CSME Fluids Engineering Conference, Montreal, 13-15 May 1974.

[27] Lewis, B., and G. van Elbe. Combustion, Flames and Explosions of Gases. Academic Press, Inc., New York, 1951.

tonative combustion yields the shock waves which are so destructive. Deflagrative combustion waves, on the other hand, produce a "whoosh" not a "bang." However, it appears that, if the initial extent of space experiencing deflagrative combustion is large enough, the subsonic pressure waves propagating away from the combustion zone may "shock up" and develop into damage-generating, finite amplitude blast waves.

Other factors not considered by this explosion model include Mach stem formation [18] and confined explosions. Although treatment of explosions resulting from the seepage of flammable vapor into a confined space is not currently implemented in the VM, the damage potential from such explosions is large as demonstrated in Appendix C5.

The Flash Fire Submodel

The major damage mechanism of the flash burning of the vapor cloud is the heat generated by the combustion. This heat may cause ignition of combustible materials within or near the burning cloud. This heat may also cause burn damage to living organisms within the affected area.

The flash burning occurs at a very rapid rate. Following the combustion, the hot gases remaining lose heat by radiation, conduction, and admixture of cooler gas. The cooling of the combustion products also occurs at a relatively rapid rate.

Damage to materiel and personnel from the flash fire is dependent on the amount of heat transferred and the nature of the heat transfer to the vulnerable receptors. The parameters affecting damage, and to some extent the damage mechanisms themselves, are roughly the same for both living and nonliving receptors. For combustible materials, the significant damage criterion is whether or not ignition has occurred. In general, the noncombustible materials will be considered undamaged by the flash fire; the level and duration of heating are expected to be low enough so that damage to noncombustibles, such as buckling of steel beams or calcination of bricks, is not expected to occur. The ignition of combustible materials is, however, expected to be a significant damage mechanism for the flash fire. The ignitability of a combustible item depends upon a plethora of physical parameters.

However, as explained in Appendix D, the only parameters used in the VM to determine ignitability are (1) radiation intensity and (2) duration of the radiation. Unfortunately, the fire hazard presented by the flash fire is quite different from the controlled experiments through which ignition and burn criteria are obtained. In the controlled experiments, the radiation intensity was maintained at a constant level; in the flash fire, the temperature of the reaction products, and therefore the radiation intensity therefrom, decreases rapidly with time subsequent to the ignition of the vapor cloud. Since ignition data for this type of radiation-time variation are not available (nor are they likely to be), the approach taken here is to use the data available for a constant radiation level. To use the available data, the variation in the radiation with time that actually occurs during the flash fire must be parameterized by a single radiation level and an effective duration time for that radiation level.

Since it has been determined that the significant parameters are the intensity and duration of radiation from the hot combustion products resulting from the flash fire, the time history of thermal radiation from the hot gases should be considered in detail before the precise forms of the parametric intensity level and time duration are chosen. Following the flash fire of a puff of flammable gac an ellipsoidal shell of hot gas remains. As mentioned previously, this layer (shell) of gas loses heat by radiative, conductive, and convective heat transfer processes.

By far the most important heat loss mechanism in this situation is radiation. Consider a prismatic volume of gas losing heat by radiation through one end surface as shown in Figure 4-2. The heat loss from the volume of gas by radiation through that surface, A_r, can be expressed by

$$q = A_r \sigma [\varepsilon_g T_g^4 - \varepsilon_a T_a^4] \qquad (4\text{-}11)$$

where

q = heat loss by radiation (J/S)

A_r = area through which the radiative heat loss occurs (m^2)

T_g, T_a = temperatures of the radiating gas and the environment to which the hot gas radiates, respectively ($^\circ K$)

$\varepsilon_g, \varepsilon_a$ = respective emissivities oi the gas and environment

σ = Stefan-Boltzmann constant* = 5.67×10^{-8} J/($^\circ K^4$-m^2-s)

Radiation from a volume of gas depends to a large extent upon the presence in that gas volume of gas molecules capable of absorbing and emitting infrared radiation. For the combustion products in which we are interested, the significant molecules are CO_2 and H_2O. The emissivity of a gas layer containing such molecules depends upon (1) the layer thickness, (2) the partial pressure of the thermally active species, and (3) the temperature of the gas. Figure 4-3 shows the emissivity of water vapor as a function of temperature and the product of partial pressure and layer thickness. Not shown is the fact that, for water vapor, emissivity is also a function of partial pressure (as well as the product of partial pressure and layer thickness). For CO_2, the behavior of emissivity is similar to that shown in Figure 4-3 for water vapor. When both CO_2 and H_2O are present, the total emissivity is not just the sum of the separate emissivities for each species, but a slightly more complicated computation must be performed to arrive at the total emissivity. Regardless of these complicating factors, it should

*The authors recognize the dual use of σ for both Stefan-Boltzmann constant and air dispersion coefficient; however, the use of σ in each discipline is so universal, that a change of symbology for this report might cause more confusion than it would prevent.

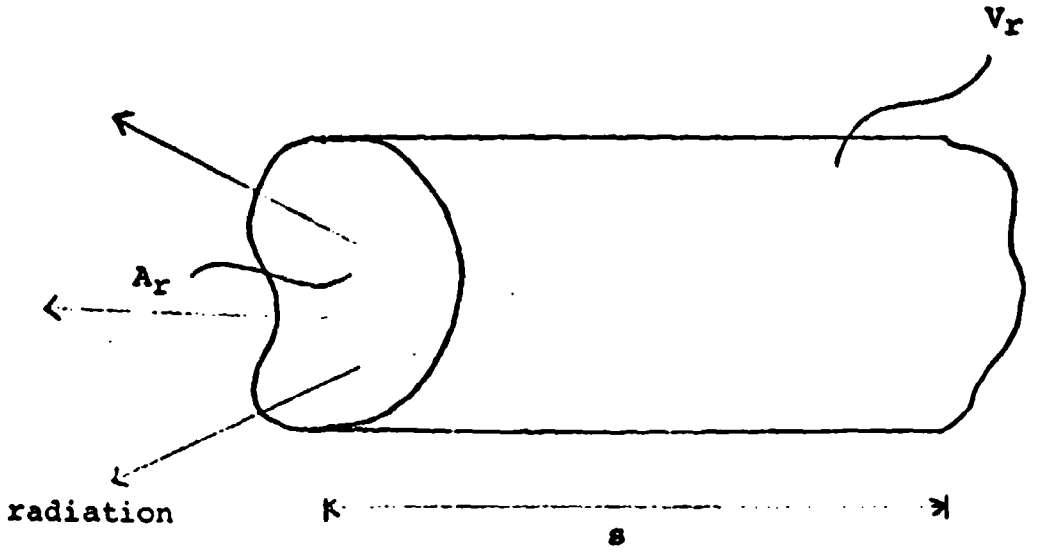

FIGURE 4-2

THERMAL RADIATION FROM A PRISMATIC VOLUME OF GAS

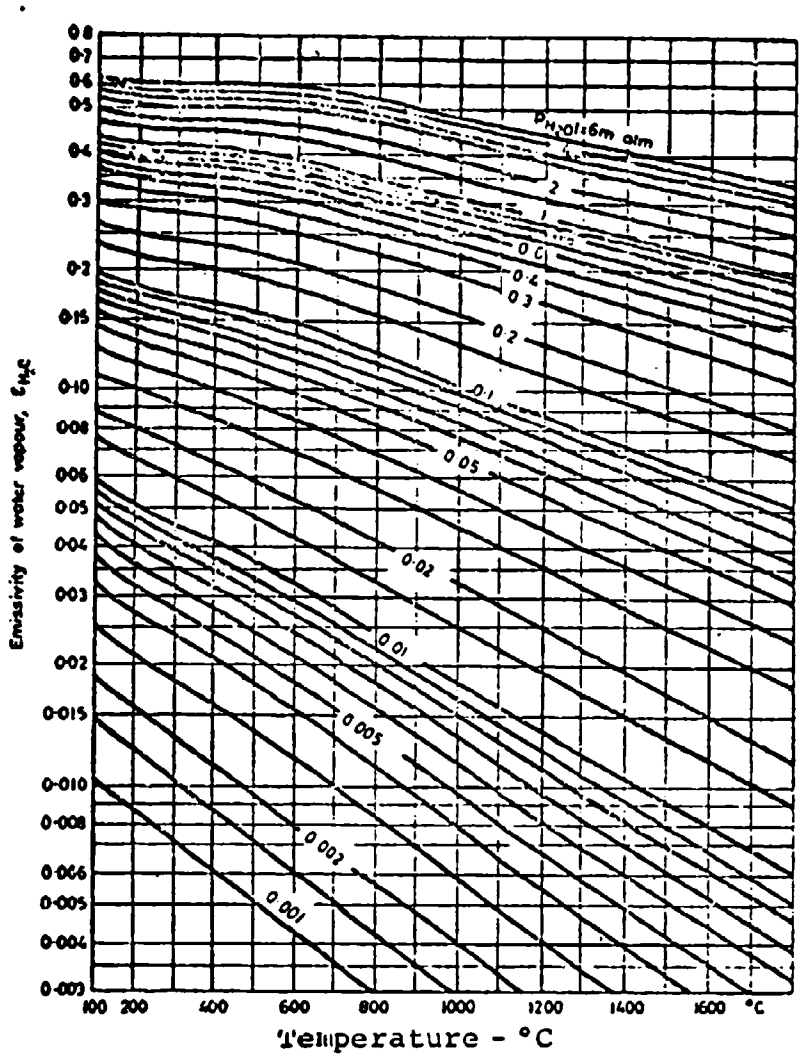

FIGURE 4-3

EMISSIVITY OF WATER VAPOR

Shown as a function of
temperature with optical thickness
(the partial pressure of H_2O times the
physical thickness) as a parameter [28]

---

[28] Kutateladze, S. S., and V. M. Borishanskii. A Concise Encyclopedia of Heat Transfer (translated by J. B. Arthur). Pergamon Press, New York, 1966.

be pointed out that, for the combustion of flammable vapors, the partial pressures of either CO_2 or H_2O are liable to be in the neighborhood of 0.1 atmospheres. On the other hand, the thickness of the ellipsoidal shells under consideration is liable to be tens of meters if not indeed hundreds of meters. Consequently, the emissivities that result will (1) be rather high values of the order of 0.5 and (2) not change very much with either temperature or layer thickness. The layer thickness to which the hot gas is radiating is essentially infinite, since the atmosphere is many hundreds of meters thick.

Although radiation is the primary mechanism by which the hot gas layer loses heat to the surroundings, other heat transfer mechanisms are occurring simultaneously. Rather than considering these processes separately, the additional heat loss can be approximated by raising the emissivity of the hot gas layer. Therefore, because of the large thicknesses of both the emitting and absorbing gas layers and because additional methods of heat transfer are to be ignored, we take as a suitable approximation that the emissivities of the hot gas and the absorbing atmosphere are both equal to one. Therefore, equation (4-11) becomes

$$q = A_r \sigma [T_g^4 - T_a^4] \tag{4-12}$$

Now the heat loss from the layer of hot gas causes the temperature of the layer to change according to the relation

$$q = -C_p \rho V_r \frac{dT_g}{dt} \tag{4-13}$$

where

C_p = specific heat at constant pressure $(J/K_g - {}^oK)$

ρ = density of the layer of hot, radiating gas (K_g/M^3)

V_r = volume of the radiating gas layer (M^3)

Although the layer of hot gas is comprised of combustion products, unburnt fuel, and air, it will nearly always be mostly air; therefore, in the computer program at this time, the density of the gas layer is set equal to that of the ambient air.

Equating the heat flows in equations (4-12) and (4-13) and solving the resulting nonlinear differential equation for temperature as a function of time gives

$$at + c = \frac{1}{2T_a^3} \left[\arctan\left(\frac{T_g}{T_a}\right) - \frac{1}{2} \ln\left(\frac{T_g - T_a}{T_g + T_a}\right)\right] \tag{4-14}$$

where

$$c = \frac{1}{2T_a^3}\left[\arctan\left(\frac{T_i}{T_a}\right) - \frac{1}{2}\ln\left(\frac{T_i - T_a}{T_i + T_a}\right)\right] \qquad (4\text{-}15)$$

and

$$a = \frac{A_r \sigma}{C_p \rho V_r} \qquad (4\text{-}16)$$

and

T_i = the initial temperature of the gas layer immediately after combustion

Equation (4-14) indicates that the temperature of the gas in the heated layer declines very rapidly at first from the initial temperature, T_i, and then the temperature declines at a diminishingly smaller rate; i.e., $T_g \to T_a$ only as $t \to \infty$. Since the time at which the gas temperature reaches the ambient temperature is not finite, let us, in a manner similar to the procedures used in nuclear physics and electronics, consider the time at which the gas temperature is midway between T_i and T_a; that is, let us consider the "half life" of the elevated temperature layer. If we take

$$T_g = \frac{T_i + T_a}{2} \qquad (4\text{-}17)$$

then the time at which this temperature is attained, $t_{1/2}$, is given by

$$t_{1/2} = \frac{1}{2aT_a^3}\left[\arctan\left(\frac{1}{\beta}\right) - \arctan\left(\frac{2}{\beta+1}\right) - \frac{1}{2}\ln\left(\frac{\beta+1}{\beta+3}\right)\right] \qquad (4\text{-}18)$$

where

$$\beta = \frac{T_i}{T_a} \qquad (4\text{-}19)$$

The variation of $t_{1/2}$ with β is shown in Figure 4-4. As β increases, i.e., as the initial temperature increases, the time required to reach the one-half temperature level decreases. This is because the heat transfer rate is proportionately higher at higher initial temperatures.

Now we are in a position to parameterize the temperature-time variation of the hot gas layer by an effective temperature and effective radiation intensity. For the effective radiation intensity, I_r, we take

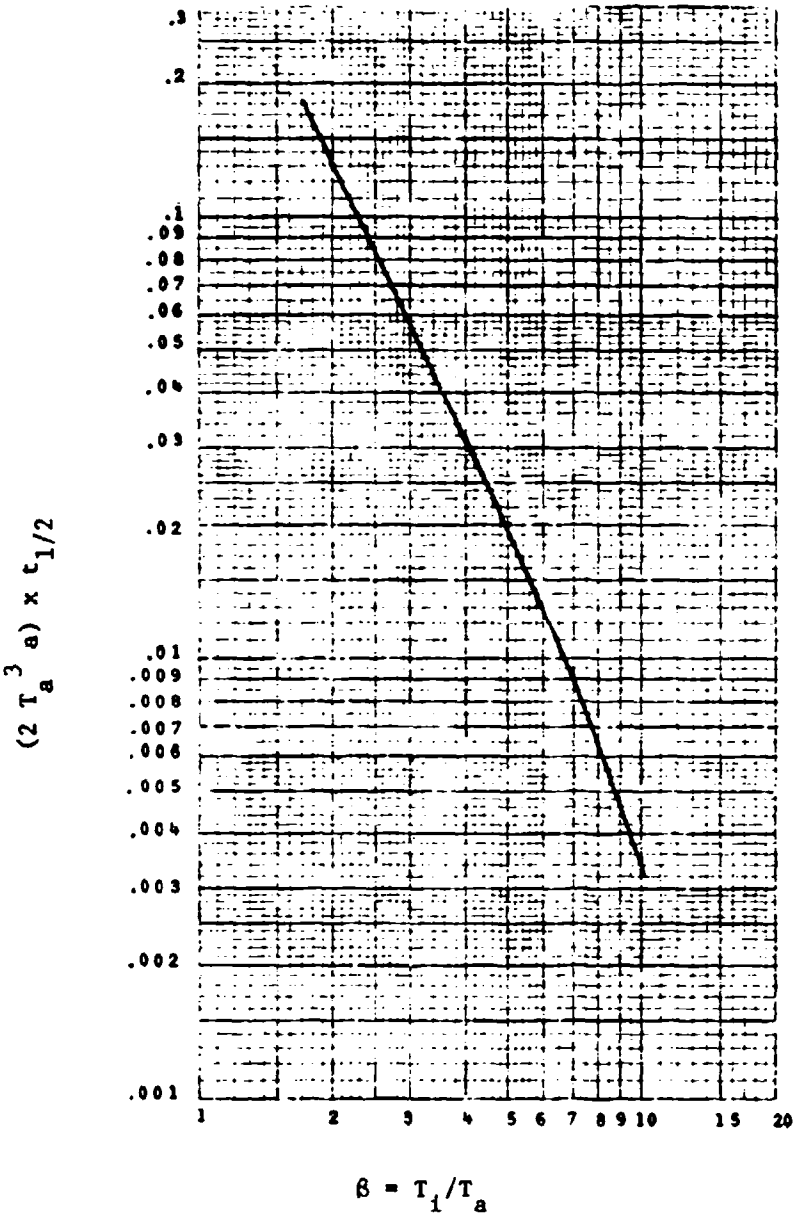

FIGURE 4-4

VARIATION OF $t_{1/2}$ with β

Variation in "half-life" time, $t_{1/2}$, as a function of temperature ratio, $\beta=(T_i/T_a)$. Note that $t_{1/2}$ is multiplied by the scale factor, $2\ T_a^3 a$ (as given by equation (4-16))

$$I_r = \sigma [T_g^4 - T_a^4] \qquad (4\text{-}20)$$

where T_g is given by equation

For the effective duration, t_{eff}, of the radiation we take

$$t_{eff} = 3t_{1/2} \qquad (4\text{-}21)$$

where $t_{1/2}$ is given by equation

The initial temperature is taken to be the adiabatic flame temperature, as is listed in the VM properties file.

To complete the formulation of the problem, the factors A_r and V_r in equation 4-10 must be given. The volume of the half ellipsoidal shell is given by

$$V_r = -\frac{2\pi}{3} \sigma_x \sigma_y \sigma_z (r_U^3 - r_L^3) \qquad (4\text{-}22)$$

and the area of radiation is given approximately by

$$A_r = \frac{2\pi}{3} (r_U^2 + r_L^2) (\sigma_x^2 + \sigma_y^2 + \sigma_z^2) \qquad (4\text{-}23)$$

where, as discussed in Chapter 3, σ_x, σ_y, and σ_z are the dispersion coefficients for the puff and

$$r_U = [2 \ln (\frac{2m}{(2\pi)^{3/2}\sigma_x\sigma_y\sigma_z K_U})]^{1/2}$$

$$r_L = [2 \ln (\frac{2m}{(2\pi)^{3/2}\sigma_x\sigma_y\sigma_z K_L})]^{1/2}$$

K_U = concentration at the upper explosive limit (Kg/m^3)

K_L = concentration at the lower explosive limit (Kg/m^3)

m = total mass of vapor released (Kg)

The origin of these terms is given in more detail in Appendix C2.

The Pool Burning Submodel

Since this submodel is largely based on models developed previously under USCG sponsorship, it is not necessary to provide detailed descriptions of them in this report. Further details are provided in Chapter 2 and in the CHRIS documentation [2].

CHAPTER 5

INPUT/OUTPUT DATA FOR PHASE I

Introduction

This chapter summarizes the input data required to run the VM and the types of output data to be provided to Phase II for use in assessing injuries to people and damage to property. In addition, the approach to preparing a geographical grid cell structure is described.

There are three types of data required to run the VM:

(1) chemical property data stored in a library file;

(2) geographical/demographic data for the general region of interest, also stored in a library file;

(3) spill and environment definition data, supplied as input by the user for each spill considered.

In the following, detailed consideration of each class of input data is given. The "Vulnerability Model User's Manual" details the mechanics of data input and output.

Chemical Properties Data

The chemical properties file is designed to contain 71 physical and chemical properties constants for more than 400 hazardous materials. The 71 properties that may be stored in the file for each material are listed in Table 5-1. This table was generated by a reporting computer program developed and run under another Coast Guard effort. The USCG currently has an ongoing program to expand the properties file and to fill many gaps that now exist.

The chemical properties file provides virtually all of the physical and chemical properties constants related to the hazardous material that are required to run the HACS programs described in the CHRIS and HACS documentation. In some instances, the properties file does not contain values for the required constant. In such cases, the computer executive automatically refers to a default property value file to obtain an estimated value. Since these estimated values are chosen to apply to a large number of substances, the errors induced by using default values can be quite significant; therefore, every effort should be made to provide missing values in the properties file, so that default values are not used. These missing values can be provided as part of the user-supplied input data and will override the default values.

TABLE 5-1. CONSTANTS CURRENTLY LISTED IN THE CHEMICAL PROPERTIES FILE

ABBREVIATION	UNITS	DESCRIPTION
MOLWT	NO	MOLECULAR WEIGHT
NBP	C	NORMAL BOILING POINT
NFP	C	NORMAL FREEZING POINT
CRTEM	C	CRITICAL TEMP
CRITPR	GM/CM2	CRITICAL PRESSURE
SPCGV	NO	SPECIFIC GRAVITY AT A POINT
SGTEMP	C	TEMP. FOR SPECIFIC GRAVITY
STATE	NO	STATE OF CHEMICAL,LIQUID - SOLID
LD1	GM/CM3	CONSTANT, LIQ DEN EQUA
LD2	*NO	COEFF LINEAR TERM, LIQ DEN EQUA
LD3	*NO	COEFF SQUARE TERM, LIQ DEN EQUA
LDUP	C	UPPER TEMP BOUND, LIQ DEN
LDLO	C	LOWER TEMP BOUND, LIQ DEN
LIQVIS	D-S/CM2	LIQUID VISCOSITY AT A POINT
LVTEMP	C	TEMP. FOR LIQ VIS
LV1	*NO	CONSTANT, LIQ VIS EQUA
LV2	*NO	COEFF 1/T, LIQ VIS EQUA
LVUP	C	UPPER TEMP. BOUND LIQ VIS
LVLO	C	LOWER TEMP. BOUND LIQ VIS
LTHCO	CAL/CMSC	LIQUID THERMAL CONDUCTIVITY AT A POINT
LTCTEM	C	TEMP FOR LIQ THER COND
LTC1	*NO	CONSTANT LIQ THER COND EQUA
LTC2	*NO	COEFF LINEAR TERM, LIQ THER COND EQUA
LTCUP	C	UPPER TEMP BOUND, LIQ THER COND
LTCLO	C	LOWER TEMP BOUND, LIQ THER COND
LHCAP	CAL/G-C	LIQUID HEAT CAPACITY AT A POINT
LHCTEM	C	TEMP FOR LIQ HEAT CAP
LHC1	NO	CONSTANT, LIQ HEAT CAP EQUA
LHC2	NO	COEFF LINEAR TERM, LIQ HEAT CAP EQUA
LHCUP	C	UPPER TEMP BOUND, LIQ HEAT CAP
LHCLO	C	LOWER TEMP BOUND, LIQ HEAT CAP
SRTEN	D/CM	SURFACE TENSION AT A POINT
STTEM	C	TEMP FOR SURFACE TENSION
IFTEN	D/CM	INTERFACIAL TENSION AT A POINT
IFTEM	C	TEMP FOR INTERFACIAL TENSION
SOLUB	G/1000	SOLUBILITY AT A POINT
SOLTEM	C	TEMP FOR SOLUBILITY
SOL1	NO	CONSTANT, SOLUBILITY EQUA
SOL2	*NO	COEFF LINEAR TERM, SOLUBILITY EQUA
VP1	*NO	CONSTANT A, VAPOR PRESSURE EQUA
VP2	*NO	CONSTANT B, VAPOR PRESSURE EQUA
VP3	*NO	CONSTANT C, VAPOR PRESSURE EQUA
VPUP	C	UPPER TEMP BOUND, VAPOR PRESSURE
VPLO	C	LOWER TEMP BOUND, VAPOR PRESSURE
VHC1	NO	CONSTANT, VAPOR HEAT CAPACITY EQUA
VHC2	NO	COEFF LINEAR TERM, VAPOR HEAT CAP EQUA
VHC3	NO	COEFF SQUARE TERM, VAPOR HEAT CAP EQUA
VHC4	NO	COEFF CUBED TERM, VAPOR HEAT CAP EQUA
VHCUP	C	UPPER TEMP BOUND, VAPOR HEAT CAP
VHCLO	C	LOWER TEMP BOUND, VAPOR HEAT CAP
FUS	CAL/G	HEAT OF FUSION
VAPOR	CAL/G	HEAT OF VAPORIZATION
COMB	CAL/G	HEAT OF COMBUSTION
DECOM	CAL/G	HEAT OF DECOMPOSITION
SOLHS	CAL/G	HEAT OF SOLUTION
SOLHR	CAL/G	HEAT OF REACTION(WITH WATER)
POLY	CAL/G	HEAT OF POLYMERIZATION
FLMLO	NO	LOWER FLAMABILITY LIMIT
FLMUP	NO	UPPER FLAMABILITY LIMIT
BRNRT	CM/S	BURNING RATE
TOXIN	PPM	TOXICITY BY INHALATION
NHALP	PPM	SHORT TERM INHALATION LIMIT
NHALT	S	SHORT TERM INHALATION
TOXLO	G/KG	LOWER LIMIT TOXICITY BY INGESTION
TOXUP	G/KG	UPPER LIMIT TOXICITY BY INGESTION
LATEYOX	NO	LATE TOXICITY
ADFLM	C	ADIABATIC FLAME TEMP
MOLRA	NO	MOLECULAR RATIO, REACTANTS TO PRODUCTS
AIRFUEL	NO	STOICHIOMETRIC AIR TO FUEL RATIO
FLMTEM	C	FLAME TEMPERATURE
MOLFRAC	NO	LIMITING VALUE, MOL FRACTION CONC

*Error in dimensional units as reported on this table.

Geographical/Demographic Data

The geographical/demographic data required as Phase I input are listed in Table 5-2. Not all of the data listed in Table 5-2 are at present used in the operation of the VM; however, space is allowed for these data and, in some cases, the data are entered in the event that further developments of the VM require this information. Those items marked by an asterisk in Table 5-2 are currently used for computations in the VM. In order to input these data, it is necessary to partition the macroregion in which the spill is to be simulated into grid cells for which representative geographical/demographic data may be supplied. To this end, a major city and its surrounding areas, including a 30-mile segment of a navigable river, were partitioned into more than 400 grid cells. These cells were determined, for simulation purposes, so that it could then be assumed that whatever occurs within a cell does so uniformly throughout the cell. The river cells are numbered in ascending order from upstream to downstream.

The approach taken to this partitioning was to equate a census tract, as defined by the U.S. Department of Commerce, to a cell. By definition, a census tract is a "...small area into which large cities and metropolitan areas are divided for statistical purposes. Tract boundaries are established cooperatively by a local committee and the Bureau of the Census and are generally designed to achieve some uniformity of population characteristics, economic status, and living conditions"[29]. Those census tracts that include both land and water were partitioned into two or more cells. The river itself was divided into 84 cells, so that no cell would be larger than 1 mile in length and so that each cell would be approximately rectangular in shape as required for river flow simulation.

Figure 5-1 is a reduced copy of a portion of the map of an urban area. Tracts on the map are identified numerically (e.g., 215, 234) and are separated from one another by solid, dark lines. For VM simulation purposes, the center of each tract (or cell) is identified by the latitude and longitude at its centermost point. For irregularly shaped tracts, a point is chosen to be representative of the tract area. Thus, the cell is identified only by a representative point, not by a description of its boundaries.

Data for each tract are available from, among other sources, the 1970 Census of Housing Report for the city. The data include, for each tract, total populaton, percent of population under 18 and over 62 years of age, assessed dollar value of houses, etc. Additional data (such as land use, etc.) were used in preparation for testing the VM; several sources of these applicable data are being used. The population statistics represent the number of persons residing in a given cell, not necessarily the number of persons in the cell at any given time. The estimated dollar value of structures is given only for residential property; these values were derived from the responses to census questionnaires. It is a limitation of the VM that the dollar values for damage assessment do not include damage to commercial property.

---

[29] U. S. Department of Commerce, Bureau of the Census, 1970 Census of Housing, Block Statistics, September 1971.

TABLE 5-2. GEOGRAPHICAL/DEMOGRAPHIC DATA INPUT FOR PHASE I

For Land Areas

* 1. Grid number
* 2. Latitude
* 3. Longitude
* 4. 0 (denotes land grid)
* 5. Total population
6. Percent of population under 18 years of age
7. Percent of population over 62 years of age
* 8. Percent of population sheltered
* 9. Total number of housing units
*10. Average assessed dollar value per unit dwelling
11. Housing construction material
12. Number of schools
13. Land use
14. Uniformity of the land topography
*15. Ignition source code

For Water Areas

* 1. Grid number
* 2. Latitude
* 3. Longitude
* 4. Depth (nonzero)
* 5. Length of cell
6. Direction of water current
* 7. Ignition source code
* 8. Speed of current
9. Tidal condition
10. Water turbulence level
11. Water temperature
12. Water density
13. Salinity

---

*These items are currently used for computing results in the VM.

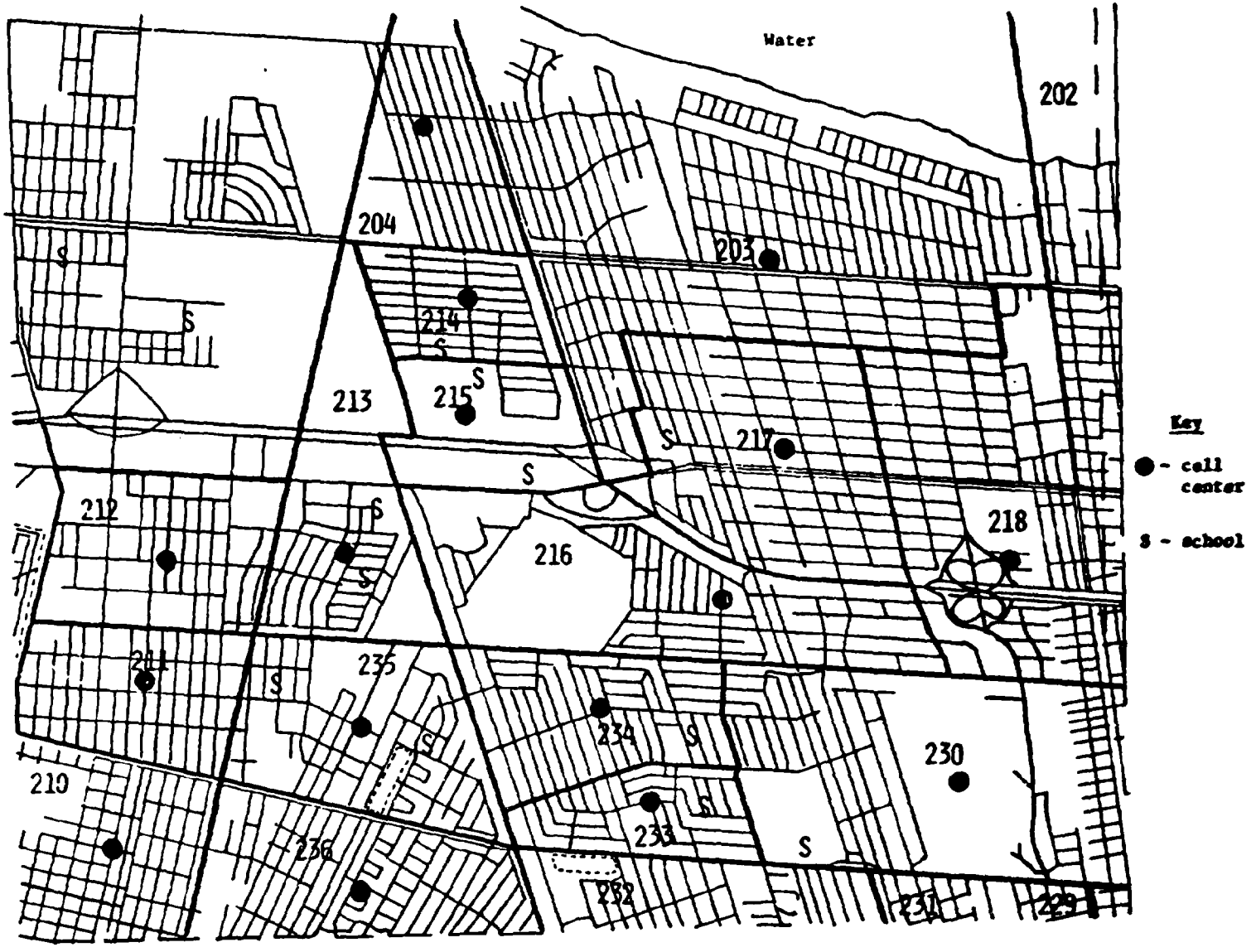

FIGURE 5-1 EXAMPLE OF A TRACT MAP FOR A PORTION OF AN URBAN AREA

Bureau of the Census publications obtained from the GPO include a description of pier facilities containing, among other information, listings of the industries that make use of the pier facilities.

Detailed 7-1/2 minute maps of the entire area selected for the test have been obtained from the United States Geological Survey Map Division in Arlington, Virginia.

The National Climatological Data Service in Asheville, North Carolina, provided meteorological data covering the years 1971 through 1973. Data include daily and monthly temperature readings, wind speed, and wind direction.

Nautical charts and other data have been obtained from the National Ocean Survey Distribution Center in Riverdale, Maryland. These include tide tables, tidal current tables, shipping lanes and river and channel depths.

Nautical charts have been obtained from the National Ocean Survey Distribution Center in Riverdale, Maryland. These include tide tables, tidal current tables, shipping lanes, and river and channel depths.

Spill and Environmental Definition Data

The third category of input data required for Phase I operation is the detailed information that defines the spill and the environment in which it occurs. There are four subcategories into which this type of input data falls, namely

1. definition of the subset of grid cells which are to be included in the simulation
2. spill definition data
3. environmental data
4. user override data

The data comprising item 1 merely constitute a list of the numbers of the grid cells which are to be considered in the simulation. Because of the manner in which the simulation proceeds, these cells need not be contiguous. However a clearer picture of what occurs is obtained if the cells considered fill out an approximately rectangular region.

The data comprising item 2 consist of spill-related data, such as:

spill location
size of spill
substance spilled
temperature and pressure in the cargo container
diameter of the vent or puncture

As with other types of input data, if no value is specified, the default value file will supply a value for the missing item.

The environmental data comprise a description of the physical background in which the spill occurs; included in these data are items such as:

air temperature
wind velocity
humidity
atmospheric stability class
barometric pressure

The final category of data consists of input items that will override default file values. That is, if the default values for constants missing from the properties file appear undesirable, the user may override the default values with his own inputs.

Phase I Output to Phase II

The type of data output from Phase I to Phase II depends upon what course of events the simulation follows. The data are presented on a cell-by-cell basis. Certain types of data, such as vapor concentration, are delivered as output for each time step. Other types of data, such as thermal radiation intensity, are delivered as output only once because of the nature of the models involved. Table 5-3 lists the types of data generated by Phase I and used by Phase II to make damage assessments.

TABLE 5-3. PHASE I OUTPUT DATA FOR EACH CELL

	Dimensional Units	Generating Submodel	Generated Every Time Interval?
1. Gas concentration	kg/m^3	AD	Yes
2. Interval duration	s	E	Yes
3. Liquid concentration	kg/m^3	WM	Yes
4. Effective thermal radiation intensity	J/m^2-s	FF	No
5. Effective time duration	s	FF	No
6. Thermal radiation	J/m^2-s	PB	No
7. Burning time	s	PB	No
8. Peak over pressure	N/m^2	EX	No
9. Dynamic impulse	$N-s/m^2$	EX	No

Key to submodel abbreviations

AD - air dispersion

E - executive

EX - explosion

FF - flash fire

PB - pool burning

WM - water mixing

CHAPTER 6

PHASE II ASSESSMENT PROCEDURES

Introduction

Phase I of the VM simulates the spill itself, the physical and chemical transformations of the spilled substance, and its dissemination in space. The history of the spill development simulated in Phase I is stored by grid cell and time interval. These data, constituting what is referred to as the "time-history" file, along with vulnerable resources data are the input to Phase II. Phase II assesses the effects of the spill on vulnerable resources: people, structures, and the environment. This chapter summarizes procedures of Phase II.

Injury and Damage to Vulnerable Resources

The vulnerable resources of interest in the VM, namely "people," "property," and "the environment," are subject to a plethora of potential hazards from spills of marine cargoes. For example, the vulnerable resource "people" may be affected by inhalation of toxic vapor; by burns from thermal radiation from a fire, either flash fire or pool burning; by peak overpressure or impulse from an explosion, manifested as direct impact or fragment injuries; by ingestion of toxic substances; by infiltration of the skin, mucous membranes, or eyes by toxic substances;by asphyxiation from high concentrations of gases not usually considered hazardous; by pulmonary burns resulting from the inhalation of burning or hot gases; by the inhalation of toxic combustion products; by frostbite from cryogenic liquids; by accidential injury resulting from individual or group panic; by complications of injuries as a result of substandard medical treatment caused by damage to or overtaxing of medical facilities and personnel; by injury from secondary events (secondary fires, secondary explosions, vehicular accidents, etc.) that are induced by the initial spill and its immediate effects.

At this time, however, only a limited number of damage mechanisms are simulated by the VM. The vulnerable resource "people" is modeled to be affected by inhalation of toxic vapor, by thermal radiation from a flash fire, and by peak overpressure or impulse from an explosion, or by some combination of these. The vulnerable resource "structures" is modeled to be affected by thermal radiation from a flash fire or burning pool and by peak overpressure or impulse from an explosion. For the vulnerable resource "environment," defined as air and water for the purposes of the VM, there is no direct calculation of damage caused by the spilled substance in its vapor or liquid phase or by a reaction product. Table 6-1 lists the specific types of injury or damage, assessed during Phase II of the VM, that are caused by toxicity, fire, and explosion, respectively. Damage and injury from explosion and fire are treated in detail in Appendix D; injury from toxic vapors is discussed in depth in Appendix E.

TABLE 6-1. PHASE II DAMAGE ASSESSMENT

Damage Causing Event	Vulnerable Resource	Type of Injury or Damage		Cause of Injury or Damage	Outdoors (Unsheltered)	
					Function	Factor(s)
TOXICITY	People*	Death		Toxic vapor: concentration or cumulative dose	T1 **	Concentration and time
		Nonlethal injury			T2 **	
		Irritation			T3 **	Concentration
EXPLOSION	People*	Death		Direct blast	E1	Peak overpressure
				Impact	E2	Impulse
		Nonlethal Injury	Eardrum rupture	Direct blast	E3	Peak overpressure
			Bone fracture	Impact	E4	Impulse
			Puncture wounds	Flying fragments	E5	
			Multiple injury	Two or more of the above	E6	Impulse or peak overpressure and impulse
	Structures	Structural damage		Direct blast	S1	Peak overpressure
		Glass breakage		Direct blast	S2	Peak overpressure
POOL BURNING	People	Death		Thermal radiation	B1 ***	Duration and magnitude of thermal radiation
		First degree burn			B2 ***	
	Structures	Ignition			B3	
FLASH FIRE	People	Death		Thermal radiation	F1	Effective duration and effective magnitude of thermal radiation
		First degree burn			F2	
	Structures	Ignition			F3	

* Comparable assessment format may be provided by age group where data are available.

** Separate functions for each chemical.

*** These functions are essentially the same as F1 and F2; however, as indicated in the adjacent column, slightly different arguments are used. These functions have not yet been implemented as part of the computer program, although to do so will be very easy.

Overview of Phase II

The function of Phase II is to read the time-history file of the simulation, to compute the damages resulting from the values of physical parameters contained in the time-history file, and then to assess damages and injury to the vulnerable resources impacted by the physical events. An overall flow chart for Phase II is presented as Figure 6-1. In most cases, the percent of the vulnerable resources affected within a given grid cell is calculated and then applied to the numbers of vulnerable resources present, giving the total numbers of vulnerable resources affected (for a given time period and given grid cell). The level of damage calculated at the center of the grid cell is assumed to apply to the entire grid cell and all of the vulnerable resources in it. The algorithm for computing the percent affected is denoted under the column headed "Function" in Table 6-1. The factor or factors computed by Phase I and used by each algorithm to assess damage are listed in the adjacent column of the table. In the case of first-degree burns resulting from the thermal radiation of a flash fire, the percent of vulnerable resource (people) affected in each cell is not computed; instead, a message is printed out indicating that the radiation intensity and duration were sufficient to cause first-degree burns in that cell. For all other damage assessment cases treated in the VM, the percent of the vulnerable resource experiencing the given type of damage is calculated.

For most of the assessment functions indicated in Table 6-1, the percent of vulnerable resource damaged is related to the causative factors computed in Phase I by probit equations (to be explained below). However five assessment procedures viz., B2, B3, F2, F3, and T3, do not use probit equations. As mentioned in the above, no percentage is calculated for F2 or B2, nonlethal injury to people from fire. For B3 and F3, ignition of structures by pool burning and flash fire, respectively, it is assumed that 25% of the structures in a given cell are ignited when the ignition criteria are met at the cell center. As explained further in Appendix D, this ad hoc assumption of 25% was used as an expedient estimate to account for shielding effects without performing a detailed analysis and calculation. Clearly some structures will be shielded from radiation by other intervening structures. For T3, toxic irritation of people, it is assumed that 100% of the subject population is irritated when the concentration criterion for irritation is met. Nonlethal injury from inhalation of ammonia is not simulated, as explained in Appendix E; thus for T2, in the case of ammonia, zero percent of the population is always assessed.

The remaining assessment calculations are based on probit functions [30]. A probit function takes the following form:

$$Pr = a + b \log_e V \qquad (6\text{-}1)$$

where the dependent variable, Pr, is a measure of the percent of the vulnerable resource affected and the independent variable, V, is some function of the factor that causes injury or damage to the vulnerable resource. The coefficients a (location parameter) and b (slope parameter) are

---

[30] Finney, D. J. Probit Analysis, 3rd ed. Cambridge University Press, London, 1971.

Figure 6-1. PHASE II FLOW CHART

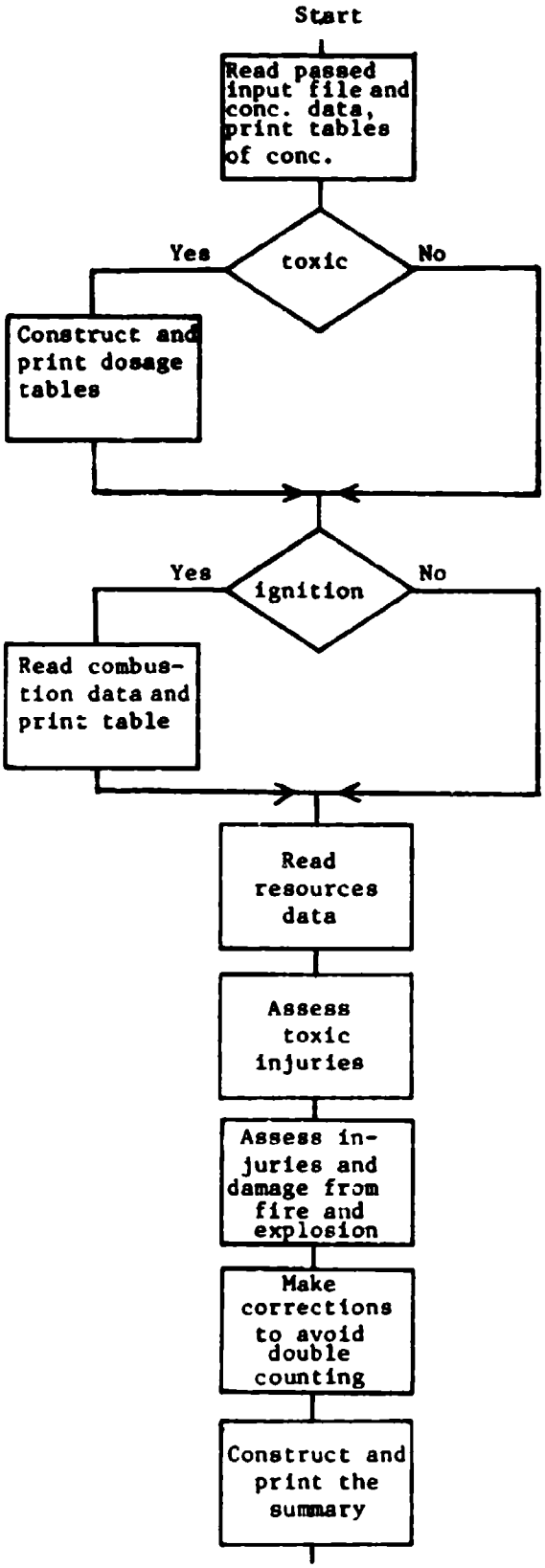

computed by maximum likelihood estimation similar to the computation of coefficients for classical regression equations. The variable Pr is referred to as a probit (probability unit). It is a Gaussian distributed random variable with mean value 5 and variance 1. The percent of the vulnerable resource affected is the percent corresponding to the cumulative distribution of Pr. This correspondence is given in Table 6-2 in which the main entries are probits and the row and column headings give the corresponding percents.

Each of the assessment equations E1, E2, E3, E4, E5, F1, B1, S1, S2, T1, and T2 (see Table 6-1) is a probit equation. For example, equation E1 is the probit equation for estimating deaths from lung hemorrhage resulting from the peak overpressure from an explosion. E1 is given by

$$Pr = -77.1 + 6.91 \log_e (P_p)$$

where P_p is the peak overpressure in N/m^2. A peak overpressure of 1.10×10^5 N/m^2, say, gives a probit of 3.11. Table 6-2 shows that this probit corresponds to approximately 3% deaths from lung hemorrhage. The coefficients (a = 77.1 and b = 6.91) were calculated from the following data, taken from Table 6-3:

Percent Affected	Probit (Table 6-4)	Peak Overpressure (N/m^2)
1	2.67	1.00×10^5
10	3.72	1.20×10^5
50	5.00	1.41×10^5
90	6.28	1.76×10^5
99	7.33	2.00×10^5

The above probits and the logarithms of the above peak overpressure values were inserted in a computer program that then calculated the values to be used for a and b.

In some cases, a function of the variable that determines injury or damage was used rather than simply the numerical value of the variable. For example, as explained in Appendix D, the probit equation F1 (deaths from burns) is given by:

$$Pr = -14.9 + 2.56 \log_e [t (I^{4/3})/10^4]$$

where t is the effective duration (in seconds) and I is the effective radiation intensity (in J/m^2 seconds). The 10^4 is used solely to reduce the magnitude of the $I^{4/3}$ value. This reduction, in turn, is absorbed in the slope coefficient, b (in this case b = 2.56). The exponent 4/3 of I was obtained iteratively to provide a good fit to the data.

The logarithm is conventionally used in probit equations, not for theoretical purposes, but because the logarithm usually transforms the relationship between causative factor and response into a Gaussian function. This frequently is the case when the variable to be computed

%	0	1	2	3	4	5	6	7	8	9
0	—	2.67	2.95	3.12	3.25	3.36	3.45	3.52	3.59	3.66
10	3.72	3.77	3.82	3.87	3.92	3.96	4.01	4.05	4.08	4.12
20	4.16	4.19	4.23	4.26	4.29	4.33	4.36	4.39	4.42	4.45
30	4.48	4.50	4.53	4.56	4.59	4.61	4.64	4.67	4.69	4.72
40	4.75	4.77	4.80	4.82	4.85	4.87	4.90	4.92	4.95	4.97
50	5.00	5.03	5.05	5.08	5.10	5.13	5.15	5.18	5.20	5.23
60	5.25	5.28	5.31	5.33	5.36	5.39	5.41	5.44	5.47	5.50
70	5.52	5.55	5.58	5.61	5.64	5.67	5.71	5.74	5.77	5.81
80	5.84	5.88	5.92	5.95	5.99	6.04	6.08	6.13	6.18	6.23
90	6.28	6.34	6.41	6.48	6.55	6.64	6.75	6.88	7.05	7.33
—	0.0	0.1	0.2	0.3	0.4	0.5	0.6	0.7	0.8	0.9
99	7.33	7.37	7.41	7.46	7.51	7.58	7.65	7.75	7.88	8.09

TABLE 6-2

RELATIONSHIP BETWEEN PERCENTAGES AND PROBITS

Probits are the three digit numbers in the table. Percents are read along the top and side margin of the table. The vertical column of percents gives the decade; the horizontal column gives the unit. The table entry appearing in the row of the decade value and the column of the unit value is the probit corresponding to that percent. The last two rows in the table provide a finer reading for very high percent, from 99.0 to 99.9. The second to last row is the tenths of percent to be added to 99%. The last row consists of the corresponding probits.

Equation Symbol	Type of Injury or Damage	Causative Variable	Parameters of Probit Equations		Data From Which the Probit Equation Was Derived					
			Constant; a	Slope; b	% Affected	Value of Variable	% Affected	Value of Variable	% Affected	Value of Variable
E1	Death from Lung Hemorrhage	P_p	-77.1	6.91	1 10	1.00×10^5 1.20×10^5	50 90	1.41×10^5 1.76×10^5	99	2.00×10^5
E2	Death from Impact	J	-46.1	4.82	0 8	18.0×10^3 28.6×10^3	31 63	37.3×10^3 45.2×10^3	96 100	49.7×10^3 60.7×10^3
E3	Eardrum Rupture	P_p	-15.6	1.93	1 10	16.5×10^3 19.3×10^3	50 90	43.5×10^3 84.3×10^3		
E4	Injuries from Impact	J	-39.1	4.45	1 50	13×10^3 20×10^3	90	28×10^3		
E5	Injuries from Flying Fragments	J	-27.1	4.26	1	1024	50	1877	99	3071
S1	Structural Damage	P_p	-23.8	2.92	1 50	6.2×10^3 20.7×10^3	99	34.5×10^3		
S2	Glass Breakage	P_p	-18.1	2.79	1	1700	90	6200		
F1	Burn Deaths from Flash Fire	$t_e \cdot e^{4/3}/10^4$	-14.9	2.56	1 1 1	1099 1073 1000	50 50 50	2417 2264 2210	99 99 99	7008 6546 6149
B1	Burn Deaths from Pool Burning	$tI^{4/3}/10^4$	-14.9	2.56	1 1 1	1099 1073 1000	50 50 50	2417 2264 2210	99 99 99	7008 6546 6149
T1	NH_3 Deaths	$\Sigma\ TC^{2.75}$	-30.57	1.385	3 3 3	37.3 90.9 44.6	50 50 50	74.6 204.6 148.6	99 99	411.8 334.4
T1	Cl_2 Deaths	$\Sigma\ TC^{2.75}$	-17.1	1.69	3 3 3	14.1×10^4 17.0×10^4 21.5×10^4	50 50 50	34.05×10^4 47.0×10^4 64.7×10^4	97 97	105.8×10^4 129.4×10^4
T2	Cl_2 Injuries	C	-2.40	2.90	1 25	6 10	50 90	13 20		

KEY: P_p = peak overpressure (N/m^2)
J = impulse ($N\text{-}s/m^2$)
t_e = effective time duration (s)
I_e = effective radiation intensity ($J/m^2/s$)
C = concentration (ppm)
T = time interval (minutes)
t = time duration of pool burning (s)
I = radiation intensity from pool burning ($J/m^2/s$)

TABLE 6-3

SUMMARY OF PROBIT EQUATIONS BASED ON INFORMATION IN APPENDIX D

is a measure of percent. It is desirable that the causative factor and response be related by a Gaussian function, because such extensive theoretical work has been performed on this distribution that the statistical treatment of such distributions reduced to the use of standard methods. For all probit equations used in the VM, the logarithm provided exceptionally good fits to the data used.

Table 6-3 summarizes the probit equations used for Phase II assessment. The first column of this table gives the equation symbol that corresponds to the function given in Table 6-1. The second column of Table 6-3 specifies the type of injury or damage for which the equation is used, and the third column specifies the types and unit(s) of measurement of the variable that affects the vulnerable resource. The next two columns give the location and slope parameters (a and b) of the corresponding probit equation. The last six columns list the data used to compute a and b, the data being given in pairs. Each pair consists of the percent of vulnerable resource affected and the magnitude of the variable that causes this percent to be affected. The above data used for estimating the coefficients a and b for equation E1, for example, are listed in the first two rows of the last six columns of Table 6-3.

In applying percent damage, whether derived from a probit equation or otherwise, to the vulnerable resource "people," it has been assumed that half of the total population is unsheltered (outdoors) and thereby subject to damage. Half the population is assumed to be sheltered (indoors) and no deaths or injuries are assessed for this portion of the population, because more complex models are required to assess injuries to people indoors. The VM does not, at this time, attempt to determine the movements and locations of the population as a function of time of day, day of week, and weather conditions, so half the population was arbitrarily placed outdoors. Furthermore, census data have been used to estimate the population distribution in the region of interest. As a consequence, people are modeled to be at their place of residence rather than at work, school, recreation, or in transit.

Double Counting

Provisions have been made in the VM to prevent double counting in three different situations. Double counting is used in this context to mean the inclusion of an element of some vulnerable resource (e.g., a person or a building) in more than one category of damage or injury. Three situations arise in which double counting will occur unless provisions are made to prevent it. The situations are as follows.

(1) A single damage mechanism from one event simultaneously causes injuries of differing severity (e.g., inhalation of toxic gas may cause death, nonlethal injury, or irritation).

(2) Two or more damage mechanisms from one event simultaneously cause injuries of the same severity (e.g., an explosion can kill people either by direct blast effects or by impact).

(3) Different events at different times both cause damage to the same resource, and the first event so severly damages some portion of the resource that further damage is irrelevant (e.g., persons killed by toxic gas cannot be further injured by a subsequent explosion).

The corrections made to damage assessment for double counting and the means by which these corrections are obtained are described in depth in Appendix G. The type of correction used for situation (1) is applied to values resulting from the sets of damage functions denoted by: (E1, E3), (E2, E4), (S1, S2), (T1, T2, T3). The type of correction used for situation (2) is applied to values resulting from the sets of damage functions giving death and injury resulting from an explosion. The type of correction used for situation (3), by the very nature of the correction, is not applied to any particular set of damage estimates; instead this type of correction is used at the termination of the simulation to arrive at the summary of damages. This correction is used for the vulnerable resource "people" when either flash fire or explosion follows inhalation of toxic gases; this correction is used for the vulnerable resources "structures" and "people" when pool burning follows either flash fire or explosion.

Damage Assessment Procedures

As it currently stands, the VM can simulate damage to vulnerable resources from four physical events; these events are:

(1) air dispersion of a toxic gas

(2) flash fire

(3) explosion

(4) pool burning

Damage to vulnerable resources is conveniently discussed in terms of (1) toxic injury, (2) explosion damage, and (3) fire damage. Detailed consideration is given to toxic damage assessment in Appendix E and to fire and explosion damage assessment in Appendix D. The assessment algorithms for toxic damage are highly dependent on the type of substance spilled; whereas the assessment algorithms for fire and explosion are independent of the type substance spilled, although the values of the variables used in the algorithm do depend on the type of substance spilled.

(1) Toxic Injury

Toxic injury is assessed only for the vulnerable resource "people."

At the present time, only inhalation toxicity is treated in the VM. Toxic injury caused by ingestion of poisonous substances is not treated. One difficulty encountered in attempting to model damage caused by ingestion of toxic material is that the amount of toxic substance ingested by a receptor is usually extremely difficult to estimate. The current treatment of inhalation toxicity is restricted to the substances directly spilled; modeling of the inhalation toxicity of combustion products or of other reaction products has been deferred. Of the five substances currently treated in the VM, only chlorine (Cl_2) and anhydrous ammonia (NH_3) are considered to have an inhalation toxicity liable to cause serious consequences. The toxic damage caused by irritant gases in general falls into three categories:

(1) death

(2) sublethal injury

(3) irritation

The category of injury sustained by exposed resources depends, in general, upon both the duration of exposure and the concentration level experienced. This dependence is nonlinear; dose, the product of concentration level and duration, is not the appropriate variable to assess response to irritant gases. As an example, for concentrations over the lethality threshold, doubling the concentration level does not halve the time required to produce the same death rate; instead, as the concentration level increases, the time to produce a given injury level decreases at a disproportionately rapid rate. This phenomenon is illustrated by the isodamage curves for chlorine lethality shown in Figure 6-2.

The dependence of toxic gas lethality on concentration and time was found to be described by a nonlinear function of the form

$$TC^n$$

where C = concentration of the toxic gas

T = time duration of the exposure

n = an exponent

For both chlorine and ammonia, the best value for the exponent, as determined by fitting the data given in Table 6-3, was found to be n = 2.75.

In the VM the concentration is not constant in time, therefore the function TC^n must be replaced by the quantity

$$\int C^n dT$$

As an approximation to this integral, the VM uses a finite sum; i.e.,

$$\int C^n dT \simeq \sum_i T_i \cdot C_i^{2.75}$$

where T_i is the duration of a time step and
C_i is the concentration during that time step at a given location.

Table 6-4 summarizes basic data on chlorine and ammonia inhalation taken from Appendix E. These data were used to generate the probit equations for lethal injuries from the inhalation of the toxic vapors of chlorine and ammonia. The midpoints of the rectangular areas defined by the data were used in the generation of probit equations Tl for chlorine and ammonia. The resulting equations for lethality are:

for chlorine, $Pr = -17.1 + 1.69 \log_e V$ (6-2a)

and

for ammonia, $Pr = -30.57 + 1.385 \log_e V$ (6-2b)

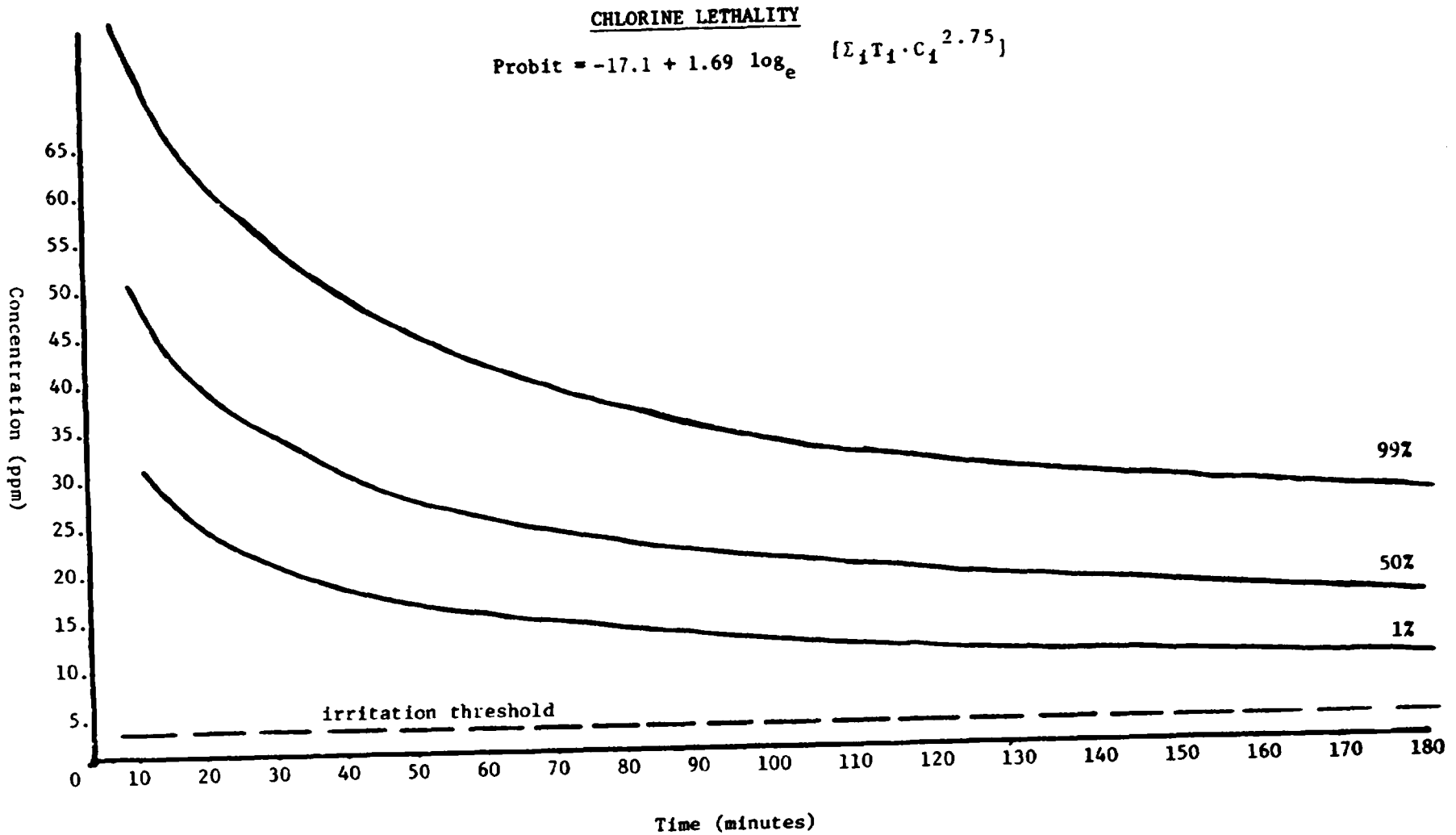

FIGURE 6-2

SELECTED CONTOUR LINES FOR CHLORINE LETHALITY EQUATION (6-2a)

TABLE 6-4. DATA USED IN DERIVING EQUATIONS FOR ESTIMATING DEATHS FROM CHLORINE AND ANHYDROUS AMMONIA GAS (Details of the data and their sources are given in Appendix E)

Effect	Deaths (%)		Time	Concentration (ppm)	
	General Population	High-Risk Population*		Cl_2	NH_3
Negligible	0	0	Any	< 3	< 100
Complaint, no risk	0	0	Any	3-5	100-300
Severe harassment (some risk)	0	25	Any	5-15	300-1000
Severe harassment/risk	0	25	< 1/2 hr.		
Lethal	3	50	1/2-1 hr.	15-25	1000-2500
Lethal	50	100	1-2 hr.		
Lethal	3	50	< 1/2 hr.		
Lethal	50	100	1/2-1 hr.	25-40	2500-4000
Lethal	97	100	1-2 hr.		
Lethal	3	50	< 5 min.		
Lethal	50	100	5-15 min.	> 40	> 4000
Lethal	97	100	15-30 min.		

* As explained in Appendix E, the high-risk population consists of the very old, the very young, and those with preexisting pulmonary pathology.

where

$$V = \sum_i T_i C_i^{2.75} \qquad (6\text{-}3)$$

Nonlethal injury is taken to mean hospitalization with or without evidence of permanent or lasting impairment. Of major concern in public disasters is the number of people whom the medical services send to hospitals. This number is interpreted as the count of nonlethal injuries for VM purposes, regardless of actual impairment.

Reports of three chlorine accidents [31-34], summarized in Table 6-5, were the primary sources of data in deriving the VM equation for estimating nonlethal injuries from chlorine. The data in Table 6-5 and the dose response considerations discussed in Appendix E can be summarized as presented in Table 6-6. Nonlethal injury can be correlated with concentration level alone, rather than with the nonlinear function of time and concentration, V, that correlates with death from chlorine inhalation. The probit equation for nonlethal injury resulting from inhalation of chlorine is

$$Pr = -2.40 + 2.90 \log_e C \qquad (6\text{-}4)$$

Since nonlethal injury from chlorine inhalation does not heal immediately (as discussed in Appendix E, it may heal spontaneously after a few days), the appropriate value for concentration in equation (6-4) is not the current level, but the maximum level that occurs in the given cell up to the current time.

Nonlethal injuries from the inhalation of ammonia (NH_3) are not assessed by the VM at this time. There seems to be some disagreement among the authorities as to whether hospitalization is appropriate after acute but nonlethal exposure to ammonia vapors. The studies relevant to this problem are few, so it has been impossible within the scope of this study (investigation of published data - no laboratory work) to obtain good estimates of the dosage required to cause injuries which require hospitalization. Therefore, the function T2 giving percent nonlethal injury from ammonia inhalation is simply:

percent injured = 0

---

[31] Kowitz, T.A., R.C. Reba, R.T. Parker, and W.S. Spicer, Jr. Effects of chlorine gas upon respiratory function. Arch. Environ. Health 14:545-558, 1967.

[32] Chasis, H., J.A. Zapp, J.H. Whittenberger, J.L. Helm, J.J. Doheny, and C.M. MacLeod. Chlorine accident in Brooklyn. Occup. Med. 4:152-176, 1947.

[33] Joyner, R.E., and E.G. Durel. Accidental liquid chlorine spill in a rural community. J. Occup. Med. 4:152-154, 1962.

[33] Weill, H., R. George, M. Schwarz, and M. Ziskind. Late evaluation of pulmonary function after acute exposure to chlorine gas. Am. Rev. Resp. Dis. 99:374-379, 1969.

TABLE 6-5. SUMMARY OF NONLETHAL INJURIES RECEIVED BY ACCIDENTAL INHALATION OF CHLORINE

Accident	Numbers of People			Hospitalized (% of Those Examined)
	Exposed	Examined	Hospitalized	
Industrial Transportation[a]	150	59	11	18
Brooklyn Subway[b]	1000	418	208	50
Morganza, Louisiana[c]	Unknown	100	17	17

[a]See reference [31] in the text.

[b]See reference [32] in the text.

[c]See references [33] and [34] in the text.

TABLE 6-6. SUMMARY DATA FOR NONLETHAL INJURIES FROM CHLORINE INHALATION

Cl_2 (ppm)	Injuries (%)
20	90
13	50
10	25
6	1

Toxic irritation is treated as an all-or-nothing case for assessment purposes. If the concentration equals or exceeds the specified concentration, every person outdoors is assessed to be irritated. Irritation is assumed to cease as soon as the concentration drops below the specified value. From the data in Appendix E, the threshold for irritation by chlorine is taken to be 3 ppm, and for ammonia it is taken to be 100 ppm. Therefore, the assessment functions T3 for chlorine and ammonia may be written as

$$\text{percent irritated} = \begin{cases} 100\% & \text{if } C > C_t \\ 0\% & \text{if } C < C_t \end{cases}$$

where $C_t = \begin{cases} 3 \text{ ppm for chlorine and} \\ 10 \text{ ppm for ammonia.} \end{cases}$

Toxic damage to the vulnerable resource "environment" is not assessed in the VM at this time. The VM predicts the concentration of a toxic substance in the air and water; comparison of these predicted concentrations to air and water quality standards appears to be an attractive method for assessing damage to the environment. Such an approach, however, has many pitfalls; among these are the following.

(a) This scheme cannot be implemented for many cargoes. Many substances carried in bulk in commerce upon the navigable waters are uncommon as pollutants, and there are no standards for these materials.

(b) For some cargoes, there may be more than one standard. For water contamination, for example, there might be one standard for drinking water, another for water safe for swimming, a third standard for the protection of fish, and a fourth level, above which shellfish living in these waters are unfit for human consumption.

(c) Because most air and water quality standards are developed for situations of chronic exposure there is a problem of exposure time. Most air and water quality standards explicitly mention the averaging time and are designed for situations in which the concentration does not change by orders of magnitude in a few minutes. One may easily conceive a situation in which a very high concentration, for example of SO_2, may exist for a few minutes, killing all of the animals at a location without exceeding the three-hour air quality standard. Although the cumulative dosage at a location may be calculated, there is little information on the response of many plants and animals to short exposures of high concentrations of many common cargoes.

(d) Some quality standards are not simply stated as concentration levels or dose levels not to be exceeded. Other factors may be involved. For example, one water quality standard for ammonia depends on concentration, water temperature, and water pH. Quality standards for other materials involve complex and expensive bioassay procedures.

Because of the problems raised by these factors, the violation of air or water quality standards has not been adopted as a viable procedure for assessment of environmental damage in the VM. Since the USCG has directed that environmental damage assessment is of lower priority than assessment of damage to people and property, no alternative method for assessing environmental damage has been implemented in the VM. However, the VM does provide the time history of pollutant concentration in air and water so the user may use this information to assess environmental damage at his option.

(2) Explosion Damage

Explosion damage is assessed for the vulnerable resources "people" and "structures." Personnel experience explosion damage in two categories, (a) death and (b) nonlethal injury. It is customary to categorize explosion damage to personnel in three categories, depending on the causative mechanism of damage:

(a) primary damage - direct blast effects (interaction between the blast wave and personnel only, with no other intervening or associated factors)

(b) secondary damage - damage from missiles and fragments

(c) tertiary damage - damage from translation and subsequent collision with an obstacle

In the VM, death is assessed for primary damage manifested as lung hemmorhage or for tertiary damage manifested as skull and body bone fractures. Nonlethal injuries are assessed for all three damage categories, including the secondary damage of puncture wounds from missile penetration. In addition, injury resulting from two or more damage mechanisms is assessed in a separate category, multiple injury. Explosion may cause eardrum rupture, bone fracture, or puncture wounds through the independent mechanisms of direct blast, impact, or flying fragments. Since the causative mechanisms are independent, an individual exposed to an explosion may experience injury from a combination of two or even three causes. That fraction of the population injured by more than one mechanism is determined by the double counting procedures described in Appendix G. Structures experience explosion damage in two categories, (a) serious structural damage and (b) window glass breakage. The physical variables that determine the extent of explosion damage are the peak overpressure and the impulse associated with the blast wave; the values for these variables are generated in Phase I of the VM. Table 6-3 summarizes the probit equations used to assess explosion damage and the data upon which the equations are based; Appendix D explains at length the formulation of the assessment procedures.

Death from direct blast damage usually is due to lung hemorrhage, although other injuries may sometimes contribute. The data in Appendix D indicate that a peak overpressure of about 1 atmosphere ($= 10^5$ N/m^2 = 14.5 psi) is the threshold for fatal injuries, and that 2 atmospheres causes close to 100% fatality. The probit equation for this type of injury, E1, is given by:

$$Pr = -77.1 + 6.91 \log_e (P_p) \qquad (6\text{-}5)$$

where P_p is the peak overpressure.

Death from tertiary explosion damage results when a person is moved by the blast wave and forcibly impacts with the ground, a wall, or some other object. The speed attained by a person subject to a blast wave is more dependent upon the impulse (roughly the integral of overpressure over time for the blast wave) than upon the overpressure associated with the explosion. Consequently, impulse is the variable used to make this assessment. The nature of the impact injury is complicated by the need to consider the person's position when struck by the blast wave, shielding by objects such as walls or buildings, and the distance to, and the nature of, any surfaces which the person might strike. As explained in Appendix D, data prepared for the Defense Civil Preparedness Agency and based on a model considering most of these factors [35] have been used to derive the probit equation E2:

$$Pr = -46.1 + 4.82 \log_e J \qquad (6\text{-}6)$$

where J is the impulse.

As discussed in Appendix D, eardrum rupture is by far the most prevalent injury which is an effect of direct blast. This mechanism operates in a straightforward manner, and there is a general consensus on the pressures required to cause damage. The equation E3, used to assess this type of injury, is:

$$Pr = -15.6 + 1.93 \log_e Pp \qquad (6\text{-}7)$$

The injuries caused by translation followed by abrupt impact upon some surface are mostly lacerations, contusions, broken bones and internal injuries. Damages caused by this mechanism are difficult to assess, as discussed above. For the assessment procedure in the VM, damage criteria established for an idealized model were adjusted to account for nonideal effects, on the basis of the relationship of ideal and nonideal criteria for death by this mechanism. This is explained more fully in Appendix D. The equation E4, used to assess this injury, is given by:

$$Pr = -3.91 + 4.45 \log_e J \qquad (6\text{-}8)$$

For most accidental explosions, penetration by flying fragments is the most common mechanism which causes nonfatal injuries. Most of the injuries which result are not serious. More injuries are caused by broken glass than by other material, such as gravel. The number of people injured from fragments is very difficult to treat accurately, because the location and exposure of the population are important and the availability of material to break and form fragments also enters into the assessment. At present, a simplified procedure, based on damage from ten-gram glass fragments, is used.

---

[35] Longinow, A., G. Ojdrovich, L. Bertram, and A. Wiedermann. People Survivability in a Direct Effects Environment and Related Topics. IIT Research Institute, Chicago, May 1973.

The resulting equation, E5, is given by:

$$Pr = -27.1 + 4.26 \log_e J \qquad (6\text{-}9)$$

Assessment of injuries from multiple causes is based on the assessment of injury from each individual cause; the procedure used to eliminate double counting in making the assessment is described in detail in Appendix G.

For the purpose of assessing major damage to buildings, a typical wood frame structure has been assumed. Most residential structures are of this type. Since the census records used to provide data on the number and value of property include only residential property, it is consistent to use damage criteria for wood frame structures. If further development of the VM provides an expanded data base that includes nonresidential structures as well as a designation of structural type, the assessment algorithms may be readily modified on the basis of data available in the literature to encompass damage to structures other than wood frame. The response of the structure has been generalized, so the damage assessment is based only on blast wave parameters. Because complex interreactions between the blast wave and structure are not considered here, the blast wave is parameterized solely on the basis of peak overpressure. The difficulty of precisely describing structure-blast wave interactions and the expediency of using a single blast wave parameter are discussed in more detail in Appendix D. The assessment equation used for major structural damage, S1, is given by:

$$Pr = -23.8 + 2.92 \log_e P_p \qquad (6\text{-}10)$$

This probit equation is used to relate the given peak overpressure to the percent structural damage caused to a building subject to the given peak overpressure; it does not give the percent of buildings in the geographical cell experiencing complete destruction. Of course, as far as the dollar value of the damage is concerned it is irrelevant whether x percent of the buildings in a cell are completely destroyed or whether all buildings in the cell experience x percent damage. Window breakage is a much simpler phenomenon than other structural response to a blast wave environment. Therefore, it is generally agreed that peak overpressure is the significant causative factor; further, the critical levels required to cause given degrees of damage are generally agreed upon. The assessment equation for glass breakage, S2, is given by:

$$Pr = -1.81 + 2.79 \log_e P_p \qquad (6\text{-}11)$$

This probit equation gives the percent of exposed windows that are broken by the blast. At this time, no assessment of the dollar value of the breakage is made.

(3) Fire Damage

Damages from fire are modeled as affecting the vulnerable resources "people" and "structures." Damage from flash fire is currently modeled to affect both personnel and structures. The current computer version of the VM assesses damage from pool burning only to structures, since it has been

assumed that personnel would have time to seek shelter or to evacuate in order to avoid injury. However, injury to personnel can readily be modeled by using the same damage criteria (as expressed in a probit equation) as are used for flash fire; the only difference is that actual radiation intensity and duration are used for pool burning, whereas effective values are used for flash fire. The damage assessed to structures is ignition. The damages assessed to personnel are (a) death and (b) nonlethal burns. For all types of damages, two parameters have been found to be significant: (a) level of thermal radiation and (b) duration of the thermal radiation; therefore a variable combining these two parameters is used for assessment purposes. The level of thermal radiation and its duration are computed by the Phase I submodels, for pool burning and flash fire, as is discussed in Chapter 4. The assessment of deaths from flash fire is based on data obtained primarily from studies of the effects of nuclear weapons. These data, presented in Appendix D, indicate that the number of deaths is proportional to the product of the duration of the radiation pulse with the four-thirds power of the intensity. The radiation pulse from a flash fire is not a square wave, of course, so an effective pulse intensity and an effective pulse duration must be calculated. This is discussed in Chapter 4. The data relating the lethality levels to the radiation dosage are presented in Appendix D. The probit equation F1, used to assess deaths from flash fire, is given by:

$$Pr = -14.9 + 2.56 \log_e\left(\frac{tI^{4/3}}{10^4}\right) \qquad (6\text{-}12)$$

where t is the effective time duration in seconds and I is the effective radiation intensity in $J/m^2/sec$. The factor 10^4 is a convenient scaling constant.

The VM does not make a quantitative assessment of nonlethal burn injuries, because of the uncertainty in determining the degree of the burns and the effects of clothing and shielding. The data in Appendix D indicate that the threshold for first-degree burns is

$$tI^{1.15} = 550{,}000$$

where t is in seconds and I is in joules/m^2/sec. In the analysis of first-degree burns it was found that an exponent of 1.15 provided a better fit to the data than the exponent 4/3 used for lethality (see page D-24). This is for exposed skin. The function F2, used to assess nonlethal injury from flash fire, is given by:

$$\text{percent subject to first-degree burns on exposed skin} = \begin{cases} 100\% & \text{for } tI^{1.15} > 550{,}000 \\ 0\% & \text{for } tI^{1.15} < 550{,}000 \end{cases} \qquad (6\text{-}13)$$

The assessment of fire damage to structures is based on studies of the ignition of wood. Factors influencing wood ignition are: (a) radiation intensity level, (b) duration of radiation exposure, (c) wood type, and (d) the presence or absence of a pilot flame near the irradiated wood. Duration and level of radiation intensity are factors computed by Phase I submodels. Wood type is not treated explicitly; average

values are used. For flash fire, the presence of a pilot flame is assumed; for pool burning, pilot flames are assumed to be absent. For flash fire, the radiation intensity is considered to be high enough to cause ignition only in that region where a flammable fuel-air mixture exists, i.e., the region where the flash fire burns. The presence of the flash fire provides an open flame, so the data for pilot ignition are used. For pool burning, the irradiated structures are generally too far from the burning pool for those flames to be considered as a pilot. Thus the data for spontaneous (no pilot) ignition are used for pool burning. The damage assessment functions and procedures for ignition of structures from pool burning, B1, and from flash fire, F3, may thus be stated.

For ignition from pool burning

1. For every grid cell, look up the radiation intensity, I_r, at the cell center.

2. The radiation intensity at the cell center must exceed the value

$$I_s = 2.54 \times 10^4 \frac{\text{Joules}}{\text{m}^2 - \text{s}}$$

3. The duration of the pool burning, t_b, must exceed the time given by

$$t_s = \left[\frac{6.10 \times 10^4}{(I_r - I_s)}\right]^{5/4} \qquad (6\text{-}14)$$

4. If $t_b \geq t_s$, then there is ignition

   If $t_b < t_s$, then there is no ignition

where in both cases

I_r = radiation intensity at the cell center

For ignition from flash fire

1. The vapor concentration at grid cell center must be between the limits of flammability for the spilled substance (this to assure the presence of a pilot flame).

2. The radiation intensity, I_r, must exceed the value

$$I_p = 1.34 \times 10^4 \frac{\text{Joules}}{\text{m}^2 - \text{s}}$$

3. The effective duration of the radiation, t_{eff}, must exceed the value given by:

$$t_p = \left[\frac{7.22 \times 10^5 \frac{\text{J}}{\text{m}^2 - \text{s}}}{(I_r - I_p)}\right]^{3/2} \qquad (6\text{-}15)$$

4. If $t_{eff} \geq t_p$, then there is ignition

   If $t_{eff} < t_p$, then there is no ignition

If ignition occurs (pool burning or flash fire), one-fourth of the structures in the cell are assumed to ignite. This assumption, recognized to be somewhat crude, was made to account for the fact that some structures will be shielded from thermal radiation by others.

An Example

To illustrate some of the assessment techniques discussed in the preceding section, consider the following hypothetical occurrence. The dispersion of a chlorine spill causes the air in a given grid cell to experience the following time history:

Phase I output for grid cell x

Concentration (ppm)	Time (min) at this Concentration
0	5
10	10
30	5
25	15

For these data, the significant assessment variable

$$V = \sum_I T_i \, C_i^{2.75}$$

has the value $V = 168{,}100$, $\log_e V = 12.03$, so the probit has the value, $Pr = 3.23$, as determined through equation (6-2a). From Table 6-4 we see that a probit of 3.25 corresponds to 4%. Thus we conclude that for this hypothetical exposure history just under 4% of the exposed population in the given cell will be killed by inhalation of toxic vapors.

During the last time interval the concentration is 25 ppm. Since concentration is the appropriate assessment variable for nonlethal injury from chlorine inhalation, we find $\log_e C = 3.22$; using this value in equation (6-4) we find the needed probit, $Pr = 6.93$. Again, from Table 6-4, it is seen that probits of 6.88 and 7.05 correspond to 97% and 98%, respectively. Therefore we assess 97% of the exposed population in the given cell as having nonlethal toxic injury. However, since the concentration during the preceding time step was the highest experienced in this cell (30 ppm), it is that value that should be used to assess nonlethal injury. For $C = 30$ ppm, $\log_e C = 3.40$ and $Pr = 7.46$. Thus 99.3% of the exposed population received nonlethal toxic injury.

Since the concentration during the last time interval exceeds 3 ppm, 100% of the exposed population is also irritated.

Thus the assessment of toxic injury for the last time interval reads:

Dead	=	4%
Nonlethal Injury	=	99.3%
Irritation	=	100%

Correcting for situation (1) double counting, we obtain:

Dead	=	4%	= 4%
Nonlethal Injury	=	(99.3 - 4)%	= 95.3%
Irritation	=	[100 - (95.3 + 4)]%	= 0.7%

CHAPTER 7

EXAMPLES OF COMPUTER RUNS FOR AN URBAN AREA

Introduction

This chapter presents the results of a number of computer runs for the five cargoes used to exercise the model. The four spill sizes for each of these cargoes used in the test computer runs are shown in Table 7-1. The very large, large, and small sizes of spills were specified by the Risk Analysis Advisory Board of the U. S. Coast Guard. The medium-sized spill was chosen by ECI to be close to the geometric mean of the small spill and the large spill, to provide a spill size intermediate between these two widely different cases. Since the very large spill differs from the large spill by a factor of only two in most cases, the computer test runs used the large, medium, and small sizes. The large and very large spills may be expected to have a significant effect on the general population (over and above those directly concerned with the cargo transport - the ships' crews, marine terminal personnel, and fire and rescue personnel).

Below, we first take up one computer run and present the results in detail, with copies of the actual computer printout. Next the runs for LNG, chlorine, and anhydrous ammonia are discussed. For these three cargoes, the effects of spills of different sizes are compared, and, in addition, one other input variable is varied. For LNG, the wind direction was changed slightly, for chlorine the stability class was changed, and for ammonia the time step was varied. Unless otherwise explicitly stated, in all the test runs that follow, the wind is blowing toward 53° at 4 m/s, and the time step is 2 minutes for cases where the effects of toxicity are being considered and 1 minute when an explosion or flash fire is expected. All spills are located at the center of cell 3, a river or harbor cell. The last computer runs discussed are those where pool burning immediately follows the spill. Medium-sized spills of LNG, methyl alcohol, and gasoline are treated in this way. The spills of methyl alcohol and gasoline are very difficult to ignite because their evaporation rates are so slow. Finally, some important features of the VM, which have been delineated by these test runs, are discussed.

Before proceeding to the first computer run, a word about the demographic data and the grid system is in order. The demographic data from 40 census tracts have been used in these runs, and each census tract has been represented by a point. For cells which appear from the pattern of streets to have a uniform population density, the center of the cell has been approximated and used to represent this cell or tract. For cells which include a great deal of unpopulated area such as cemeteries, parks, marshes, lakes, etc., these areas have been excluded, and what appears to be the center-of-mass for the populated area has been chosen. For irregularly shaped tracts, however, the tract center has always been placed within the tract boundaries.

For these test runs, 50 cells were used, 10 river cells and 40 census tracts. The location of these cell centers is shown in Figure 7-1. These

	Very Large	Large	Medium	Small
LNG Liquified Natural Gas	2 ship tanks 50,000 m^3 20,750 MT	1 ship tank 25,000 m^3 10,375 MT	200 m^3 83 MT	500 gallons 2 m^3 0.8 MT
Chlorine (Cl_2)	1 barge load 1,200 short tons 727 m^3 1,090 MT	1 barge tank 300 short tons 182 m^3 272 MT	10 m^3 15 MT	1 short ton 0.60 m^3 0.90 MT
Anhydrous Ammonia (liquid NH_3)	2 ship tanks 20,000 m^3 16,340 MT	1 ship tank 10,000 m^3 8,170 MT	300 m^3 251 MT	10 m^3 8.2 MT
Methanol (Methyl Alcohol) (CH_3OH)	2 ship tanks 30,000 m^3 23,800 MT	1 ship tank 15,000 m^3 11,900 MT	120 m^3 95 MT	300 gallons 1.10 m^3 0.9 MT
Gasoline	2 ship tanks 4,000 long tons 5,820 m^3 4,060 MT	1 ship tank 2,000 long tons 2,910 m^3 2,030 MT	100 m^3 70 MT	2 long tons 2.9 m^3 2.0 MT

TABLE 7-1

SPILL SIZES (MT = METRIC TON = 10^3 kg)

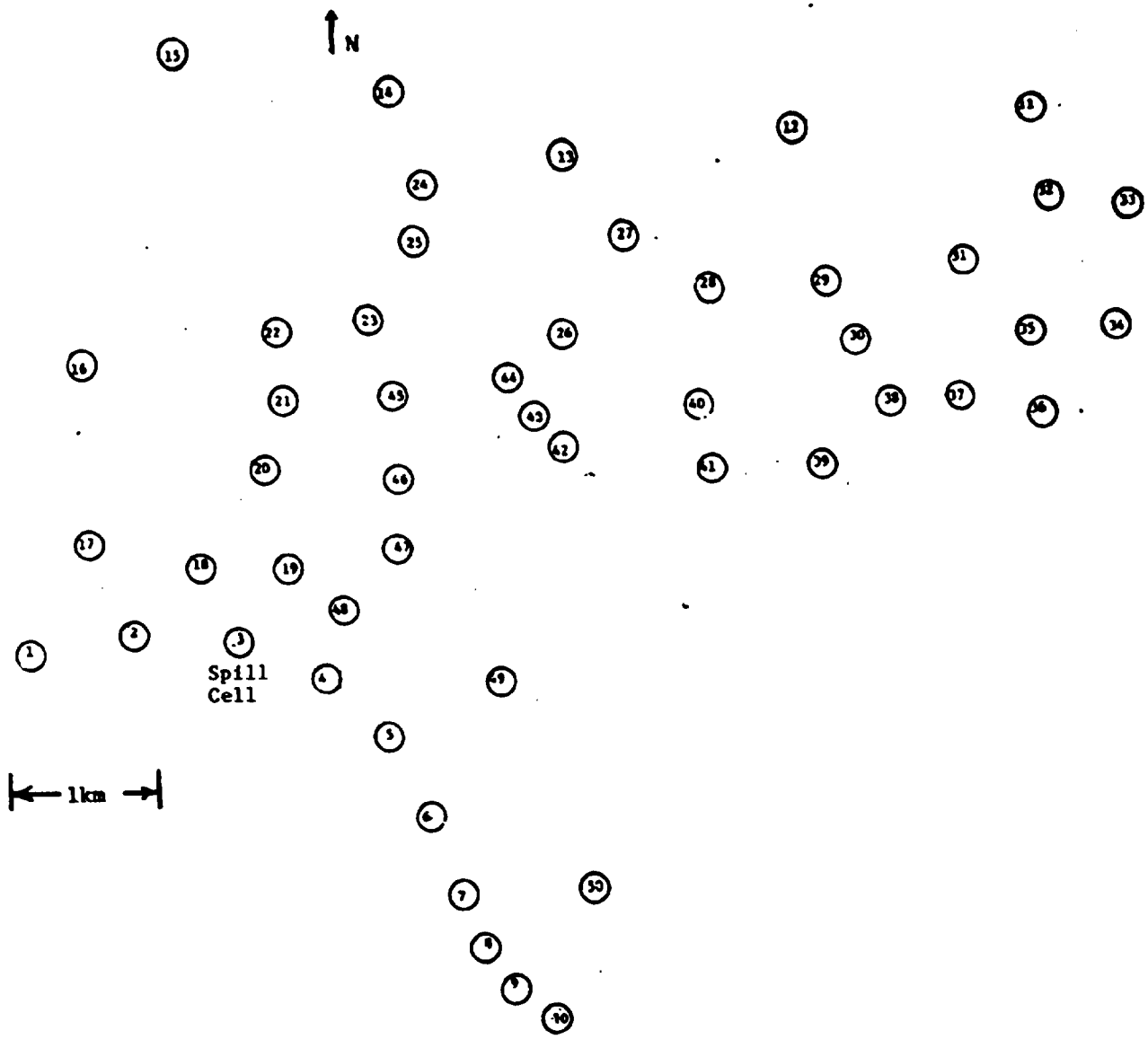

FIGURE 7-1

RELATIVE LOCATION OF THE GRID CELLS FOR THE TEST RUN
Cells 1 through 10 are river or harbor cells, which are assumed to contain no people or structures.

data were obtained from census statistics for an actual city. In this study, we considered only one phase of a more complete risk analysis - it was assumed here that a spill of a certain size has occurred. A complete analysis would consider the chances of such a spill taking place. Factors such as the number of ships or barges carrying this sort of cargo, their capacity, the type of waters which they are navigating, the other traffic in these waters, the visibility, currents, tides, and so on must be considered in determining the probability that a certain spill will occur in a particular place over a given period. As this project was to consider only the assessment of damage after the spill had occurred, consideration of this probability was not addressed, and any realistic appraisal of a spill must take the probability of occurrence into account. Therefore any analysis of the damage that may result from the transportation of hazardous cargoes by ship or barge cannot be made on the basis of this study alone. In the development of this model, wherever possible, approximations were made in a manner such that the damage would be overestimated. Thus the resulting damage assessments, although credible, may be somewhat high. The injury and damage figures which follow must be interpreted in this light.

The Output of an LNG Run

Tables 7-2 a to j present the details of a computer run for a medium-sized spill of LNG. Following printing of the properties file (not reproduced), the next page of output, Table 7-2a, gives spill and environmental information. The first column in Table 7-2a contains the number which is associated with each variable, and which is necessary for understanding the computer program operations, and provides a convenient way to refer uniquely to each variable. The second column contains an abbreviation of the variable name or a brief description of the variable. The third column gives the value of this variable, the fourth column lists the units of the value given for the variable, and the last column shows the origin of the value for the variable. Table 7-3 explains the designation printed to denote the source of the value for the variable.

The values of the variables are generally given in the CGS system. The letters N.A. mean that the units for that variable are not available in the file of units. If the units column is blank, then the variable has no units. The items listed under spill definition data are self-explanatory except for variable 2006 which is a flag which is set = 1 if adiabatic wall conditions in the tank are to be used and = 0 if isothermal wall conditions are to be used. Variable 2015 is the height of the hole above the water surface, and variable 2009 is the number of increments to be used in calculating the rate of spilling.

For the environmental data, variable 2058 gives the direction toward which the wind is blowing, in degrees. Variable 2017 is the stability or turbulence class, and variable 2014 is the height above the ground at which the concentrations are to be calculated. Variable 5022 is the ambient atmospheric pressure, and variable 5011 is the density of the water (a density different from 1.00 might occur due to salinity). Variable 2018 is a flag indicating whether the spill is restricted to a channel or is

LNG SPILL, MEDIUM, 200M3 = 83MT

SPILL DEFINITION DATA

1001	CHEM NAME	=	LNG			
2007	INITIAL MASS	=	0.830E 08	G	,	USER
2001	TANK VOLUME	=	0.200E 09	CM3	,	USER
2002	TANK HEIGHT	=	500.	CM	,	USER
2004	TEMP START	=	-151.	C	,	USER
2005	TANK PRESS	=	0.203E 07	G/CM2	,	USER
2006	ISO=0, ADB=1	=	1		,	USER
2003	HOLE HEIGHT	=	100.	CM	,	USER
2008	HOLE DIAM	=	50.0	CM	,	USER
2015	HT OVER SURF	=	0.0	CM	,	USER
2009	NUM MASS INC	=	200		,	DEFAULT

ENVIRONMENTAL DATA

2016	WIND SPEED	=	400.	CM/S	,	USER
2059	WIND TOWARD	=	50.0	DEG	,	USER
2017	ATMOS COND	=	4		,	USER
2014	COMB Z	=	100.	CM	,	USER
2054	AIR TEMP	=	15.0	C	,	DEFAULT
5022	PRESSURE AMB	=	0.101E 07	G/CM2	,	USER
2023	WATER TEMP	=	20.0	C	,	USER
5011	DENS WATER	=	1.00	G/CM3	,	USER
2018	CHL=1, RIV=2	=	2		,	USER
2020	CHANNEL WIDTH	=	0.610E 05	CM	,	USER
2047	STREAM VEL	=	100.	CM/S	,	DEFAULT
2043	DIF COEF H2O	=	50.0	CM2/S	,	DEFAULT
2022	FLUX,CM1,LM2	=	1		,	USER
2048	TIDAL VEL	=	50.0	CM/S	,	DEFAULT
2049	TIDAL PERIOD	=	0.518E 06	S	,	DEFAULT
2050	PHASE LAG	=	0.0	S	,	DEFAULT
2051	DECAY COEFF	=	0.0		,	DEFAULT
2052	HARKING FACT	=	0.300E-01	CM3	,	DEFAULT
2053	DIF COEF V A	=	0.100E 00	CM2/S	,	DEFAULT

TABLE 7-2a

SPILL DEFINITION AND ENVIRONMENTAL DATA

radial in nature. Variable 2043 is the diffusion coefficient of the liquid cargo in water. Variable 2022 is a flag for cryogenic spills to indicate whether the flux of heat from the water to the liquid cargo pool is constant (flux var = 1) or is limited by the formation of ice (flux var = 2). The next five variables are used by the submodel that calculates the mixing and dilution in rivers and tidal estuaries. The Manning factor concerns the roughness of the river bottom. Variable 2053 is the diffusion coefficient of the cargo vapor in air and is estimated by a subroutine if it is not given by the user.

Selected chemical and physical properties of the cargo are printed on the next page, Table 7-2b. Most of these variable names are sufficiently explanatory, but variables 1010, 1011, and 1012 are constants in the vapor pressure equation. The vapor pressure equation is of the form

$$P = 10^{\left[A - \frac{B}{(T+C)}\right]}$$

where P is the vapor pressure, T is the temperature, and A, B, C are the constants given, respectively, by 1010, 1011, and 1012.

Table 7-2c shows the page which displays the geographical data. The latitude and longitude columns originally contained the location of each cell center in degrees, minutes, and seconds, but in the sample page the degrees column has been omitted. The first column gives the cell number, by which all further reference to the cell is made. The second column contains identifying information about each cell. An "R" indicates a river or harbor cell. The other numbers may be block number, census tract numbers, or some other means of entering demographic information. The ignition code has been discussed in Chapter 4. Columns x and y give the location of the cell in a coordinate system in which the spill location is at the origin and the positive x axis is in the direction toward which the wind is blowing.

Table 7-2d shows the page containing spill and ignition information. Variables 4001, 4002, and 4003 give the amount of cargo spilled, and variable 4004 gives the time for the spill to take place. Variable 2038 is the average release rate, and variable 5027 gives the maximum dimension of the pool of liquid cargo on the water surface. This dimension is the radius for a circular pool and the upstream-downstream extent for a spill restricted by the channel (see variable 2018 in environmental data). Variable 5010 is a flag which is set = 0 if the puff (instantaneous source) air dispersion model is to be used and which is set = 1 if the plume (continuous source) model is to be used. If the user does not specify the value of the variable, the VM decides whether the puff model or the plume model is more appropriate.

The first six variables in the ignition data list are self-explanatory. Variables 5042 and 5043 give the effective values of the intensity and duration of the flash fire radiation. For an explosion, variable 5044 gives the mass of cargo vapor which exploded, variable 5045 gives the explosive yield in calories, and variable 5047 gives the yield equivalent in (short) tons of TNT. Variable 4019 is the mass of cargo remaining in the pool at the time of ignition. In this case, it is zero so that no pool burn can follow a flash fire or explosion. Thus the last four variables which concern the flame from the burning pool are zero as well.

LNG SPILL, MEDIUM, 200M3 = 83MT

CHEMICAL PROPERTIES DATA

1002	MOLEC WEIGHT	=	16.0	G/MOLE ,	USER
1003	BOIL TEM LIQ	=	-161.	C ,	CHM PROP
5012	FREEZING PT	=	-182.	C ,	USER
1004	DENS LIQ AMB	=	0.409	G/CM3 ,	CHM PROP
1005	VISCOSITY-BP	=	0.141E-02	D-S/CM2 ,	CHM PROP
1006	VISCOSITY-AM	=	0.102E-02	D-S/CM2 ,	CHM PROP
1007	HEAT CAPC LQ	=	0.864	CAL/G-C ,	CHM PROP
1008	SURF TENSION	=	14.0	D/CM ,	CHM PROP
1009	DEN FUEL VPR	=	0.716E-03	G/CM3 ,	COMPUTED
1010	VPR COEFF A	=	6.61	,	CHM PROP
1011	VPR COEFF B	=	390.	,	CHM PROP
1012	VPR COEFF C	=	266.	,	CHM PROP
1013	HEAT CAPC VP	=	0.02	CAL/G-C ,	EST PROP
1014	HEAT OF VPR	=	122.	CAL/G ,	EST PROP
1019	FLAME TEMP	=	800.	C ,	DEFAULT
1020	MOLE FRACTN	=	0.100E-01	,	DEFAULT
1021	LIQ DENS BP	=	0.424	G/CM3 ,	CHM PROP
5013	CONC, LO PCT	=	5.30	,	USER
5014	CONC, UP PCT	=	14.0	,	USER
5015	AIR/FUEL RAT	=	9.52	,	COMPUTED
5023	CONC, LO LIM	=	0.379E-04	G/CM3 ,	COMPUTED
5024	CONC, UP LIM	=	0.100E-03	G/CM3 ,	COMPUTED
5025	CONC, STOICH	=	0.680E-04	G/CM3 ,	COMPUTED
5016	HEAT COMBUST	=	-0.13[illegible]E 05	CAL/G ,	USER
5017	ADFLAME TEMP	=	0.188E 04	C ,	USER
5018	BURNING RATE	=	0.209E-01	CM/S ,	USER
5019	MOLES OXYGEN	=	2.00	,	USER
5020	FLASHPOINT	=	-161.	C ,	USER
5021	SPC HEAT RAT	=	1.40	,	USER
5002	MISCIBLE IND	=	0	,	USER
5003	REACTIVE IND	=	1	,	USER
5004	TOXICITY IND	=	0	,	USER

TABLE 7-2b

SELECTED CHEMICAL AND PHYSICAL PROPERTIES OF THE CARGO

GEOGRAPHICAL DATA

SPILL ORIGIN IS 5800 1500 WITH WIND TOWARD 50.0

CELL #	CELL ID	IGN CODE	LATITUDE	LONGITUDE	X, KM	Y, KM
1	201	0	5800	1540	-0.819	0.687
2	202	0	5800	1520	-0.410	0.344
3	203	0	5800	1500	0.0	0.0
4	204	0	5740	1420	0.424	-1.161
5	205	0	5720	1340	0.846	-2.321
6	206	0	5640	1330	0.257	-3.440
7	207	0	5620	1320	0.065	-4.085
8	208	0	5550	1310	-0.325	-4.966
9	209	0	5530	1300	-0.517	-5.611
10	210	0	5520	1250	-0.511	-6.019
11	201.00	-4	0100	0830	11.559	-2.446
12	202.00	-4	0100	1020	9.307	-0.556
13	203.00	-4	0100	1200	7.258	1.163
14	204.00	-4	0130	1320	6.215	3.247
15	205.00	-4	0200	1500	4.762	5.675
16	206.00	-4	0000	1600	1.153	3.869
17	207.00	-4	5840	1600	-0.435	1.977
18	208.00	-4	5820	1530	-0.019	1.225
19	209.00	-4	5830	1420	1.415	0.021
20	210.00	-4	5900	1430	1.806	0.902
21	211.00	-4	5940	1430	2.599	1.848
22	212.00	-4	0010	1420	3.400	2.386
23	213.00	-4	0010	1330	4.424	1.527
24	214.00	-4	0100	1300	6.030	2.194
25	215.00	-4	0030	1300	5.435	1.485
26	216.00	-4	0000	1200	6.068	-0.256
27	217.00	-4	0030	1140	7.074	0.109
28	218.00	-4	0120	1100	7.674	-0.814
29	219.00	-4	0000	1000	8.526	-2.318
30	220.00	-4	5940	1000	8.129	-2.792
31	221.00	-4	0050	0900	10.151	-2.376
32	222.00	-4	0020	0830	10.964	-3.155
33	223.00	-4	0030	0740	11.989	-4.015
34	224.00	-4	5940	0800	10.586	-4.354
35	225.00	-4	5940	0840	9.767	-4.167
36	226.00	-4	5900	0840	8.974	-5.113
37	227.00	-4	5920	0910	8.756	-4.124
38	228.00	-4	5920	0940	8.142	-3.609
39	229.00	-4	5940	1010	6.734	-4.039
40	230.00	-4	5930	1100	6.702	-1.998
41	231.00	-4	5930	1100	5.512	-3.417
42	232.00	-4	5940	1200	4.481	-2.148
43	233.00	-4	5920	1220	4.864	-0.859
44	234.00	-4	5930	1230	4.859	-0.451
45	235.00	-4	5930	1330	3.629	0.580
46	236.00	-4	5900	1320	3.034	-0.129
47	237.00	-4	5940	1330	2.638	-0.592
48	238.00	-4	5920	1400	1.627	-0.559
49	239.00	-4	5730	1300	1.864	-2.772
50	240.00	-4	5620	1220	1.234	-5.116

TABLE 7-2c

GEOGRAPHICAL DATA

LNG SPILL, MEDIUM, 200M3 = 834T

SPILL OUTPUT DATA

5009	SPILL CELL	=	3		,	COMPUTED
4001	TOT MASS GAS	=	0.1768 05	G	,	COMPUTED
4002	TOT MASS LIQ	=	0.654E 08	G	,	COMPUTED
4003	TOT VOL LIQ	=	0.154E 09	CM3	,	COMPUTED
4004	TIME OF REL	=	42.4	S	,	COMPUTED
2038	AVG ESC RATE	=	0.155E 07	G/S	,	COMPUTED
5027	LIQ REM TANK	=	0.175E 08	G	,	COMPUTED
4025	MAX DIA POOL	=	0.523E 04	CM	,	COMPUTED
4016	TIME TO EVAP	=	70.6	S	,	COMPUTED
4023	MASS VAP LIB	=	0.654E 08	G	,	SYSTEM
5010	FLAG,ISW,CSL	=	0		,	USER

IGNITION OUTPUT DATA

5040	TIME AT IGN	=	339.	S	,	COMPUTED
5007	IGNITN CELL	=	12		,	COMPUTED
5008	IGNITN CODE	=	-4		,	COMPUTED
5041	PUFF CENTER	=	0.135E 06	CM	,	COMPUTED
5028	SIGY,DISPERS	=	0.615E 04	CM	,	COMPUTED
5029	SIGZ,DISPERS	=	0.295E 04	CM	,	COMPUTED
5042	FL FIRE RADN	=	2.97	CAL/CM2S	,	COMPUTED
5043	FL FIRE TIME	=	4.54	S	,	COMPUTED
5044	MASS VAP EXP	=	0.257E 08	G	,	COMPUTED
5045	PCT VAP EXP	=	39.2		,	COMPUTED
5046	EXPL YIELD	=	0.697E 12	CAL	,	COMPUTED
5047	TNT EQUIV	=	557.	N.A.	,	COMPUTED
4010	VOL LIQ POOL	=	0.0	CM3	,	COMPUTED
2018	CHL=1, FIRE=2	=	2		,	USER
2019	CUR DIA POOL	=	0.5231 04	CM	,	SYSTEM
2020	CHANNEL WIDTH	=	0.610E 05	CM	,	USER
4007	DIAM FLAME	=	0.0	CM	,	DEFAULT
4008	FLAME ANGLE	=	0.0	RAD	,	DEFAULT
4018	POOL FLM HGT	=	0.0	CM	,	DEFAULT
5048	PL PUFF TIME	=	0.0	S	,	DEFAULT

TABLE 7-2d

SPILL AND IGNITION DATA

LNG SPILL, MEDIUM, 200M3 = 83MT

VAPOR CONCENTRATION, KG/M3

TIME(MIN)	CELL NUMBER 1	2	3	4	5	6	7	8	9	10
1.00	0.0	0.0	0.0	0.0	0.0	0.0	0.0	0.0	0.0	0.0
2.00	0.0	0.0	0.0	0.0	0.0	0.0	0.0	0.0	0.0	0.0
3.00	0.0	0.0	0.0	0.0	0.0	0.0	0.0	0.0	0.0	0.0
4.00	0.0	0.0	0.0	0.0	0.0	0.0	0.0	0.0	0.0	0.0
5.00	0.0	0.0	0.0	0.0	0.0	0.0	0.0	0.0	0.0	0.0
5.63	0.0	0.0	0.0	0.0	0.0	0.0	0.0	0.0	0.0	0.0

TIME(MIN)	CELL NUMBER 11	12	13	14	15	16	17	18	19	20
1.00	0.0	0.0	0.0	0.0	0.0	0.0	0.0	0.0	0.0	0.0
2.00	0.0	0.0	0.0	0.0	0.0	0.0	0.0	0.0	0.0	0.0
3.00	0.0	0.0	0.0	0.0	0.0	0.0	0.0	0.0	0.0	0.0
4.00	0.0	0.0	0.0	0.0	0.0	0.0	0.0	0.0	0.0	0.0
5.00	0.0	0.0	0.0	0.0	0.0	0.0	0.0	0.0	0.0	0.0
5.63	0.0	0.0	0.0	0.0	0.0	0.0	0.0	0.0	0.682E-04	0.0
									0.406E-01	0.0

TIME(MIN)	CELL NUMBER 21	22	23	24	25	26	27	28	29	30
1.00	0.0	0.0	0.0	0.0	0.0	0.0	0.0	0.0	0.0	0.0
2.00	0.0	0.0	0.0	0.0	0.0	0.0	0.0	0.0	0.0	0.0
3.00	0.0	0.0	0.0	0.0	0.0	0.0	0.0	0.0	0.0	0.0
4.00	0.0	0.0	0.0	0.0	0.0	0.0	0.0	0.0	0.0	0.0
5.00	0.0	0.0	0.0	0.0	0.0	0.0	0.0	0.0	0.0	0.0
5.63	0.0	0.0	0.0	0.0	0.0	0.0	0.0	0.0	0.0	0.0

TIME(MIN)	CELL NUMBER 31	32	33	34	35	36	37	38	39	40
1.00	0.0	0.0	0.0	0.0	0.0	0.0	0.0	0.0	0.0	0.0
2.00	0.0	0.0	0.0	0.0	0.0	0.0	0.0	0.0	0.0	0.0
3.00	0.0	0.0	0.0	0.0	0.0	0.0	0.0	0.0	0.0	0.0
4.00	0.0	0.0	0.0	0.0	0.0	0.0	0.0	0.0	0.0	0.0
5.00	0.0	0.0	0.0	0.0	0.0	0.0	0.0	0.0	0.0	0.0
5.63	0.0	0.0	0.0	0.0	0.0	0.0	0.0	0.0	0.0	0.0

TIME(MIN)	CELL NUMBER 41	42	43	44	45	46	47	48	49	50
1.00	0.0	0.0	0.0	0.0	0.0	0.0	0.0	0.0	0.0	0.0
2.00	0.0	0.0	0.0	0.0	0.0	0.0	0.0	0.0	0.0	0.0
3.00	0.0	0.0	0.0	0.0	0.0	0.0	0.0	0.0	0.0	0.0
4.00	0.0	0.0	0.0	0.0	0.0	0.0	0.0	0.0	0.0	0.0
5.00	0.0	0.0	0.0	0.0	0.0	0.0	0.0	0.0	0.0	0.0
5.63	0.0	0.0	0.0	0.0	0.0	0.0	0.0	0.0	0.0	0.0

TABLE 7-2e

CONCENTRATIONS IN THE CELLS (AS COMPUTED AT THE CELL CENTERS) FOR EACH TIME STEP

LNG SPILL, MEDIUM, 200M3 = 83MT

VAPOR CONCENTRATION, PPM

	CELL NUMBER									
TIME(MIN)	1	2	3	4	5	6	7	8	9	10
1.00	0.0	0.0	0.0	0.0	0.0	0.0	0.0	0.0	0.0	0.0
2.00	0.0	0.0	0.0	0.0	0.0	0.0	0.0	0.0	0.0	0.0
3.00	0.0	0.0	0.0	0.0	0.0	0.0	0.0	0.0	0.0	0.0
4.00	0.0	0.0	0.0	0.0	0.0	0.0	0.0	0.0	0.0	0.0
5.00	0.0	0.0	0.0	0.0	0.0	0.0	0.0	0.0	0.0	0.0
5.63	0.0	0.0	0.0	0.0	0.0	0.0	0.0	0.0	0.0	0.0

	CELL NUMBER									
TIME(MIN)	11	12	13	14	15	16	17	18	19	20
1.00	0.0	0.0	0.0	0.0	0.0	0.0	0.0	0.0	0.0	0.0
2.00	0.0	0.0	0.0	0.0	0.0	0.0	0.0	0.0	0.0	0.0
3.00	0.0	0.0	0.0	0.0	0.0	0.0	0.0	0.0	0.0	0.0
4.00	0.0	0.0	0.0	0.0	0.0	0.0	0.0	0.0	0.0	0.0
5.00	0.0	0.0	0.0	0.0	0.0	0.0	0.0	0.0	0.100E 03	0.0
5.63	0.0	0.0	0.0	0.0	0.0	0.0	0.0	0.0	0.598E 05	0.0

	CELL NUMBER									
TIME(MIN)	21	22	23	24	25	26	27	28	29	30
1.00	0.0	0.0	0.0	0.0	0.0	0.0	0.0	0.0	0.0	0.0
2.00	0.0	0.0	0.0	0.0	0.0	0.0	0.0	0.0	0.0	0.0
3.00	0.0	0.0	0.0	0.0	0.0	0.0	0.0	0.0	0.0	0.0
4.00	0.0	0.0	0.0	0.0	0.0	0.0	0.0	0.0	0.0	0.0
5.00	0.0	0.0	0.0	0.0	0.0	0.0	0.0	0.0	0.0	0.0
5.63	0.0	0.0	0.0	0.0	0.0	0.0	0.0	0.0	0.0	0.0

	CELL NUMBER									
TIME(MIN)	31	32	33	34	35	36	37	38	39	40
1.00	0.0	0.0	0.0	0.0	0.0	0.0	0.0	0.0	0.0	0.0
2.00	0.0	0.0	0.0	0.0	0.0	0.0	0.0	0.0	0.0	0.0
3.00	0.0	0.0	0.0	0.0	0.0	0.0	0.0	0.0	0.0	0.0
4.00	0.0	0.0	0.0	0.0	0.0	0.0	0.0	0.0	0.0	0.0
5.00	0.0	0.0	0.0	0.0	0.0	0.0	0.0	0.0	0.0	0.0
5.63	0.0	0.0	0.0	0.0	0.0	0.0	0.0	0.0	0.0	0.0

	CELL NUMBER									
TIME(MIN)	41	42	43	44	45	46	47	48	49	50
1.00	0.0	0.0	0.0	0.0	0.0	0.0	0.0	0.0	0.0	0.0
2.00	0.0	0.0	0.0	0.0	0.0	0.0	0.0	0.0	0.0	0.0
3.00	0.0	0.0	0.0	0.0	0.0	0.0	0.0	0.0	0.0	0.0
4.00	0.0	0.0	0.0	0.0	0.0	0.0	0.0	0.0	0.0	0.0
5.00	0.0	0.0	0.0	0.0	0.0	0.0	0.0	0.0	0.0	0.0
5.63	0.0	0.0	0.0	0.0	0.0	0.0	0.0	0.0	0.0	0.0

TABLE 7-2f

CONCENTRATIONS IN THE CELLS (AS COMPUTED AT THE CELL CENTERS) FOR EACH TIME STEP

Tables 7-2e and 7-2f list the concentrations in the cells (as computed at the cell centers) for each time step. In this case, the ignition subroutine has calculated that the cloud ignited at 5.63 minutes, so this time is listed in addition to the 1-minute time steps. Table 7-2e gives the concentrations in kg/m^3, and Table 7-2f gives them in parts per million (by volume).

Table 7-2g lists the results of both the flash fire and the explosion. For these computer runs, the program was altered so that, if ignition occurred, the results of both were computed in the same run, which saved considerable computer time. The distance listed is the distance from the puff center at the time of ignition. Thermal radiation from a flash fire was calculated only for those cells in which the concentration was above the lower flammable limit. Since the vapor cloud ignited at cell 19, the first cell in its path in this example, there is a non-zero radiation value only for that cell. The liquid pool had completely evaporated prior to ignition, so there was no pool burning in this example.

Tables 7-2h and 7-2i list the damage and injuries which resulted from the explosion, first for each cell and then a summary for all cells. Table 7-2j shows the analogous information for the flash fire case.

Results of Test Runs

The test runs for the five cargoes used to exercise the VM are listed in Table 7-4. There are six or more runs for LNG, ammonia, and chlorine, but since the clouds resulting from methyl alcohol and gasoline spills did not have high enough concentrations to ignite when they reached the first land cell downwind, for these two cargoes only the case where pool burning was initiated immediately after the spill was run. Methyl alcohol, gasoline, and LNG are not toxic, so the hazard from them is due to fire or explosion. Chlorine is toxic but incombustible, so the hazard from chlorine stems from inhalation only. Ammonia is both toxic and flammable, so all types of damage may result. The concentrations of ammonia which result in death in a minute or so may be considerably below the lower flammable limiting concentration. Ammonia inhalation will cause death in a minute or so at concentrations which are below the lower flammable limiting concentration, so for the cells on the x axis (directly in the path of the cloud) the people are killed by the toxic effects before the explosion occurs. After an explosion or flash fire, pool burning takes place if there is any liquid remaining in the pool. No injuries or damage to structures resulted from the burning pools because the pool in the center of a water cell was more than 1 km from the nearest land cell where the injuries and damage were assessed.

The results for the LNG, chlorine, and ammonia runs are discussed in the following sections, and then the three cases of immediate pool burning are taken up. Finally, a few points concerning certain features of the VM are discussed.

LNG Spills

The results of the simulations of six spills of LNG are shown in Table 7-5. For each of the three sizes of spills, the VM was run with the

LNG SPILL, MEDIUM, 200M3 = 83MT

IGNITION AT TIME(MIN) = 9.63

CELL #	EXPLOSION PEAK OVERPRESSURE N/M2	EXPLOSION IMPULSE MS/M2	EXPLOSION DISTANCE KM	FLASH FIRE THERMAL RAD'N J/M2S TEFF(MIN) = 0.08	POOL BURNING THERMAL RAD'N J/M2S TEFF(MIN) = 0.0
1	3371.	528.	2.28	0.	0.
2	4437.	671.	1.79	0.	0.
3	5931.	864.	1.35	0.	0.
4	5366.	791.	1.49	0.	0.
5	3172.	502.	2.38	0.	0.
6	1427.	264.	3.61	0.	0.
7	1003.	201.	4.28	0.	0.
8	1049.	192.	5.24	0.	0.
9	1071.	187.	5.91	0.	0.
10	953.	169.	6.30	0.	0.
11	620.	116.	10.50	0.	0.
12	652.	121.	7.98	0.	0.
13	1033.	182.	6.02	0.	0.
14	1090.	190.	5.85	0.	0.
15	876.	157.	6.62	0.	0.
16	1217.	234.	3.87	0.	0.
17	2651.	433.	2.66	0.	0.
18	4332.	653.	1.34	0.	0.
19	1235999.	11013.	0.07	124458.	0.
20	9092.	1076.	1.01	0.	0.
21	3464.	540.	2.23	0.	0.
22	1937.	336.	3.15	0.	0.
23	1559.	209.	3.43	0.	0.
24	1017.	189.	5.17	0.	0.
25	980.	197.	4.35	0.	0.
26	930.	185.	4.72	0.	0.
27	1129.	196.	5.72	0.	0.
28	930.	166.	6.40	0.	0.
29	704.	130.	7.54	0.	0.
30	729.	135.	7.33	0.	0.
31	620.	116.	9.26	0.	0.
32	620.	116.	10.12	0.	0.
33	620.	116.	11.37	0.	0.
34	620.	116.	10.43	0.	0.
35	620.	116.	9.39	0.	0.
36	620.	116.	9.18	0.	0.
37	620.	116.	8.48	0.	0.
38	686.	127.	7.69	0.	0.
39	850.	153.	6.73	0.	0.
40	1133.	196.	5.71	0.	0.
41	1120.	199.	5.38	0.	0.
42	1272.	242.	3.80	0.	0.
43	1420.	263.	3.62	0.	0.
44	1497.	274.	3.54	0.	0.
45	3219.	508.	2.35	0.	0.
46	4686.	705.	1.69	0.	0.
47	5630.	829.	1.42	0.	0.
48	16063.	1772.	0.62	0.	0.
49	2399.	399.	2.82	0.	0.
50	996.	187.	5.12	0.	0.

TABLE 7-2g

RESULTS OF BOTH FLASH FIRE AND EXPLOSION

TIME = 5.6 MIN	CELL # 14				CELL # 16				CELL # 17				CELL # 18			
	% - PEOPLE - #				% - PEOPLE - #				% - PEOPLE - #				% - PEOPLE - #			
	IN	OUT	IN	OUT	IN	OUT	IN	OUT	IN	OUT	IN	OUT	IN	OUT	IN	OUT
BLAST DEATHS (E1)	0	0	0	0	0	0	0	0	0	0	0	0	0	0	0	0
IMPACT DEATHS (E2)	0	0	0	0	0	0	0	0	0	0	0	0	0	0	0	0
BLAST INJURY (E3)	0	0	0	0	0	0	0	0	0	0	0	0	0	0	0	0
IMPACT INJURY (E4)	0	0	0	0	0	0	0	0	0	0	0	0	0	0	0	0
FRAGMENT INJURY(E5)	0	0	0	0	0	0	0	0	0	0	0	0	0	0	0	0
MULTIPLE INJURY(E6)	0	0	0	0	0	0	0	0	0	0	0	0	0	0	0	0
	STRUCTURES				STRUCTURES				STRUCTURES				STRUCTURES			
	%	#	$		%	#	$		%	#	$		%	#	$	
STRUCTURAL DMG (S1)	0	0	0		0	0	0		0	0	0		0	0	0	
GLASS BREAKAGE (S2)	0	0	0		0	0	0		13	105	0		60	538	0	

TIME = 5.6 MIN	CELL # 19				CELL # 20				CELL # 21				CELL # 22			
	% - PEOPLE - #				% - PEOPLE - #				% - PEOPLE - #				% - PEOPLE - #			
	IN	OUT	IN	OUT	IN	OUT	IN	OUT	IN	OUT	IN	OUT	IN	OUT	IN	OUT
BLAST DEATHS (E1)	0	109	0	921	0	0	0	0	0	0	0	0	0	0	0	0
IMPACT DEATHS (E2)	0	0	0	0	0	0	0	0	0	0	0	0	0	0	0	0
BLAST INJURY (E3)	0	0	0	0	0	0	0	1	0	0	0	0	0	0	0	0
IMPACT INJURY (E4)	0	0	0	0	0	0	0	0	0	0	0	0	0	0	0	0
FRAGMENT INJURY(E5)	0	0	0	0	0	1	0	19	0	0	0	0	0	0	0	0
MULTIPLE INJURY(E6)	0	0	0	0	0	0	0	0	0	0	0	0	0	0	0	0
	STRUCTURES				STRUCTURES				STRUCTURES				STRUCTURES			
	%	#	$		%	#	$		%	#	$		%	#	$	
STRUCTURAL DMG (S1)	100	561	8963800		1	6	114600		0	0	0		0	0	0	
GLASS BREAKAGE (S2)	0	0	0		97	1060	0		36	315	0		2	12	0	

TIME = 5.6 MIN	CELL # 23				CELL # 27				CELL # 40				CELL # 41			
	% - PEOPLE - #				% - PEOPLE - #				% - PEOPLE - #				% - PEOPLE - #			
	IN	OUT	IN	OUT	IN	OUT	IN	OUT	IN	OUT	IN	OUT	IN	OUT	IN	OUT
BLAST DEATHS (E1)	0	0	0	0	0	0	0	0	0	0	0	0	0	0	0	0
IMPACT DEATHS (E2)	0	0	0	0	0	0	0	0	0	0	0	0	0	0	0	0
BLAST INJURY (E3)	0	0	0	0	0	0	0	0	0	0	0	0	0	0	0	0
IMPACT INJURY (E4)	0	0	0	0	0	0	0	0	0	0	0	0	0	0	0	0
FRAGMENT INJURY(E5)	0	0	0	0	0	0	0	0	0	0	0	0	0	0	0	0
MULTIPLE INJURY(E6)	0	0	0	0	0	0	0	0	0	0	0	0	0	0	0	0
	STRUCTURES				STRUCTURES				STRUCTURES				STRUCTURES			
	%	#	$		%	#	$		%	#	$		%	#	$	
STRUCTURAL DMG (S1)	0	0	0		0	0	0		0	0	0		0	0	0	
GLASS BREAKAGE (S2)	1	4	0		0	0	0		0	0	0		0	0	0	

TIME = 5.6 MIN	CELL # 42				CELL # 43				CELL # 44				CELL # 45			
	% - PEOPLE - #				% - PEOPLE - #				% - PEOPLE - #				% - PEOPLE - #			
	IN	OUT	IN	OUT	IN	OUT	IN	OUT	IN	OUT	IN	OUT	IN	OUT	IN	OUT
BLAST DEATHS (E1)	0	0	0	0	0	0	0	0	0	0	0	0	0	0	0	0
IMPACT DEATHS (E2)	0	0	0	0	0	0	0	0	0	0	0	0	0	0	0	0
BLAST INJURY (E3)	0	0	0	0	0	0	0	0	0	0	0	0	0	0	0	0
IMPACT INJURY (E4)	0	0	0	0	0	0	0	0	0	0	0	0	0	0	0	0
FRAGMENT INJURY(E5)	0	0	0	0	0	0	0	0	0	0	0	0	0	0	0	0
MULTIPLE INJURY(E6)	0	0	0	0	0	0	0	0	0	0	0	0	0	0	0	0
	STRUCTURES				STRUCTURES				STRUCTURES				STRUCTURES			
	%	#	$		%	#	$		%	#	$		%	#	$	
STRUCTURAL DMG (S1)	0	0	0		0	0	0		0	0	0		0	0	0	
GLASS BREAKAGE (S2)	0	1	0		0	2	0		0	4	0		29	337	0	

TABLE 7-2h

CELL BY CELL ASSESSMENT OF INJURY AND DAMAGE CAUSED BY EXPLOSION

TIME = 5.6 MIN	CELL # 46				CELL # 47				CELL # 48				CELL # 49			
	% - PEOPLE - #				% - PEOPLE - #				% - PEOPLE - #				% - PEOPLE - #			
	IN	OUT	IN	OUT	IN	OUT	IN	OUT	IN	OUT	IN	OUT	IN	OUT	IN	OUT
BLAST DEATHS (E1)	0	0	0	0	0	0	0	0	0	0	0	0	0	0	0	0
IMPACT DEATHS (E2)	0	0	0	0	0	0	0	0	0	0	0	0	0	0	0	0
BLAST INJURY (E3)	0	0	0	0	0	0	0	0	0	2	0	40	0	0	0	0
IMPACT INJURY (E4)	0	0	0	0	0	0	0	0	0	0	0	0	0	0	0	0
FRAGMENT INJURY (E5)	0	0	0	0	0	0	0	1	0	41	0	1011	0	0	0	0
MULTIPLE INJURY (EM)	0	0	0		0	0	0	0	0	1	0	29	0	0	0	0
	STRUCTURES				STRUCTURES				STRUCTURES				STRUCTURES			
	%	#	$		%	#	$		%	#	$		%	#	$	
STRUCTURAL DMG (S1)	0	0	0		0	0	0		30	419	8044800		0	0	0	
GLASS BREAKAGE (S2)	68	1368	0		84	920	0		70	972	0		8	233	0	

LNG SPILL, MEDIUM, 200M3 = 83MT

SUMMARY — ALL CELLS

	PEOPLE
BLAST DEATHS (E1)	921
IMPACT DEATHS (E2)	0
BLAST INJURY (E3)	41
IMPACT INJURY (E4)	0
FRAGMENT INJURY (E5)	1031
MULTIPLE INJURY (EM)	29

TOTAL DEATHS	921
TOTAL INJURIES	1101

	# - STRUCTURES - $	
STRUCTURAL DMG (S1)	986	17023200
GLASS BREAKAGE (S2)	5871	0

TOTAL STRUCTURES	986
TOTAL VALUE	$17023200

TABLE 7-21

CONTINUATION OF CELL BY CELL ASSESSMENT OF INJURY AND DAMAGE CAUSED BY EXPLOSION AND THE SUMMARY FOR ALL CELLS

TIME = 9.6 MIN CELL # 19

	% - PEOPLE - #			
	IN	OUT	IN	OUT
FL FIRE DEATHS (F1)	0	67	0	617
FL FIRE BURNS (F2)	1ST DEGREE BURNS			
	STRUCTURES			
	%	#	$	
FL FIRE IGNTN (F3)	25	140	2212000	

LNG SPILL, MEDIUM, 200M3 @ 83MT

SUMMARY ALL CELLS

	PEOPLE		
FL FIRE DEATHS (F1)	617		
		TOTAL DEATHS	617
		TOTAL INJURIES	0
	# - STRUCTURES - $		
FL FIRE IGNTN (F3)	140	2212000	
		TOTAL STRUCTURES	140
		TOTAL VALUE	2212000

TABLE 7-2j

CELL BY CELL ASSESSMENT OF INJURY
AND DAMAGE CAUSED BY FLASH FIRE
AND THE SUMMARY FOR ALL CELLS

Hierarchical Source Code	Source Designation Printed	Source of Value
0	---	Value is missing in the Chemical Properties File.
1	DEFAULT	Value is taken from the default file.
2	EST PROP	Value taken from the Chemical Properties File is estimated.
3	CHM PROP	Value taken from the Chemical Properties File is an accepted value.
4	COMPUTED	Value is computed by the program.
5	USER	Value is supplied by the user.
6	SYSTEM	Value is computed by the program and will override a user-supplied code.

TABLE 7-3

DESIGNATION DENOTING SOURCE OF VALUE FOR THE VARIABLE

The source designation printed indicates the source of the value printed out for a given variable. Each value has associated with it a hierarchical source code; for a given variable a value with a numerically higher source code will override (replace) a value with a numerically lower source code.

Case	Definition of Test Case								Results																				
	Case Parameters		Environmental Parameters					Int. Para.	To Ignition Or End Of Simulation		Portion of Evaporated Mass Combusting	Explosion					Flash Fire			Pool Burning				Toxicity		Case
		Amount in tank metric tons	Wind Speed m/s	Wind Dir. °	Stab. Class	Ign. Type	Time Step Δt min.	Time min.	Distance m		Yield tons of TNT	Deaths #	Injuries #	Structures Damaged MS	Structures with Broken Windows #	Deaths #	Injuries # Cells Assessed	Structures Ignited MS	Amount in Pool m²	Flame Height m	Burning Time min.	Structures Ignited MS	Deaths #	Injuries #	
L1	[illegible]	[illegible]	4	50	4	E	1	4.2	1,010	12.1	40,700	984	77,542	129.5	29,490				7,590	455	1.1	0			L1
L2	[illegible]	20,750	4	53	4	E	1	4.2	1,010	12.1	41,200	1,238	77,753	131.1	29,628				7,200	456	1.0	0			L2
L3	[illegible]	20,750	4	53	4	F	1	4.2	1,010	12.1	41,200					534	1	2.2	7,200	456	1.0	0			L3
L4	[illegible]	93	4	50	4	E	1	5.6	1,350	39.2	657	921	1,101	17.0	5,871										L4
L5	[illegible]	83	4	50	4	F	1	5.6	1,350	39.2	657					617	1	2.2							L5
L6	[illegible]	83	4	53	4	E	1			DNI															L6
L7	[illegible]	83	4	53	4	F	1			DNI															L7
L8	[illegible]	0.83	4	50	4	E	1			DNI															L8
L9	[illegible]	0.83	4	50	4	F	1			DNI															L9
L10	[illegible]	0.83	4	53	4	E	1			DNI															L10
L11	[illegible]	0.83	4	53	4	F	1			DNI															L11
L12	[illegible]	22	4	53	4	P	1	1											43	18	0.4	0			L12
M1	Methanol	95	4	53	4	P	1	1											117	18	117	0			M1
[illegible]	Gasoline	70	4	53	4	P	1	1											100	55	5.8	0			[illegible]
A1	Ammonia	16,350	4	53	4	E	1	11.8	2,600	7.9	4,110	T	11,419	68.3	15,720				15,200	146	19.5	0	6,726	[illegible]	A1
A2	Ammonia	16,350	4	53	4	F	1	11.8	2,800	7.9						T	T	9.23	15,200	146	19.5	0	6,726	[illegible]	A2
A3	Ammonia	16,350	4	53	4	N	2	30	7,200														18,151	[illegible]	A3
A4	[illegible]monia	251	4	53	4	E	1	15	3,600	DNI													4,554	[illegible]	A4
A5	[illegible]monia	251	4	53	4	F	1	15	3,600	DNI													4,554	[illegible]	A5
A6	[illegible]monia	251	4	53	4	N	2	30	7,200														8,033	[illegible]	A6
A7	[illegible]monia	8.2	4	53	4	E	1	15	3,600	DNI													0	0	A7
A8	[illegible]monia	8.2	4	53	4	F	1	15	3,600	DNI													0	0	A8
A9	[illegible]monia	8.2	4	53	4	N	2	30	7,200														0	0	A9
C1	[illegible]rine	1,030	4	53	4	N	2	30	7,200														13,679	337	C1
C2	[illegible]rine	1,030	5	53	3	N	2	25	7,200														28,712	8,946	C2
C3	[illegible]rine	35	4	53	4	N	2	30	7,200														9,095	845	C3
C4	[illegible]rine	35	4	53	3	N	2	30	7,200														1,000	6,736	C4
C5	[illegible]rine	35	5	53	3	N	2	24	7,200														340	7,425	C5
C6	Chlorine	0.9	4	53	4	N	2	30	7,200														277	5,748	C6
C7	Chlorine	0.9	5	53	3	N	2	24	7,200														0	2	C7

TABLE 7-4

TEST RUNS FOR THE URBAN GRID

These test runs were made to exercise the VM. These results do not necessarily represent the results that would be obtained from a more complete VM, since the model in its current state of development (a) does not treat all damage mechanisms rigorously, (b) does not model all aspects of spill development with sophistication sufficient to guarantee very precise results, and (c) does not give a completely realistic treatment to population density and shifts of density with time of day and season of the year.

KEY TO TABLE 7-4

COLUMN HEADING	ABBREVIATION	MEANING
Cargo	LNG	Liquefied natural gas.
Ignition Type	E	Ignition source set to produce an explosion.
	F	Ignition source set to produce a flash fire.
	P	Pool burning initiated at the first time step.
	N	Ignition not allowed (for NH_3) or not possible (for Cl_2).
Portion of Evaporated Mass Combusting	DNI	Fuel cloud did not ignite.
Deaths or Injuries	T	Deaths or injuries would have occurred but the population of the cell was already dead from toxic inhalation.
Toxicity/Injuries	NA	Toxic injuries are not assessed in the VM for this substance (NH_3).

Case Number	Amount (Metric Tons)	Wind Direction (Toward) (°)	Ignition		Portion of Mass Combustible (%)	Explosive Yield (Tons of TNT)	Explosion				Flash Fire	
			Time (min)	Distance (m)			Deaths (#)	Injuries (#)	Structural Damage (M$)	Structures with Broken Windows (#)	Deaths (#)	Structures Ignited (M$)
L1	20,750	50	4.2	1,010	12.1	40,700	984	77,542	129.5	29,490		
L2, L3	20,750	53	4.2	1,010	12.1	41,200	1,238	77,753	131.1	29,628	534	2.2
L4, L5	83	50	5.6	1,350	39.2	657	921	1,101	17.0	5,871	617	2.2
L6, L7	83	53	DID NOT IGNITE									
L8, L9	0.8	50	DID NOT IGNITE									
L10, L11	0.8	53	DID NOT IGNITE									

TABLE 7-5

LNG SPILLS

Distance is the distance from the spill location to the center of the puff at the time that ignition occurred.

wind toward 50° and then with the wind toward 53°. When the vapor cloud from the very large spill detonated at cell 19, the resulting explosion was calculated to have been immense - equivalent to about 40,000 tons of TNT. Such explosions are known to be unlikely; moreover, they are not known to be physically possible. Bear in mind that there are few LNG ships in operation and few planned compared to the total number of all ships or even all tankers operating. These ships will call at few ports and are expected to be subject to unusual operating constraints in the port calls they do make. There are very few ways in which any spill, much less a major spill, can occur from such specially designed vessels, and exceptional precautions are taken to preclude such an event. Although the probability of such a rare event as an LNG spill is difficult and expensive to estimate reliably, it is known to be very low relative to the total number of LNG ships (say, 42 to 85) which will operate in U.S. waters (a small part of their total operating time) over the full life cycle of LNG importation (say, 15 to 25 years). The next point to bear in mind is that, even if an LNG spill were to occur, it is far more likely that the material would burn in the immediate vicinity of the ship than that a cloud of vapor would disperse away from the ship. Even if the material did disperse, it would enter a populated area only if the wind direction carried it to that area rather than away from such an area. Even if an LNG vapor cloud were to approach a populated area, it appears far more likely that it would be ignited when only the leading edge of the cloud was in that area and while the bulk of the cloud was still over water. If the cloud were to move over a populated area without ignition, as it was warmed by the air and ground, it would tend to rise (at ambient temperatures LNG is lighter than air) and to disperse harmlessly into the atmosphere. Even if the cloud were to be ignited while over a populated area and before its natural buoyancy carried it up and away from people and buildings, it is known that it could burn in a flash fire or deflagration; it is not known whether unconfined parts of the cloud could detonate. In this respect, methane (the major component of commercial LNG) is less dangerous than some other hydrocarbon vapors, such as propane or ethylene oxide. A possibility that has not been fully researched (and would be very expensive to research) is that a detonation from a confined explosion of a portion of the methane cloud (see Appendix C5) could accelerate the deflagrative combustion wave in portions of the unconfined cloud to supersonic speeds, thus producing detonation(s) there. Also, it is not known how much of the unconfined cloud would be detonated or how much of the cloud would be impacted by the initiating detonation wave.

Cases L1 and L2 in Table 7-4, then, represent hypothetical events which may not be even physically possible and which are definitely extremely unlikely ever to happen. Why, then, should such cases be explored at all in a model? If it can be established that even very rare types of accidents will not result in major damage, then unnecessarily expensive safety precautions and/or scientific research on safety problems can be avoided. Where major accidents cannot be conclusively ruled out, then careful consideration of safety precautions, accident probability estimates, and/or further scientific research is indicated. Even so, no final decisions can be made on the basis of this model alone. If the risks (probability times consequences) are apparently comparable to other dangers to the public, then deciding factors may be the the benefits of an activity and/or cost-effective application of additional safety measures.

One final caution is that extensive scientific research can be time-consuming as well as expensive; frequently decisions are time-limited such that it is unfeasible to obtain all of the scientific input desirable when it is needed. All production and transportation of hazardous materials involve some risk; the key question is whether drastic constraints affecting the economics of these materials involve even greater risks.

The reason that there were more deaths for the very large spill with the wind toward 53° is that the ignition time varied by two seconds and this changed the yield slightly. The extra yield was just enough to increase the effect in cell 48 from 2% dead to 13% dead. As cell 48 is a very densely populated cell, this accounts for the excess deaths in the case where the wind was blowing toward 53°. With the wind toward 50°, the flash fire was assessed to have killed 58% of the population in cell 19, and the radiation level there was high enough to have caused first-degree burns on the remainder of the persons in the cell if they had been exposed.

The LNG spills of medium size are of interest, because of the fact that ignition occurred with the wind toward 53° and did not occur when the wind was toward 50°. In the case which ignited, the center of cell 19 was 21 m off the x axis, and, in the case where it failed to ignite, the center of cell 19 was 95 m off the x axis. Early in the dispersion of a puff of gas, when the diffusion coefficients are still small, this difference can be enough for the concentration to reach the flammable range in one case and fail to reach it in another. The concentration was evaluated at 6 minutes when the puff center was only 25 m from the cell center, so adjusting the time step would have no effect on the case which failed to ignite. For the neutral stability condition, at 1400 m, σ_y is approximately equal to 65 m thus in one case the cell center was about 0.3 σ_y from the puff center and in the case with the wind from 50° the cell center was about 1.5 σ_y from the puff center, so the failure to ignite is understandable. For the 50° case, cell 46 was only 30 m from the x axis but was 3037 m from the spill location, and, by the time the puff had traveled that far, it was too diffuse to ignite. The LNG spills of small size resulted in a vapor cloud which was not concentrated enough to ignite at the first downwind cell.

Chlorine Spills

For chlorine, the results of seven computer runs are shown in Table 7-6. For all three spill sizes, there are results for a wind speed of 5 m/s and unstable conditions as well as for a wind speed of 4 m/s and neutral conditions. In addition, the medium size spill was run for a wind speed of 4 m/s and unstable conditions. With stability class 4 (neutral), the values of σ_y and σ_z are smaller than they are for stability class 3 (unstable), so the resulting puff is smaller and more dense after traveling the same distance. Whether the smaller, denser puff affects more people depends on the size of the spill. Table 7-6 shows that the small spill of 900 kg is calculated to have killed 277 people and injured over 5000 people in the neutral case, but, in the unstable case, the more diffuse puff was too dilute to cause any deaths and is calculated to have injured only two people. For the very large spill, on the other hand, there is so much chlorine that the more diffuse puff is calculated to have caused more deaths as well as more injuries. Even though the concentration is lower near the center of the

Case Number	Amount (Metric Tons)	Wind Speed (m/s)	Stability Class	Time (min)	Distance (km)	Toxicity	
						Killed (#)	Injured (#)
C1	1,090	4	4	10	2.4	921	0
C2	↓	5	3	8	2.4	1,823	5,734
C1		4	4	16	4.8	7,328	17
C2		5	3	20	4.8	10,932	4,943
C1		4	4	30	7.2	13,628	937
C2		5	3	24	7.2	18,152	4,946
C3	15	4	4	10	2.4	921	0
C4	↓	4	3	10	2.4	921	0
C5		5	3	8	2.4	0	921
C3		4	4	20	4.8	7,327	1
C4		4	3	20	4.8	1,020	5,768
C5		5	3	16	4.8	340	6,446
C3		4	4	30	7.2	9,995	865
C4		4	3	30	7.2	1,020	6,334
C5		5	3	24	7.2	340	7,425
C6	0.90	4	4	10	2.4	277	645
C7	↓	5	3	8	2.4	0	0
C6		4	4	20	4.8	277	5,111
C7		5	3	16	4.8	0	2
C6		4	4	30	7.2	277	5,748
C7		5	3	24	7.2	0	2

TABLE 7-6

CHLORINE SPILLS

The various cases for each spill size are listed here in order of distance traveled to facilitate the comparison of the effect of wind speed and stability class on the effects of the spill. The distance is the distance from the spill location to the center of the puff for the time listed.

more diffuse puff, it is still more than high enough to cause 100% deaths there, so the more widespread puff causes fatal and nonfatal injuries over a wider area. Because of the large number of casualties assessed for the very large spills of chlorine, it should be mentioned once again that they are hypothetical and represent only the use of realistic demographic data for a theoretically possible incident.

For the medium-sized spill, one may compare two runs with the same stability with different wind speeds and two runs with the same wind speeds but with different stability classes. Examination of these three runs in detail points out some interesting features of the VM and of atmospheric dispersion. First, note that at cell 19, 2.4 km from the spill location, the case with the wind speed equal to 5 m/s has 921 injuries whereas the other cases have 921 deaths. As all the chlorine was released as gas in 17.3 s, this is not due to any difference in travel time. (The release time is 17.3 s for all three spill sizes due to the fact that the submodel involved [MODI and EVDRP] assumes that all the liquid chlorine breaks up into individual drops which do not occupy a large fraction of the volume of the water and liquid chlorine mixture.) The difference is due to the fact that the puff passes over cell 19 while it is very small, so that the exact time at which the concentration is calculated is important. For the 4 m/s, stability class 3 case, the concentration at 6 minutes was 312 ppm. At this time, the puff center was at x = 1440 m, very close to the center of cell 19 at x = 1412 m, y = 95 m. For the 5 m/s, stability class 3 case, the highest concentration calculated was at 4 minutes, when the puff center was at x = 1200 m, about 200 m from the center of cell 19. Of course, at 4.8 minutes the puff center was at x = 1440 in this case, but the time step was 2 minutes, so the concentration was not calculated then. Thus the smaller number of deaths with the wind at 5 m/s is due primarily to the large value used for the time step.

This artifact in the assessment can, of course, be eliminated by using very short time steps or by calculating the factor determining toxic lethality ($\int c^n dt$ as explained in Chapter 6) at a given geographical point by analytic means. A short time step requires more computer time, on which there are economic constraints. The analytic calculation of the factor determining lethality at a geographical point appeared to be a level of detail for which the VM is not ready at this time. The problem is most severe when the puff is small shortly after the release of the cargo gas. As the puff expands with distance, the problem becomes less severe. Running the VM with 10 s time steps would have caused the assessment of identical numbers of dead and injured for the 4 m/s case and the 5 m/s case with unstable conditions, but the computation time for each run would have increased by a factor of twelve. Cost is roughly proportional to computation time, so the cost would have increased by about an order of magnitude.

Comparing the two medium-sized spills which have the same wind speed, but different stability classes, it is clear that the smaller dense puff resulted in more dead but fewer injured. Cells 44, 46 and 26 were close enough to the x axis (i.e., close enough to being directly downwind) so that the higher concentrations in the neutral stability case caused 100% deaths to be assessed, whereas in the unstable case the lower concentrations resulted in the assessment of many injuries but only a few deaths.

Anhydrous Ammonia Spills

The results of the ammonia runs are shown in Table 7-7. Each of the three spill sizes was run with ignition possible at the cell centers, and with ignition precluded. In evaluating test runs in which the ammonia did burn, the reader should note that ammonia is difficult to ignite under most conditions; however, it will burn or even explode under certain conditions. There is no known record of an unconfined ammonia cloud explosion.

The small spill of 8.2 tons caused no toxic deaths and did not ignite. Toxic injuries are not assessed for ammonia, as discussed in Chapter 6. When ignition was possible, the time step, Δt, was set to 1 minute since ignition usually occurs fairly soon if it is going to occur. With no ignition sources at the cell centers, it was desirable to run the program for 30 minutes so $\Delta t = 2$ minutes was used. In Table 7-7, the case with ignition possible at $\Delta t = 1$ minute is listed first.

The very large spill of over 16,000 metric tons of anhydrous ammonia ignited, not at the first cell in its path (cell 19) but later at cell 46. The reason for this is the evaporation time and the manner in which the puff model treats long release times. It took 20.8 minutes for all of the ammonia to escape in gaseous form, but the puff submodel starts the puff moving from the spill location when the first gas escapes and increases the amount of cargo gas in the puff as it escapes. Thus, as the puff moves away downwind, the mass in the puff increases. In this case, the mass in the puff increased fast enough to more than compensate for the spreading of the puff; the concentration increased from the time the puff was near cell 19 (6 min), so that by the time it was close to cell 46 (12 min) ignition was possible. At the time of ignition at 11.8 minutes, 7.9% of the spilled mass was combustible. In the case that the ignition set off an explosion, this amount of ammonia is equivalent to 4110 tons of TNT. The resulting damage is shown in Table 7-7. There were no deaths from explosive effects because the people in cells 46 and 47, 210 m and 490 m, respectively, from the blast center, were already dead from the toxic vapors. Explosion injuries were assessed as far away as 4350 m at cell 16, where one person was calculated to have received injuries from flying fragments. Seven buildings 6500 m from the blast center in cell 12 were assessed as having broken windows. In the case of flash fire, structures were ignited only in cell 46.

For the very large spill without ignition, it is interesting to note that the 2-minute time step resulted in more deaths from toxic vapors at 10 minutes after gas release started than the run with $\Delta t = 1$ minute, but the number of deaths at 11.8 minutes in the one case was the same as the number of deaths at 12 minutes in the other case. This is due to the use of Δt in calculating the dosage. In this example, the concentration at cell 47 was increasing so that the VM had, by 11.8 or 12 minutes, assessed all of the outdoors population in that cell as dead. Changing the size of the time step does not always have an effect; Table 7-7 shows that for the medium-sized spill the number assessed as dead is the same at 10 and at 14 minutes for $\Delta t = 1$ and $\Delta t = 2$.

Case Number	Amount Spilled (Metric Tons)	Time (min)	Distance (km)	Toxicity Deaths (#)	Explosion			Flash Fire	Δt (min)
					Injuries (#)	Structural Damage (M$)	Structures with Broken Windows (#)	Structures Ignited (M$)	
A1, A2	16,340	10	2.4	1,412					1
		11.8	2.8	6,726	11,419	68.35	15,720	9.23	1
A3	16,340	10	2.4	2,177					2
		12	2.8	6,726		NO IGNITION ALLOWED			2
		30	7.2	18,151					2
A4, A5	251	10	2.4	921		DID NOT IGNITE			1
		14	3.4	4,584					1
A6	251	10	2.4	921					2
		14	3.4	4,584		NO IGNITION ALLOWED			2
		30	7.2	8,033					2
A7, A8	8.2	ANY	ANY	NONE		DID NOT IGNITE			1
A9	8.2	ANY	ANY	NONE		NO IGNITION ALLOWED			2

TABLE 7-7

AMMONIA SPILLS

No explosion deaths and no flash fire deaths or injuries are listed because inhalation of toxic ammonia fumes had killed those people in cell 19 who would have been killed by the explosion or killed or injured by the flash fire. Toxic injuries are not listed because toxic injuries are not assessed for ammonia (see Chapter 6 and Appendix E). Distance is the distance from the spill location to the center of the puff.

Immediate Pool Burning - Methanol, Gasoline, and LNG

Methyl alcohol and gasoline evaporate much more slowly than do LNG and ammonia, with the result that the concentration at the first downwind cell (cell 19) is so low that even the maximum credible spill does not result in ignition. As the puff moves downwind, the amount of vapor it contains increases. but the dispersion coefficients increase as well, and the concentration does not approach the lower flammable limit concentration at later times either. For these two cargoes, the spill location was moved 30 m upwind from the center of the river cell, and a very short time step was used; however, even in these cases the concentration was too low to ignite. Finally, the VM was reprogrammed so that the user may set a flag which indicates that the simulation should proceed immediately to pool burning after the spill is complete.

The results of runs for medium-sized spills of LNG, methyl alcohol and gasoline with immediate pool burning are shown in Table 7-8. The radiation given is for cell 3, the cell in which the spill occurred. For these spills, the location of the spill was chosen to be the center of cell 3. In the radiation calculation, entering a zero for the distance from the center of the pool to the observer causes the flux to be equal to infinity; thus, in cases like this, the program removes the observer to a distance equal to the pool radius plus 10 m. In the simulation, there are no structures in the river cell in which the pool burning takes place, and the nearest land cell center is about 1.2 km away; the radiation levels there were not high enough to ignite any structures, so no damage is assessed in each of these three cases.

It may seem strange that the burning time varies so widely among these three cases whereas the radiation intensity varies very little. This is partially due to the ways in which some of the submodels operate. First, it is assumed that the pool stops spreading when ignition occurs. Second, a simplifying assumption in the calculation of the radiation flux is that the flux is primarily a function of the adiabatic flame temperature. Finally, the burning rates of large pools (in terms of reduction of depth per unit time) were found for these three materials, and the depth of the pool was used with these data to give the burning time. Since the total energy radiated through a right circular cylinder around the flame is the product of the cylinder's area, the radiation flux, and the burning time, the amount of energy radiated is not calculated in a direct way from the energy contained in the spilled cargo pool.

Let us compare the results of LNG, which has the shortest burning time, with those for methyl alcohol which has the longest burning time. The available energy in the pool at the instant of ignition is given by the product of the heat of combustion with the mass of the cargo in the pool. Thus, assuming that the combustion is complete, one finds that the LNG pool contained 3.5×10^{12} joules, whereas the methyl alcohol pool contained 1.8×10^{12} joules. The size of the cylinder around the flame was chosen to be such that the radiation flux calculated for cell 3 may be used. In these examples, the spill was exactly at the center of cell 3, and the radiation level could not be calculated there since this point was inside the burning pool. Therefore, the radiation flux was calculated at a point

10 m beyond the edge of the pool, and the cylinder had a radius 10 m greater than the pool radius. The area of such a cylinder is 40,700 m^2 for the LNG case, but only 2650 m^2 for the methyl alcohol pool since the methyl alcohol pool was smaller and the flame was shorter. Thus, 0.044×10^{12} joules were radiated away in the LNG case, and 0.71×10^{12} joules were radiated in the methyl alcohol case. The two cases differ in radiated energy, then, by a factor of about 16, not the factor of over 200 which one might get if only the burning times were considered. Still, in the methyl alcohol case 39% of the available energy is calculated to have been radiated away, whereas in the LNG case this figure is only 1.2%. The remainder of the available energy in both cases is convected away.

The long burning time calculated for methyl alcohol results from the fact that the pool of methyl alcohol spreads more slowly than the pools of LNG or gasoline. Thus, when ignition occurred after one time step of 60 s, the methanol pool was about 2 cm thick, which is the reason why the methyl alcohol burning time is so long. For pools which are less than a millimeter thick at ignition, the assumption of no further spread during burning is reasonable. But, in the case of methyl alcohol, this assumption gives a pool which retains a radius of 13.7 m for almost 2 hours while it burns. It also results in a burning time which is much longer than the time that it would take the pool to evaporate, as calculated by the HACS submodel MODR.

Conclusions

These test runs show the great range of injuries and damage that may result from spills of hazardous cargoes. The size of the spill and the material spilled primarily determine the order of magnitude of the results, but the wind direction and atmospheric stability also play important roles. It is noteworthy that the methyl alcohol and gasoline spills did not evaporate fast enough to form a cloud concentrated enough to ignite at the first grid point downwind. This point was 1400 m away; however, computer experiments showed that ignition of the vapor cloud would not occur for distances as short as 30 m. These results may correctly simulate physical phenomena for spills of this type, but further validation seems to be required. Thus further investigation of the experiments and theory relating to this problem may be appropriate.

Because the very large spills of LNG, ammonia, and chlorine were assessed to have killed and injured thousands of people, it should be remembered that in this model approximations have been made in such a way as to maximize the potential damage wherever feasible and that the probability of spills this large in a densely populated area has not been taken into account.

Ignition

Since a change in the wind direction of only 3° in the medium-sized spills determined whether or not the vapor cloud would ignite, consideration should be given to making the ignition less dependent upon the wind direction. At the present time in many cases, the center of the puff must pass very closely to a cell center for ignition to occur. This is due to the fact that ignition in the VM is possible only at the cell centers at this time and

Case Number	Cargo	Amount in Tank (MT)	Amount Spilled (MT)	Pool Radius (m)	Flame Height (m)	Burning Time (min)	Radiation Flux ($J/m^2/s$)
L13	LNG	83	65	50.7	106	0.43	42,405
M1	Methyl Alcohol	95	93	13.7	17.8	117	37,867
G1	Gasoline	70	68	37.1	54.9	5.8	37,325

TABLE 7-8

IMMEDIATE POOL BURNING

There are no deaths or injuries from the pool burning because it is assumed that there is no resident population in the river or harbor cell where the pool burning occurs; furthermore, the nearest land cell is far enough away that the radiation from the pool does not cause any injuries or the ignition of any structures there. The radiation flux is calculated at a point 10 m beyond the edge of the pool.

that these are rather coarsely spaced with respect to the puff size during the early stages of dispersion. A quick solution to this problem would be to subdivide the census tracts presently in use. This should solve the ignition problem, as well as making the assessment results less markedly dependent on small variations in direction.

For the long run, a more sophisticated solution may be in order. One such solution would be to assign an ignition probability, which would have the units of 1/area/time, to each census tract or subdivision thereof. Thus the product of the ignition probability with the area in which the concentration is in the combustible range would have the units of 1/time. For each time step, this product would be multiplied by the duration of the time step and added to the sum of similar products from previous time steps. This sum would increase with each time step, and, when a threshold value, such as one-half is reached, ignition would occur. This method would more realistically simulate both slow-moving clouds hanging over an area with sparsely distributed ignition sources, as well as clouds which move quickly over an area in which ignition sources are dense.

Resource Distribution

The fact that the VM currently treats the resources in each cell as if they were all located at the cell center makes the assessment of damage dependent on slight changes in the spill location or the wind direction, or both. This is due directly to the coarseness of the grid of cells. Census tracts are often more than 1 km across and are less than 500 m across only in the most densely populated areas. Although the use of whole census tracts as cells has been adequate for this developmental work, subdivision of census tracts will be necessary if the development of the VM proceeds much further.

Ideally, the resources would be described in a grid system which has a scale smaller than the horizontal diffusion coefficient of the air dispersion model for the conditions prevailing at the time of interest. Since the dispersion coefficients differ widely with the stability class and distance, no single scale can be ideal for all conditions. For the most stable conditions within a few hundred meters of the source, the horizontal dispersion coefficient is less than 10 m, and cells on this scale are computationally infeasible; even so, consideration might be given to making the cells smaller along the river or harbor than they are a kilometer or so inland.

Time Step Selection

The test runs have shown that the VM, at its current stage of development, is sensitive to the choice of time step under certain conditions. If development proceeds, this could be addressed by a number of actions. An increase in the density of the cells and a more sophisticated treatment of the ignition problem will largely resolve the current situation in which the concentration of the puff at the cell center is not evaluated during the time that this concentration is near its maximum; however, it may be necessary to introduce an internal limit in time step duration and to use a short time step for the early stages of the dispersion and a longer time step later on. These procedures will also remedy the problem for toxic gases where the concentration is not evaluated for representative values.

Validation

Extensive validation of the VM by reference to actual accidental spills of hazardous materials has not been feasible. The large disasters happen only infrequently and are usually not well documented. Smaller spills, on the order of the medium size or smaller, happen more often, but they too are usually not well documented and, fortunately, they commonly occur in rural areas. Moreover, upon close examination, almost every accident seems to have features which make it atypical.

For example, consider the case of the freight train derailment in Crete, Nebraska, in February of 1969 [36]. In some respects this case is ideal for study since the accident involved a substantial amount of ammonia (111 m^3) and occurred near the center of town. On the other hand, the accident took place at 0630 when the temperature was very low (-15.5°C) and there was no wind. Thus very few people were out of doors, and all of the houses were tightly closed. These conditions contributed to the fact that only 6 persons were killed and 28 seriously injured from ammonia inhalation in this accident.

The Phase I submodels could be validated individually or as a group by field experiments. Some work of this type has been performed and more is currently underway; however, the cost of large-scale field experiments is high in resources and time. The Phase II submodels are generally based on extrapolated animal experiments. In some instances, reports of accidents have contributed to the evolution of assessment procedures. Nevertheless, in any event the validation of Phase II submodels by planned experiments is ethically unacceptable.

Cost

The cost of running the VM will vary depending upon the computer system used and the scenario simulated. The test runs were made on an IBM 360/65 computer. Running times were generally between 15 and 35 CPU seconds. Typically 1000 to 2000 lines of output were produced. The typical cost of a run was between three and eleven dollars. A cost of five dollars was average.

Closure

The examples in this chapter were presented to allow the reader to see the type of information obtained by running the VM and to judge the reasonableness of the results in view of the approximations inherent in the development of the VM. Neither the probability of a spill nor the probability of any other factors has been considered in the VM, since it is a damage assessment, not a risk assessment tool. The probability of

---

[36] U. S. Department of Transportation, National Transportation Safety Board. Railroad Accident Report (Chicago, Burlington, and Quincy Railroad Company, Train 64 and Train 824, Derailment and Collision with Tank Car Explosion, Crete, Nebraska, Feburary 18, 1969). U. S. Department of Transportation, Washington, D.C., February 24, 1971. Report No. NTSB-RAR-71-2.

the events comprising a simulation scenario, as well as the validity of the approximations and assumptions made in the course of VM development, should always be borne in mind when the test runs are contemplated, interpreted, or discussed by the reader.

CHAPTER 8

SENSITIVITY ANALYSIS

Plan of the Analysis

The concept of sensitivity analysis has been extensively discussed in the literature related to control systems and other physical systems [37, 38]. Although the theoretical concepts considered are relatively sophisticated, simplification can be made to apply these methods to a sensitivity analysis of the VM.

Typically one considers a system with n output variables, Y_i, $i = 1, 2, \ldots, n$, and with m input variables, X_j, $j = 1, 2, \ldots, m$. Then we may write

$$Y_i = f_i (X_j)$$

to represent the functional dependence of the n output variables on the m input variables.

Consider now the differential change in one of the output variables, dY_i. By the chain rule we have

$$dY_i = \frac{\partial f_i}{\partial X_1} dX_1 + \frac{\partial f_i}{\partial X_2} dX_2 + \ldots + \frac{\partial f_i}{\partial X_m} dX_m$$

The factors, $\partial f_i / \partial X_j$, are usually termed the sensitivity coefficients and give, for small changes in the input variables, a measure of the effect on the output variable.

For a detailed sensitivity analysis, each of the sensitivity coefficients must be considered and its variation over the range of the several variables must be determined. One way to summarize the output variation would be to consider functions such as

$$g_j = \sum_{i=1}^{n} \left(\frac{\partial f_i}{\partial X_j}\right)^2$$

which gives the "change in arc length" generated in the n dimensional space of output variables by incremental changes in the jth input variable.

In the present stage of the development of the VM, such a rigorous sensitivity analysis is considered to be: (a) too detailed, exacting, and time consuming considering the priorities of other tasks in the program and (b) too abstract and devoid of physically tenable measures to assist the USCG. Therefore, a simpler, less sophisticated, less conventional form of sensitivity analysis has been chosen.

---

[37] Radanovic, L. (ed.). Sensitivity Methods in Control Theory. Pergamon Press, New York, 1966.

[38] Tomovic, R. Sensitivity Analysis of Dynamic Systems. McGraw-Hill, New York, 1963.

In this modified analysis, a square grid with a uniform density of population and structures was used. Therefore, input variables such as spill location and wind direction, which change only the location but not the magnitude of the damage, should have no effect. This is true as long as the area in which the damage or injuries occur always falls within the grid, and as long as the mesh of the grid is small with respect to the size of the damage mechanism.

For the sensitivity analysis computer test runs, a 15 x 15 grid with a spacing of 500 m was set up. Each grid point represented 1000 people (all assumed to be outdoors) and 100 structures. The spill took place at the central point, and the wind was in the positive x direction (toward the east). For a distance of 1 km, the horizontal dispersion coefficient for the puff is less than 10 m for the very stable condition and about 85 m for the unstable condition. Thus the grid spacing is not small with respect to the size of the puff at this distance, so the wind direction and spill location will influence the damage assessment. Consider, as an example, the case of a toxic gas with stable atmospheric conditions. The cloud will be small and concentrated, and the wind will carry it down the x axis directly over each grid point along the axis, killing all of the people at each point. If the release point is moved half a grid space to the north (in the positive y direction), the wind will carry the cloud down the corridor between the grid points, and no deaths at all may be assessed. This effect, due to changing the spill location, is completely artificial and results from the coarseness of the grid. In theory, or for an infinitely fine mesh, the wind direction and spill location have no influence on the damages assessed for a resource which has a uniform density. Therefore, since a grid spacing smaller than the size of the puff is not economically feasible, and since the wind direction and spill location do not affect the damage assessment for a very fine mesh, the spill location and wind direction are not changed in this analysis, even though they will affect the assessment due to the coarseness of the grid.

The plan for these computer runs was to vary only the size of the spill, the wind speed, and the stability class, but it became necessary to vary the time step in certain cases as well. The puff model was used for all runs, and the time step was 1 minute unless otherwise stated. As methyl alcohol and gasoline evaporated so slowly that they would not ignite, and since these cargoes are not currently treated as toxic in the VM, the sensitivity analysis test runs were made only for chlorine, anhydrous ammonia, and liquefied natural gas (LNG). For each cargo, the standard or reference run was a medium-sized spill with neutral stability and a wind speed of 4 m/s. After this reference run had been made, six other runs were made, and in each of them only one parameter varied from the reference case. The stability was changed to more and less stable conditions, and the wind speed was reduced from 4 to 2 m/s and then increased to 10 m/s. Finally, the size of the spill was changed to the very large size and then to the small size.

Results

1. Toxic effects

The results of the runs which concentrated on the toxic effects are given in Table 8-1. Since there were only 7 cells downwind of the spill on the x axis, the 7000 dead for the first (reference) ammonia run represent the maximum number that can be killed unless the puff is large enough to affect the cells off the x axis. Had the grid been larger and the runs extended for a longer period of time, the casualties would have been greater since this spill was causing 100% deaths when it reached the edge of the grid. The puff is less dense and more widely distributed in the

Cargo	Amount (MT)	Wind Speed (m/s)	Stability Class	Dead (#)	Injured (#)	Notes
NH_3	251	4	N	7,000		Reference case
↓	251	4	U	4		t_{evap} = 7.8 min.
	251	4	S	7,000		
	251	4	N	7,000		
	251	2	N	7,000		
	251	10	N	2,949		Δt = 1 min.
	16,340	4	N	13,042		Lethalities in off-axis cells
	8.2	4	N	2,175		
Cl_2	15	4	N	7,000	0	Reference case
↓	15	4	U	4,580	2,460	
	15	4	S	3,000	850	Δt = 1 min.
	15	4	S	7,000	0	Δt = 20 sec.
	15	2	N	7,000	0	
	15	10	N	3,000	924	Δt = 1 min.
	15	10	N	6,000	0	Δt = 20 sec.
	1,090	4	N	7,000	0	
	0.90	4	N	3,865	3,135	

TABLE 8-1

SUMMARY OF TOXIC EFFECTS

For these runs, a square grid with cells 500 m apart was used. The wind blew in the direction of the positive x axis, and the time step was 1 minute unless otherwise indicated. Each cell contained 1,000 people outdoors and 100 structures. A square grid structure comprised of 15 x 15 cells was used with the spill always at the center, so there were 7 cells downwind of the spill. The stability classes are denoted as follows: N=neutral, U=unstable, and S=stable.

unstable case, and the concentrations just barely reached the lethality threshold. (No injuries are assessed for ammonia, as discussed in Chapter 6.) The medium-sized ammonia pool takes 7.8 minutes to evaporate, so the puff is more than halfway down the x axis before it contains the entire amount of the spilled cargo. Thus the vapor cloud did not contain all of the spilled ammonia when it passed over the first grid points; this partly explains why very few deaths were assessed with unstable conditions, since the concentration at the center of the puff is lower than with other stability conditions. Use of the puff model, as described in Chapter 3, requires that the vapor liberated at later times be added to the puff at its downwind position, without passing over the intervening area. This anomaly is produced by the lack of an extant air dispersion model to treat cases between instantaneous and continuous releases. The results for the unstable case were not affected by the value of the time step.

The cases with stable conditions and the slow wind speed caused 100% deaths on the x axis as might be expected. The low number of assessed fatalities in the fast wind speed case is due to the use of a time step of 1 minute which is too large for a wind speed of 10 m/s. Although this run reported no fatalities in the first cell downwind because the puff center was 100 m away when the concentration was calculated, a short run with a time step of 10 s found 89% dead for this cell. Since the evaporation is completed just before the puff leaves the grid, and the run with Δt = 1 minute calculated 100% dead when the puff center was at the center of the sixth cell on the x axis at 3 minutes, it is clear that if the time step had been 50 s to insure evaluation of the concentration when the puff center was exactly at each cell center, the number of fatalities would have been over 6000.

The very large spill caused over 13,000 deaths because it was so big that the puff was capable of causing toxic concentrations in the cells adjacent to the x axis. The first cell off the axis to have deaths assessed was at x = 2 km, and the cells at 3.0 and 3.5 km had 100% fatalities. As the evaporation took almost 21 minutes for this size spill, fatalities would have been caused for at least 10 km downwind if the grid had extended that far. The small spill caused considerably fewer deaths than did the reference case, which is to be expected.

The medium-sized chlorine spill is less than one tenth the mass of the medium-sized ammonia spill, but chlorine is much more toxic than ammonia, so the chlorine spill is also assessed to have killed everyone on the x axis. The unstable case resulted in 4580 deaths, many more than the ammonia spill with unstable conditions. The difference is primarily due to the fact that all of the chlorine evaporates in only 17.3 s, so that the entire mass spill is present in the vapor cloud when it reaches the first grid point. The stable case was assessed to have killed all persons in cells on the x axis only if a time step of 20 s is used. With Δt = 1 minute, the assessment was much less. For the case with the wind at 10 m/s, even with Δt = 20 s, the cell center was 100 m from the puff center for the first cell, which was too far. With Δt = 10 s, 25 s, or 50 s, 100% in all the cells on the x axis would have been assessed as killed. Even the small spill of less than a ton of chlorine killed almost 4000 people. A run with an extra long grid showed that the reference case was capable of 100% lethalities more than 7 km downwind on the x axis. There were no deaths in the cells adjacent to the axis, but there were some injuries.

To sum up, the toxic deaths show a greater dependence on stability class than they do on wind speed, a result which was expected. This assumes that the length of the time step is reduced as the wind speed is increased, otherwise too infrequent evaluation of the gas concentration will result in inaccurate assessment of the injuries. For the medium-sized spills of chlorine and ammonia, the unstable condition resulted in many fewer casualties than did the neutral condition. For a very large spill, however, this may not be the case.

2. Effects of Explosions and Fires

The results of the sensitivity runs for the flammable cargoes being considered, LNG and ammonia, are shown in Table 8-2. In the case of ammonia, the concentration levels necessary to cause death in a couple of minutes or less are below the lower flammable limit concentration, so the inhabitants of the cell at which the ignition occurs are already dead before the explosion or flash fire occurs. Thus there are no injuries or deaths from the explosion or flash fire for ammonia in the ignition cell. And the very large spill is the only ammonia spill which causes a large enough explosion to affect people outside the ignition cell.

The slow rate at which the ammonia evaporates is the reason that the vapor cloud failed to ignite in three of the medium-sized spills. Ignition did occur in the stable case where the puff is smaller and more concentrated and in the slow wind case where more of the liquid was able to evaporate before the puff reached the first cell downwind. The very large spill is interesting in that it did not ignite at the first cell downwind, but did ignite at the third cell. This was due to the continued evaporation of the ammonia as the puff moved downwind. The increase in mass countered the increasing size of the dispersion coefficients and caused the concentrations on the x axis to increase with time.

The failure of the LNG spills to ignite for the unstable mixing condition and the small spill is not unexpected. The case with stable conditions resulted in a smaller explosion than the reference case because the smaller values of the dispersion coefficients allowed less of the methane to be in the flammable concentration range. In the low wind speed case as in the reference case, evaporation was complete and no liquid pool remained when the cloud ignited at the first downwind cell. In the high wind speed case, however, ignition occurred when the evaporation was little more than half completed; consequently, even though a larger portion of the vapor exploded, the resulting blast was less powerful than the one in the reference or low wind speed cases. Note that the blast in the very large spill case treated here is much smaller than it was in the test cases with an actual grid of census tracts. This is due to the fact that here ignition occurred about 310 m from the spill location, whereas in the case reported in Chapter 7 the puff moved just over 1000 m before ignition. This extra movement allowed time for additional LNG to evaporate, and for the cloud to disperse more widely, so the portion of the methane in the range of flammability was greater.

The LNG spill for the 10 m/s wind did not ignite with the usual time step of 60 s. A value of Δt such as 10 s, 25 s, or 50 s, which causes the concentration to be calculated when the puff center is exactly at the first grid point, does result in ignition. With $\Delta t = 60$ s, the puff center and cell center did not coincide at an evaluation time until 5 minutes after the

Cargo	Amount (MT)	Wind Speed (m/s)	Stability Class	Toxic Deaths (#)	Explosion					Flash Fire	
					Deaths (#)	Injured (#)	Structural Damage (#)	Fraction of Mass Exploding (%)	Yield (Short Tons of TNT)	Deaths (#)	Structures Ignited (#)
NH_3	*251	4	N	7,000		DID NOT IGNITE					
	251	4	U	4		DID NOT IGNITE					
	251	4	S	1,000			100	2	3.5		0
	251	2	N	1,000			100	8	52		0
	251	10	N	2,949		DID NOT IGNITE					
	16,340	4	N	3,000		6,550	593	8	1,020		25
	8.2	4	N	2,175		DID NOT IGNITE					
LNG	*83	4	N		1,000	20	125	13	215	10	25
	83	4	U			DID NOT IGNITE					
	83	4	S		1,000	0	100	3	54	0	0
	83	2	N		1,000	20	125	13	215	10	25
	83	10	N		1,000	10	112	25	159	19	25
	20,750	4	N		1,000	28,456	958	8	2,500	183	25
	0.8	4	N			DID NOT IGNITE					

*Reference test runs.

TABLE 8-2

SUMMARY OF THE EFFECTS OF EXPLOSIONS AND FLASH FIRES

The grid and abbreviations used are described in the caption to Table 8-1. For the explosions of ammonia, all those people who were in a position to be killed or injured by the explosion had already been assessed as dead from toxic effects prior to ignition. For the ignition of structures by flash fire, only 25 structures in the cell in which ignition occurs are set on fire because the program assumes that only 25% of the structures in a cell are ignitable in this fashion.

spill when the puff center was at the sixth cell downwind of the spill location. At this time, the concentration at the center of the puff was not great enough to cause ignition. (It is not true that the puff center and the grid point must coincide for ignition; however, when the fuel concentration is above the lower flammable limit only near the center of the puff, then the center of the puff must come very close to the ignition source if ignition is to occur.)

Summary and Conclusions

It is clear that, of the three parameters varied, the size of the spill had the greatest effect on the damage assessed. This was partially obscured in the case of the very large spills of toxic cargoes because when the vapor clouds from these spills leave the grid, they have concentrations far above that needed to cause death in a few minutes. The small spills of the toxic substances caused many fewer fatalities than did the medium-sized spills. The small spills of the flammable cargoes also caused many fewer deaths than did the medium-sized spills, but here one of the primary reasons was the failure of the vapor cloud to ignite. Unlike the toxic case, for flammable materials the relationship of input parameters to damage caused was discontinuous, with the discontinuity occurring at the ignition threshold. The small spills did not result in clouds dense enough to ignite at the first grid point, so there is no damage from fire and explosion for these cases.

Of the remaining two variables, the stability class had a more marked effect than did the wind speed. In the toxic case, the number killed was lower for unstable case atmospheric conditions than for the reference case with neutral stability. For ammonia, changing to unstable conditions almost eliminated the fatalities. For chlorine, the reduction was less pronounced. The effects of stable conditions do not show up as well in this sensitivity analysis because of the small number of cells downwind from the spill location. A note of caution is in order, however. For the very large spills, the change from neutral to unstable conditions may result in more deaths and injuries. This is due to the fact that an increase in dosage above the lethal level has no effect. For a big spill in which the concentration might be above the lethal concentration in the cells adjacent to the x axis, fewer people may be assessed as killed if the lethal concentration of toxic gas is contained near the axis and does not extend to the adjacent cells. Since the populations of the cells on the x axis are all killed anyway, increasing the concentration there will have no further effect.

Finally, we come to the variations in wind speed. For the materials which evaporated before the puff reached the first grid point with the 10 m/s wind, the wind speed had no effect on the damage assessed as long as the time step was reduced accordingly. For cargoes which took longer to ignite, the increased wind speed could mean the difference between ignition and no ignition. For ammonia, for example, the release of the gas was slow enough so that only for the 2 m/s case was the concentration high enough to ignite when the puff reached the first grid point. It should be pointed out that the wind speed and the stability condition are not unrelated. The most stable atmospheric conditions are invariably associated with calms or very light winds. Thus, specification of strong winds and stable conditions is not realistic.

CHAPTER 9

THE HISTORICAL SURVEY SUBTASK†

This chapter describes the work performed on the VM under the historical survey subtask. This subtask consisted mainly in researching and compiling data about unconfined vapor cloud explosions, data that would be helpful in the development of the VM, but that might not be readily available. Ongoing research activities and plans related to VM development were also surveyed.

In the following text, Section 1 presents a summary of the major findings of the historical survey subtask. Section 2 is a review of private sector safety research and development plans relevant to the development of the VM. Section 3 is a listing of respondents interviewed or contacted. In addition, Appendix F contains a detailed account of fourteen case studies of accidental explosion incidents. In the following text, numbered cases (such as Case F.9) refer to the descriptions provided in Appendix F.

1. OVERVIEW

This section presents an introduction to and a summary of the major findings of this study, as well as a discussion of the major data gaps and recommendations for filling them.

1.1 Objectives and Scope of the Study

This study was undertaken to seek real world verification of the predictions of the VM, by collecting available data on actual vapor cloud fires and explosions.

The initial thrust of the investigation was to visit private, mostly industrial, organizations which had experienced or investigated actual vapor cloud explosions and to ask for access to their data. It was known that some such studies existed but were largely unpublished. Such studies are typically not published, because the details intrude too far into areas the organizations consider private and confidential. Nevertheless, it was expected that the strictly safety aspects of internal reports would usually be shared in face-to-face conferences where confidential information could be kept private.

It turned out that some very instructive studies were indeed obtained in this fashion, but overall a disappointingly small number of really usable case studies were found. A number of commonly-listed "gas" explosions, upon review, turned out to have occurred inside a reactor or

†The historical survey reported in this chapter was performed under contract to ECI by Dr. John A. Brown of John Brown Associates, Inc., Berkeley Heights, New Jersey.

inside a building and were not at all the unconfined vapor cloud events of interest here. Some companies would talk only under seal of privacy, and their data could be used only to enhance the perspective on the reportable cases. A few companies would not talk at all.

But mostly, the detail desired simply does not exist. Industrial disasters have seldom been investigated in anything like the detail lavished on, say, an airline disaster. Industrial emphasis is placed on proximate causes and on prevention of recurrences, and relatively minor attention is paid to such elements as the exact amount of fuel participating in an explosion or the resulting damage profiles. Reconstruction of industrial explosion disasters in detail comparable to that provided by the VM would require a vastly greater investigative effort than private organizations are willing or able to mount.

In the end, only two industrial explosion case studies were selected for presentation herein, and this study was extended to include the more numerous and better-documented studies of transportation-related vapor cloud accidents. In all, nineteen visits and interviews were carried out, and fourteen case studies were selected as sufficiently instructive for inclusion in this report. Lessons learned are summarized in Section 1.2, and the cases are reported in detail in Appendix F.

The existence of several previously unlisted industrial explosions was discovered during the course of investigations supporting this study, but visits to the investigators of these explosions could not be arranged in the time remaining between discovery of the incident and the termination of this program. They are listed in Table 9-1. It is not recommended that they be pursued. The two case studies presented herein are by far the most detailed of those seen, and even they are sketchy by VM standards. Conferences with numerous respondents with first or second-hand knowledge of the unexplored cases indicate that further case studies are not likely to add materially to the picture.

It must not be inferred from the remarks on privacy that important safety data are being withheld in any significant number of cases. They are not. Details impacting litigation and liability were sometimes withheld, but every respondent saw to it that the key safety information was made available, even if permission was not given to use the actual case study or to cite the source.

TABLE 9-1. ADDITIONAL MISHAP INCIDENTS MENTIONED DURING INTERVIEWS AND RECOMMENDED FOR SPECIFIC EXPLORATION WITH THE RESPECTIVE RESPONDENTS LISTED

- "Vapor cloud 800' x 200' x 20'" -- Cities Service, Lake Charles, La., "1967 or 68".
- Ethylene oxide tank car -- Dow Chemical, Midland, Mich.
- "Several incidents" -- PPG Industries, Lake Charles, La.
- Butadiene explosion -- Union Carbide, Texas City, Texas, 7 Sept 70.
- Isoprene plant explosion -- Goodyear, Beaumont, Texas, 27 Nov 74.

1.2 Findings and General Conclusions

The extraction of quantitative generalizations from records of such capricious events as accidental fires and explosions should be approached with extreme caution and with application of extremely wide confidence limits, but a number of clear qualitative conclusions do emerge from this study.

As explained in Chapter 4, the VM models the combustion of the vapor-air cloud as either a deflagration, producing no significant overpressure, or a detonation, producing a shock wave of potentially destructive overpressure. This strict dichotomy between deflagration and detonation is based on the classical Chapman-Jouget theory of combustion waves. As mentioned in Chapter 4, more modern studies indicate the possibility that deflagration (subsonic) combustion may, under certain circumstances, produce damage-generating, finite amplitude blast waves. In this Chapter, the terms "explosion" and "blast" are used to refer to damage-causing overpressures without regard to the nature of the combustion (deflagrative or detonative) which gave rise to the overpressures. Thus "deflagrative air blast" refers to an event causing explosion damage but thought to originate from deflagrative, rather than detonative, combustion.

The Results of Vapor Cloud Ignitions Vary Widely

The consequences of vapor cloud ignitions range from a huge but simple fire through deflagrative air blasts to true gas detonations without any apparent way to make confident predictions. Fireballs ranging up to hundreds of feet in height and diameter are almost universally reported, and about half the incidents involve air blasts which break windows and strip metal sheets from nearby buildings but do not strip leaves from trees or shatter heavy structures. Detonations are rare; the four reported herein form a disproportionately large sample from the population. They are over-reported because their disproportionate destructiveness has attracted more attention and more detailed reporting than have the results of the lesser deflagrative blasts. Spills studied ranged from a few thousand pounds of hydrocarbon to more than 100,000 pounds, but there was no visible relationship between the size of the spill and any tendency to deflagration vs. detonation. No clear trigger mechanism for detonation was identified, either: two of the cases were attributed to burning under confinement; another is thought to have been a case of burning to detonation in the open; and the other case is thought to have been initiated by the shock wave from an exploding diesel engine.

Probably neither the upper nor the lower end of the damage spectrum has been found. The largest spill on which a report was found was approximately 100,000 pounds, which is still far less than the half million or so barrels of LNG carried by some of the larger ocean-going tankers. Calculations by Burgess et al. [39] offer hope that flammable spill clouds may have a maximum size limited in each case by diffusion and mixing rates; but the maximum blast possible -- if there really is such a limit -- has not been established. At the other end of the scale, small spills have received little study because they do little damage;

---

[39] Burgess, D., J.N. Murphy, M.G. Zabetakis, and H.E. Perlee. Volume of flammable mixture resulting from the atmospheric dispersion of a leak or spill. To be submitted to the Fifteenth Symposium (International) on Combustion, The Combustion Institute, 1974.

and there is a widespread feeling that many of them are never even reported at all.

It may be that the overwhelming majority of all spills fail to ignite. That would be consistent with the reluctance of chemical plant operators to install pilot lights to insure the immediate ignition of spills and to prevent the growth of vapor clouds, but data on the point are not at hand.

Devastation is Never Total

One of the most striking features of aerial photos of disaster areas such as Crescent City (Case F.9) or Decatur (Case F.3) is the apparent normalcy of the scene. Houses and commercial buildings all look intact, automobiles are parked normally all along the streets, trees and shrubbery look untouched, and no smoke or flame is in evidence. Using high magnification, one can see broken windows and an occasional wrinkled roof; but one has to look hard. Damage there surely is, but the community is not destroyed as it is by, say, a tornado.

Moreover, most of the damaged buildings are repairable at relatively minor cost. In fact, they typically get repaired, and the people go on living in them. Even in Decatur, where 67 residences were posted as unsafe, 90% of the damage was termed "minor." It was typified by broken windows and loose ceiling tiles, not by collapsed buildings.

The damage that does occur is distributed very unevenly. One house will suffer severe structural damage while the adjacent house is virtually untouched. Some windows in a given wall will be broken, whereas others in the same wall are intact, even deep within the general window breakage zone. The damage counts and the claim maps do not give a clear picture of this, because they concentrate on the damaged buildings and do not list the much larger numbers of essentially undamaged buildings intermingled with them.

The spottiness of blast damage is a puzzling but typical feature of explosions. It does not seem to be due to variations in the strength of the structures, but rather to random fluctuations in the strength of the advancing blast wave front. No one has yet modeled that in detail.

There is Seldom Severe Blast Damage Beyond Half a Mile

For spills of up to about 100,000 pounds of fuel, there appears to have been little severe blast damage at distances of more than about half a mile:

Case No.	Approximate amount of fuel spilled	Approximate limit of severe blast damage	Location
F.2	5,000 lb. ethylene	1500 feet	Longview, Texas
F.4	27,000 lb. vinyl chloride monomer	1500 feet	Climax, Texas
F.1	100,000 lb. cyclohexane	1/4 mile	Flixborough, England
F.5	100,000 lb. propylene	1/2 mile	East St. Louis, Illinois
F.3	117,000 lb. propane	1/2 mile	Decatur, Illinois
F.6	130,000 lb. propane	2 miles	Franklin County, Missouri

The exception of Case F.6 was a rare detonation rather than the usual deflagrative blast, and it is the only case of its kind so far known. Since it did happen, two miles might be taken as a more conservative limit; but half a mile is the more typical limit. Another exception is the occurrence of caustics -- the focusing of blast waves, by atmospheric inhomogeneities such as temperature inversions, back down into an anomalous area of severe damage well outside the general area of severe damage. However, caustics are usually an order less severe than the central damage area, and they do not seriously invalidate the generalization.

Since the data are few, the above conclusion should be reviewed in the light of each new incident as it occurs. One should also keep in mind Burgess' point [40] that the size of a flammable or detonable cloud is a stronger function of wind and weather than it is of the size of the spill. Nevertheless, the severe blast damage actually observed in actual explosions has usually not exceeded about half a mile. The half mile damage limit may not hold for the more destructive detonative combustion cases.

The Central Fireball is Deadly

All the cases studied, plus a number of others which were not detailed enough for inclusion here, featured an enormous fireball which may or may not have been accompanied by a blast. In several cases (notably Cases F.13 and F.14), people were enveloped in the fireball, and they were almost always killed. The few who survived were severely burned. Buildings which were enveloped in such fireballs were ignited and usually burned to the ground. Fence posts and telephone and power poles were charred, and wires were melted.

The fireballs also radiate enormous amount of thermal energy and can ignite fires hundreds of feet beyond their edges. Report after report tells of firemen severely burned or forced to seek shelter hundreds of feet from fireballs, and a firemen's training film cited in Case F.11 warns that firemen have died from burns received as far away as 250 feet from large fireballs. In Case F.8, paint was blistered 600 feet from a fireball. In Case F.12, the paint on a fire truck was scorched and plastic light components were warped 300 to 450 feet from a fireball, and a bystander was burned 600 feet from the fireball. In Case F.10, a fireman 1600 feet from a fireball had to stop work and cover his head with his coat.

It has sometimes been anticipated that "flash fires" in stoichiometric fuel-air clouds would be so evanescent that little if any damage or injury would result from them. This study cannot address that point, but the real vapor cloud fires analyzed in this study all exhibited intensely hot, deadly, central fireballs. It would appear that such a fireball is an inherent feature of any spill large enough to cause

---

[40] Burgess, D.G., and M.G. Zabetakis. Detonation of a Flammable Cloud Following a Propane Pipeline Break -- the December 9, 1970 Explosion in Port Hudson, Missouri. U.S. Bureau of Mines, Washington, D.C., 1973. Report No. RI 7752.

concern. As Burgess has illustrated in some data [40], the vapor cloud from a large fuel spill should consist of three concentric zones: an inner zone too rich to burn, a shell wherein the composition is within the upper and lower flammable or explosive limits, and the rest of the world where the composition is too lean to burn. Ignition could occur only within the flammable shell, and the flame would travel outward to the lean limit and inward to the rich limit. At the rich limit, the flame would stop and continue to burn there as a diffusion flame at the interface between the rich cloud and fresh air brought in by turbulence. Fireballs do form. The cloud of heated gas would be expected to rise like a balloon, and fireballs have been reported with heights of up to 1,000 feet (Case F.9).

In the context of the VM, the combustion of that portion of the vapor-air cloud premixed between flammable limits is modeled. However the turbulent diffusion flame resulting from the combustion of the rich portion of the cloud, which is believed to produce the deadly fireball, is not treated at present in the VM. This phenomenon is extremely complex and to be modeled would have required more time and resources than were available. Furthermore the great damage potential of this mechanism, as indicated herein, was not known at the time that the fire and explosion models were formulated.

A Firestorm May Follow a Large Gas Explosion

In World War II, one of the most fearsome effects of firebombings was the widespread firestorm which sometimes ensued. A ground fire of sufficient extent creates an overwhelming updraft which draws in high winds from all directions. The resulting flaming whirlwind depletes the oxygen of the air, and it is said that more people died from suffocation than from burns in World War II firebombings.

Something of that sort happened in Case F.6. "In the seconds following detonation, a firestorm was observed to 'roll' in a generally east to west direction -- up the sloping terrain toward [the] highway" [40]. A footnote explained "firestorm" as: "That is, a diffusion flame with very high winds which consumed the remainder of the propane."

In a sense of course, every billowing fireball is a small firestorm; but we are talking here about the much worse <u>area</u> firestorm that results from the coalescing of many fireballs or the burning of a very <u>large</u> vapor cloud. Case F.6 is the only example encountered wherein a firestorm was specifically mentioned; but it was also the largest fuel spill encountered, and the incidence of firestorms would be expected to increase with the size of the spill. Thus an increase in spill size may change the possible class of events that follow from a spill, rather than just changing key parameters in a fixed set of consequences.

Exploding Tank Segments Can Fly up to Half a Mile

If an accident involves liquefied fuel gas tanks enveloped in a fire, still another hazard mechanism exists: the internal pressure in the tanks builds up to the bursting point, and the tanks rupture explosively. They not only then release enormous quantities of hot gas to make a fireball, but the tank segments fly off like rockets for distances up to half a mile, inflicting impact damage where they land and setting new, spot fires there. In Case F.9, exploding LPG tankcars hurled blazing segments up to 1750 feet into the heart of Crescent City where they smashed buildings and set fires. In Case F.10, the same

thing happened in the center of Laurel, Mississippi. It happened in the single-tanktruck fire of Case F.12 on the New Jersey Turnpike. The overpressure safety valves on such tanks are not adequate to relieve the excess pressure and prevent the explosions. It is truly a rocket effect; long, cylindrical, tank segments fly farther than shorter segments and much farther than random fragments hurled by the rupture explosion.

This hazard is an important one, because such tanks are to be expected where gaseous fuels are being handled. The effect where a tank hits is comparable to that from wartime demolition and incendiary bombs.

1.3 Data Gaps

This study, although instructive, has raised as many questions as it has answered. One wants more detail on the cases analyzed, one wants more cases, and one wants information on larger explosions and on marine spills.

The case studies found in this survey have typically had disappointingly little detail on damages and injuries. They have been heavy on the dollar value of damages and on numbers of deaths, because those data fulfilled the purposes for which they were made; but they have been relatively light on the fine details needed to break new ground in the understanding of explosion effects. The more recent case studies -- particularly those by the National Transportation Safety Board -- have contained more detail as awareness of its value has emerged; but one needs much more yet. One can find map plots of buildings made unsafe, for example; but one also needs to know just what kind of damage made each one unsafe, and which side of the house faced the blast. One also needs to know the condition of the adjacent houses which, being unmentioned, were presumably not much damaged. One needs an actual count of broken windows, house by house and street by street. One needs to know how many houses were in a given area as well as how many were damaged. One needs similar detail on injuries.

Much of this detail is gone forever, but much of it could still be reconstructed by sifting through raw insurance and newspaper archives, by study of the stacks of record photographs which were made in some cases and of city maps, and by field work at the explosion site. Such in-depth studies were far beyond the resources provided for this program.

One wants more cases, to test the tentative conclusions drawn from the ones analyzed, and yet the data scatter seen thus far make one doubt the value of simply more of the same. There are more industrial explosion cases sitting in people's files, but their collection is not strongly recommended unless they can be studied in much greater depth than was possible on this program.

One would like data on larger explosions (both deflagrative and detonative explosions). This study found and analyzed explosions of up to 100,000 pounds of fuel (about 50 MT $\cong$ 83 m^3), but data on a million-pound blast resulting from a spill would add perspective (1 million pounds $\cong$ 500 MT $\cong$ 830 m^3). Theoretical considerations suggest that the blast damage would by no means increase proportionately, but the point needs confirmation.

One would like data on spills which did not result in ignition, because they ought to contain clues on how to prevent ignition. Such events are not major accidents, of course, and seldom get much attention. The unignited Pensacola spill of hot cyclohexane is a fortunate exception in that some detail was recorded and in its frightening similarity to the Flixborough spill which did ignite. It would probably repay deeper study even at this late date. One would also like to know -- if only for perspective -- how many nondisastrous spills there are per year in comparison to the number of disastrous ones.

Further Studies that Appear Worthwhile

Although there are more industrial and transportation explosion cases which could be collected, a further canvass is not strongly recommended. The chances are that they would just be more of the same and would not add greatly to the picture. It would be far more productive to go back and reinvestigate selected, already identified accidents in much greater detail, and the following cases are recommended.

- The June 1974 cyclohexane explosion at Flixborough

  This explosion is fresh enough that it is still under intensive study, and much of the physical evidence is still available. It is one of the largest disasters in terms of dollar value of damage, and it offers an unusually dense gridwork of damage effects to indicate ranges of effects. It is uniquely instructive in that it appears to have involved a rare open-air detonation, and in that it can be compared to an almost exactly similar spill that did not ignite. The European investigation appears to be impressively thorough and would provide an unusually complete picture.

- The July 1972 propane explosion in Decatur, Illinois

  This explosion is still under investigation by the National Transportation Safety Board, and their file of observations and photographs is unusually extensive. It is fresh enough that local memories and records will still be vivid and accurate for still more detail. It is accessible for on-the-scene, street-by-street review of the patterns of damage and injuries. Occurring as it did in a densely built, urban area, it offers a rich lode of damage data with valid, side-by-side comparisons available.

- The 1944 LNG spill in Cleveland, Ohio

  This accident is thirty years old, so there is nothing fresh about it; but by the same token there is also no longer anything sensitive about it and existing data ought to be freely available. Morever, it was investigated by Zabetakis, of the Bureau of Mines, which suggests that the record will be thorough and comprehensive. It is also of interest because it was a large spill of LNG in an urban area.

- The 1969 LPG tankcar explosions in Laurel, Mississippi

This accident is recommended partly because of the unusually large number of buildings suffering damage and partly because of the existence of a very tantalizing claims map at Southern Railways. Two different kinds of claims are plotted on it within a radius of about five miles, but no one was found who remembered what they were! The information could doubtless be recovered from Southern's files, and their claims office has offered generous cooperation. The map also does not indicate the density of undamaged buildings, but this too could readily be reconstructed from local information.

2. PRIVATE SECTOR SAFETY RESEARCH AND DEVELOPMENT PLANS

Literally no planned, privately sponsored, explosion safety research and development programs were found in the course of this survey. The study was not exhaustive of course, but five of the largest fuel and chemical companies were included, and four major R&D companies who have been actively attempting to market such programs were included; and it is unlikely that so large a sample would fail to uncover any significant programs under consideration. Respondents interviewed on the point included:

Fuel and chemical companies and associations:

- Exxon Chemical Company USA
- El Paso Algeria Company
- Institute of Gas Technology
- Texas Eastman Company
- Monsanto Company

R&D companies:

- Calspan Corporation
- Science Applications, Inc.
- Systems, Science and Software
- Aerotherm-Acurex Corporation

Some commercial companies have been contemplating safety R&D programs, but their managements are currently taking the position that safety R&D is not a proper unilateral activity. They point out that any useful results therefrom would be instantly shared with the community rather than being used to advance the company's competitive interests, and that therefore such R&D is not a proper use of funds derived from one company's earnings. In the same breath, though, they go on to say that they would consider joining in, and contributing to the funding of, multicompany safety R&D programs, perhaps at the trade association level.

There is precedent for such joint R&D. Trade associations such as the American Gas Association and the American Petroleum Insitute have sponsored R&D on common problems, using members' funds, for many years, and their work is well known. There are less formal associations, too. For example, an Ad Hoc Committee of 25 major chemical companies was formed in 1971 under the leadership of W. H. Doyle, then of Factory Insurance Association and since retired, to support work on the effect of water sprays on the burning of flammable gases. This work has been completed and will soon be published, probably first at an AIChE Loss Prevention Symposium. Two members of the Steering Group were interviewed by the writer; and it is the writer's opinion that this Ad Hoc organization, or one descended from it, could be induced to support additional safety R&D, given some meritorious proposals and assurance of broad participation.

Ideas for safety R&D abound. A detailed report on ideas which have not crystallized into plans is beyond the scope of this study, but they include the following.

- Modeling of the formation and diffusion of gas clouds.
- Modeling of deflagrative explosions.
- Determination of the TNT equivalent of large gas explosions.
- Study of cloud control and flame suppression.
- Study of ignition limits and extinguishants.
- Analysis of gas container vulnerabilities.
- Modeling of fireballs and radiation fluxes.
- Development of pool fire models.
- Study of transition from deflagration to detonation.
- A more quantitative understanding of caustics.
- Study of the electrostatic ignition of gas clouds.
- Study of flame arrestors.
- Research on atmospheric stability factors.
- Research on maximum cloud and fireball size.

In the course of the present study, the writer was shown a number of proposals and capability documents on the above subjects. They were mostly "not for citation" and none of them was scheduled for early implementation.

The American Gas Association has a recommended plan based on an industry-wide poll of LNG research needs, both foreign and domestic. It recommends over $5 million in safety R&D. A detailed analysis of the plan is beyond the scope of this study, but the chart that follows illustrates its general outlines.

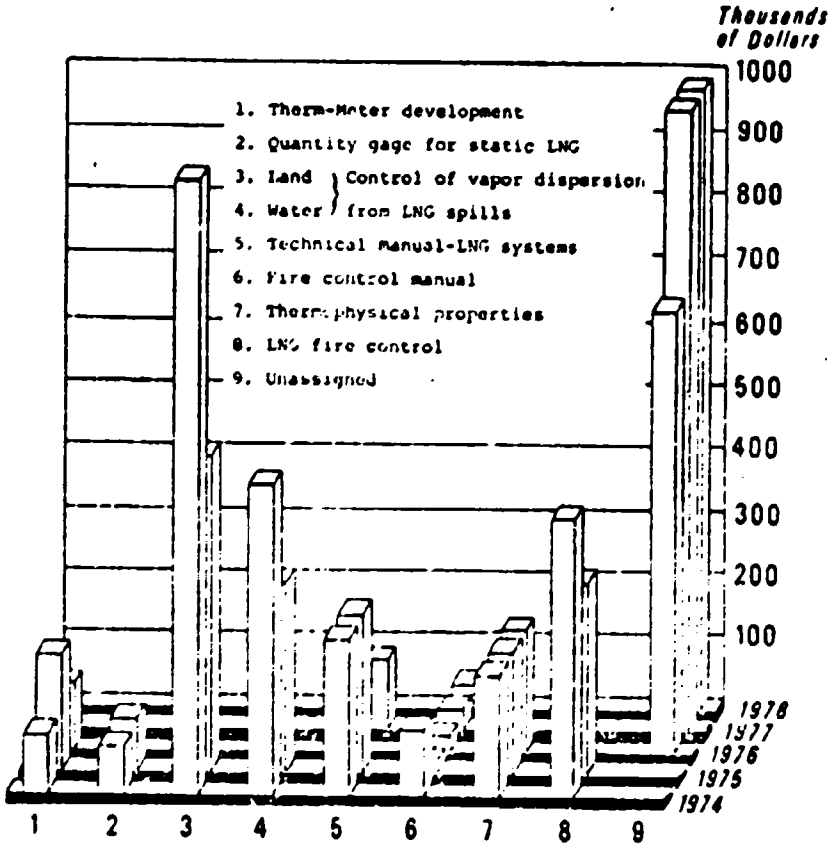

AGA LNG Research Plan. (After Sarkes [41])

The Plan is available from AGA, and a review of it was published at the Fourth International Conference on Liquified Natural Gas in Algiers on 24-27 June 1974 [41].

With research ideas aplenty and with potential co-sponsors not unwilling to participate on a team basis, what is mainly needed is some leadership and the selection of a limited number of specific projects. Some seed funding would probably be needed to attract industrial funding, but the most pressing need is for organization.

---

[41] Sarkes, L.A. A survey of LNG technological needs in the USA - 1974 to beyond 2000. Presented at the Fourth International Conference on Liquified Natural Gas, Algiers, 24-27 June 1974.

3. RESPONDENTS INTERVIEWED

The following individuals and organizations were canvassed and interviewed as to their accident experiences and R&D plans.

- Exxon Company USA, Houston, Texas

  Personal visit. Discussion of gas spills in Exxon facilities and possible R&D programs.

- El Paso Algeria Corporation, Houston, Texas

  Telephone interview; a visit could not be scheduled due to host's travel commitments. No spill incidents on record and no R&D plans.

- LP Gas Administration, Oklahoma City, Oklahoma

  Personal visit. Search through files of investigations of local gas spills and resulting fires and explosions.

- Monsanto Company, St. Louis, Missouri

  Personal visit. Discussions of cyclohexane spills like Flixborough, spread of gas clouds, and ad hoc committee safety R&D.

- Professor Roger Strehlow, University of Illinois

  Personal visit. Discussions of East St. Louis and Decatur explosions, NTIS studies, calculation of TNT equivalents and further information sources.

- Institute of Gas Technology, Chicago, Illinois

  Telephone interview, following a visit to the Washington office. A Chicago visit could not be scheduled. No accidents on record and no R&D plans.

- Texas Eastman Company, Longview, Texas

  Personal visit. Discussions of ethylene cloud explosions and water sprays. Range of blast damages.

- Calspan Corporation, Buffalo, New York

  Personal visit. Search of clipping files of accidents. Discussion of potential R&D programs.

- Systems, Science & Software, La Jolla, California

  Personal visit, telephone interview and correspondence. Discussions of industry R&D plans and S^3 proposals. Literature exchange.

- Science Applications, Inc., La Jolla, California

  Personal visit plus an escorted visit to Enviro Control. Discussion of R&D programs.

- Aerotherm Division of Acurex Corporation, Mountain View, California

  Telephone interview plus evening conference at JANNAF-AIAA meeting. Safety R&D proposals.

- Bureau of Mines Explosive Research Center, Pittsburgh, Pennsylvania

  Telephone interview plus correspondence. Discussions of gas explosions and specific incidents. References to additional contacts.

- Naval Surface Weapons Center, Dahlgren, Virginia

  Personal visit, with Coast Guard personnel. Discussions of Navy data on cloud travel and instrumentation. Introduction of Coast Guard to Navy computerized data base.

- Exxon Research and Engineering Company, Florham Park, New Jersey

  Multiple telephone interviews. Discussions of explosion in Bayway facility not for citation because in litigation. Discussions of past safety R&D on LNG.

- American Gas Association, Washington, D.C.

  Telephone interview; visit could not be scheduled. Discussion of Gas Industry Research Plan - 1974-2000.

- National Transportation Safety Board, Washington, D.C.

  Study of files on recent accidents still under investigation and collection of issued reports. Discussion of characteristics of accidents and explosions.

- Mr. W. H. Doyle, retired, formerly of Factory Insurance Association

  Telephone interview; visit could not be scheduled in time available. Chairman of the 25-company, ad hoc committee that sponsored the study of water sprays.

- Southern Railway System, Washington, D.C.

  Personal visit. Further details on the Laurel, Mississippi, tank car explosions.

- Federal Railway Administration, Washington, D.C.

  Personal visit. Additional details on Climax, Texas, vinyl chloride tank car explosion.

- Mr. D. H. Slater, Cremer and Warner, Consulting Engineers, London, England

  Correspondence. Additional details on the Flixborough cyclohexane explosion.

The following additional respondents were listed for interview, but visits could not be arranged in the time remaining for this study.

- Naval Weapons Center, China Lake, California
- Stanford Research Institute, Menlo Park, California
- Dow Chemical Company, Midland, Michigan
- Factory Mutual Research Corporation, Norwood, Massachusetts
- Eglin Air Force Base, Florida
- BuMines Enforcement and Safety Administration, Washington, D.C.
- Air Force Office of Scientific Research, Washington, D.C.
- National Fire Protection Association, Boston, Massachusetts
- Cities Service Company, Lake Charles, Louisiana
- PPG Industries, Lake Charles, Louisiana
- Union Carbide Company, South Charleston, West Virginia
- American Petroleum Institute, Washington, D.C.
- American Chemical Society, Washington, D.C.
- Manufacturing Chemists Association, Washington, D.C.

CHAPTER 10

CONCLUSIONS AND RECOMMENDATIONS

Conclusions

The primary conclusion of this study is that the concept of the VM is feasible for use in risk analysis. The material required to operate such a model, viz., the input data and the predictive submodels, is either available or attainable. Although some aspects of the modeling are not at the highest level of sophistication, the VM yields results that appear to be consistent with the historical survey of actual accidental spills. Technical details of conclusions drawn from the operation of the VM are given in Chapters 7 and 8. Some of the more significant conclusions are listed below.

- The injuries and damage resulting from the detonation of a vapor cloud are highly dependent upon the exact nature of the air dispersion. This dependence upon the spill characteristics (location of spill, rate of gas release) and the atmospheric conditions (temperature, wind, stability) is a realistic reflection of the complexities of the actual world and is not considered to be an inaccuracy or quirk in the modeling used.

- The injuries resulting from the release of toxic gas into the air are highly dependent upon the nature of the air dispersion, just as in the case of explosion. This is a realistic aspect of the simulation.

- In general the parameters that are input to the VM have a certain level of importance in determining damage; three such parameters, listed in descending order of importance, are:

  (1) spill size
  (2) stability class
  (3) wind speed

- For flammable and toxic cargoes there is a spill size below which the VM does not assess any damage even though some may occur in reality; this minor anomaly is primarily the result of using in the VM a grid cell system of finite spacing.

The simulation shows that for each flammable cargo spilled under a given set of environmental conditions, there is a critical spill size such that spills smaller than this do not cause any damage. This occurs because by the time mass has gone from the spill into the air in a large enough amount to cause damage, the fuel-air cloud is too diffuse to ignite. That is, this critical size is that for which the evaporation rate is slow enough relative to the dispersal rate, that the fuel concentration is never above the lower flammable limit except within a few tens of meters of the spill site. This aspect of the simulation is only qualitatively correct.

In the real world, the damage-causing potential of a spill decreases as the spill size decreases, but it does not necessarily go to zero. The finite size of the grid cells with their associated ignition points and the limitations on the correct application of the Phase I submodels only on geographical scales over tens of meters cause the simulation to predict zero damage for spills below a certain size when, in fact, a small damage-causing potential could be present.

Similarly for each toxic cargo spilled under a given set of environmental conditions, there is a critical spill size such that spills smaller than this are not capable of causing significant injury. This occurs because toxic material is dispersed to below an injurious concentration level at distances close to the spill. That is, the evaporation rate is slow enough relative to the dispersal rate so that the concentration is never above the threshold for inhalation injuries except within a few tens of meters of the spill site.

Recommendations

Recommendations are given for improvements to specific submodels, aspects of submodels, overall model architecture, and data sources, collection, and analysis. Improvements to the VM should be considered in view of (1) need, and (2) feasibility. The need for an improvement is determined by the magnitude of changes in output produced by making the improvement. The greater the change effected, the greater is the need. The feasibility of an improvement is determined by the facility, both technical and financial, with which the improvement can be made. Improvements, which are more tenable technically and lower in cost, are more feasible.

On this basis recommendations arising from this study may be grouped in four categories.

(1) Recommendations for improvements of greatest need without regard to feasibility. These improvements will have a large effect on the output of the VM.

(2) Recommendations for improvements of lesser, but significant, need and unquestionable feasibility. These improvements will have a significant effect on the output of the VM and are both technically and financially feasible.

(3) Recommendations for improvements of questionable significance or feasibility, but not both. These improvements are either (1) of significant effect, but questionable feasibility, or (2) of questionable significance, but unquestionable feasibility.

(4) Recommendations for improvements of questionable significance and feasibility.

The degree to which any of these improvements can be implemented is, of course, largely dependent on the amount of resources, time and level of effort, that is allocated. In addition, however, improvements, especially to specific aspects of modeling and to overall model structure, are further constrained by factors inherent to the VM.

- Improvements requiring an extensive increase in the amount of data input are undesirable since an exorbitant cost for data collection, manipulation, and computer storage will make usage of the VM impractical.

- Improvements requiring an extensive increase in computer running time and/or storage requirements will make operation of the VM too expensive to be useful; the use of certain very accurate, but costly, finite difference models is therefore precluded.

Within the context of these constraints, recommendations for further work to improve the VM are listed below.

Recommended Improvements of Greatest Significance:

(1) The VM will be modified to assess deaths and injuries suffered by indoor sheltered populations due to all relevant damage mechanisms. Consideration will be given to the varying degrees of shelter afforded by different types of structures. For injury caused by inhalation of toxic gases, assessment of injury to the indoor population will involve considerations of seepage of the toxic substance into structures.

For injury caused by explosion, assessment of injury to the indoor population will involve the degree of shelter afforded by a particular building type and also the degree of shelter afforded by the placement of the people in the building.

Injury to persons inside buildings as a result of flash fire or pool burning is much less likely to occur as a primary damage mechanism than injury to sheltered populations from explosion or toxic substances.

The treatment of death and injury to people inside structures is feasible and will have a significant effect on the damage calculation performed by the VM.

(2) The damage assessment models should consider secondary (non-immediate or not direct) damage mechanisms; for example, a spill of flammable liquid ignites producing a moderate fire hazard, but this spill-based fire ignites a nearby petroleum refinery producing fires and explosions that cause calamitous damage.

(3) An effort should be made to restructure the VM and the required submodels to allow simulation of phenomena actually occurring simultaneously as such. Thus, for example, spilling, evaporation, and air dispersion are currently modeled as a sequence of events, even though all three may happen at the same time. Restructuring Phase I of the VM in this way appears to be feasible, although not necessarily easy. For certain simulations, a quite different picture will result if events are modeled simultaneously instead of sequentially.

(4) The movement of vulnerable resource populations with time of day, season of the year, and other factors should be researched and modeled to give a more realistic description of the resources at risk. For example, the census tract data currently used give low population densities to commercial etc., even though the population density in such locations can be very high at selected times. It appears to be feasible to account for population shifts caused by work, recreation, and travel. Shifting of the vulnerable resources will, of course, strongly affect the damage assessment.

(5) An alternative to locating the ignition sources at discontinuous points (cell centers) should be considered. A treatment is desired which would consider ignition potential as a true function of area, rather than the current treatment which considers ignition sources to be concentrated at the center of a grid cell. By describing ignition sources in a manner other than locating the sources at discrete sites (the cell centers), a more realistic assessment of time to ignition and distance between ignition point and spill may be obtained. Such a treatment of ignition sources is feasible and is expected to have a significant effect on damage assessment results by changing the time for ignition.

Recommended Improvements of Definite Feasibility and Significant Need:

(1) The flash fire should be modeled so that damage beyond the flame location is allowed. The calculation of radiation levels at locations distant from the flame is definitely feasible. Some sources report significant damage to both personnel and property at locations moderately far from fires.

(2) Modeling should be added to permit accurate treatment of subsurface spills. The release of cold, soluble chemicals underwater is of special interest. Such modeling is definitely feasible. The ability to treat this additional class of spills will enhance the utility of the VM.

(3) The VM should be modified to treat the ingestion of water containing toxic concentrations of pollutant. Estimating a specific level of injury or percent of population injured is not possible since the quantity and rate of ingestion are highly variable and unpredictable. What is required is some indication of the toxic hazard presented by a given concentration of spilled substance. One possible approach is to establish levels of hazards. The VM should be modified to inform the user when and where these hazard levels exist in the water body. This modification is definitely feasible and will make the output of the VM significantly more useful.

(4) The VM should incorporate a better treatment of the ignition of structures. A more precise method to account for shielding from thermal radiation should be devised. The current criterion that 25% of the structures are ignited in a cell subject to radiation sufficient to cause ignition should be replaced by a criterion that has a variable percentage ignited and the percentage ignited is to be calculated on the basis of physical principles. This improvement is feasible and will significantly affect the damage assessed to structures.

(5) Further toxicological considerations are required so that additional toxic substances may be treated by the VM. Since the additional toxic substances may be other than irritant gases, the assessment procedures used for the added substances may differ from those used previously for NH_3 and Cl_2. The additional toxicological considerations are feasible and will enhance the applicability of the VM.

(6) The water mixing model should be expanded to include water mixing and reaction. Such modeling is certainly feasible, but separate models may be required for each class of reactions. The inclusion of this modeling in the VM will increase the number of substances for which spills can be simulated.

(7) The capability to treat spills of dissolvable solids, liquids, and gases should be added to the VM. The treatment of substances with finite solubilities is feasible. The ability to simulate substances of this type will enhance the value of the VM.

(8) Advantages may result from treating the population density of vulnerable resources in a continuous rather than a discrete, cell-based manner. The use of discrete cells requires that a greater number of smaller cells be used in order to obtain greater accuracy for a simulation over the same geographical area. Since the damage simulated is often highly localized, only part of the detailed data base, maintained and used at considerable cost, is actually required for a given simulation. It is feasible to treat vulnerable resources in a manner such that the geographical area impacted by damage is defined and the vulnerable resource data for that area only are retrieved. Such a change in the treatment of vulnerable resource data will make the VM more precise and more efficient.

(9) Computational efficiency may be increased by the use of look-ahead techniques. Preliminary calculations may be made to estimate the region impacted by damage mechanism. Detailed calculations and data retrieved need only be performed for the region estimated to be affected. Savings in computer time and cost will result. Such look-ahead techniques are certainly feasible.

(10) The VM should be modified to model the heating, rupture, and release of pressurized cargo in a fire. These phenomena could result in significantly different damages than release of a cargo without additional heating. The modeling is feasible.

Recommended Improvements of Questionable Feasibility or Need, But Not Both:

(1) The analytical and experimental background applicable to "the roiling fireball." The roiling fireball seems to be the very rich, but gas phase, portion of a flammable vapor cloud that results in a burning process significantly different from the diffusion flame described by the pool burning model or the combustion of the premixed cloud described by the flash fire model. The roiling fireball should be investigated to determine whether and how this phenomenon might be modeled because as suggested by the historical survey, this may be a significant damage mechanism. The roiling fireball is distinguished from the flash fire by: (1) combustion in the flash fire is rapid, compared to combustion in the fireball; and (2) the burning mixture in the fireball is rich and is supported by turbulent diffusion, whereas the burning mixture in the flash fire is premixed within flammable limits. It is recognized that this phenomenon may also induce significant overpressures. Significance is moderate to great; feasibility is questionable.

(2) The VM should be modified to treat damage caused by the inhalation of toxic combustion products. Although some limitations of the ability to treat injury from toxic combustion products may not yield to analysis, the model should be modified at the very least to inform the user of the existence of this damage mechanism. Significance is moderate; feasibility, questionable.

(3) Injury by asphyxiation should be addressed. Although an extensive effort in this area is not envisioned, some means of determining the seriousness of this damage mechanism is desired. The assessment approach should take into account the time varying concentration of the asphyxiant. For substances which exhibit both asphyxiant and toxic effects (e.g., dichlorodifluoromethane), the problem of combined effects needs to be addressed. Significance is indeterminate; feasibility, definite.

(4) The air dispersion model should be made more realistic by incorporating the ability to treat the arbitrary time variation of source strength and source location. Significance is unknown; feasibility, definite.

(5) The pool burning submodel should include a more realistic treatment of simultaneous spreading and burning. Feasibility is definite; significance is unknown.

(6) The VM should be modified so that the release and migration of heavy insolubles on river beds can be modeled. Feasibility is definite; significance is unknown, since heavy insolubles would appear to offer less of a threat to people and property than other classes of substances.

(7) The effects of water wave action and of wind on the spread of a surface spill should be considered. Feasibility is definite; significance, unknown.

(8) The air dispersion model should be extended to include the dispersion of reacting chemicals. Feasibility is definite; significance is questionable, since spills of relatively few cargoes would seem to result in the air dispersion of a reacting substance.

(9) Air dispersion by gravity spreading in calms should be modeled. Feasibility is definite; significance, unknown.

(10) Micrometeorological effects, and meandering effects, presently treated analytically, should be implemented in the computer models. Feasibility is definite; significance, unknown.

(11) Instead of computing damages at a given sequence of cell centers, techniques capable of yielding isodamage contours would be, in some respects, more appealing. Feasibility is definite; significance, unknown.

(12) Buoyancy considerations should be incorporated into the air dispersion modeling. Feasibility is definite; significance, unknown.

(13) Consideration of topological features should be incorporated into the air dispersion models. Feasibility is definite; significance, unknown.

Recommended Improvements of Questionable Feasibility and Need:

(1) The effect of explosion on the liquid spill should be considered; it is conceivable that streams of flaming liquid could be sprayed long distances by a vapor cloud exploding over a spill.

(2) The assessment of damage from inhalation of toxic fumes should consider that the toxic concentration varies in space and time in a stochastic manner; the receptor response to these concentration variations may be different from the currently modeled response to an average concentration.

(3) Further consideration should be given to the significant ways in which diffuse explosions differ from conventional explosions, both in physical characteristics and in damage phenomena.

(4) The effects of precipitation should be assessed, and modeled as required, for the air dispersion, surface spreading, and water mixing submodels.

Recommended Improvements to Data:

The following are data items that may be available from investigations of accidental spills and are useful for improving the VM modeling; in all cases it is desired that the data gathered be as precise and complete as possible. These recommendations are included at the direction of the Risk Analysis Advisory Board of the USCG.

I. In the case of damage from toxic materials:

A. Source and Spill Development Data

1. Chemical and physical nature of the spilled substance
2. Quantity spilled
3. Local weather conditions prevailing at the time of spill
   a. wind speed and direction } each as a function of
   b. temperature } height, if available
   c. inversion characteristics
   d. humidity and precipitation
4. Visual or photographic observations of the travel of a visible toxic cloud

B. Receptor Data

1. Best possible estimate of population at risk
2. More precise definition of:
   a. nature of effects on receptors
   b. duration of effects on receptors
   c. severity of effects
   d. treatment provided affected receptors
   e. state of health of receptors prior to incident
   f. age of receptors
3. Effects on nonhuman receptors - animals and plants

II. In the case of damage from fire and/or explosion:

A. Source and Spill Development Data

1. Chemical and physical nature of the spilled substance
2. Quantity spilled
3. Sequence of spillage and ignition
4. Data
   a. wind speed and direction
   b. temperature
   c. inversion characteristics
   d. humidity and precipitation

   } each as a function of height, if available
5. Observations of cloud size and travel before ignition

B. Receptor Data

1. Damage maps
   a. location of dead and cause of death
   b. location of injured and severity of injuries
   c. location and severity of physical damage
2. Extensive photography

Closing Remark

The listing of such a large number of recommendations was intended to point the way toward areas related to the VM for which additional effort is believed to have the greatest potential for benefit. This list of recommendations is not, nor is it intended to be, an indictment of the VM. To the contrary the VM, in this its first stage of development, is believed to be a useful, practical tool for use in the risk analysis of marine spills. Further development of the VM will make this already functional tool more useful, more precise, and more widely applicable.

REFERENCES

[1] Dunn, W.A., and P.M. Tullier. Spill Risk Analysis Program Phase II Methodology Development and Demonstration. Operations Research, Inc., Silver Spring, Md., August 1974. USCG Tech. Report #840.

[2] Raj, P.P.K., and A.S. Kalelkar. Assessment Models in Support of the Hazard Assessment Handbook. Arthur D. Little, Inc., Cambridge, Mass., January 1974. USCG Report No. CG-D-65-74 (NTIS AD 776617).

[3] Hazard Assessment Computer System (HACS) User Manual. Arthur D. Little, Inc., Cambridge, Mass., December 1974.

[4] Raj, P.P.K., J. Hagopian, and A.S. Kalelkar. Prediction of Hazards of Spills of Anhydrous Ammonia on Water. Arthur D. Little, Inc., Cambridge, Mass., January 1974. D.O.T. Report No. CG-D-74-74 (NTIS AD 779400).

[5] Slade, David H. (editor). Meteorology and Atomic Energy. U. S. Atomic Energy Commission, July 1968.

[6] Tyron, G.H. (editor-in-chief). National Fire Protection Association, Boston, 1969.

[7] Eckert, E.R.G., and R.M. Drake. Heat and Mass Transfer. McGraw-Hill, N. Y., 1959. Ch. 14.

[8] Pasquill, F. The estimation of the dispersion of windborne material. Meteorology Mag. 90(1063):33-49, 1961.

[9] Pasquill, F. Atmospheric Diffusion. Van Nostrand, London, 1962.

[10] Turner, D. Bruce. Workbook of Atmospheric Dispersion Estimates. Environmental Protection Agency Publication No. AP-26, Revised 1970, pp.37-38.

[11] Stewart, N.C., H.J. Gale, and R.N. Crooks. The atmospheric diffusion of gases discharged from the chimney of the Harwell Reactor BEPO. Int. J. Air. Pollution 1:87-102, 1958.

[12] Cramer, H.E. Engineering estimates of atmospheric dispersal capacity. Amer. Ind. Hyg. Assoc. J. 20(3):183-189, 1959.

[13] Nonhebel, G. Recommendations on heights for new industrial chimneys. J. Inst. Fuel 33:479-513.

[14] Fay, J.A. Unusual fire hazard of LNG tanker spills. Combustion Sci. Tech. 1:47, 1973.

[15] Feldbauer, G.W., et al. Spills of LNG on Water - Vaporization and Downwind Drift of Combustible Mixtures. Esso Research & Engineering Company, Report No. EE61E-72 (Released by the Am. Petroleum Institute, Re 6Z32), March 1973.

[16] Strehlow, Roger A. Unconfined vapor-cloud explosions - an overview. In Proceedings of the International Symposium on Combustion, 1972.

[17] Brown, John A. A Study of the Growing Danger of Detonation in Unconfined Gas Cloud Explosions. John Brown Associates, Inc., Berkeley Heights, N. J., December 1973.

[18] Kinney, Gilbert F. Explosive Shocks in Air. The Macmillan Co., New York, 1962, p.11.

[19] Strehlow, Roger A. Equivalent Explosive Yield of the Explosion in the Alton and Southern Gateway Yard, East St. Louis, Illinois, January 22, 1972. Engineering Experiment Station, College of Engineering, University of Illinois, Urbana, June 1973. AAE TR 73-3, UILU-ENG-73 05-05.

[20] Kinney, Gilbert F. Engineering Elements of Explosions. Naval Weapons Center, November 1968. NWC TP-4654.

[21] Kirk, P.L. Fire Investigation. John Wiley & Sons, Inc., New York, 1969, p.193ff.

[22] Hawkins, S.J., and J.A. Hicks. A New Explosives Technique for Synthesizing a Wide Range of Pressure Waveforms in Air, Part 1: Approximate Theory of Air Blast from Extended Explosive Charges. Ministry of Technology, Explosives Research and Development Establishment, Waltham Abbey, Essex, October 2, 1968. Report No. ERDE 9/R/68.

[23] Woolfolk, R.W., and C.M. Ablow. Dependence of the blast wave from an explosion on the energy release rate. In Proceedings of the Fifteenth International Symposium on Combustion, August 1974.

[24] Strehlow, R.A., L.D. Savage, and G.M. Vance. On the measurement of energy release rates in vapor cloud explosions. Combustion Science and Technology 6:307-312, 1973.

[25] Strehlow, R.A., and A.A. Adamczyk. On the Nature of Non-Ideal Blast Waves. Engineering Experiment Station, College of Engineering, University of Illinois, Urbana, April 1974. AFOSR-TR-0834.

[26] Karim, G.A., and P. Tsang. Flame propagation through atmospheres involving concentration gradients formed by mass transfer phenomena. Presented at ASME-CSME Fluids Engineering Conference, Montreal, Quebec, May 13-15, 1974.

[27] Lewis, B., and G. von Elke. Combustion, Flames and Explosions of Gases. Academic Press, Inc., New York, 1951.

[28] Kutateladze, S.S., and V.M. Borishanskii. A Concise Encyclopedia of Heat Transfer (J.B. Arthur, trans.). Pergamon Press, New York, 1966.

[29] U.S. Department of Commerce, Bureau of the Census. 1970 Census of Housing, Block Statistics, September 1971.

[30] Finney, D.J. Probit Analysis, 3rd edit. Cambridge University Press, 1971.

[31] Kowytz, T.A., et al. Arch. Environ. Health 14:545, 1967.

[32] Chasis, H., J.A. Zapp, J.H. Whittenberger, J.L. Helm, J.J. Doheny, and C.M. MacLeod. Chlorine accident in Brooklyn. J. Occup. Med. 4:152, 1947.

[33] Joyner, R.E., and E.G. Durel. Accidental liquid chlorine spill in a rural community. J. Occup. Med. 4:152-154, 1962.

[34] Weill, H., G.M. Schwarz, and M. Ziskind. Late evaluation of pulmonary function after ecute exposure to chlorine gas. Am. Rev. Respiratory Disease 99:374-379.

[35] Longinow, A., G. Ojdrovich, L. Bertram, and A. Wiedermann. People Survivability in a Direct Effects Environment and Related Topics. IIT Research Institute, Chicago, May 1973.

[36] U.S. Department of Transportation, National Transportation Safety Board. Railroad Accident Report (Chicago, Burlington and Quincy Railroad Company, Train 64 and Train 824, Derailment and Collision with Tank Car Explosion, Crete, Nebraska, February 18, 1969). Report No. NTSB-RAR-71-2, Washington, D.C., February 24, 1971.

[37] Radanovic, L. (editor). Sensitivity Methods in Control Theory. Pergamon Press, New York, 1966.

[38] Tomovic, R. Sensitivity Analysis of Dynamic Systems. McGraw-Hill, New York, 1963.

[39] Burgess, D., J.N. Murphy, M.G. Zabetakis, and H.E. Perlee. Volume of flammable mixture resulting from the atmospheric dispersion of a leak or spill. Advance copy, to be submitted to the Fifteenth Symposium (International) on Combustion, The Combustion Institute, 1974.

[40] Burgess, D.G., and M.G. Zabetakis. Detonation of a Flammable Cloud Following a Propane Pipeline Break -- the December 9, 1970 Explosion in Port Hudson, Missouri. U.S. Bureau of Mines, RI 7752, 1973.

[41] Sarkes, L.A. A survey of LNG technological needs in the USA - 1974 to beyond 2000. Session VII, Paper 1, Fourth International Conference on Liquified Natural Gas, Algiers, 24-27 June 1974.

APPENDIX A

PHASE I FLOW CHARTS WITH NARRATIVE

This appendix described the Phase I Vulnerability Model (VM) flow diagrams. In general, available submodels from HACS are used wherever possible. Where submodels are still to be developed, they are so indicated.

The inadvertent release of all or a portion of a hazardous cargo is characterized by many quantities, most of which are listed in the attached symbol list. In addition, many quantities describing the ambient air and water conditions must be given. The cargo may be either solid, liquid, or gas, or a combination of gas and liquid. (This last condition will usually be the case for a tank containing a fluid under pressure or at reduced temperature or both.) The puncture, rupture or vent may occur above or below the water line, so we must consider the possibility that the cargo will escape in three different phases and that it may escape into air or into water.

Because of their extremely rare occurrence, the following possibilities are not considered.

1. A fluid cargo is being transported at less than ambient air pressure.

2. The fluid cargo is such that it changes to the solid state (freezes) upon contact with ambient conditions (air or water).

3. The cargo is lighter than air in its liquid or solid phases.

Because the vent will almost always be within 15 m of the water surface ($\pm$ z) we assume the following:

a. For the case of a gas venting into water, no significant advection by the current will occur before the gas reaches the water surface. (This assumption is reasonable because the rise of the gas to the water surface will be very fast compared to the advection processes being considered.)

b. For the case of a liquid venting into air, no significant advection by the wind will occur before the liquid reaches the water surface, and no significant evaporation of the cargo will occur in the time it takes the liquid to reach the water surface. (This assumption is also reasonable because of the relatively short time required for the liquid to fall to the surface. The exception would be a rupture in a tank holding a liquid cargo under pressure, which results in a fountain of the liquid cargo, directed upwards. This is extremely unlikely, however, as a rupture in the top of the tank will result in the escape of the cargo in gaseous form in virtually every case, and a rupture in the side of the tank below the gas-liquid interface would result in a fountain directed primarily in the horizontal direction.)

The flow chart is entered at the top of chart 1, at "SPILL". The first thing that must be done is to enter the many quantities needed to describe the cargo, vessel location, ambient conditions and the puncture or rupture. For some common cargoes, the physical and chemical properties such as critical point temperature, viscosity, concentration at lower flammability limit, and molecular weight may be obtained from the HACS Properties File. But other quantities such as the temperature, pressure and amount of the cargo will have to be supplied by the user. The difference between the two types of information needed is distinct. The properties of a cargo are inherent, and will not change from spill to spill, so they may be stored in the computer memory once and recalled when needed. The quantities which the user must supply each time are those which may vary with the spill, such as location of the spill, size of the vent, and the ambient conditions.

With this information available, the first task is the calculation of the rate of escape of the cargo, and the phase of the cargo which escapes. For a tank containing both gas and liquid phases, the height of the vent z_v would have to be compared with the height of the phase change of the gas-liquid interface z_{pc}. Further, if the vent is located below this interface, the escaping cargo may change from liquid to gas when sufficient cargo has escaped to lower the interface level to the vent level. Generally the vent or puncture area will be given, and the rate of release calculated, but the user may stipulate an instantaneous release. A solid spill must be assumed to be instantaneous at this time, as there is no extant subroutine to calculate rate of a solid spill. For liquids and gases, the HACS/CHRIS model is being used. This model takes the tank walls to be either isothermal or adiabatic, and for the venting of a gas, the subroutine uses either choked (sonic flow) or unchoked (subsonic flow) equations as appropriate.

At this point it might be mentioned that the tie-points 1 through 8 represent intermediate conditions, which might be called meta-stable states. The cargo may exist, of course, in three phases or states -- gas, liquid or solid. Since cargo spills upon land are outside the scope of this study, the cargo can be in the air, in the water, or it can occupy space at the interface between the air and the water. This last case is considered worthy of separate treatment because the spread of the cargo will be significantly different in this case than it will in the other two cases. The three cargo phases and the three locations lead to nine possible combinations, but the case where a gaseous cargo is in the water is considered too transient. This first chart, then, treats the escape of the cargo and its rapid transition to one of the eight intermediate states. The states, represented by tie-points 1 through 8, are not necessarily the final disposition of the cargo, but states in which the cargo remains for several minutes at least. This is long enough that transport of the cargo by diffusion, the wind, or the current must be considered. The processes on chart 1, on the other hand, generally take place in several seconds, so that advection during this period may be ignored at this time.

GASEOUS RELEASE

For the case where all or part of the escaping cargo is in the gaseous phase, the flow diagram on chart 1 is followed to the left, to point G1, where different paths are followed depending upon whether the vent is above or below the water. In the former case, at G2 we determine whether some of the escaping gas will condense to the liquid phase, forming a mist or fog comprised of droplets of the cargo.

The escaping gas has been assumed to have expanded to the ambient air pressure, P_a, by a throttling process, without mixing with the air. If the gas is considered to be a perfect gas, in such a throttling process the final temperature of the gas is the same as its initial temperature, and the expanded gas will be superheated and dry. The gas at the edge of the cloud will soon come to equilibrium with the air temperature, however, and condensation of the cargo will occur there if the vapor pressure of the cargo at the ambient air temperature is less than the air pressure, that is, if $P_{vc}(T_a) < P_a$.

If it is determined that liquid drops of the cargo form a mist, the portion of the cargo in each phase is calculated (at G3), and for each quantity one proceeds to specific models through tie-points 1 and 3. In the case that no mist forms, all the escaped cargo is in vapor form, and at G4 it is asked whether the gaseous cargo is heavy enough so that it mixes only slightly into the air and primarily floats upon the water surface. This is an unlikely case, but it is possible for exotic gases or for very cold gases. If the gas mixes with air, we proceed to chart 2 through tie-point 1. If the gas is very dense, one proceeds to chart 3 through tie-point 2.

Returning to G1, in the case where the gas is escaping below the water line of the vessel, at G5 we calculate the amount of the escaping cargo which goes into solution as the gas bubbles rise to the surface. The portion going into solution is treated as liquid in water, through tie-point 4 to chart 5, and the portion remaining as a gas escapes to the surface. For this gas at G6, we ask if it mixes into the air or remains at the interface, and proceed to tie-points 1 or 2 accordingly, as in the case of an escape of gas directly into the atmosphere. At the present time, the calculation of the portion of the cargo going into solution has not been considered, and we temporarily assume that all the escaping gas reaches the water surface. It should be pointed out that it is not possible for the water pressure to force the escaping gas into liquid phase. If the water pressure outside the puncture were great enough to liquify the gaseous cargo, then the water pressure would force water into the cargo tank while liquifying the cargo in the tank, and very little cargo would escape.

LIQUID RELEASE

If the escape rate calculation indicates that some or all of the cargo escapes in liquid form, one proceeds to L1 where the vent height, z_v, is compared with the height of the water surface, $z=0$, to determine whether the leak is above or below the water. If the liquid cargo is escaping into air, we assume that it reaches the water surface without advection or loss, as discussed above. Next, at L3, we determine whether the liquid floats or sinks. If it sinks, we have the liquid in water case, and proceed to chart 5 through tie-point 4.

For the case in which the liquid cargo escapes underwater, at L4, it is asked whether the cargo floats or sinks. As in the case where the cargo was released into the air, the original temperature of the cargo in the tank is used in calculating the density of the cargo, for it is assumed that a spill of sufficient mass to be of interest will take some time to come to ambient temperature, and the temperature change of the cargo is considered on the flow charts which follow this first one. Most cargoes will have a density at least 10% different from that of water, but in the cases where

they do not, the water temperature and salinity may be used to calculate the density of the water more precisely. If the liquid cargo sinks, we again proceed to tie-point 4. If the cargo floats, one considers that case further through tie-point 5.

SOLID RELEASE

The case of a spill of a hazardous cargo which is in solid phase has been given a lower priority than the case of a cargo in a fluid state. Therefore many of the calculation subroutines are in undeveloped condition, but the decision pathways are fairly clear regardless. There is currently no routine available to calculate the rate of a solid phase spill, so it will be declared to be instantaneous. The spill rate calculation for solid cargoes may be developed later as time and interest dictate. Since a cargo consisting of fist-sized chunks will spill at a very different rate from a cargo consisting of grains about the size of sand grains, the spill rate calculation will have to take into account the size range of the particles which make up the cargo.

Having decided that all or part of the spill is solid, at S1 the decision is made as to whether the puncture is above or below the water line of the vessel. If the cargo escapes into air, at S2 we wish to calculate how much of the cargo is carried away by the wind, and how much falls to the water surface. At present this subroutine has not been designed, so it is assumed that all of the escaping cargo falls to the wate surface. This will be inaccurate only for a cargo consisting of very fine particles of a light material when a high wind is present.

The cargo having fallen to the water surface, at S3 it is decided whethe· the particles float or sink. One then proceeds to follow the case of solid in water in more detail on chart 8 through tie-point 7, or the solid on water surface case on chart 9 through tie-point 8. If the solid cargo is escaping below the water line, at S4, the density of the cargo is ascertained, and in the case that it sinks, one proceeds to tie-point 7. If the cargo particles rise to the surface and float, one should calculate the portion lost by going into solution during the brief period it takes the particles to reach the water surface. This has not been implemented yet, however, so currently there is no such loss, and all the escaping cargo arrives at the surface and is treated later through tie-point 8. The route to the liquid in water case through tie-point 4 is shown, however.

GAS IN AIR

For the case of a gaseous cargo escaping into the air, the detailed events are followed on chart 2 through tie-point 1. First the air temperature, stability or mixing characteristics, and wind velocity are used to calculate the dispersion of the cargo. At present this calculation assumes that all the escaping cargo has been released instantly. This model has been discussed in some detail in chapter 2 of this report, so we proceed to the decision at G11 on the reactivity of the cargo. This information will come from the properties file, or will be entered by the user for cases of unusual spills where the properties file does not have this information. For many, if not most, of the hazardous cargoes, the cargo will be reactive.

At G12 on the basis of flammability limiting concentrations and ignition temperatures, it is decided whether the situation is such that combustion is possible. If it is, it is next determined whether an ignition source is present, and if so we proceed through tie-point 9 to the fire and explosion model, which is discussed in detail elsewhere in this report. If the gaseous cargo is not combustible, or if it has not been ignited, the path followed is to G13 where a series of calculations determine what reactions will take place, how much heat is liberated, what reaction products are formed and at what rates. This model is still in the germinal stage. Finally, the spread and dispersal of the reaction products must be determined. While the methods to be used for this are much the same as for the dispersal of the cargo originally, the use of these methods to trace the spread of the reaction products has not been implemented at this time. This will be necessary at some point, for there are a number of cases, though not very common, where the reaction products are more toxic or dangerous than the original cargo.

GAS ON WATER SURFACE

The case for a heavier-than-air gas resting on the water surface has not been programmed at this time, but on chart 3 the calculations which should be performed are indicated. For the case of a gas that is heavier than air primarily because of its low temperature, the calculation of the spread of the gas should be similar to the calculations used to determine the spread of a cryogenic liquid, and should present no major difficulties. The rate of heat input to the gaseous cargo should also have much in common with the flow of heat to a cryogenic liquid spill. As the cargo attains a density not too different from that of air the cargo can be expected to mix into the air, and with this rate calculated, at G21, one then goes to the gas-in-air calculations, which have just been discussed. While the case of a gas which owes its very high density to its very low temperature will be more common, the case of gases which are inherently much heavier than air, even at ambient temperature and pressure may also be treated by this model. As in the case of a cold gas, the spilled cargo will eventually disperse into the air, but the rate of such a dispersal will depend not upon the rate of warming of the gas, but primarily upon the wind speed and local turbulence conditions. The calculation at the top of chart 3 should consider this type of loss into the air as well as heat transfer and gravity-induced spreading upon the water surface.

LIQUID IN AIR

Chart 4 takes up the case of a liquid in air - a mist or fog whose droplets are composed of the cargo in liquid phase. The dispersion calculation will be the same as for the dispersion of gas in air, with the addition of a subroutine to calculate the loss of the cargo in liquid phase due to evaporation and rainout. Rainout may occur either due to the incorporation of the drops into existing precipitation, or when the density and size of the drops allows them to grow in size while decreasing in number until the surviving drops fall due to their own weight. The increase of the number of drops might be precipitated by a reduction in the termperature in the cloud, which would reduce the vapor pressure of the cargo, and lead to more condensation.

In most cases, however, evaporation will reduce the amount of cargo in the liquid phase. The mixing of the originally concentrated cargo plume with ever larger amounts of air during the course of dispersal is the cause of this. The amount of cargo per unit volume in the plume will have to be more than the air can absorb at saturation in order for mist droplets to form. The mixture of the original volume of the spill into a larger amount of air will increase the amount of cargo that the air can hold in vapor phase, so, in the absence of a marked temperature decrease during the spreading of the plume, evaporation of the droplets can be expected.

After the calculation of the rates of phase change for the cargo, at L11, the portion evaporating is treated through tie-point 1, and the portion raining-out is treated through tie-point 3 or 4 depending upon the density of the cargo in its liquid phase. The cargo remaining in liquid phase is next assessed for its combustibility at L12. If it is combustible, and if it ignites, then one proceeds to the fire and explosion model through tie-point 9. If the cargo is incombustible or is not ignited, one proceeds to the evaluation of toxicity, air pollution, reduced visibility (which may be a navigation hazard). and other damage.

LIQUID IN WATER

Chart 5 takes up the case of a liquid in water - entry from the main flow chart by means of tie-point 4. Since the behavior of the spilled liquid will depend on whether it mixes with water or not, the immediate question concerns the cargo's miscibility. A miscible liquid will mix into the water and disperse much like a gas dispersing into air. An immiscible liquid, on the other hand, will maintain its own separate identity and stay separate from the water. If lighter than water, the immiscible liquid will remain on the surface and that possibility is treated through tie-point 5. Here only immiscible liquids which have a density greater than that of water are considered. They will, of course, sink to the bottom, and there, if the current is strong enough, and the cargo is not too heavy and viscous, significant transport of the immiscible cargo along the bottom may occur. Thus the transport of the spilled liquid will be considerably different for the immiscible spill than it is for the miscible spill, and different calculations are indicated at L22 and L23.

The considerations of boiling of the liquid spill and of reactions are not significantly dependent upon the miscibility of the spill, so no differentiation has been shown here. If the liquid has a boiling point lower than the water temperature, all of the spill will eventually escape into the air, and this path is indicated by the left branch from the decision point at L24. If no boiling takes place, the possibility of reactions is considered, at L26, and the gaseous reaction products escape from the water and are treated through tie-point 1. The unreacted cargo and other reaction products go on to produce water pollution and possibly toxicity hazards.

LIQUID ON WATER SURFACE

For a liquid floating on the surface of the water, the development of the spill is continued on chart 6 through tie-point 5. This case is presently programmed and running in abbreviated form because common hazardous cargoes such as gasoline and liquified natural gas fall into this case, and it

was given top priority. After determining whether the cargo is miscible or not, at L31, the spread of the cargo is calculated. At L34 it is determined whether the spreading miscible spill boils at ambient conditions. If so, one proceeds to the gas in air model after calculating the rate of gas formation at L35. If the spill does not boil, the cargo may still pass to the gaseous state by evaporation, so this is considered at L36, and the possibility of reactions is also considered at this time. The portion of the cargo evaporating and the gaseous reaction products go to the gas in air model via tie-point 1. For the portion of the spill remaining on the water surface, some may be lost by going into solution in the water, but this calculation is not available yet, so it is assumed that all of the spill which does not evaporate or react remains in the pool on the surface. At L37 we ask whether this pool can burn, and if so whether it is ignited. (Ignition would normally occur from an explosion or flash fire resulting from the spread of the cargo in vapor phase.)

For the liquid which does not mix with water at L43 it is determined whether this liquid boils at ambient temperature. If the answer is yes (as it would be for a liquid natural gas spill, for example) at L44 the rate of escape of the cargo in the gas phase is calculated, and the consideration of the problem shifts to the gas in air model. If the spill does not boil, loss by evaporation is calculated at L45 (this would be the case for gasoline), and the escaping gas is again treated by the gas in air model. Reactions are considered at L45 for the unevaporated portion remaining. The possibility of fire is considered at [4] for the pool of cargo and/or reaction products floating.

SPILL OF SOLID CARGO

The case of a spill of a solid phase cargo is taken up on charts 7, 8, and 9 depending on whether the spill has come to be temporarily in the air, on the water, or in the water. We have excluded from consideration the possibility that a solid cargo may be combustible if it is in the water or on the water surface. While these possibilities do exist, they are extremely rare, and other considerations have higher priorities. The case that a solid cargo suspended in the air (in small particles) may explode or burn, is explicitly considered, however, since substances usually harmless, such as wheat flour, have caused explosions when the conditions were right.

The calculation of the spread of fine particles of the solid cargo in the air, reached through tie-point 6, on chart 7 is much the same as the dispersion calculation used for the spread of a gaseous cargo, with the addition that the loss of cargo due to fallout (with or without agglomeration) and the rainout must be considered. For a solid in water (chart 8), the calculation of transport in the water will be much like that for an immiscible liquid, except that the settling rate will be different. The loss of the solid cargo through reactions and solution are next considered at S22. For liquid and gaseous reaction products, and the portion of the solid going into solution, the further consideration proceeds through tie-points 1 and 4 as appropriate. Chart 9 takes up the last of our 8 possibilities, the spill of a solid phase cargo which floats upon the surface by the water. After a calculation of the spread and transport of the cargo by winds and currents, S31, the rates of disappearance due to sublimation, going into solution, and reactions are calculated. Liquid reaction products and cargo going into solution are treated by the liquid in water model through tie-point 4, and the gaseous reaction products and sublimed cargo go to the gas in air model through

tie-point 1. None of the calculations for a solid spill has been programmed at present, but the knowledge needed for many of the subroutines is available.

SYMBOL LIST FOR FLOW CHARTS WITH NARRATIVE

x, y, z : Cartesian coordinates

+z is in the upward direction, z=0 at the water surface

+x is in the direction toward which the wind is blowing

t: time, t=0 at the commencement of the spill

subscripts:

c	cargo
s	spill
a	air
w	water
G	gas phase of the cargo
L	liquid phase of the cargo
S	solid phase of the cargo

Cargo information supplied by user

T_c Temperature at which the cargo is stored

P_c The pressure above ambient air pressure at which the cargo is stored

S_c State of cargo (gas, liquid or solid) - for a cryogenic or pressurized cargo a code will indicate whether the cargo is partly liquid and partly gaseous

z_{pc} Height of the phase change (liquid-gas interface) for a fluid cargo which exists in the tank in both phases

V_c Volume of cargo potentially affected

M_c Mass of cargo potentially affected

Comment: If only one of a number of tanks or holds on a vessel is ruptured or punctured, V_c and M_c are the volume and mass of the affected tank. Note that V_c and M_c will not necessarily be equal to the amount spilled. The nature and location of the puncture may preclude all of the cargo in the tank from escaping.

ρ_c Density of cargo

Comment: V_c, M_c, and ρ_c are inter-related, and all three need not be given in most cases. From T_c and P_c, and other known constants, ρ_c can be calculated for a liquid or gas, and thence M_c if V_c is known, which will usually be the case. For a solid cargo, ρ_c will be the density of the individual grains or chunks, and $M_c \neq \rho_c V_c$ because the packing fraction will have to be taken into account, but in most cases M_c will be known and V_c will not be needed.

Cargo information obtained from the properties file

T_b Boiling point of the cargo at atmospheric pressure

T_f Freezing point of cargo at atmospheric pressure

T_{FP} Flash Point temperature

χ_L, χ_U Concentration of the cargo in gas phase at the Lower and Upper Flammability limits

P_v Vapor pressure, as a function of temperature

λ Solubility

m Miscibility

Spill information supplied by user

M_s or V_s Mass or Volume of spill for an instantaneous spill

A_v Area of puncture, rupture, or vent - needed only if the spill is not instantaneous

z_v Height of puncture, rupture, or vent

Comment: If the spill is not to be instantaneous, then the spill rate as a function of time may be calculated from the area of the vent and the cargo conditions.

Information about Ambient Conditions supplied by the user

T_a Air Temperature

P_a Air Pressure

H Relative Humidity

$\bar{v}_a$ Wind vector

S_a Atmospheric Stability Class

T_w Water Temperature

$\bar{v}_w$ Current vector

N Salinity - may be needed to calculate the water density ρ_w

CHART 1

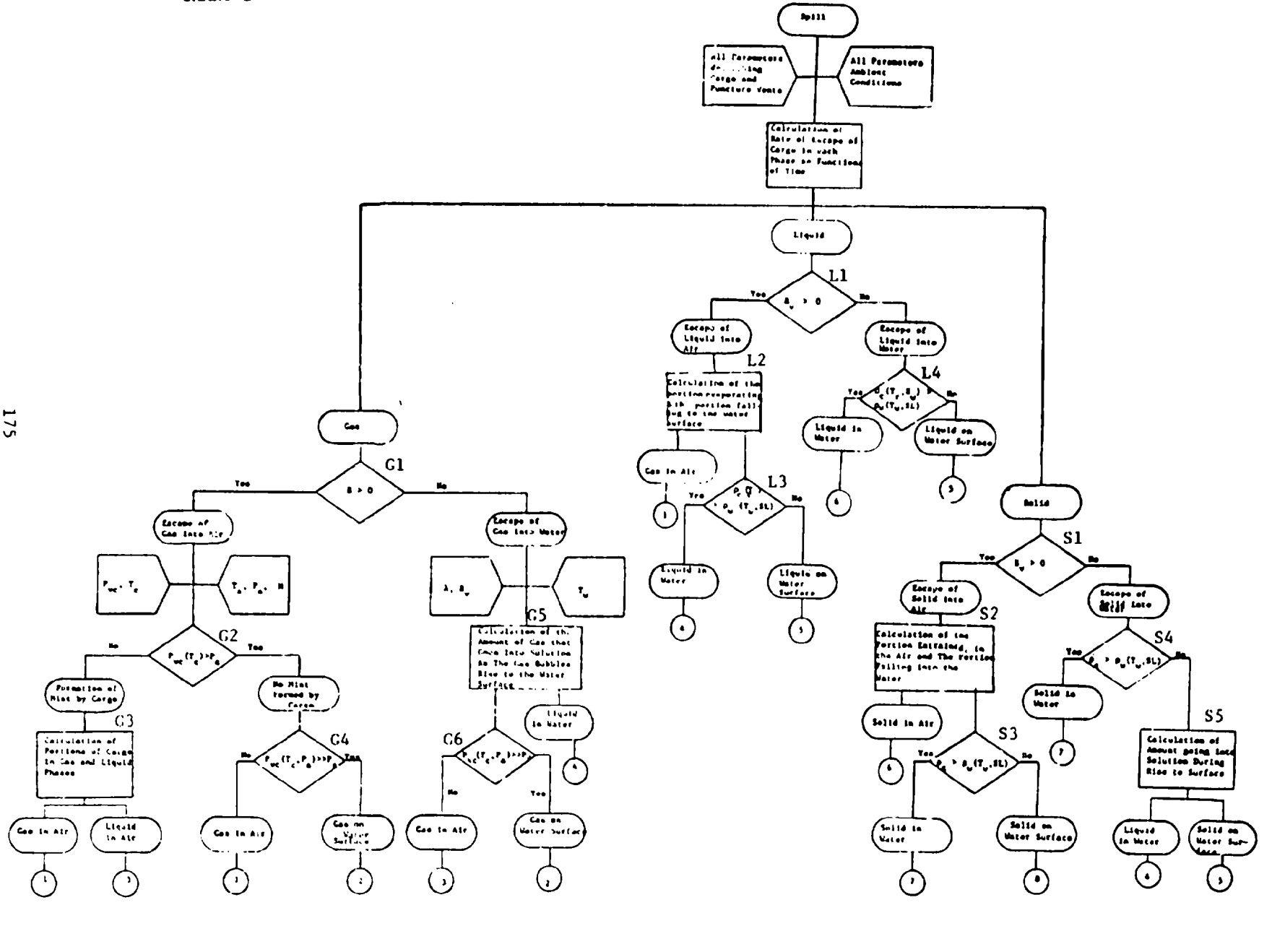
Spill
All Parameters Ambient Conditions
Calculation of Rate of Escape of Cargo in each Phase as Function of Time
Liquid
L1
Yes
No
Escape of Liquid into Air
Escape of Liquid into Water
L2
L4
Liquid in Water
Liquid on Water Surface
Gas in Air
L3
Liquid in Water
Liquid on Water Surface
Gas
G1
Yes
No
Escape of Gas into Air
Escape of Gas into Water
G2
G5
G3
G4
G6
Formation of Mist by Cargo
No Mist formed by Cargo
Calculation of Portions of Cargo in Gas and Liquid Phases
Gas in Air
Liquid in Air
Gas in Air
Gas on Water Surface
Gas in Air
Gas on Water Surface
Liquid in Water
Solid
S1
Escape of Solid into Air
Escape of Solid into Water
S2
S4
S3
S5
Solid in Air
Solid in Water
Solid in Water
Solid on Water Surface
Liquid in Water
Solid on Water Surface

CHART 2

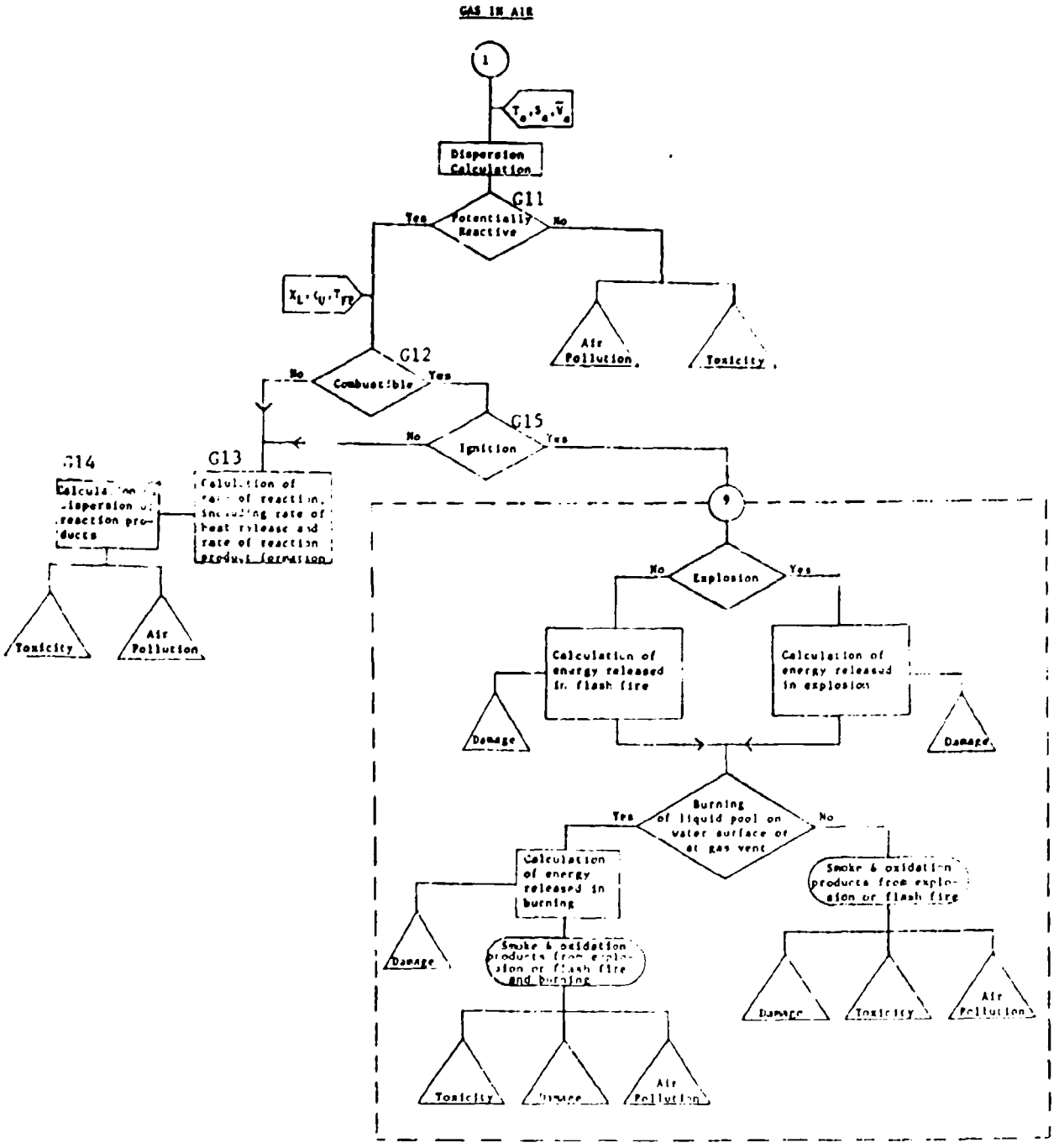
GAS IN AIR
1
$T_a, S_a, \bar{V}_a$
Dispersion Calculation
G11
Potentially Reactive
Yes
No
X_L, C_U, T_{FP}
Air Pollution
Toxicity
G12
Combustible
No
Yes
G15
Ignition
No
Yes
G13
Calculation of rate of reaction, including rate of heat release and rate of reaction product formation
G14
Calculation of dispersion of reaction products
Toxicity
Air Pollution
9
Explosion
No
Yes
Calculation of energy released fr. flash fire
Calculation of energy released in explosion
Damage
Damage
Burning of liquid pool on water surface or at gas vent
Yes
No
Calculation of energy released in burning
Smoke & oxidation products from explosion or flash fire
Damage
Smoke & oxidation products from explosion or flash fire and burning
Damage
Toxicity
Air Pollution
Toxicity
Damage
Air Pollution

CHART 3

GAS ON WATER SURFACE

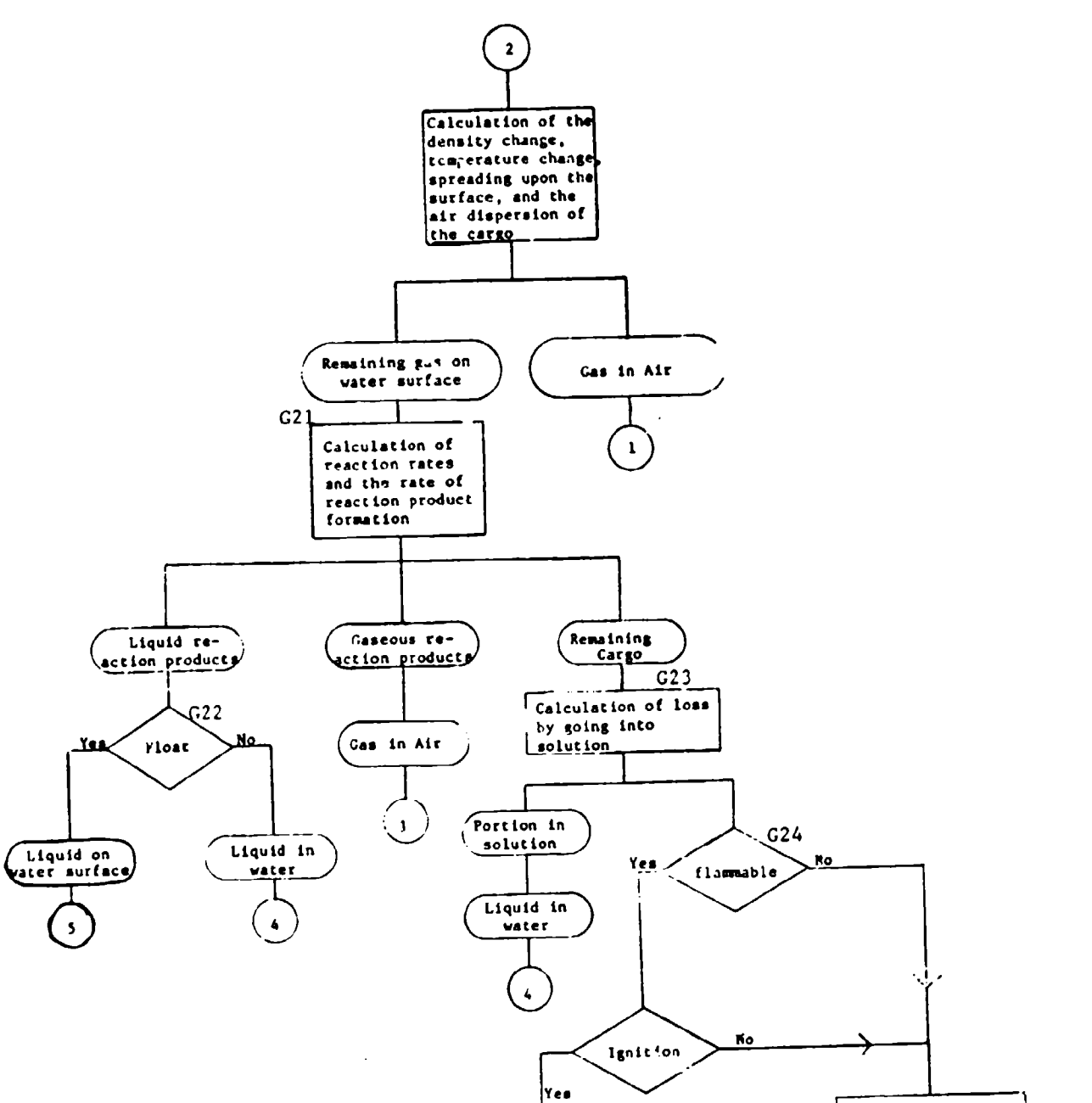

LIQUID IN AIR

CHART 4

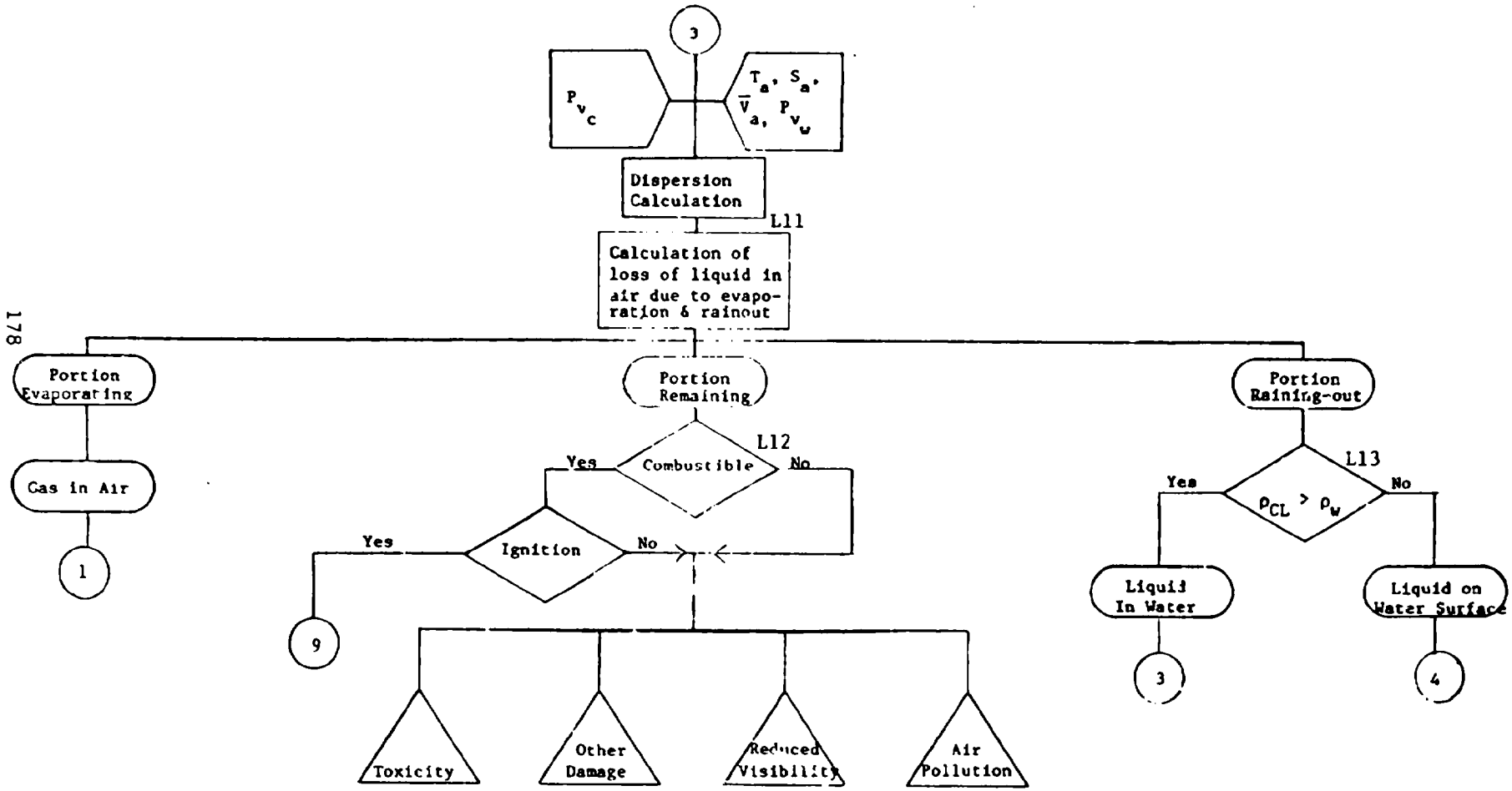

CHART 5

LIQUID IN WATER

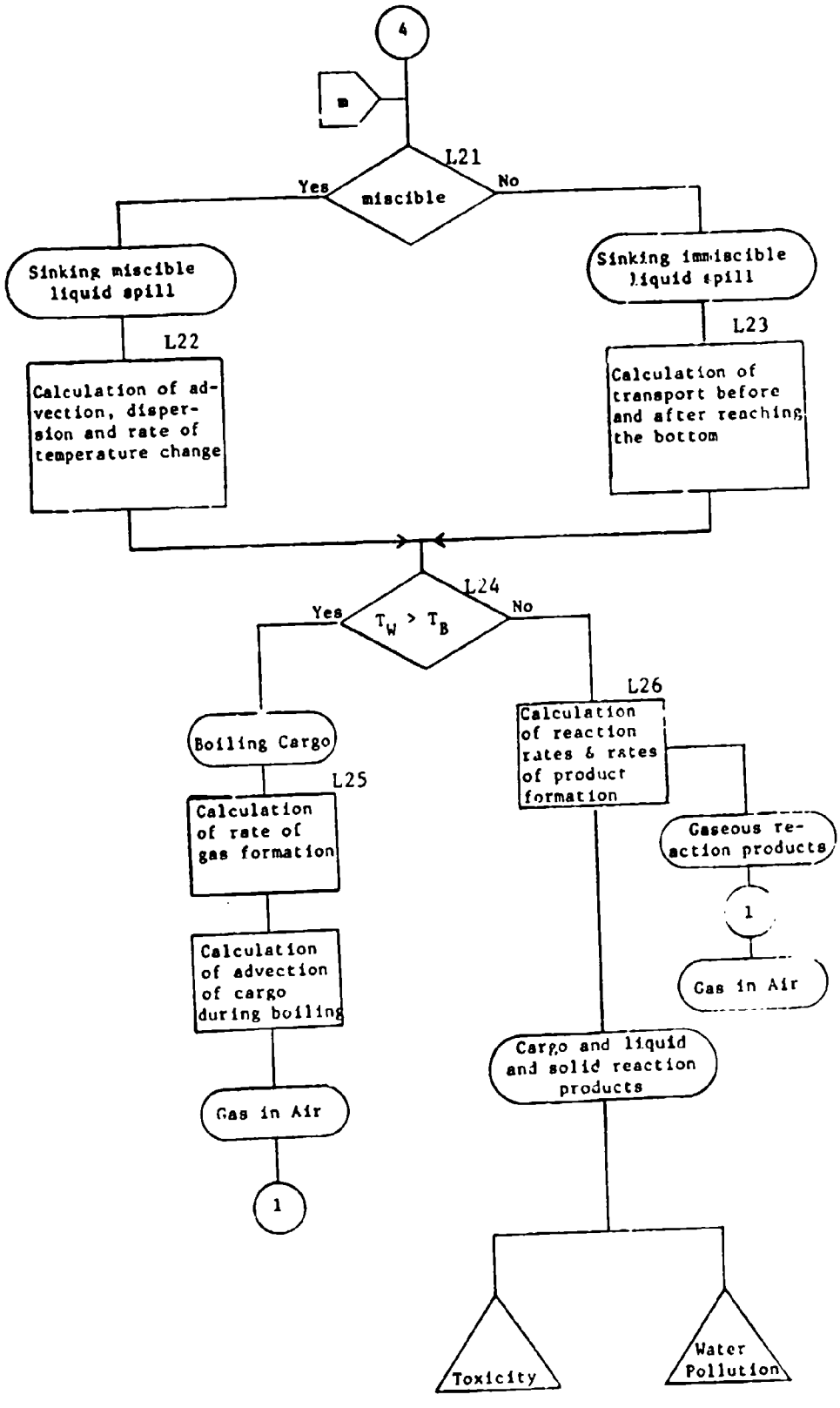

CHART 6

LIQUID ON SURFACE OF WATER

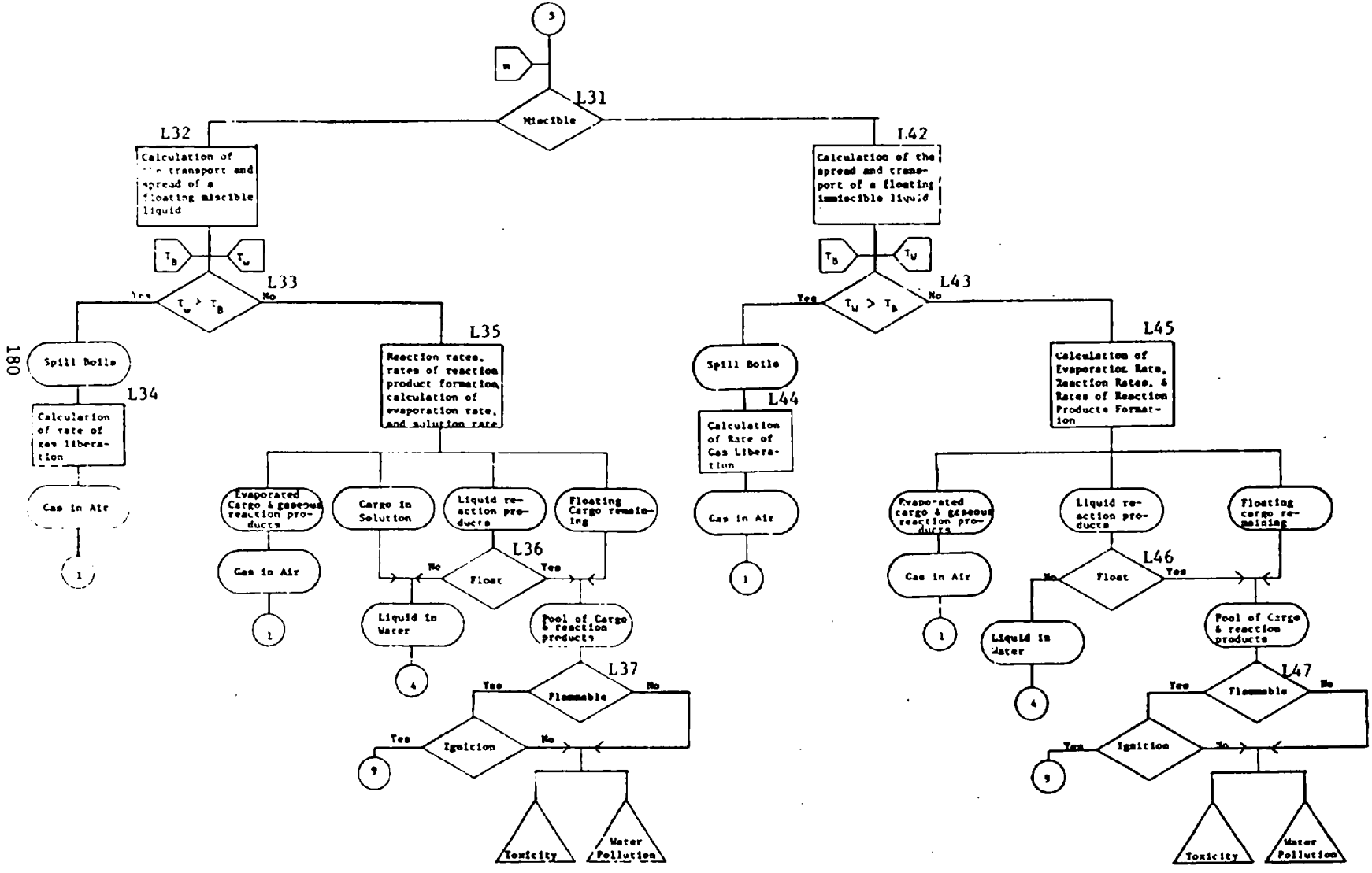

CHART 7

SOLID IN AIR

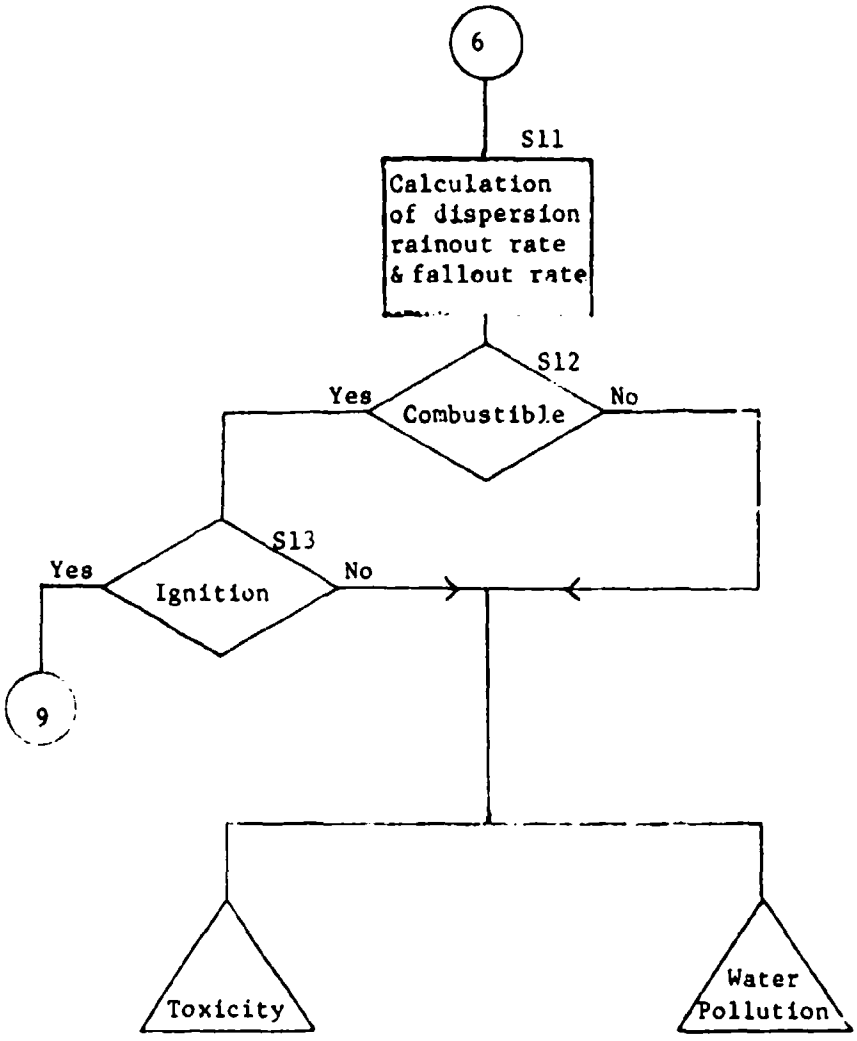

CHART 8

SOLID IN WATER

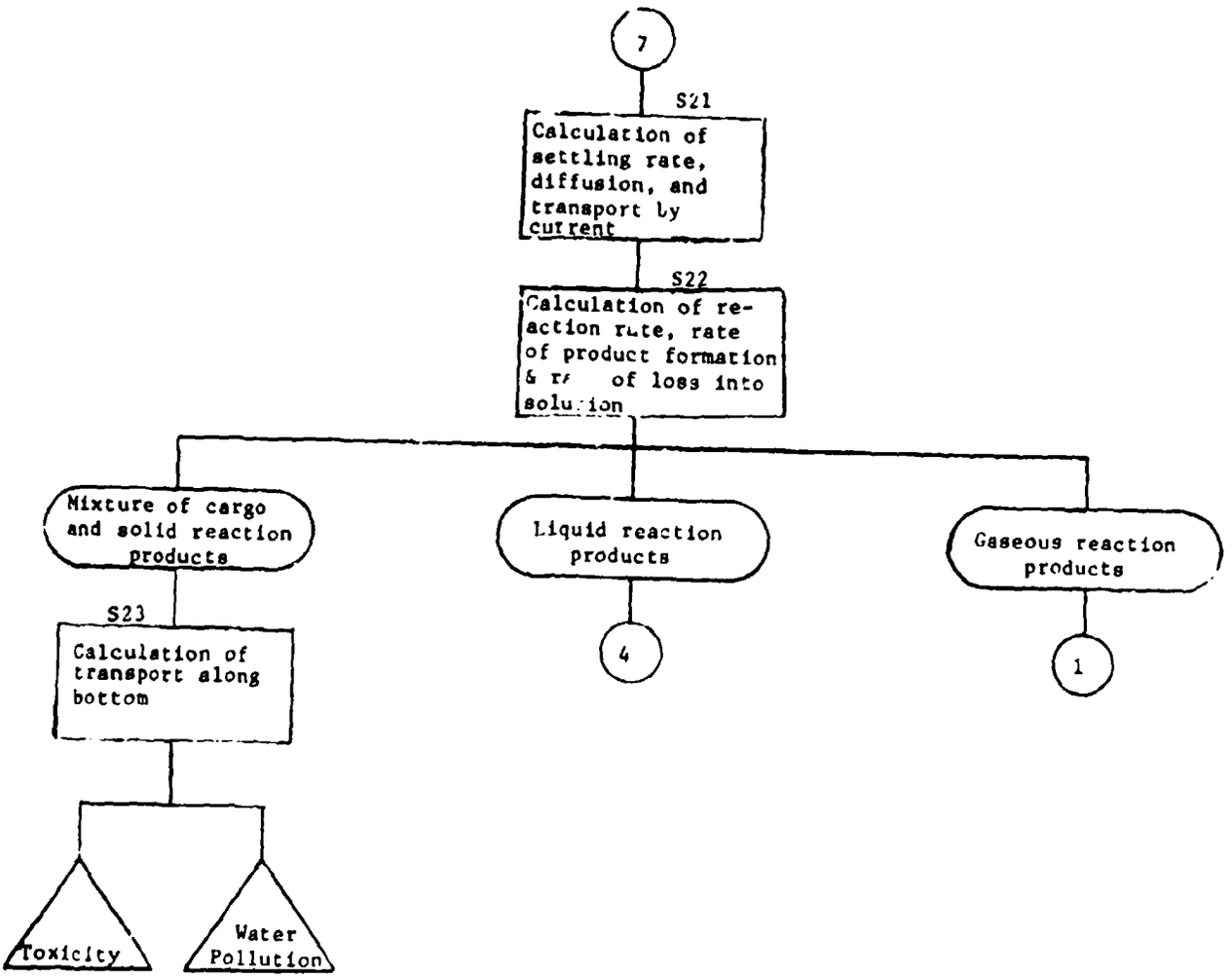

CHART 9

SOLID ON WATER SURFACE

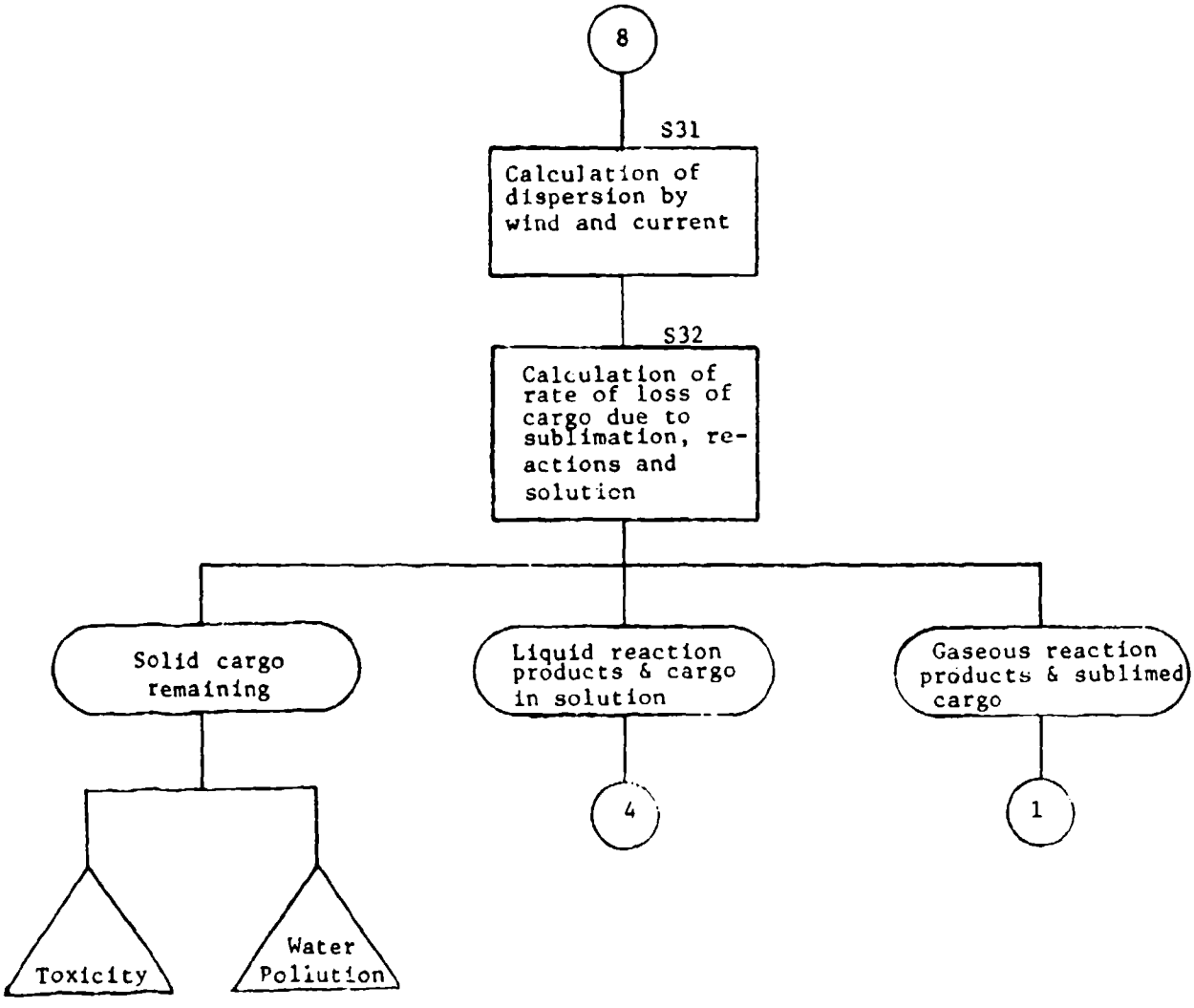

APPENDIX B1

MODIFICATION OF THE GAUSSIAN PUFF MODEL

Since the Gaussian puff model is primarily intended for use with low concentrations, when applied very close to a large source the unmodified Gaussian puff equation may give a concentration of the vapor-phase cargo which is greater than the density of the pure cargo vapor at ambient atmospheric pressure and temperature. This is not physically possible, of course, and the computer model has been modified to preclude such a concentration being given.

In the case when the unmodified Gaussian puff equation would give a concentration greater than pure cargo at ambient conditions, what is actually present is a glob of nearly pure cargo, surrounded by a volume in which the concentration decreases from the density of pure gaseous cargo towards zero. It is reasonable to assume that the concentration decreases in a Gaussian manner from the surface of the glob of pure or nearly pure cargo.

To treat this mathematically, let us first transform from the physical x,y,z coordinate system into one which is scaled by the diffusion coefficients:

$$x' = \frac{x-Ut}{\sigma_x}, \quad y' = \frac{y}{\sigma_y}, \quad z' = \frac{z}{\sigma_z} \tag{B1-1}$$

where U is the wind speed. Since the point of liberation of the gas is at the water surface, z=0, in this coordinate system, let the glob be a hemisphere centered at x'=y'=z'=0. Let us take the radius of this hemisphere to be R', and assume that it is pure cargo-gas. If C_p is the density of the cargo in gas phase at ambient temperature and pressure, and $(r')^2 = (x')^2 + (y')^2 + (z')^2$ is the square of the distance from the center of the puff to the observation point in the new coordinate system, then the concentration C at x',y',z' will be

$$\begin{aligned} C &= C_p \text{ if } r' \leq R' \\ C &= C_p \exp\left(-\frac{(r'-R')^2}{2}\right) \text{ if } r' > R' \end{aligned} \tag{B1-2}$$

The term $(r' - R')^2$ in the exponent is the correct distance factor, but it appears unusual. It is clear that the Gaussian function depends on the square of the distance from some point, line, or surface. The usual Gaussian diffusion equations are written with respect to a point (puff model) or a line (plume or continuous source model). In these cases, the distance from the point or line may be conveniently expressed in the Gaussian coordinate system, by the familiar equations. Here, however, we have a case where it is the distance from the surface of a sphere which is important, and this is expressed conveniently only in spherical coordinates.

The reader familiar with the diffusion equation or time-dependent heat flow problems may have noticed that (B1-2) is not the solution to

$$\frac{\partial C}{\partial t} = K \nabla^2 C \qquad \text{(B1-3)}$$

with

$$\left.\begin{array}{ll} C = C_p & \text{for } r \leq r_1 \\ C = 0 & \text{for } r > r_1 \end{array}\right\} \quad \text{at } t = 0 \qquad \text{(B1-4)}$$

which is the rigorous statement of the problem of the dispersion of material which forms a sphere at $t = 0$. (The equation for the diffusion of particles is identical to the equation for the transfer of heat by conduction, and the thermal problem antedates the diffusion problem, so the treatment in many books is in terms of heat flow. Analytic solutions to the diffusion equation for a number of simple cases may be found in standard texts such as Kreyszig [B1] or Landau and Lifshitz [B2]).

While this problem could be solved for the concentration as a function of time and space for the early period of the puff's dispersal, the problem of matching this solution to the Gaussian puff solution at a later time when the puff model is appropriate would remain. This matching would require shifting from the solution to (B1-3) to the empirically determined Gaussian puff concentration over an arbitrary period of time by means of interpolation of spline functions. To make a smooth transition, the matching would be quite complex. Since the Gaussian puff should need modification to avoid unrealistically high densities only for a short time after the puff begins dispersing, this complication was not considered worthwhile. The chosen solution (B1-2) approximates the theoretical solution to (B1-3) well enough for the use the VM will make of it, and the transition to the Gaussian puff distribution is trivial.

Further, the type of flat-topped profile of concentration as a function of radial distance which (B1-2) gives, is in accordance with

---

[B1] Kreyszig, E. Advanced Engineering Mathematics. John Wiley & Sons, Inc., New York, 1967. (See Section 9.5 and 9.6)

[B2] Landau, L.D., and E.M. Lifshitz. Fluid Mechanics. Pergamon, London, 1959. (See Chapter 5 and 6.)

other work. Figure B1-1 shows a profile calculated by Lind [B3], which clearly shows a region of constant concentration. While this concentration is not 100% as it is in (B1-2), it is clear from the figure that very close to the spill a concentration close to 100% would occur. Lind's method of calculation is based upon that used by Esso, which was experimentally verified [B4].

In equation (B1-2), R' marks the boundary between the hemisphere of pure cargo vapor and the region in which the vapor is mixed with air. The value of R' is determined by the necessity of conserving mass:

$$M = \iiint_{\substack{\text{all}\\\text{space}}} C\,dv = \iiint_{\substack{\text{all}\\\text{space}}} C\left(\frac{dv}{dv'}\right) dv' = \iiint_{\substack{\text{all}\\\text{space}}} C(\sigma_x\sigma_y\sigma_z)dv' \qquad \text{(B1-5)}$$

where $dV = dxdydz$, and $dV' = dx'dy'dz'$.

It may seem that the concentration used should be converted to the primed coordinate system, but this is not necessarily the case. It is incorrect to transform the limits of integration, the unit volume, and the concentration or density. However, one may define $C' = C\sigma_x\sigma_y\sigma_z$ to be the new density if one so desires*.

[B3] Lind, C.D., Explosion Hazards Associated with Spills of Large Quantities of Hazardous Materials - Phase I. Report No. CG-D-30-75, United States Coast Guard, Dept. of Transportation, 18 October 1974.

[B4] Feldbauer, G.W., et al. Spills of LNG on Water - Vaporization and Downwind Drift of Combustible Mixtures. Esso Research and Engineering Company, Report No. EE61E-72 (Released by the American Petroleum Inst., Re 6232), March 1973.

* That this new integral is correct may be demonstrated by a simple example. In the x,y,z system let the density be some constant value, C_o, in a rectangular region with slides $\sigma_x,\sigma_y,\sigma_z$, respectively, and zero outside this region. Clearly:

$$M = \int_o^{\sigma_x}\int_o^{\sigma_y}\int_o^{\sigma_z} C_o\,dxdydz = C_o\,\sigma_x\sigma_y\sigma_z$$

Taking care to transform the limits of integration, in the x',y',z' system we have

$$M = \int_o^1\int_o^1\int_o^1 C_o\sigma_x\sigma_y\sigma_z dx'dy'dz' = C_o\sigma_x\sigma_y\sigma_z$$

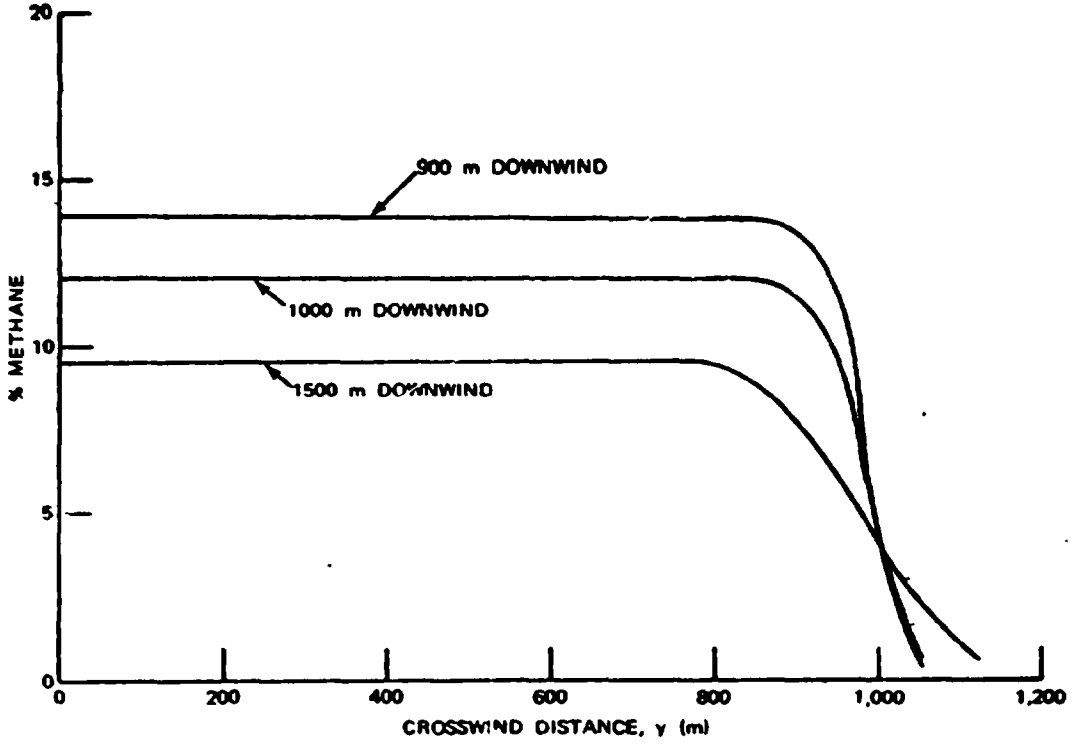

FIGURE B1-1. Sea Level Concentration Profile, 10,000 m^3 Spill. [B3]

It will be easiest to do the integral in spherical coordinates in the new coordinate system so equation (B1-5) becomes:

$$M = \int_{\phi'=0}^{2\pi} \int_{\theta'=0}^{\pi/2} \int_{r'=0}^{\infty} C\,(\sigma_x\sigma_y\sigma_z)\,(r')^2\,\sin\theta' dr' d\theta' d\phi' \qquad \text{(B1-6)}$$

where the integral over θ' only goes from 0 to $\pi/2$ because the gas can only occupy the +z half-space.

The ϕ' and θ' integrals can be done at once, leaving

$$\frac{M}{\sigma_x\sigma_y\sigma_z} = 2\pi \left[\int_0^{R'} C_p (r')^2 dr' + \int_{R'}^{\infty} C_p \exp(-\tfrac{1}{2}(r'-R')^2)(r')^2 dr' \right] \qquad \text{(B1-7)}$$

Let the second integral above be denoted by $A\,C_p$, and we have

$$\frac{M}{\sigma_x\sigma_y\sigma_z} = 2\pi C_p \frac{(R')^3}{3} + 2\pi A C_p \qquad \text{(B1-8)}$$

The integral A is evaluated by making the substitution $s = r' - R'$:

$$A = \int_{R'}^{\infty} \exp\left(-\tfrac{1}{2}(r'-R')^2\right)(r')^2 dr' = \int_0^{\infty} e^{-\frac{s^2}{2}} (s^2 + 2sR' + (R')^2)\, ds$$

$$= \int_0^{\infty} s^2 e^{-\frac{s^2}{2}} ds + 2R' \int_0^{\infty} s\, e^{-\frac{s^2}{2}} ds + (R')^2 \int_0^{\infty} e^{-\frac{s^2}{2}} ds \qquad \text{(B1-9)}$$

$$= \left(\frac{\pi}{2}\right)^{1/2} + 2R' + (R')^2 \left(\frac{\pi}{2}\right)^{1/2}$$

The second of the three integrals in s is trivial, and the other two are tabulated definite integrals.* With the integral A evaluated, from (B1-8) we have:

$$\frac{M}{\sigma_x\sigma_y\sigma_z} = C_p \left[\frac{2}{3}\pi (R')^3 + 2\pi \left(2R' + (1+(R')^2)\left(\frac{\pi}{2}\right)^{1/2}\right)\right] \qquad \text{(B1-10)}$$

which is a cubic equation in R'.

---

*It may seem odd that $\int_0^{\infty} s^2 e^{-\frac{s^2}{2}} ds = \left(\frac{\pi}{2}\right)^{1/2} = \int_0^{\infty} e^{-\frac{s^2}{2}} ds$, but such is indeed the case. This may be proved by integration by parts. We have

(cont'd)

$$(R')^3 + p(R')^2 + qR' + s = 0$$

$$\text{with } p = \frac{3}{2}(2\pi)^{1/2} \qquad \text{(B1-11)}$$
$$q = 6$$
$$s = p - \frac{3M}{2\pi C_p \sigma_x \sigma_y \sigma_z}$$

In use, at each time step the concentration at the center of the puff is calculated by the usual Gaussian puff equation:

$$C = \frac{2M}{(2\pi)^{3/2}\sigma_x\sigma_y\sigma_z} \qquad \text{(B1-12)}$$

If this concentration does not exceed C_p, the usual Gaussian puff equation is used. If this concentration exceeds C_p, then equation (B1-11) is solved for R', and then the concentrations are calculated from equation (B1-2) with:

$$r' = \left[\left(\frac{x-Ut}{\sigma_x}\right)^2 + \left(\frac{y}{\sigma_y}\right)^2 + \left(\frac{z}{\sigma_z}\right)^2\right]^{1/2} \qquad \text{(B1-13)}$$

---

*(cont'd)

$\frac{d}{ds}(fg) = \frac{df}{ds}g + f\frac{dg}{ds}$, and since $\int \frac{d}{ds}(fg)ds = fg$, $\int_0^\infty f\frac{dg}{ds}ds =$ $[fg]_0^\infty - \int_0^\infty (\frac{df}{ds})\,gds$. Let $\frac{dg}{ds} = se^{-\frac{s^2}{2}}$ and $f = s$, then $g = -e^{-\frac{s^2}{2}}$ and $\frac{df}{ds} = 1$. Thus $\int_0^\infty s^2 e^{-\frac{s^2}{2}}ds = [-se^{-\frac{s^2}{2}}]_0^\infty - \int_0^\infty (-e^{-\frac{s^2}{2}})ds$ which gives $\int_0^\infty s^2 e^{-\frac{s^2}{2}}ds = \int_0^\infty e^{-\frac{s^2}{2}}ds$.

Both these integrals are evaluated in tables of definite integrals, and are equal to $(\frac{\pi}{2})^{1/2}$. (For example, see integrals 423 and 426 on p. 304 of [B5].)

[B5] C.R.C. Standard Mathematical Tables, 11th ed. C. D. Hodgeman (Editor-in-Chief), Chemical Rubber Publishing Company, Cleveland, Ohio, 1957.

In the case that an explosion or flash fire occurs while the puff is still so close to the source that the unmodified Gaussian puff model gives unrealistic values for the concentration, the VM must be able to calculate the amount of cargo vapor which explodes or burns for the modified distribution we have been discussing. In Appendix C it is shown that the mass which will explode or burn will be given by

$$M_e = \int\int\int_{S_s}^{S_l} C\,dV + \int\int\int_{S_u}^{S_s} PC\,dV \qquad \text{(B1-14)}$$

where S_u is the surface on which $C = C_u$
S_s is the surface on which $C = C_s$
S_l is the surface on which $C = C_l$
C_u = the upper flammable limiting concentration
C_s = the stoichiometric concentration
C_l = the lower flammable limiting concentration

and where

$$P = \frac{0.21}{N_O}\left(\frac{C_p}{C} - 1\right) \qquad \text{(B1-15)}$$

is the fraction of the fuel which burns when the mixture is richer than stoichiometric. N_O is the number of moles of oxygen consumed for every mole of fuel burned.

As before it will be easiest to work in the primed coordinate system (equation B1-1) and in spherical coordinates in this system (equation B1-13). In this coordinate system the surfaces of constant concentration will be spheres. Let

r'_u = radius of the surface on which $C = C_u$

r'_s = radius of the surface on which $C = C_s$

r'_l = radius of the surface on which $C = C_l$

Values for these radii may be obtained by setting C equal to C_u, C_s, or C_l in equation (B1-2). (Since pure fuel vapor cannot burn - there is no oxygen present - C_u must be less than C_p, and we need only consider the region in which r' is greater than R'.) The values for the radii are easily obtained:

$$r'_u = R' + (2\ell n(C_p/C_u))^{1/2}$$
$$r'_s = R' + (2\ell n(C_p/C_s))^{1/2} \qquad \text{(B1-16)}$$
$$r'_l = R' + (2\ell n(C_p/C_l))^{1/2}$$

So with (B1-2) and (B1-15), equation (B1-14) may be written

$$M_e = \int_{\phi'=o}^{2\pi} \int_{\theta'=o}^{\pi/2} \int_{r'=r'_u}^{r'_s} \left[\frac{0.21}{N_O} C_p \left(1-\exp\left[-\frac{(r'-R')^2}{2}\right]\right)\right] \cdot$$

$$\sigma_x\sigma_y\sigma_z (r')^2 \sin\theta' dr' d\theta' d\phi' \quad + \quad \text{(B1-17)}$$

$$\int_{\phi'=o}^{2\pi} \int_{\theta'=o}^{\pi/2} \int_{r'=r'_s}^{r'_1} C_p \exp\left[-\frac{(r'-R')^2}{2}\right] \sigma_x\sigma_y\sigma_z (r')^2 \sin\theta' dr' d\theta' d\phi'$$

The transformation used to obtain this expression is analogous to the one used to go from (B1-5) to (B1-6). And here also the ϕ' and θ' integrals can be done at once giving

$$\frac{M_e}{2\pi C_p \sigma_x\sigma_y\sigma_z} = \frac{0.21}{N_O} \int_{r'_u}^{r'_s} (r')^2 dr' \quad - \quad \text{(B1-18)}$$

$$\frac{0.21}{N_O} \int_{r'_u}^{r'_s} \exp\left[-\frac{(r'-R')^2}{2}\right] (r')^2 dr' + \int_{r'_s}^{r'_1} \exp\left[-\frac{(r'-R')^2}{2}\right] (r')^2 dr'$$

Now the first integral is trivial and gives $(r')^3/3$. The other two integrals may be done by considering integrals of the form

$$I = \int_a^b s^2 \exp\left(-\frac{s^2}{2}\right) ds \quad \text{(B1-19)}$$

which we treat by integration by parts. With $dg/ds = s \exp(-s^2/2)$ and $f(s) = s$, then $g(s) = -\exp(-s^2/2)$ and $df/ds = 1$. Since

$$\int_a^b \frac{dg}{ds} f ds = [fg]_a^b - \int_a^b \frac{df}{ds} g ds \quad \text{(B1-20)}$$

we have

$$\int_a^b s^2 \exp\left(-\frac{s^2}{2}\right) ds = \left[-s \exp\left(-\frac{s^2}{2}\right)\right]_a^b - \int_a^b -\exp\left(-\frac{s^2}{2}\right) ds$$

$$= a \exp\left(-\frac{a^2}{2}\right) - b \exp\left(-\frac{b^2}{2}\right) + \int_a^b \exp\left(-\frac{s^2}{2}\right) ds \quad \text{(B1-21)}$$

Now let $s = r' - R'$; then $r' = s + R'$ and $(r')^2 = s^2 + 2sR' + (R')^2$ so we have

$$A = \int_{r'_u}^{r'_s} \exp\left[-\frac{(r'-R')^2}{2}\right] (r')^2 dr' = \int_{r'_u-R'}^{r'-R'} \exp\left(-\frac{s^2}{2}\right)[s^2+2sR'+(R')^2] ds \quad \text{(B1-22)}$$

Let $a = r'_u - R'$, $b = r'_s - R'$, and $c = r'_l - R'$. Then (B1-22) becomes

$$A = \int_a^b s^2 \exp\left(-\frac{s^2}{2}\right)ds + 2R' \int_a^b s \exp\left(-\frac{s^2}{2}\right)ds + (R')^2 \int_a^b \exp\left(-\frac{s^2}{2}\right)ds \quad \text{(B1-23)}$$

Using (B1-21) this becomes

$$A = a \exp\left(-\frac{a^2}{2}\right) - b \exp\left(-\frac{b^2}{2}\right) + \int_a^b \exp\left(-\frac{s^2}{2}\right)ds$$
$$+ 2R' \left[a \exp\left(-\frac{a^2}{2}\right) - b \exp\left(-\frac{b^2}{2}\right)\right] + (R')^2 \int_a^b \exp\left(-\frac{s^2}{2}\right)ds \quad \text{(B1-24)}$$

The similar terms may be combined to give

$$A = (1+2R') \left[a \exp\left(-\frac{a^2}{2}\right) - b \exp\left(-\frac{b^2}{2}\right)\right] + \left[1+(R')^2\right] \int_a^b \exp\left(-\frac{s^2}{2}\right)ds \quad \text{(B1-25)}$$

Now the remaining integral has an integrand which differs from the normal curve of error only by a constant, and the normal curve of error, $\phi(x)$, is related to the error function, erf(t) by

$$\int_o^t \phi(x)dx = \int_o^t (2\pi)^{-1/2} \exp\left(-\frac{x^2}{2}\right)dx = 1/2 \operatorname{erf}\left(\frac{t}{\sqrt{2}}\right) \quad \text{(B1-26)}$$

The error function is a tabulated special function, and we may express the integral A in terms of it by using the identity

$$\int_a^b f(s)ds = \int_o^b f(s)ds - \int_0^a f(s)ds \quad \text{(B1-27)}$$

and so we have

$$A = (1+2R') \left[a \exp\left(-\frac{a^2}{2}\right) - b \exp\left(-\frac{b^2}{2}\right)\right] +$$
$$+ \left[1+(R')^2\right] \left(\frac{\pi}{2}\right)^{1/2} \left[\operatorname{erf}\left(\frac{b}{\sqrt{2}}\right) - \operatorname{erf}\left(\frac{a}{\sqrt{2}}\right)\right] \quad \text{(B1-28)}$$

But r'_s was defined by

$$C_s = C_p \exp\left[-\frac{(r'_s-R')^2}{2}\right] = C_p \exp\left(-\frac{b^2}{2}\right) \quad \text{(B1-29)}$$

and r'_u and r'_l were defined in an analogous manner so we have

$$A = (1+2R') \left[a(C_u/C_p) - b(C_s/C_p)\right] + \left[1+(R')^2\right] \left(\frac{\pi}{2}\right)^{1/2} \cdot$$
$$\left[\operatorname{erf}\left(\frac{b}{\sqrt{2}}\right) - \operatorname{erf}\left(\frac{a}{\sqrt{2}}\right)\right] \quad \text{(B1-30)}$$

The third integral in (B1-18) is the same as the second integral except for the limits so we have, by analogy:

$$B = \int_{r'_s}^{r'_1} \exp\left[-\frac{(r'-R')^2}{2}\right] (r')^2 dr' = (1+2R')\left[b(C_s/C_p) - c(C_1/C_p)\right]$$

$$+ \left[1+(R')^2\right] \left(\frac{\pi}{2}\right)^{1/2} \left[\mathrm{erf}\left(\frac{c}{\sqrt{2}}\right) - \mathrm{erf}\left(\frac{b}{\sqrt{2}}\right)\right] \qquad \text{(B1-31)}$$

and the mass exploding or burning, from equation (B1-18) can finally be written as:

$$M_e = 2\pi C_p \sigma_x \sigma_y \sigma_z \left[\frac{0.21}{3N_0}\left((r'_s)^3 - (r'_u)^3\right) - \frac{0.21}{N_0} A + B\right] \qquad \text{(B1-32)}$$

APPENDIX B2

GAUSSIAN PLUME AIR DISPERSION MODEL

In cases where the liberation of the cargo in vapor phase takes a long time, it is more appropriate to use a Gaussian plume model (continuous source model) than a Gaussian puff model (instantaneous source model). The question of how long the gas release time should be in order to use the plume model is discussed in chapter 4 and the following section of this appendix.

The Gaussian plume model is discussed in chapter 5 of the CHRIS documentation [B6], and equation (B2-1) below is essentially equation (5.2) from p. 54 of this work. The CHRIS documentation does not discuss the possibility of the vapor release rate varying as a function of time. Equation (B2-1) allows for this possibility, but as programmed the model uses an average release rate which is not a function of time. The reason for this limitation in the program is twofold: first, if an explosion or flash fire occurs, the amount of fuel which explodes or burns must be found by integration of the concentration distribution between given concentrations. Not only is this much easier for the case where the release rate is constant, but the various subroutines make no provision for storing the release rate as a function of time, so a number of HACS subroutines would have to be modified if the average release rate was not used. Second, some of the HACS submodels which treat the release of cargo vapor do not calculate a release rate as a function of time, but output only the amount of vapor released and the time at which the release is complete.

The Gaussian plume model is undefined when the wind speed is zero. Since this is the case, and the plume model is not appropriate for use when the wind speeds are low, the VM uses the puff model whenever the wind speed is below 2 m/s.

The details of the calculation are as follows; let:

C = the concentration of the cargo in vapor phase.

x,y,z = the position of the observer (or the cell center) in a coordinate system in which the origin is at the spill or vent location (which is assumed to be at the water surface) and the positive x axis is in the direction toward which the wind is blowing.

t = the time at which the concentration at x,y,z is to be calculated.

t = o, when the vapor release begins.

t_v = t - x/U = the time at which the cargo vapor observed at x,y,z at time t would have escaped or evaporated if the wind speed was steady at U and there was no diffusion in the x direction.

[B6] Raj, P.K., and A.S. Kalelkar, Assessment Models in Support of the Hazard Assessment Handbook, A.D. Little, Inc., Cambridge, Mass., January 1974. Dept. of Transportation Report No. CG-D-65-74, NTIS AD 776617.

t_e = time at which the gas venting or evaporation is complete.

F_e = the rate of liberation of the cargo in gaseous state.

σ_y, σ_z = the diffusion parameters in the y and z direction, respectively. They are functions of x and of the atmospheric stability, of the Form ax^b.

U = the wind speed. U is taken to be a constant.

It is clear that F_e should be evaluated at time t_v, since the rate of vapor liberation at the pool or vent at the same time that the concentration is being measured many hundreds of meters or many kilometers downwind is irrelevant. What is relevant is release rate at t_v, since the time it has taken the vapor to travel with the wind from the origin to x is just x/U.

If the conditions are suitable for use of the plume equation as opposed to the puff equation, the concentration is given by

$$C(x,y,z,t) = \frac{F_e}{\pi U \sigma_y \sigma_z} \exp\left[-\frac{1}{2}\left(\frac{y}{\sigma_y}\right)^2 - \frac{1}{2}\left(\frac{z}{\sigma_z}\right)^2\right] \text{ for } 0 \leq t_v \leq t_e \qquad \text{(B2-1)}$$

$$C(x,y,z,t) = 0 \text{ for } t_v < 0 \text{ and } tv > te$$

where F_e is evaluated at t_v. In this equation it has been assumed that the gas is released at the water surface and a factor of two has been incorporated to account for the reflection about the z=0 plane, i.e., for the fact that the gas escapes into the positive-z half-space.

Next we consider how much of the cargo vapor which is dispersing in a Gaussian plume will explode or burn in a flash fire. The basic assumptions are that no fuel will burn where the concentration is less than the lower flammable concentration, and that no fuel will burn where the concentration is above the upper flammable concentration. Where the concentration is between the stoichiometric concentration and the upper flammable concentration, it is assumed that all of the oxygen will be consumed, but that not all of the fuel will be consumed. This assumption is discussed in detail in appendix C.

In addition to the items defined above, let:

C_p = concentration or density of pure cargo vapor at ambient atmospheric temperature and pressure.

C_s = stoichiometric concentration.

C_u = upper flammable concentration limit.

C_l = lower flammable concentration limit.

t_i = time of ignition.

x_i, y_i, z_i = coordinates of ignition source.

x_e = coordinate of the source-end of the plume:

$x_e = 0$ if $t_i \leq t_e$

$x_e = U(t_i - t_e)$ if $t_i > t_e$.

N_O = number of moles of oxygen consumed per mole of fuel.

M_e = mass of cargo consumed in flash fire or explosion.

P = portion of fuel burned when the fuel concentration is greater than stoichiometric.

Let us begin by finding an expression for the curve in the yz plane where $C = C_s$. The concentration is given by

$$C = \frac{2F_e}{2\pi U\sigma_x\sigma_y} \exp\left[-\frac{1}{2}\left(\frac{y}{\sigma_y}\right)^2 - \frac{1}{2}\left(\frac{z}{\sigma_z}\right)^2\right] \qquad \text{(B2-2)}$$

Where the factor of two in the numerator comes from the assumption that the source is at z=0, and the escaping gas can only go into the positive-z half-space. With $C=C_s$, rearranging (B2-2) we have

$$\left(\frac{y}{\sigma_y}\right)^2 + \left(\frac{z}{\sigma z}\right)^2 = 2 \ln\left(\frac{F_e}{\pi U\sigma_y\sigma_z C_s}\right) \qquad \text{(B2-3)}$$

This is the equation for an ellipse. The mathematics will be simplified if we transform to a coordinate system in which we have a circle rather than ellipse. Let

$$y' = \frac{y}{\sigma_y}, \quad z' = \frac{z}{\sigma_z}, \quad (r')^2 = (y')^2 + (z')^2 = \left(\frac{y}{\sigma_y}\right)^2 + \left(\frac{z}{\sigma_z}\right)^2 \qquad \text{(B2-4)}$$

If $r' = R'_s$ on the circle in the primed coordinate system where $C=C_s$, then

$$(R'_s)^2 = 2 \ln\left(\frac{F_e}{\pi U\sigma_y\sigma_z C_s}\right) \qquad \text{(B2-5a)}$$

Likewise, R'_l given by $(R'_l)^2 = 2 \ln\left(\frac{F_e}{\pi U\sigma_y\sigma_z C_l}\right)$ (B2-5b)

is the radius of the circle on which $C=C_l$, and R'_u, given by

$$(R'_u)^2 = 2 \ln\left(\frac{F_e}{\pi U\sigma_y\sigma_z C_u}\right) \qquad \text{(B2-5c)}$$

is the radius of the circle on which $C=C_u$.

Now the fraction of fuel consumed when the fuel concentration is greater than stoichiometric is

$$P = \frac{0.21}{N_O} \left(\frac{C_p}{C} - 1 \right) \tag{B2-6}$$

as discussed in appendix C.

The mass of cargo vapor which explodes or burns in a flash fire is then

$$M_e = \int_{x_e}^{x_i} \left[\iint_{C=C_s}^{C=C_l} C dy dz + \iint_{C=C_u}^{C=C_s} PC \, dy dz \right] dx \tag{B2-7}$$

where the limits on the y and z integrals are the curves on which the concentration is equal to C_l, C_s, or C_u. The y-z integrals will be most easily done in the primed coordinate system in plane polar coordinates. The first integral is

$$\iint_{C=C_s}^{C=C_l} C dy dz = \iint_{C=C_s}^{C=C_l} C \sigma_y \sigma_z dy' dz' = \int_{\sigma'=R_s'}^{\sigma'=R_l'} \int_{\phi=-\pi/2}^{+\pi/2} \frac{F_e}{\pi U \, y \, z} e^{-\frac{(r')^2}{2}} \sigma_y \sigma_z r' dr' d\phi'$$

$$= \frac{F_e}{U} \left[e^{-\frac{(R_s')^2}{2}} - e^{-\frac{(R_l')^2}{2}} \right] \tag{B2-8}$$

But with R_1' and R_2' given by (B2-5) we have

$$\iint_{C=C_s}^{C_l} C dy dz = \frac{F_e}{U} \left(\frac{\pi U \, \sigma_y \, \sigma_z}{F_e} \right) (C_s - C_l) = \pi \, \sigma_y \, \sigma_z \, (C_s - C_l) \tag{B2-9}$$

Using (B2-6) the second y-z integral in (B2-7) is

$$\iint_{C=C_u}^{C=C_s} PC dy dz = \iint_{C=C_u}^{C=C_s} \frac{0.21}{N_O} (C_p - C) \, \sigma_y \sigma_z dy' dz'$$

(B2-10)

$$= \frac{0.21}{N_O} \int_{-\pi/2}^{+\pi/2} \left[\int_{r'=R_u'}^{R_s'} C_p \sigma_y \sigma_z \, r' dr' - \int_{r'=R_u'}^{R_s'} \frac{F_e}{\pi U \sigma_y \sigma_z} e^{-\frac{(r')^2}{2}} \sigma_y \sigma_z r' dr' \right] d\phi'$$

In this expression, the ϕ' integral and the r' integral are trivial, and the second r' integral is similar to the integral evaluated in (B2-8) and (B2-9), we we have

$$\iint_{C=C_u}^{C=C_s} PCdydz = \left(\frac{0.21}{N_0}\right) \pi\sigma_y\sigma_z \left[C_p \left(\frac{(R_s')^2 - (R_u')^2}{2}\right) - (C_u - C_s)\right] \qquad \text{(B2-11)}$$

Thus (B2-7) becomes

$$M_e = \int_{x_e}^{x_1} \pi\sigma_y\sigma_z \left[(C_s - C_1) + \left(\frac{0.21}{N_0}\right) \frac{C_p}{2} \left((R_s')^2 - (R_u')^2\right) - \left(\frac{0.21}{N_0}\right) (C_u - C_s)\right] dx \qquad \text{(B2-12)}$$

Let $\sigma_y = ax^b$, $\sigma_z = cx^d$, then

$$M_e = \pi A \int_{x_e}^{x_1} acx^{b+d}\, dx = \pi A \left(\frac{x_1^{b+d+1} - x_e^{b+d+1}}{b+d+1}\right) ac \qquad \text{(B2-13a)}$$

where

$$A = C_s - C_1 + \frac{0.21}{N_0} \left[C_p \log_e (C_u/C_s) + C_s - C_u\right] \qquad \text{(B2-13b)}$$

In practice, all the quantities in (B2-13) will be known at the time it is calculated that the ignition occurs, except R_s' and R_u'. These quantities may be calculated from (B2-5), however. In the CHRIS/HACS models, σ_y and σ_z are not always given by an expression of the form ax^b. However, in most cases the plume will not be more than several km long when it is ignited, and expressing σ_y and σ_z in ax^b form for such a range of distance is an acceptable approximation.

Appendix B3

SCALE ANALYSIS

Consideration of the lengths and times which are characteristic of air dispersion enables one to come to some useful conclusions. Scale analysis is used in this section of appendix B to show that the advection of a gaseous cargo by the wind will be much more effective in spreading the gas than will eddy diffusion alone, and it is used to indicate how a suitable time step might be chosen, and how to decide whether the plume or puff model is the more appropriate. Finally, it is shown that certain spills are too small to be treated accurately by the VM.

Let us define the following scale quantities:

L = 100 m = horizontal scale of surface roughness.

V = 30 m = vertical scale of surface roughness.

H = 3000 m = scale of distance over which a hazardous condition might exist.

U = 5 m/s = typical wind speed

K = 1000 m^2/s = horizontal eddy diffusivity on the scale of H.

t_r = duration of gas release.

From these basic parameters we may derive several other quantities:

$t_h = H/U$ = 10 min = transport time for scale length H.

$t_k = H^2/K$ = 2.5 hr = diffusion time for scale length H.

$t_l = L/U$ = 20 s = transport time for the scale length L.

In fluid dynamics it is customary to characterize the roughness of a surface by a representative length. Most surfaces, over which a fluid may flow, have surface imperfections of a random nature. In a pipe the surface roughness is caused by scratches, pits, and protuberances on the inner surface. For atmospheric flows the surface roughness is caused by topological features of the ground. In an urban area the vertical scale of surface roughness would be approximately the average height of the buildings. The horizontal scale of surface roughness would be close to the average distance between individual buildings or between groups of adjacent buildings of similar height. The surface roughness lengths have been taken to be characteristic of an urban area, for this is the area in which a spill would be most objectionable. For grassland or the open sea, the parameters L and V would have values about 1/100 of the values used above. The value of K, the horizontal turbulent diffusion coefficient, is taken from the data of Richardson as presented on p. 93 of [B7].

[B7] Slade, D. H., ed. Meteorology and Atomic Energy. U.S. Atomic Energy Commission, TID-24190, 1968.

The quantities above are representative values, and only give the orders of magnitude involved. This is sufficient for the problems addressed here. For example, comparison of t_h and t_k indicates the relative importance of wind advection and turbulent diffusion in dispersal of a substance in the atmosphere. For almost any wind speed above zero, the transport by the wind will be more important in spreading the material than will diffusion. For any scale distance H and wind speed U, the ratio of the wind transport time to the diffusion time is given by the dimensionless ratio K/H/U. For the values used above, this ratio is 1/15.

Choice of Time Step

The choice of the time step to be used in the air dispersion submodel of the VM must be based on the scale of the problem as well as the computational and cost factors. Only the input from scale considerations are considered here. Because the air dispersion model is not intended for use on the scale of the surface roughness, a time step, Δt, on the order of t_1 is not appropriate. Although the VM will function perfectly well for any size time step, the use of a time step as small as t_1 or smaller may easily lead one to make unwarranted inferences about the accuracy of the VM. There is little if anything to be gained by the use of time steps less than t_1.

On the other hand, the VM is intended for use on the scale H, and is reasonably accurate on such a scale. To get some detail on events on this scale, Δt must be chosen smaller than t_h. There are no definite rules, but typically one might choose Δt to be between $t_h/10$ and $t_h/5$. Interpretation will be easiest if Δt is an even number of convenient units. For the scale distances and wind speed listed above, t_h = 10 min, so either Δt = 1 min or Δt = 2 min would be reasonable choices. To follow a cloud of toxic gas over long distances, one might wish to increase Δt somewhat.

Plume Model or Puff Model

The characteristic times defined above are useful in determining whether the plume or the puff model is the most appropriate. Clearly the puff model is inappropriate if the time of gas release is as long or longer than the time needed to traverse the scale of distance over which damage may reasonably be expected. Thus if the time over which gas is released, t_r, is greater than t_h, the plume model should be used. It is also evident that the puff model is called for if t_r is less than t_1. For the case where t_r is between t_1 and t_h, there is no obvious dividing line between the cases for which the plume model is appropriate and the cases for which the puff model is appropriate. The line might well be drawn in the region between $3t_1$ and $t_h/3$, however. If Δt is chosen to be about $t_h/10$, then the plume model may be specified if t_r is greater than $3\Delta t$ or $5\Delta t$.

Lower Limit of Applicability

For a spill to be capable of causing damage, and also to be validly treated by the VM, it must exceed a certain size. When the vapor cloud

from a small spill is concentrated enough to be hazardous, it may be smaller than surrounding structures, and so the air dispersion submodel will not predict its motions and spreading correctly. If, when the cloud has expanded to a size such that the air dispersion submodel will treat it adequately, the concentration of cargo vapor is so low that the event is no longer of interest, then such a spill is too small to be considered by the VM. If the glob of vapor which is of interest is considerably smaller than the scale of the roughness of the surface, then this glob, if near the surface, will be inaccurately treated by the air dispersion models. Since vapors are no longer a threat when considerably elevated, the VM treats only vapors near the ground or water surface.

The scales L and V above were chosen for urban areas. For suburban areas, these scale lengths must be reduced by a factor of 2 or 3. For open fields or the sea surface, reduction by a factor near 100 is in order. Since most of the vulnerable resources are concentrated in urban areas, the lengths used above were chosen.

It is clear from the way in which the gaussian models were developed, and from observations of the eddies around buildings, that a glob of vapor which is much smaller than the buildings among which it is found will not be treated accurately by the VM. It follows then, that a glob of vapor with a radius of L/10 = 10 m is one for which the VM is inapplicable. Since we are interested in spills and vapors near the ground, let us consider a hemisphere of radius 10 m, which has a volume of 2100 m^3.

An idea of the minimum amount of material for which the model is applicable can be obtained by calculating how much of the substance this hemisphere would contain at some lower significant concentration. For flammable substances this concentration is taken to be the lower flammable limiting concentration, also known as the lower flammable limit. For toxic substances, the concentration which causes immediate irritation has been used as the significant concentration.

As a rough estimate of the lower limit of the amount of a cargo which must be spilled in order for the dispersion model to be applicable, the amount of the cargo necessary to create a hemisphere of radius 10 m with a uniform concentration at the significant level has been calculated for each of the primary cargos. The results are given in Table B3-1.

This table is interpreted as follows: For the case of LNG, it takes 53 gallons to create a hemisphere 10 m in radius at the lower flammable concentration. A hemisphere this small cannot be treated accurately by the VM in an urban area because of the size of the surrounding buildings. If the cloud were to expand to a size which the VM does treat accurately, then the vapor would be so diffuse that it could not ignite and the danger of explosion or fire is not present. Thus, a spill of 53 gallons = 0.20 m^3 of LNG is too small to be treated by the VM.

Since the volume of a hemisphere is proportional to the cube of its radius, a spill of 53,000 gallons = 200 m^3 is necessary to create a hemisphere of radius 100 m at the lower flammable concentration. This hemisphere

is on the same scale as the surface roughness, and therefore represents the order of magnitude of the spill large enough to be treated adequately by the VM. Between 0.20 m^3 and 200 m^3, the air dispersion submodel becomes more and more applicable as the size of the spill is increased, but no definite line can be drawn to separate a region of applicability from a region of inapplicability.

Thus the volumes in the two righthand columns of table B3-1 represent spill sizes for which the VM is not applicable. The VM is certainly applicable for a spill of 1000 times as much cargo as listed in these columns, however, and for spills between these two sizes the VM must be applied with caution.

TABLE B3-1

Volume of Liquid for the Five Priority Cargos
Which Is Necessary to Create a Hemisphere
of Radius 10 m at the Significant Concentration

Cargo	Significant Concentration	Mass in Hemisphere	Volume in Liquid Phase	
		kg	m	gallons
LNG	5.3%	80	0.20	53
Methyl Alchohol	7.3%	210	0.27	71
Gasoline	1.4%	130	0.19	50
Chlorine	45 mg/m^3	0.084	0.000056	0.015
Anhydrous Ammonia	700 mg/m^3	1.5	0.0018	0.48

APPENDIX C1

IGNITION SOURCE CONSIDERATIONS

As a further refinement to the fire and explosion modeling it has been suggested that gradations within the classes of ignition sources be considered. Such gradations would permit the user to specify at a given location a type of ignition source that would be capable of igniting some flammable materials but not others.

The approaches to implementing some type of ignition source gradation in the VM is based on a somewhat unconventional use of the concept of flashpoint. According to one standard text:

> Flash Point of a liquid is the lowest temperature of the liquid at which it gives off vapor sufficient to form an ignitible mixture with the air near the surface of the liquid or within the vessel used. By "ignitible mixture" is meant a mixture within the flammable range (between upper and lower limits) that is capable of the propagation of flame* away from the source of ignition when ignited. Combustion is not continuous at the flash point. This term applies mostly to flammable liquids, although there are certain solids, such as camphor and naphthalene, that slowly sublime (change from a solid to a vapor) at ordinary room temperature and therefore have flash points while still in the solid state.[C-1]

---

*By "propagation of flame" is here meant the spread of flame from layer to layer independently of the source of ignition. A gas or vapor mixed with air in proportions below the lower limit of flammability may burn at the source of ignition, that is, in the zone immediately surrounding the source of ignition, without propagating (spreading) away from the source of ignition.

Thus flashpoint is seen to be a property of the flammable substance; flashpoint is related to two more fundamental properties of the substance, viz. the limits of flammability and the dependence of vapor pressure on temperature. Nevertheless flashpoint gives a measure of the ease by which a particular substance may be ignited. The lower the flashpoint, the easier it is to ignite the material.

Since flashpoint is a commonly accepted measure of flammability, it seems reasonable to "turn-the-tables" and use flashpoint as the basis for

---

[C-1] Fire Protection Handbook, p. 4-8 ff. G. H. Tryon, ed.-in-chief. National Fire Protection Association, Boston, 1969.

a measure of ignition source strength.

At the present time it seems undesirable to perform the data preparation and modeling required to characterize real-world ignition sources, their ability to ignite a certain hazardous cargo, and their distribution spatially and temporally. Instead a less detailed model, that is more easily developed and used, is desired. Again the user should be able to keep all parameters of a simulation fixed except the type of flammable substance and have an ignition for one substance, but no ignition for another. Basing the ignition source strength on flashpoint permits the user to have this capability. Powerful ignition sources will ignite all combustible materials; weak ignition sources will only be able to ignite very flammable substances, i.e. those with very low flashpoints.

One approach to providing such gradations would be to designate an ignition temperature for each ignition source. Those materials (generally flammable liquids) that have a flashpoint less than or equal to the given ignition temperature would be ignited (provided of course that the vapor-air mixture had a concentration within the ignitable range), while those materials with a flashpoint above the given ignition temperature would not be ignited. This rather unconventional application of the concept of flashpoint is primarily an attempt to allow the user to specify ignition sources of different strengths; thus two simulations having the same input data, except for the type of substance spilled, will yield ignition in one case but not in the other. Flashpoint, of course, is a material property encompassing a set of physical and chemical parameters such as volatility, ignitibility, specific heat, and vapor density. The use of flashpoint to characterize ignition sources is recognized to be an artifice without a clear phenomenological basis. However, it does allow the user of the VM, albeit in an artificial manner, to vary the strength of the ignition sources specified. Another approach to providing gradations of the fire-type ignition source would be to characterize ignition sources on the basis of the standard classifications of flammable liquids. Table C1-1 shows the ICC and NFPA classifications for flammable liquids. An ignition source given a certain level designation would be capable of igniting all those substances whose flashpoints fell within the limits for that level and would be capable of igniting all those substances whose hazard level was greater. For example, using the NFPA classification an ignition source designated moderate could ignite methyl alcohol (flashpoint = +65°F, within the moderate range) as well as gasoline (flashpoint = -50°F, within the high range); however, it would not ignite spirits of turpentine (flashpoint = 95°F, within the slight range) nor would it ignite olive oil (flashpoint = 437°F, within the combustible range).

For the Vulnerability Model, the NFPA classification of flammable substances is used as the basis for ignition source differentiation. The flashpoint of flammable substances is not currently included in the properties file; consequently this information will be provided as input data until the properties file is revised. Guidelines will be provided to the user suggesting which type of ignition source to use depending on the land use or some other indicator of human activity. For computerization the ignition sources are denoted by a single digit code as indicated in Table C1-2. An ignition source designated by "0" means no ignition regardless of the flammability class of the spilled substance.

For ignition source codes 1 through 4 ignition will occur provided the flashpoint of the material spilled is less than or equal to the upper bound of the NFPA range indicated. This relationship between ignition source code and the flashpoint of substances subject to ignition is given in Table C1-3. If the sign of the code is positive, then the ignition source is understood to cause conflagration only; i.e., the flash fire submodel is to be selected. If the sign of the code is negative, then the ignition source is understood to cause detonation; i.e., the explosion submodel is to be selected.

I. ICC:

flash point	fire hazard
< 80°F	high
80°F-350°F	moderate
> 350°F	slight

II. NFPA:

flash point	fire hazard
< 20°F	high
20°F-70°F	moderate
70°F-200°F	slight
> 200°F	combustible

TABLE C1-1

CLASSIFICATION SYSTEMS FOR FLAMMABLE LIQUIDS [C-2]

Code	NFPA Classification		Ignition potential of the source
	Flash point of substances ignited by the source	Fire hazard of substances ignited by the source	
0	--	--	none
1	< 20°F	high	low
2	20°F-70°F	moderate	moderate
3	70°F-200°F	slight	high
4	> 200°F	combustible	all combustibles

TABLE C1-2

NUMERICAL DESIGNATION OF
IGNITION SOURCE STRENGTH USED IN THE VM

Ignition Source Code	Flash point of Spilled Material	
	Ignition	No Ignition
0	none	all
1	F.P. $\leq$ 20°F	F.P. > 20°F
2	F.P. $\leq$ 70°F	F.P. > 70°F
3	F.P. $\leq$ 200°F	F.P. > 200°F
4	all combustibles	only non-combustibles

TABLE C1-3

RELATIONSHIP BETWEEN IGNITION SOURCE
CODE AND FLASH POINT OF SUBSTANCE IGNITED OR NOT IGNITED

[C-2] Dangerous properties of industrial materials, 3rd ed., p. 198. N.I. Sax, ed. Van Nostrand Reinhold Co., New York, 1968.

APPENDIX C2

CALCULATION OF THE AMOUNT OF FUEL CONSUMED

Three ways of calculating the mass of fuel consumed were considered. An upper bound on the quantity consumed is provided by assuming that all the fuel at a concentration above the lower limit of flammability burns completely; i.e.

$$m_{e_1} = \int_{V_1} C(x,y,z)\, d\tau \qquad \text{(C2-1)}$$

where

$C(x,y,z,t)$ = the concentration of the fuel (kg/m^3)
$d\tau$ = element of volume
V_1 = the region enclosed by the surface, $C(x,y,z,t) = K_L$ (lower explosive limit*) in the half-space $z \geq 0$.

A second estimate of the quantity of fuel consumed is obtained by assuming that all the fuel at a concentration between the upper and lower flammability limit is consumed; for this case

$$m_{e_2} = \int_{V_2} C(x,y,z,t)\, d\tau \qquad \text{(C2-2)}$$

where V_2 is the region enclosed by the two surfaces, $C(x,y,z,t) = K_L$ and $C(x,y,z,t) = K_U$ (upper explosive limit) on the half-space $z \geq 0$.

A lower limit of the quantity of fuel consumed is obtained by assuming (1) only fuel at concentrations within the flammability range is consumed and (2) the fuel is not necessarily consumed completely, but is consumed only to the extent that sufficient oxygen is present. Thus, for this case

$$m_{e_3} = \int_{V_3} C(x,y,z,t)\, d\tau + \int_{V_4} F(C)\, C(x,y,z,t)\, d\tau \qquad \text{(C2-3)}$$

where

V_3 = the region enclosed by the surfaces $C(x,y,z,t) = K_L$ and $C(x,y,z,t) = K_s$ (stoichiometric) in the half space $z \geq 0$.

V_4 = the region enclosed by the surfaces $C(x,y,z,t) = K_U$ and $C(x,y,z,t) = K_s$ in the half space $z \geq 0$.

and $F(C)$ is a weighting function giving the fraction of the fuel present that enters into the combustion reaction. That is, if the fuel-air mixture is richer than stoichiometric then we desire to compute the weighting

*Although some authors distinguish between flammable and explosive limits of concentration, many other authors, including several standard references do not. Certainly for many cases of diffuse vapor clouds the distinction may well be impossible to make. Therefore, for the purposes of the VM, explosive and flammable limits are taken to be identical.

function, F (C), which is the mass fraction of fuel present that is consumed, i.e.

$$F(C) = \frac{M_c}{M_p} \qquad (C2\text{-}4)$$

M_c = the mass of fuel consumed
and M_p = the mass of fuel present.

These masses are, of course, proportional to the number of moles in each category, i.e.

$$M_c = n_c M_f \qquad (C2\text{-}5a)$$

$$M_p = n_p M_f \qquad (C2\text{-}5b)$$

where

n_c = number of moles of fuel consumed
n_p = number of moles of fuel present
M_f = molecular weight of the fuel.

Then the mass fraction consumed can be written as,

$$F(C) = \frac{n_c}{n_p} \qquad (C2\text{-}6)$$

The combustion reaction of the fuel can always be written in the form,

1 mole fuel + L moles O_2 → reaction products.

Since air is 21% oxygen by weight, if one mole of fuel requires L moles of of oxygen for complete combustion (i.e. a stoichiometric mixture), then one mole of fuel will require (L/0.21) moles of air. Phrased another way, each mole of reacting air will consume (0.21/L) moles of fuel. Hence the number of moles of fuel consumed, n_c, can be related to the moles of air present in the rich mixture by,

$$n_c = \left(\frac{0.21}{L}\right) n_a \qquad (C2\text{-}7)$$

where ,

n_a = number of moles of air present in the rich mixture (all the O_2 is presumed consumed).

Thus the mass fraction is written as,

$$F(C) = \left(\frac{0.21}{L}\right) \frac{n_a}{n_p} \qquad (C2\text{-}8)$$

The quantities n_a and n_p represent the number of moles of each component present in the two-component fuel-air mixture. The total number of moles present is given by,

$$n = n_a + n_p \qquad (C2\text{-}9)$$

where ,

n = the total number of moles in the two component mixture.

Now assuming that the perfect gas law holds for the fuel, the air, and the mixture of the two, we may write for a system containing hypothetical fuel only,

$$P = \frac{\rho_f RT}{M_f} \qquad \text{(C2-10}$$

where

P = the total pressure
T = the temperature
R = the perfect gas law constant
ρ_f = the density of the fuel at temperature, T, and pressure, P

But the perfect gas law may also be written, for an elemental volume V of the mixture as,

$$P = \frac{nRT}{V} \qquad \text{(C2-11)}$$

or

$$n = \frac{PV}{RT}$$

hence by the use of equation (C2-10), where identical temperatures and pressures are assumed for the mixture and the system containing only fuel,

$$n = \frac{V\rho_f^*}{M_f} \qquad \text{(C2-12)}$$

Now for an elemental volume of the mixture the mass of fuel present is gi en by,

$$M_p = CV \qquad \text{(C2-13)}$$

hence the number of moles present is given by,

$$n_p = \frac{M_p}{M_f} = \frac{CV}{M_f} \qquad \text{(C2-14)}$$

Rearranging equation (C2-9),

$$n_a = n - n_p$$

---

*Also note that

$$n = \frac{V\rho_a}{M_a}$$

This is a consequence of Aragandro's Law.

and substituting equations (C2-12) and (C2-14) in the result yields,

$$n_a = \frac{V\rho_f}{M_f} - \frac{CV}{M_f}$$

$$= \frac{V}{M_f} (\rho_f - C) \qquad \text{(C2-15)}$$

Note that when $C=\rho_f$ the mixture is pure fuel and the number of moles of air as given by equation (C2-15) is zero. Using this result and equation (C2-14) the mass fraction, as given by equation (C2-8) can be written as,

$$F(C) = \left(\frac{0.21}{L}\right) \frac{\frac{V}{M_f}(\rho_f - C)}{\frac{CV}{M_f}}$$

or

$$F(C) = \left(\frac{0.21}{L}\right)\left(\frac{\rho_f}{C} - 1\right) \qquad \text{(C2-16)}$$

Now that the weighting function, F (C), has been determined the third estimate, m_{e_3} (the estimate ultimately used) for fuel participating in rapid combustion, can be computed.

Thus equation (C2-3) becomes

$$m_{e_3} = \int_{V_3} C d\tau + \frac{0.21}{L} \left[\rho_f \overline{V}_4 - \int_{V_4} C d\tau\right] \qquad \text{(C2-17)}$$

where

$\overline{V}_4$ is the volume of region V_4.

To simplify the treatment of the volume integrals that occur in equations (C2-1), (C2-2), and (C2-17), only surface spills will be considered. This is consistent with restrictions already made in this program. Furthermore, the general behavior is expected to be the same regardless at what height the spill occurs. For a surface spill, the concentration according to the CHRIS model is given by,

$$C(x,y,z,t) = \frac{2m}{(2\pi)^{3/2}\sigma_x\sigma_y\sigma_z} \exp - \left[\frac{(x-Ut)^2}{2\sigma_x^2} + \frac{y^2}{2\sigma_y^2} + \frac{z^2}{2\sigma_z^2}\right] \qquad \text{(C2-18)}$$

where

$\sigma_x, \sigma_y, \sigma_z$ = the variances of the Gaussian concentration profile in the respective directions (m)

m = the total mass of spill in the vapor phase
x,y,z, = coordinates
U = wind velocity
t = time

By performing the coordinate transformation,

$$[\frac{x-Ut}{\sigma_x}] = r \sin\theta \cos\phi$$

$$[\frac{y}{\sigma_y}] = r \sin\theta \sin\phi \qquad \text{(C2-19b)}$$

$$[\frac{z}{\sigma_z}] = r \cos\theta \qquad \text{(C2-19c)}$$

the volume integrals bounded by surfaces of constant concentration can be transformed to a more convenient form. Thus, for example, for equation (C2-1) we get,

$$m_{e_1} = \frac{2m}{(2\pi)^{1/2}} \int_0^{r_L} e^{-r^2/2} r^2 \, dr \qquad \text{(C2-20a)}$$

where

$$r_L = [2 \ln (\frac{2m}{(2\pi)^{3/2}\sigma_x\sigma_y\sigma_z K_L})]^{1/2} \qquad \text{(C2-20b)}$$

and K_L = concentration at the lower explosive limit (kg/m^3).

If the quantity

$$\frac{2m}{(2\pi)^{3/2}\sigma_x\sigma_y\sigma_z K_L}$$

is less than one, the logarithm is negative; i.e. there is no real solution for r_L. What this means physically is that the variances ($\sigma_x, \sigma_y, \sigma_z$) are so large that the concentration everywhere in the vapor plume is less than K_L. For such a case the exploding mass ie obviously to be taken to be zero. On the other hand when the variances are small (this is the case soon after the time of release of the vapor), r_L becomes very large. In such a case

$$\frac{1}{(2\pi)^{1/2}} \int_0^{r_L} e^{-r^2/2} r^2 \, dr = \frac{1}{2} \qquad \text{for} \qquad r_L >> 1$$

so that $m_{e_1} \simeq m$.

In other words almost the entire mass of vapor released burns or explodes. Since the explosive yield of spills never seems to be greater than 10 percent of the total yield available from all the material spilled[C3], the approximation given by m_{e_1} may grossly overestimate the yield. The overestimation will occur at times soon after the spill when most of the mass is still undiffused and therefore contained within the lower explosive limit contour. Therefore, m_e is rejected as a suitable approximation to the mass of vapor that enters in the explosive reaction.

[C3] Brown, John A. A study of the growing danger of detonation in unconfined gas cloud explosions. John Brown Associates, Inc., Berkeley Heights, New Jersey. December 1973.

The second estimate of exploding mass given by equation (C2-2) gives more reasonable answers; however this estimate also seems to give values which are generally too high. Thus equation (C2-2) becomes,

$$m_{e_2} = \frac{2m}{(2\pi)^{1/2}} \int_{r_U}^{r_L} e^{-r^2/2} \, r^2 \, dr \qquad \text{(C2-21a)}$$

where r_L is given by equation (25-b) and

$$r_U = [2 \, \ell n \, (\frac{2m}{(2\pi)^{3/2}\sigma_x\sigma_y\sigma_z K_U})]^{1/2} \qquad \text{(C2-21b)}$$

and K_U = concentration at the upper explosive limit (kg/m^3)

Equations (C2-20b) and (C2-21b) may be combined to yield,

$$r_L^2 - r_U^2 = 2 \, \ell n \, [\frac{K_U}{K_L}] \qquad \text{(C2-22)}$$

From equation (C2-22) it is clear that the integration limits in equation (C2-21a), viz. r_L and r_U, are not independent. In a sense m_{e_2}/m, the fraction of available mass that this estimate gives as exploding, can be treated as a function of the lower limit of integration r_U, with the explosive limits ratio, $[K_U/K_L]$ a parameter. For any given r_U the integration interval (hence m_{e_2}/m) is increased as the ratio, $[K_U/K_L]$, is increased. This is what one would expect physically.

If r_U is taken to be very large, r_L is also very large and the integral is small. The case of r_U large corresponds to times soon after the spill when very little mass is contained in the region between the explosive limits. As stated previously, whenever the argument of the square root in equations (C2-20b) and (C2-21b) is negative the radius, r_U or r_L, is to be set equal to zero. Thus for very diffuse vapor clouds both r_U and r_L approached zero. In that case the integral also zero. Thus the estimate m_{e_2} has the desirable property that very rich or very lean vapor clouds both tend to have small explosive yield, while at some intermediate point the explosive yield is maximum. This behavior is what is expected to occur.

It appears that the largest yield is obtained when $r_U = 0$. Values of m_{e_2}/m are plotted as a function of K_U/K_L in Figure C2-1. Values of K_U/K_L for four flammable substances of special interest are given in Table C2-1. As shown in Figure C2-1, when K_U/K_L is large (e.g. for acetone $K_U/K_L = 32$) nearly the entire mass of vapor is within combustible limits. Even for substances less pernicious than acetone, for example, methanol with $K_U/K_L = 5$, more than 60% of the vapor explodes. This estimate gives yields which are several times more than the five to ten percent of mass spilled that has been observed. Consequently it seems appropriate to use the lowest estimate, m_{e_3}.

By using the transformation of coordinates given by equations (C2-19), equation (C2-17) may be rewritten as,

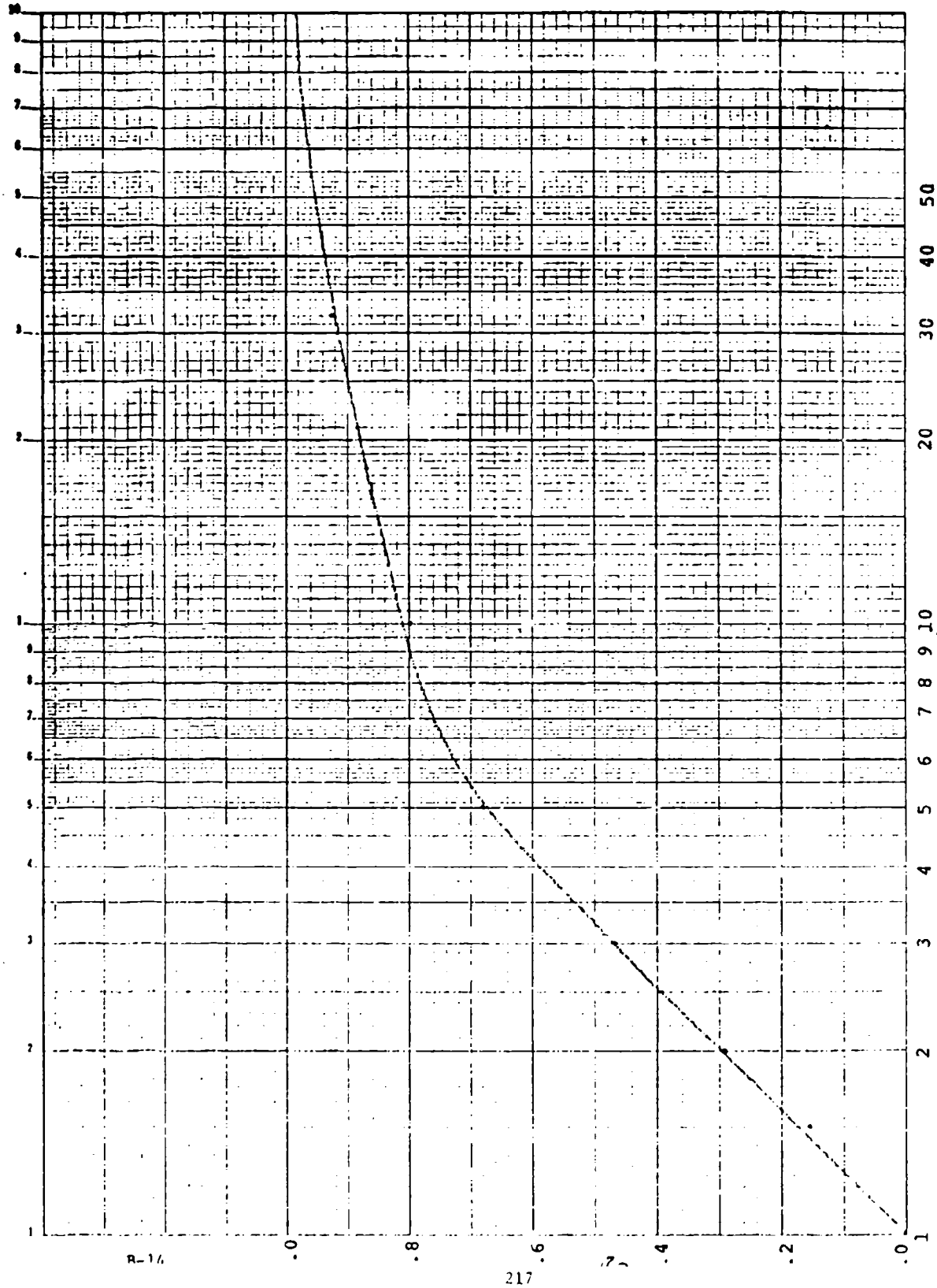

FIGURE C2-1. Variation of m_{e_r}/m with K_U/K_L for $r_U = 0$

	K_U/K_L
Ammonia	1.563
Gasoline	5.429
Methane	2.642
Methanol	5.00

TABLE C2-1

RATIOS OF UPPER EXPLOSIVE LIMIT CONCENTRATION, K_U, TO LOWER EXPLOSIVE LIMIT CONCENTRATION, K_L, FOR FOUR SUBSTANCES OF SPECIAL INTEREST.

$$\frac{m_{e_3}}{m} = 2\,[S(r_L)-S(r_S)] - 0.42\,[S(r_S)-S(r_U)] \qquad \text{(C2-23)}$$

$$+ \frac{0.21}{L} \frac{\rho_f \bar{V}_4}{m}$$

where

$$r_S = \left[2 \ln \left(\frac{2m}{(2\pi)^{3/2}\sigma_x\sigma_y\sigma_z K_S}\right)\right]^{1/2} \qquad \text{(C2-24)}$$

K_S = stoichiometric concentration (kg/m^3)

and where

$$S(r) = \int_{-\infty}^{r} \frac{1}{(2\pi)^{1/2}} e^{-\frac{x^2}{2}} x^2\, dx \qquad \text{(C2-25)}$$

or

$$S(r) = P(r) - \frac{1}{\sqrt{2\pi}} r\, e^{-\frac{r^2}{2}} \qquad \text{(C2-26)}$$

where

$$P(r) = \int_{-\infty}^{r} \frac{1}{(2\pi)^{1/2}} e^{-\frac{x^2}{2}} dx \qquad \text{(C2-27)}$$

is the cumulative normal probability function. Now from equation (C2-21b)

$$\frac{2m}{(2\pi)^{3/2}\sigma_x\sigma_y\sigma_z V_U \rho_f} = e^{r_U^2} \qquad \text{(C2-28)}$$

since

$$K_U = V_U \rho_f$$

where V_U is the volume fraction of vapor at the upper explosive limit. Furthermore, the volume of the ellipsoidal shell comprising V_4 is given by,

$$\bar{V}_4 = \frac{2\pi}{3} \sigma_x\sigma_y\sigma_z (r_S^3 - r_U^3) \qquad \text{(C2-29)}$$

Combining these two results gives,

$$\frac{\rho_f \bar{V}_4}{m} = \frac{2\, e^{-r_U^2} (r_S^3-r_U^3)}{3\,(2\pi)^{1/2} V_U} \qquad \text{(C2-30)}$$

hence the mass ratio given by equation (C2-23) becomes,

$$\frac{m_{e_3}}{m} = 2[S(r_L)-S(r_S)] - \frac{0.42}{L}\,[S(r_S)-S(r_U)]$$
$$+ \frac{0.21}{L} \frac{2\, e^{-r_U^2} (r_S^3-r_U^3)}{3(2\pi)^{1/2} V_U} \qquad \text{(C2-31)}$$

Again this estimate appears to give a maximum value when $r_U = 0$. For that condition and for methanol ($K_U/K_L = 5$, $K_U/K_S = 2.9723$) m_{e3}/m has a value of 0.216. This value is still higher than observed explosions; however, the value of $m_{e3}/m = 0.216$ is favorably smaller than the value $m_{e_2}/m = .641$ obtained for $K_U/K_L = 5$. Therefore m_{e3} should be used as the estimate of mass exploded because (1) this estimate exhibits a maximum value as expected physically, (2) the apparent maximum value for a typical explosive vapor is conservative; i.e. the explosive yield predicted is probably larger than that actually obtained, and (3) this estimate depends upon the stoichiometric concentration as well as the upper and lower explosive limits; therefore, it is physically more realistic.

APPENDIX C3

EQUIVALENCY OF CHANGE IN HELMHOLTZ FREE ENERGY AND CHANGE IN ENTHALPY FOR ESTIMATING THE YIELD OF VAPOR-AIR EXPLOSIONS

To show the close agreement between the change in Helmholtz free energy and the change in enthalpy, proceed as follows. By definition,

$$H = E + PV \tag{C3-1}$$

where,

H = enthalpy
E = internal energy
P = pressure
V = volume

Differentiation of equation (C3-1) yields,

$$dH = dE + P\,dV + V\,dP$$

and for an isobaric process this becomes

$$dH = dE + P\,dV \tag{C3-2}$$

The usually accepted standard heat of combustion is the change in enthalpy resulting from the combustion of a substance, in the state that is stable at 25°C and atmospheric pressure, with the combustion beginning and ending at a temperature of 25°C. Thus the tabulated values for change in enthalpy resulting are for an isobaric process. Thus equation (C3-2) may be written as,

$$\Delta H = \Delta E + P\,\Delta V \tag{C3-3}$$

According to Kinney [C4], the energy yield of an explosion is given approximately by the change in Helmholtz free energy, $-\Delta A$; $-\Delta A$ is computed using,

$$-\Delta A = -\Delta E + T\,\Delta S \tag{C3-4}$$

where,

ΔE is the heat of explosion measured at constant volume

T is the temperature and

ΔS is the change in entropy for the isothermal process.

[C4] Kinney, Gilbert Ford. Explosive Shocks in Air, p. 11. The MacMillan Co., New York, 1962.

The quantity E has the same meaning in equation (C3-3) and (C3-4). Combining equations (C3-3) and (C3-4) gives

$$-\Delta A = -\Delta H + P\,\Delta V + T\,\Delta S$$

or

$$(-\Delta A + \Delta H) = P\,\Delta V + T\,\Delta S \qquad \text{(C3-5)}$$

Equation (C3-5) states that the difference between $-\Delta A$ and $-\Delta H$, the alternative quantities used to compute explosive yield, is given by $(P\,\Delta V + T\,\Delta S)$.

Consider the combustion of methane by the reaction,

$$CH_4 + 2\,O_2 \rightarrow CO_2 + 2\,H_2O \qquad \text{(C3-6)}$$

Since three moles of gaseous reactants combine to produce three moles of gaseous combustion products, there is no change in volume, i.e., at the same temperature and pressure (by definition the reactants and products are brought to 760 mm Hg at 25°C), volumes of gas containing equal number of moles are of equal volumes (Avogadro's Law [C5]). Thus for the reaction given by equation (C3-6), ΔV in equation (C3-4) is zero.

Now for a mixture of ideal gases, the entropy is given by,

$$S = R \sum_{k=1}^{N} n_k \,(\sigma_k - \ln P - \ln X_k) \qquad \text{(C3-7)}$$

where

$$\sigma_k = \frac{1}{R}\left[\int \frac{C_{p_k}\,dT}{T} + S_{o_k}\right] \qquad \text{(C3-8)}$$

and

S = entropy of mixture

n_k = number of moles of gas species "k"

P = pressure

X_k = mole fraction of gas species "k"

C_{p_k} = specific heat of gas species "k"

R = gas constant

S_{o_k} = standard molar entropy at STP

[C5] Hougen, O.A., K.M. Watson, and R.A. Ragatz. Chemical Process Principles, Part I, p. 305. John Wiley & Sons, Inc., New York, 1959.

Equation (C3-7) now can be used to calculate the entropy on both sides of the reaction (C3-6) so that the change in entropy can be computed. Note that the terms

$$- R \sum_{k=1}^{2} n_k \ln P$$

and

$$- R \sum_{k=1}^{2} n_k \ln X_k$$

are identical on either side of the reaction. Hence,

$$\Delta S = S_R - S_L = S_{o_{CO_2}} + 2\, S_{o_{H_2O}} - S_{o_{CH_4}} - S_{o_{O_2}}$$

(where S_R, S_L are the entropy on the right and left hand sides respectively of the reaction (C3-6).

Following through the computation with tabulated values gives,

$$\Delta S = -1.28 \ \frac{\text{cal}}{\text{g-mole-}^\circ\text{K}} \qquad \text{(C3-9)}$$

hence,

$$T\Delta S = -381.44 \ \frac{\text{cal}}{\text{g-mole}} \qquad \text{(C3-10)}$$

Referring again to equation (C3-5) we see that the difference between $-\Delta A$ and $-\Delta H$ is -381.44 cal/g-mole. However the value of ΔH for the combustion of methane is -212.798×10^3 cal/g-mole. In other words, for this reaction the error made in using $-\Delta H$ to represent $-\Delta A$ is of the order of 1/10 of one percent.

Now consider the combustion of n-octane by the reaction,

$$C_8H_{18} + \frac{25}{2}\, O_2 \rightarrow 8CO_2 + 9H_2O \qquad \text{(C3-11)}$$

Again using equation (C3-7) we obtain,

$$\Delta S = 107.385 \ \frac{\text{cal}}{\text{g-mole-}^\circ\text{K}} \qquad \text{(C3-12)}$$

In the combustion of n-octane, however, the number of moles of gas changes, hence the term $P\Delta V$ in equation (C3-5) is not zero. From the perfect gas law,

$$PV = nRT \qquad \text{(C3-13)}$$

it can be shown for a reaction in which the reactants and product are brought to the same temperature and pressure, that

$$\Delta V = \Delta nRT \qquad \text{(C3-14)}$$

where Δn is the change in the number of moles in the gas phase by virtue of the reaction. For the reaction given by equation (C3-11)

$$\Delta n = -3.5$$

Thus the total difference between $-\Delta A$ and $-\Delta H$ is

$$2.993 \times 10^4 \ \frac{\text{cal}}{\text{g-mole}}$$

But the heat of combusion, $-\Delta H$, for n-octane is 1.307×10^6 cal/g-mole. In other words, the error is of the order of two percent.

These rather lengthy calculations have been performed to demonstrate that the change in enthalpy is indeed a good approximation to the change in Helmholtz free energy. The energy available from the terms $P\Delta V$ and $T\Delta S$ are very important for the condensed phase explosives with which Kinney [C4] was mainly concerned; however, for gas mixture explosions, with which we are concerned, these terms are negligible.

APPENDIX C4

CORRECTION TO HEATS OF COMBUSTION

Correction for Water Heat of Vaporization

The value for heat of combustion, $-\Delta H$, used in Chapter 4 to determine explosive yield (equation 4-2), is for final products that include water vapor; most handbooks give $-\Delta H$ for final products that include liquid water. These values for $-\Delta H$ must be corrected for the heat of vaporization of water.

This correction is given by,

$$-\Delta H_w = -\Delta H - n_w \lambda_w \qquad \text{(C4-1)}$$

where

$-\Delta H_w$ = heat of combustion corrected for water vaporization
$-\Delta H$ = handbook value for heat of combustion
n_w = number of moles of water formed per mole of fuel burned
λ_w = heat of vaporization of water.

For the combustion of methane as given in equation (C3-6) the correction factor is -19.43×10^3 cal/g-mole or about a nine percent correction. For the combustion of n-octane as given by the reaction in equation (C3-11) the correction factor is 0.08745×10^6 cal/g-mole or about a seven percent correction.

Correction for Fuel Heat of Vaporization

The value for heat of combustion, used in Chapter 4 to determine explosive yield (equation 4-2), $-\Delta H$, is for an initially vaporized (gaseous phase) fuel.

Heats of combustion are usually reported for the substance in the normal state at 25°C. Since the reaction of interest is for a substance normally a liquid at 25°C, then unless specified otherwise, the handbook value must be corrected to account for the heat of vaporization of the fuel. This correction is given by,

$$-\Delta H_f = -\Delta H - \lambda_f \qquad \text{(C4-2)}$$

where

$-\Delta H_f$ = heat of combustion corrected for fuel vaporization
λ_f = heat of vaporization of the fuel.

Since methane is gaseous at 25°C and 760 mm H_g, no correction is required for the combustion of methane. For n-octane, which is a liquid at standard conditions, the correction factor is -9221 cal/g-mole or about 0.7 percent. For substances less easily vaporized the correction factor will, of course, be larger.

APPENDIX C5

DAMAGE POTENTIAL OF CONFINED EXPLOSIONS

The following two charts give a measure of the damage potential of confined explosions. The charts consider the energy yield available when confined spaces are filled with combustible mixtures. The charts do not address the more sophisticated consideration of what seepage rates into and out of structures will produce combustible mixtures in the presence of a time varying atmospheric concentration. Neither do the charts address the additional hazard from fragments expected for confined, rather than unconfined explosions.

The first chart gives the explosive yield as a function of volume resulting from the ignition of a stoichiometric mixture of the materials noted, presuming the volume is completely filled with a stoichiometric mixture.

The second chart shows the effect on energy yield as a function of volume when the concentration is varied away from stoichiometric; of course for any concentration other than stoichiometric the energy yield is less given the same enclosed volume of vapor-air mixture. The substance is methanol. Ratios of 0.6 and 3 correspond approximately to the lower and upper explosive limits, respectively.

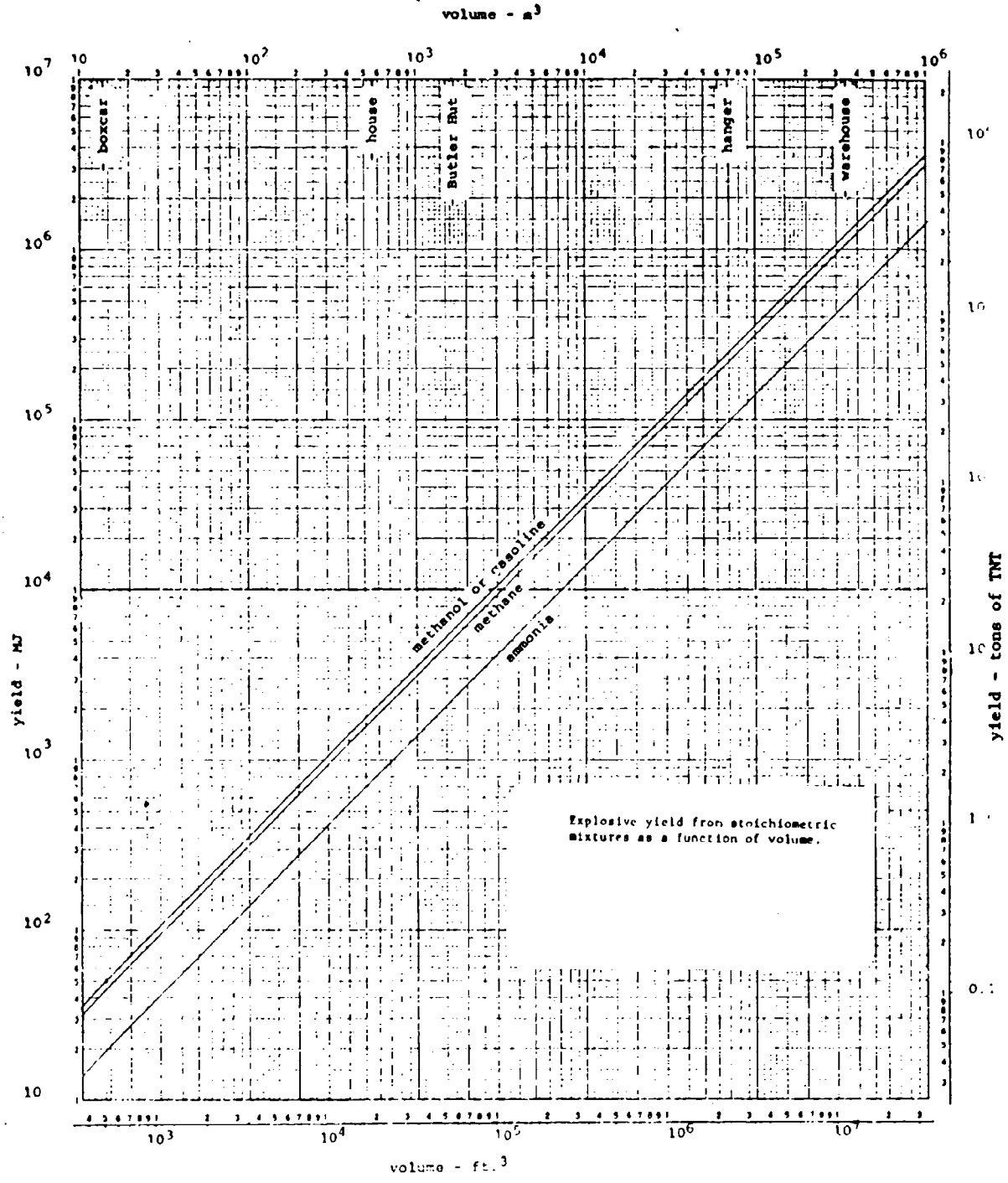
volume - m³
10
10²
10³
10⁴
10⁵
10⁶
10⁷
boxcar
house
Butler Hut
hanger
warehouse
methanol or gasoline
methane
ammonia
yield - MJ
yield - tons of TNT
Explosive yield from stoichiometric mixtures as a function of volume.
10³
10⁴
10⁵
10⁶
10⁷
volume - ft.³

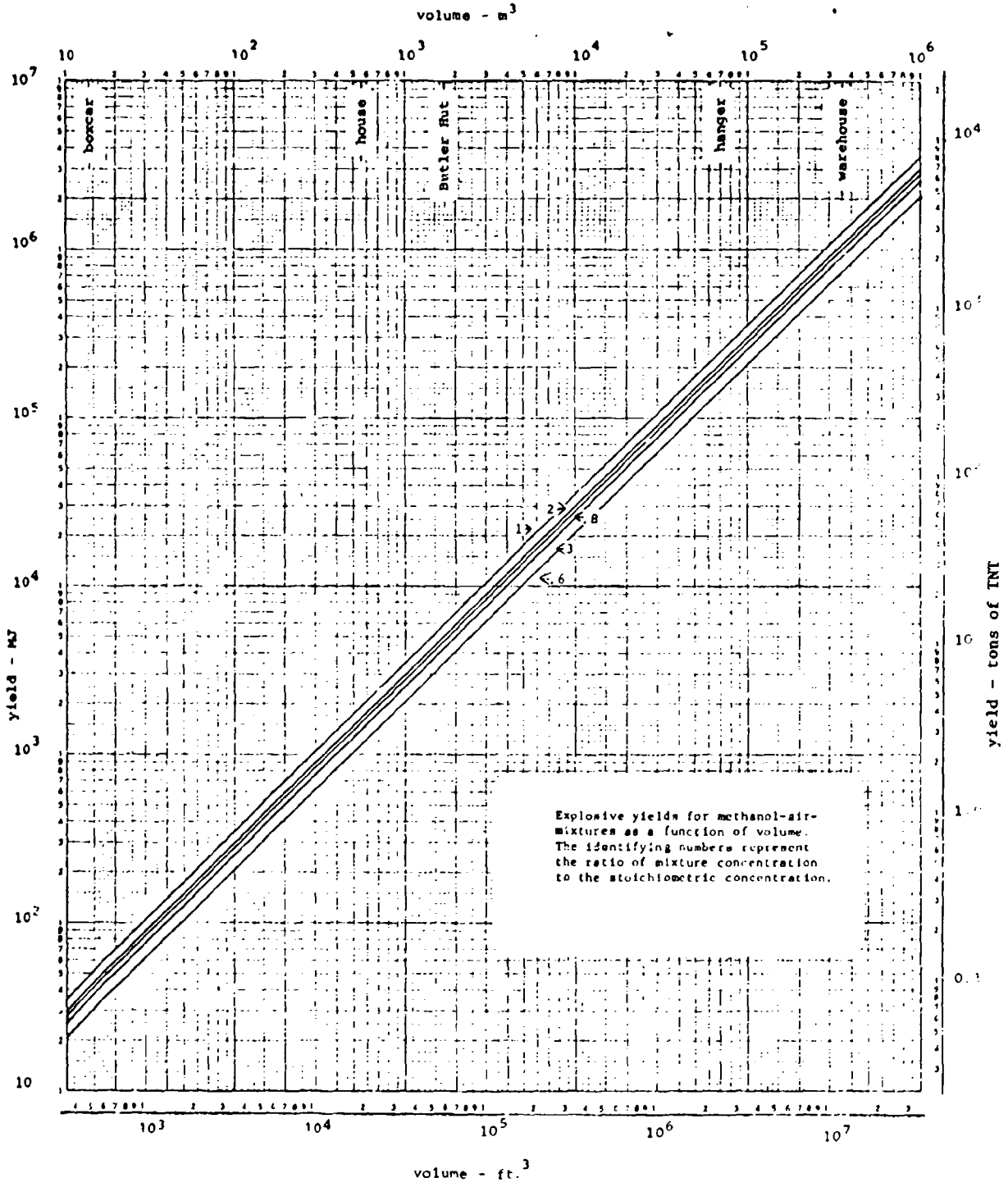
volume - m3
10
10^2
10^3
10^4
10^5
10^6
10^7
boxcar
house
Butler hut
hangar
warehouse
yield - MJ
yield - tons of TNT
1
2
8
3
6
Explosive yields for methanol-air-mixtures as a function of volume. The identifying numbers represent the ratio of mixture concentration to the stoichiometric concentration.
10^3
10^4
10^5
10^6
10^7
volume - ft.3

APPENDIX D

DAMAGE TO VULNERABLE RESOURCES FROM FIRE AND EXPLOSION

In this appendix further detail is provided about the basis for damage assessment in the event of fire or explosion. Since the physical phenomena causing the damage in a fire are quite different from the damage-causing phenomena in an explosion, the damage assessment for fire is discussed separately from that for explosion. Furthermore under each of the separate discussions for fire and explosion, damage to each type of vulnerable resource is treated separately; people and structures are the two types of vulnerable resource considered. Damage from explosion will be described first since damage from this source is likely to be more serious than from either a flash fire or pool burning.

EXPLOSION DAMAGE

In assessing damage from explosions that result from spills of hazardous materials, considerable use is made of studies performed for and by the military; these studies assess damage from both conventional and nuclear weapons.

As mentioned in Chapter 4 of this report, the blast wave resulting from a diffuse explosion behaves differently than a standard condensed phase explosion (like TNT) and certainly behaves differently than a nuclear explosion. Nevertheless, the assumption that diffuse and condensed phase explosions are similar yields small errors compared to those errors given by some other assumptions. Since much of the damage assessment analysis is presented in terms of basic blast wave parameters (say overpressure, rather than the TNT yield), if the analyses becomes available to predict the behavior of diffuse explosions, these predicted values may be used with the preexisting data to provide a more accurate damage assessment. In the absence of a convincing and complete analysis of diffuse explosions, the approach will be to treat the diffuse explosions as condensed phase explosions and assess damage accordingly. This approach is certainly state-of-the-art and is consistent with approximations in modeling made elsewhere in the VM.

Damage to Personnel

In choosing models to describe damage from explosions several sources were consulted, but primary among these is a recent document [D1] prepared for the Department of Defense Explosives Safety Board which is a compendium of assessment techniques for damage from conventional explosions. In this and other references, damage to personnel is classified into three categories:

[D1] Fugelso, L.E., L.M. Weiner, and T.H. Schiffman. Explosion effects computation aids. General American Research Division, General American Transportation Corporation, Niles, Illinois, June 1972. GARD Project No. 1540, AD903279 L - (the limited distribution denotation on this document has recently been lifted).

(1) primary damage - direct blast effects (interaction between the blast wave and personnel only, with no other intervening or associated factors)

(2) secondary damage - damage from missiles and fragments

(3) tertiary damage - damage from translation and subsequent collision with an obstacle.

These categories of blast injury are based on the mechanism of damage and are independent of which of the basic blast wave parameters (peak overpressure or dynamic impulse) is used to assess damage of that category.

The discussions that follow, taken largely from references [D1] and [D2] explain in more detail, the nature of these categories of blast injury to personnel.

(1) Direct Blast Injury

When the human body is exposed to the environmental pressure variation accompanying a blast wave, the wave is transmitted in complex patterns throughout the body but, more important, the body wall is pushed violently inward. As a consequence of this implosive effect, very high transient internal pressures occur. These often exceed the external pressures by considerable amounts. Severe disruptive forces are produced at junctions of tissues of different densities such as bone with soft tissue or in air-containing organs such as the lungs and abdominal viscera. Only for "long" duration typical blast waves is the severity of the injury sustained roughly proportional to the magnitude of the peak overpressure; otherwise, and in addition, the hazard is a function of the duration and the rate and character of the rise of the pressure pulse. In general, except for the ears and sinuses, the human body is far more resistant to direct blast injury than are rigid structures such as buildings.

While eardrum rupture may occur at peak overpressure as low as 5 psi, the best value of the peak overpressure for 50 percent probability of rupture appears to be between 15 and 20 psi. Though painful, eardrum rupture is not serious. However, infection, fracture and displacement of the ossicles, including the foot plate of the stapes, may result in impaired hearing and require specialized treatment.

Blast injuries to the chest begin to occur at about 10-12 psi for "long" duration waves. These include bruising of the soft tissues of the chest wall adjacent to the ribs and rupture of small vascular elements of the pulmonary

---

[D2] Department of the Army. Nuclear Handbook for Medical Service Personnel. TM8-215, 1969.

> tissue. Rupture of pulmonary vessels is always associated with interstitial hemorrhage and/or bleeding into the airways. Also, the risk of pulmonary edema is considerable and serious. With severe tearing and rupture, air emboli may occur with grave, frequently fatal, cardiac or cerebral complications. Clinical signs of pulmonary injury may be misleadingly mild until heart failure and edema appear: the heart failure and pulmonary edema are the primary treatment problems. . . .
>
> Blast injuries of the abdomen may include rupture of the liver and spleen, and rarely in airblast, perforations of the intestine. Organ perforations, especially in the lower ileum, cecum, and colon are much more common in underwater blast. Also, in airblast hemorrhages of the mesentery and gut wall are almost invariably present. Frequently there is abdominal wall rigidity without perforation of hemoperitoneum, and the significance of the signs and symptoms are difficult to assess. . . . ([D2], pp. 6-7)

The primary cause of lethality from direct blast effects is lung hemorrhage. Data on direct blast injury to personnel have been obtained by experimentally determining overpressure-duration relationships for animals, and extrapolating these to humans. That is, the level of injury depends upon both peak overpressure level and the duration of the overpressure. For large-scale conventional explosions and most probably for all diffuse explosions, the duration of the blast wave may be considered "long". Thus it is current practice to use the free field (side on) overpressure, associated with various levels of lethality at infinitely large durations to assess deaths from direct blast effects. Table D-1 shows the relationship between overpressure and lethality from direct blast effects. The data in table D-1 were used to derive the probit equation E1:

$$\text{Probit} = -77.1 + 6.91 \ \text{Log}_e \ (Pp) \qquad \text{(D-1)}$$

where Pp is the peak overpressure measured in N/m^2.

The main nonlethal injury resulting from direct blast effects is eardrum rupture. Unlike the lungs for which overpressure and blast wave duration together determined damage, eardrums are damaged in response to overpressure alone since the characteristic period of the ear vibration is small compared to the duration of a blast wave from even low yield explosions. The relationship between the overpressure and the probability of eardrum rupture is given in Table D-2. These data were used to generate the probit equation E3:

$$\text{Probit} = -15.6 + 1.93 \times \log_e \ (Pp) \qquad \text{(D-2)}$$

where Pp is the peak overpressure measured in N/m^2.

Damage	Peak Overpressure (psi)	Peak Overpressure (N/m^2)
Threshold (1% Lethality)	14.5	100,000
10% Lethality	17.5	120,000
50% Lethality	20.5	140,000
90% Lethality	25.5	175,000
99% Lethality	29.0	200,000

TABLE D1

CRITICAL OVERPRESSURES FOR LUNG DAMAGE TO HUMANS

The relationship between overpressure and death for direct blast effects. It is assumed that the pressure pulse duration is infinite and that lung hemorrhage is the operative cause of lethality. This table is based on data given in "Explosive Effects Compulation Aids" [D1].

Probability of Eardrum Rupture	Free-Field Peak Overpressure (psi)	Free-Field Peak Overpressure (N/m^2)
Threshold (1%)	2.4	16,500
10%	2.8	19,300
50%	6.3	43,500
90%	12.2	84,000

TABLE D2

PROBABILITY OF EARDRUM RUPTURE

The relationship between peak overpressure and probability of eardrum rupture. This table is based on data given in "Explosive Effects Compulation Aids [D1].

(2) Indirect Blast Injury

The transfer of momentum by a blast wave to objects in its path can result in injury from secondary missiles (both penetrating and nonpenetrating) or from displacement of the human body resulting in subsequent severe impact or decelerative tumbling; these are secondary and tertiary blast effects respectively. The injuries which result include wounds, such as contusions and fractures, which result from being thrown against an object. In addition, crush injuries from falling debris, should they occur, would be particularly more common in urban areas and less common in the open. Certain kinds of indirect blast injuries, such as violent decelerations or sharp blows to the head from blunt debris, are known to produce significant lethality just as does direct blast injury to the lung. However, the magnitude and severity of indirect hazards are very much dependent on the conditions of exposure, range, and explosive yield.

(a) Secondary Blast Injury

The missiles involved in secondary damage in the VM result from normal environmental debris (e.g., pebbles), damaged structures (e.g., broken glass), and fragments of cargo containers (e.g., ship hull fragments). Studies of military weapons have modeled missiles generated purposefully by weapon design (such as fragmenting shell casings) [D1]. Nevertheless nuclear weapon effects research has considered the effects of missiles resulting from debris set in motion by the nuclear blast waves [D3]. These studies have considered personnel damage from both penetrating and nonpenetrating missiles. The injuries which may result are lacerations and punctures from penetrating missiles or contusions, fractures, and internal injuries from large nonpenetrating objects. Penetrating missiles are light (10 grams or less in mass) compared to nonpenetrating missiles capable of causing injury (thousands of grams in mass). At the current stage of development the interest is for the VM to model diffuse, rather than condensed phase explosions. The occurrence of heavy missiles, capable of causing serious nonpenetrating woulds, is expected to be less common in diffuse explosions than in condensed phase or nuclear explosions. Therefore, the only kind of secondary damage currently considered by the VM is the nonlethal damage caused by penetrating missiles. Table D-3 gives damage criteria for both penetrating and nonpenetrating missiles. The critical parameter used to assess damage is the impact velocity of the missile. Another source [D2] gives data for penetrating missiles that are virtually the same, as shown in Table D-4.

For use in the VM the damage criteria based on missile impact velocity must be related to a blast wave parameter; it is clearly beyond the scope of the VM to treat the detailed motion of the thousands

---

[D3] White, Clayton S. The nature of the problems involved in estimating the immediate casualties from nuclear explosions. Lovelace Foundation for Medical Education and Research, Albuquerque, New Mexico, March 1971. CEX 71.1.

Kind of Missile	Critical Organ or Event	Related Impact Velocity ft/sec
Nonpenetrating 10-lb object	Cerebral Concussion:	
	Mostly "safe"	10
	Threshold	15
	Skull Fracture:	
	Mostly "safe	10
	Threshold	15
	Near 100 per cent	23
Penetrating 10-gm glass fragments	Skin Lacetration:	
	Threshold	50
	Serious Wounds:	
	Threshold	100
	50 per cent	180
	Near 100 per cent	300

TABLE D3

TENTATIVE CRITERIA FOR INDIRECT BLAST EFFECTS INVOLVING SECONDARY MISSILES

The relationship between medical damage from secondary missiles and missile characteristics. Based on data from reference [D3].

Injury	Peak Over-Pressure-PSI	Impact Velocity (meters/sec)	Range in Kilometers 1KT	10KT	100 KT
(Penetrating Missiles-10 Gram Glass Fragment)					
Skin laceration threshold	1-2	15 m/sec	1.8	4	9
Serious wound threshold	2-3	30 m/sec	1.2	2.5	5.5
Serious wounds near 50% probability	4-5	55 m/sec	.75	1.8	4
Serious wounds near 100% probability	7-8	90 m/sec	.55	1.3	2.5

TABLE D4

INJURY CRITERIA FOR PENETRATING MISSILES

Relationship between secondary effect damage and missile characteristics for three different sizes of nuclear weapons. Based on data from reference [D2].

of missiles that an accidental explosion could cause. The impact velocity is most properly related to the dynamic overpressure impulse, rather than the peak overpressure. The dynamic overpressure impulse, J, is defined as the integral of pressure over time for the duration of the positive phase of a blast wave; i.e.:

$$J = \int_{t_a}^{t_o} P(\tau)\, d\tau \qquad \text{(D-4)}$$

where,

$P(\tau)$ = the overpressure as a function of time at a given location

t_a = the arrival time of the blast wave at the given location

t_o = the time at which the positive phase of the blast wave ends.

Figure D-1 further illustrates this definition. The dynamic overpressure impulse is called simply "the impulse" elsewhere in this report ("dynamic overpressure impulse" is used by Fugelso [D1]; "impulse" and "impulse per unit area" are used by Kinney [D4]).

The relationship between missile impact velocity and the impulse of the blast wave is given by,

$$M V_i = C_D A J \qquad \text{(D-5)}$$

where,

M = mass of the missile

V_i = impact velocity

C_D = drag coefficient of the missile, taken to be unity here

A = presented area of the missile

J = impulse

Now we may also write

$$M = \rho \bar{V} \qquad \text{(D-6)}$$

where,

[D4] Kinney, Gilbert Ford. Explosive Shocks in Air, p. 11, The Macmillan Co., New York, 1962.

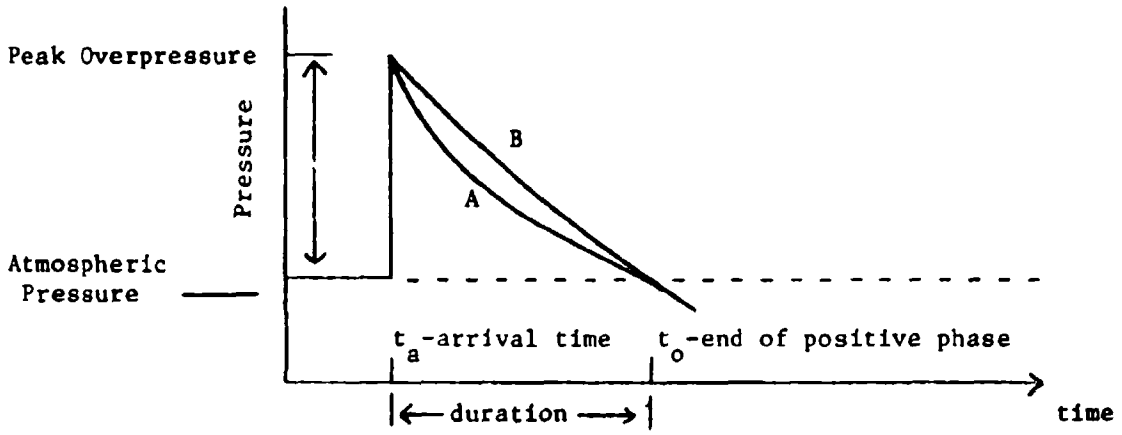

FIGURE D-1

Pressure-time graph of two typical blast waves at a given observation point. Blast wave "A" decays faster and shows a smaller impulse than blast wave "B" even though their durations and the peak overpressures are identical.

ρ = density of the missile

$\bar{V}$ = volume of the missile

But

$$\bar{V} = \frac{4\pi}{3} r^3 \tag{D-7}$$

where we have assumed a spherical fragment of radius, r, and

$$A = \pi r^2 \tag{D-8}$$

Thus we have from equation (D-5),

$$J = \frac{MV_i}{C_D A}$$

or combining with equations (D-6), (D-7), and (D-8),

$$J = \frac{\rho(\frac{4\pi}{3} r^3)\ V_i}{1 \cdot \pi r^2} = \frac{4\rho r V_i}{3} \tag{D-9}$$

Furthermore from (D-7) and (D-6)

$$r = \left[\frac{3M}{4\pi\rho} \right]^{1/3} \tag{D-10}$$

Now for M = 10 grams and $\rho \cong 2.65$ g/cm^3, a typical density for glass, then,

$r = 0.9658$ cm.

hence from equation (D-9),

$$J = (3.4125 \text{ g/cm.}^2)\ V_i \tag{D-11}$$

Substituting values for impact velocity, V_i, from Table D-4 into equation (D-11) generates a corresponding set of values for impulse as given by Table D-5. The data given in Table D-5 are the criteria used to establish the probit equation E5:

$$\text{Probit} = -27.1 + 4.26 \log_e J \tag{D-12}$$

where J is in N-S/m^2.

An assumption implicit in equation (D-5) of the preceding derivation is that no forces other than those of the blast wave are exerted on the missile. That is the forces involved when the missile breaks away from its pre-blast position, slides or rolls along the ground, or impacts intervening objects are all neglected. Furthermore, it is assumed that missiles are always available to be set in motion by the blast wave.

Injury	Free Field Impulse Level		
	dyne-s/cm^2	N-s/m^2	psi-msec
Skin laceration threshold	5120	512	74.2
Serious wound threshold	10240	1024	148.4
Serious wounds near 50% probability	18770	1877	272.1
Serious wounds near 100% probability	30710	3071	445.3

TABLE D5

DAMAGE CRITERIA FOR PENETRATING MISSILES IN TERMS OF CRITICAL IMPULSE

Relationship between penetrating missile damage and free field impulse level. Equation D-11 and the data given in Table D4 were used to obtain these values.

These values were obtained by assuming a missile of 10 grams mass.

Also all personnel (not inside buildings) in a region traversed by a blast wave of sufficient strength are assumed to suffer injury from missiles; the density of flying fragments and the target area presented by people are not factors affecting the probability of injury in this analysis. Evidently then the estimate of fragment injury given by the probit equation equation, E5 (D-12), is too large. Since there appears to be no facile method for correcting this assessment, the overestimate of damage given by equation (D-12) is currently used in the VM.

(b) Tertiary Blast Injury

Injury to personnel by tertiary effects is related to the maximum translation velocity that the body attains subject to the blast. Injury is caused when the body set in motion by the blast wave strikes an obstacle. The probability of lethality for body impact has been determined as a function of the impact velocity. Lethality criteria have also been determined for impact of the head against an obstacle. Table D-6 shows the impact velocity associated with several levels of lethality.

Again the problem is to relate the damage criteria in table D-6 based on impact velocity to some free field, blast wave parameter. One reference [D1] indicates that a method that may be used to relate impact velocity and free field impulse is the same as that used for missiles in the above. Similar to equation (D-5) we write,

$$J_i = \frac{MV_i}{C_D A} \qquad \text{(D-13)}$$

where,

J_i = critical impulse for impact damage

M = mass of the body

V_i = critical velocity for impact damage

C_D = drag coefficient of the body, taken here to be unity

A = cross-sectional area of the body presented to the blast

For each impact velocity, V_i, of interest a corresponding impulse, J_i, may be calculated using equation (D-13). We may calculate J_i assuming a typical grown male adult, using a weight of 155 pounds and an area of 8 square feet. Table D-7 (taken from [D1]) gives both the impact velocity, Vm, that causes a certain level of damage and the dynamic impulse corresponding to that velocity for the grown male adult described above. Note, however, that the critical levels for lethality from body impact given in Table D-7 are significantly different from those levels given in Table D-6. The disagreement is considerable and places some doubt on the assessment procedure. The levels given in

Condition Critical Organ or Event	Related Impact Velocity ft/sec
Skull Fracture	
Mostly "safe" (0%)	10
Threshold (10%)	13
50 per cent	18
Near 100 per cent	23
Total Body Impact	
Mostly "safe" (0%)	10
Lethality Threshold (10%)	21
Lethality 50 per cent	54
Lethality near 100 per cent	138

TABLE D6

TENTATIVE CRITERIA FOR INDIRECT (TERTIARY) BLAST EFFECTS INVOLVING IMPACT

Relationship between impact velocity and damage to the head and body. Based on data in reference [D3].

Lethality	Body		Head	
	V_m	J_c	V_m	J_c
Threshold	20	83.6	13	54.3
50%	26	108.6	18	75.2
99%	30	125.4	23	96.1

TABLE D7

LETHALITY DUE TO CRITICAL IMPACT VELOCITY AND CRITICAL IMPULSE (V_m in ft/sec and J_c in psi-msec)

Relationship between impact lethality and impact velocity or impulse. From reference [D1].

Table D-7 are preferred since the publication from which it comes is more recent and the levels given are more conservative. The data given in Table D-7 was used to generate a probit equation. It was assumed that for any given impact, there is a 20% chance of head impact and an 80% chance of body impact; the casualty rates were calculated on this basis assuming that the entire population outdoors is subject to impact for a given blast wave strength.

This assessment procedure, however, gave unrealistic results. Far too many people were killed for the explosive yields and distances considered. The critical impulse levels for a given lethality rate shown in Table D-7 were found to be an order of magnitude lower than expected from observed explosions. The cause for the overestimation of damage from a given impulse level is that certain mitigating factors have not been considered. Some of the factors reducing the likelihood of death are: (1) Friction of the body sliding and rolling along the ground reduces the peak velocity attained on exposure to the blast; (2) During the passage of the blast wave the body may tumble, thereby reducing the area presented to the wave and the momentum absorbed from it; (3) Not all the momentum absorbed by the body is converted to velocity of impact, since both rotational and translational acceleration of the body may occur; (4) Sublethal impact with the ground or obstacles may prevent the body from ever attaining a lethal impact velocity. A model for impact injury that gives consideration to these various factors has been developed for use in civil defense studies [D5]. A plane rigid body subject to a blast environment simulates the trajectory of a person and determines the impact velocities experienced. Lethality is then determined from the data given in Table D-6, since the impact velocity and part of body impacted are predicted by the model. Since at the present time the VM does not model individual damage receptors in a locally detailed environment, this detailed model of impact injury is inappropriate for use in the VM. However, repeated operation of the impact injury model for a given size nuclear weapon showed that mortality could be parameterized on the basis of peak overpressure and distance to a vertical obstacle (wall); the parameterized results for the surface burst of a one megaton nuclear weapon are given in Table D-8. The survivability fractions given in the table are related to probability of death by,

$$\% \text{ dead} = 100\% \, [1-S] \qquad \text{(D-14)}$$

where S is the survivability value given in Table D-8. Similar data for initially prone bodies was also available, but not used.

By use of the explosion scaling laws (cf. Kinney [D6]) the peak overpressures for a 1MT blast given in Table D-8 may be converted to

---

[D5] Longinow, A., G. Ojdrovich, L. Bertram, and A. Wiedermann. People Survivability in a Direct Effects Environment and Related Topics. IIT Research Institute, Chicago, May 1973.

[D6] Kinney, G.F. Engineering Elements of Explosions. Naval Weapons Center, November 1968, NWC TP-4654.

SURVIVABILITY FOR STANDING POSITIONS														
OVERPRESSURE (PSI)	DISTANCE TO WALL (FT)													
	0	5	10	15	20	25	30	35	40	45	50	55	60	NO WALL
2	1.00	.92	1.00	1.00	1.00	1.00	1.00	1.00	1.00	1.00	1.00	1.00	1.00	1.00
3	1.00	.92	.96	.96	1.00	1.00	1.00	1.00	1.00	1.00	1.00	1.00	1.00	1.00
4	1.00	.95	.92	.91	1.00	1.00	1.00	1.00	1.00	1.00	1.00	1.00	1.00	1.00
5	1.00	.82	.81	.87	.88	.50	.75	.75	.75	.75	.75	.75	.75	.75
6	.70	.69	.69	.23	.36	.00	.50	.50	.51	.51	.51	.51	.51	.51
7	.50	.49	.53	.11	.20	.03	.25	.25	.29	.25	.25	.25	.25	.49
8	.31	.26	.37	.00	.05	.06	.03	.04	.00	.00	.00	.00	.00	.47
9	.20	.20	.25	.00	.03	.03	.02	.02	.00	.00	.00	.00	.00	.23
10	.10	.13	.14	.00	.01	.00	.00	.00	.00	.00	.00	.00	.00	.00
11	.01	.09	.10	.00	.00	.00	.00	.00	.00	.00	.00	.00	.00	.00
12	.00	.03	.06	.00	.00	.00	.00	.00	.00	.00	.00	.00	.00	.00
13	.00	.02	.04	.00	.00	.00	.00	.00	.00	.00	.00	.00	.00	.00
14	.00	.01	.02	.00	.00	.00	.00	.00	.00	.00	.00	.00	.00	.00
15	.00	.01	.03	.00	.00	.00	.00	.00	.00	.00	.00	.00	.00	.00
16	.00	.00	.03	.00	.00	.00	.00	.00	.00	.00	.00	.00	.00	.00
17	.00	.00	.01	.00	.00	.00	.00	.00	.00	.00	.00	.00	.00	.00
18	.00	.00	.00	.00	.00	.00	.00	.00	.00	.00	.00	.00	.00	.00
19	.00	.00	.00	.00	.00	.00	.00	.00	.00	.00	.00	.00	.00	.00
20	.00	.00	.00	.00	.00	.00	.00	.00	.00	.00	.00	.00	.00	.00

TABLE D8

Relationship between damage from impact and the parameters, overpressure, and distance to obstacle, for the surface burst of a one megaton nuclear weapon. Percent deaths = 100 x (1- survivability)

impulse levels; thus deaths from impact may be related to impulse. Table D-9, derived from the data in Table D-8, gives the relationship between deaths from impact and impulse level for a wall distance of ten feet (3.3 meters). The spread in overpressure between the threshold of damage and the threshold of complete lethality is largest for a wall distance of ten feet; thus the dose-response relationship for this set of data is least discontinuous. Ten feet is a reasonable impact distance for urban areas. Furthermore the change in wall distance is not that significant in determining the relationship between impact injury and overpressure (hence, impulse). For all these reasons the data for an impact surface ten feet distant were used to generate Table D-9 and subsequently the probit equation, E2. Based on the data in Table D-9 the probit equation, E2, is:

$$\text{Probit} = -46.1 + 4.82 \log_e J \qquad \text{(D-15)}$$

where J is in $N\text{-}S/m^2$.

This probit equation gives estimates of deaths from impact that are much more in accord with observed events than does the probit equation based on the less sophisticated model used first.

In addition to death, tertiary effects can cause nonlethal injuries -- mainly broken bones. Table D-10 gives a variety of nonlethal injuries (as well as lethal injuries) and the impact velocities at which such injuries occur. As previously indicated, the range data for various sizes of nuclear weapons are unimportant; the critical impact velocities are significant for the VM. It is interesting that the lethality levels from this source [D2] agree reasonably well with those given in Table D-7 for body impact.

Using equation (D-13) to relate impulse level to impact velocity, one can generate a new table relating injury to impulse level by using the values given in Table D-10. Again, the calculations are for a 155 pound adult male with an effective area of 8 square feet. These computations are compiled in Table D-11. Notice, however, that the impulse levels for injury is below the levels for death given in Table D-9. The reason for this, as before, is that the data in Table D-11 are for an ideal transfer of momentum from the blast wave to the body, while the data in Table D-9 are for the more realistic model of momentum transfer. Obviously the injury criteria given in Table D-11 are unacceptable. Unfortunately the study [D5] using the more realistic model for impact damage does not include a parametric study of nonlethal injury, as it did for death. In order to circumvent this problem, an assumption was made about the relationship between the ideal model and the more realistic model of injury from impact. The more realistic model gives levels of impact for a given percent lethality that are approximately 50 times larger than the levels given by the ideal model for the same percent lethality. It was assumed that the relationship between the ideal and more realistic model would be the same regardless of whether lethal or nonlethal injury was considered. Therefore the impulse levels given in Table D-11 for ideal momentum transfer were multiplied by the same proportionality factor that held for lethal injury levels in order to give the data shown in Table D-12.

Probability of Death (%)	Impulse Level ($N-s/m^2$)
1	18,000
8	28,600
31	37,300
63	45,100
86	49,700
100	60,800

TABLE D9

RELATIONSHIP OF DEATH BY IMPACT TO IMPULSE

Relationship between impact injury and impulse level. Based on results for a surface burst of a one megaton nuclear weapon and a distance to impact of ten feet (3.3 meters).

Injury	Peak over-Pressure-PSI	Impact velocity (meters/sec)	Range in kilometers		
			1 KT	10 KT	100 KT
(PHYSICAL DISPLACEMENT OF MAN WITH IMPACT WITH HARD SURFACE)*					
Mostly safe (whole body)	3–5	3 m/sec	.75	1.8	4.5
Skull fracture threshold	4–6	4 m/sec	.65	1.6	4
Fractured feet and legs	4–6	4.3 m/sec	.6	1.5	3.6
Skull fracture near 50% probability	5–7	5.5 m/sec	.55	1.4	3.5
Lethality threshold (whole body)	6–8	6 m/sec	.52	1.3	3.1
Skull fracture near 100% probability	6–9	7 m/sec	.49	1.2	3
Lethality near 50% probability (whole-body)	7–10	8 m/sec	.45	1.1	2.8
Lethality near 100% probability (whole-body)	8–11	9.1 m/sec	.4	1	2.5

* In 3 meters of travel.

TABLE D10

TENTATIVE CRITERIA FOR PRODUCTION OF INDIRECT BLAST INJURIES WITH RANGES FOR VARIOUS YIELD WEAPONS (FAST RISING, LONG DURATION OVERPRESSURE IN AIR)

Relationship between impact velocity and injury. Taken from reference [D2, p. 9].

Injury	Impulse	
	psi-msec	$\frac{N-s}{m^2}$
Mostly safe (whole body)	41.15	283.8
Fractured feet and legs	58.98	406.8
Lethality threshold (whole body)	82.30	567.6

TABLE D11

CRITERIA FOR NONLETHAL INJURIES FROM IMPACT

Relationship between nonlethal impact injury and impulse, calculated assuming a 155-pound male adult with an effective cross-sectional area of 8 square feet.

Probability of Serious Injury (%)	Impulse ($N\text{-}s/m^2$)
1	13,000
50	20,000
90	28,000

TABLE D12

RELATIONSHIP BETWEEN NONLETHAL INJURIES FROM IMPACT AND IMPULSE

Relationship between percent injury and impulse level based on data for ideal momentum transfer and an assumption of proportionality between the results on the ideal and more realistic impact model.

The probit equation derived from the data in Table D-12 and used to make the damage assessment is given by:

$$\text{Probit} = -39.1 + 4.45 \log_e J \qquad \text{(D-16)}$$

where J is in $N\text{-}S/m^2$.

This concludes the discussion of explosion injury to the vulnerable resource, people.

Explosion Damage to Structures

To begin the discussion of explosion damage to structures, it is worthwhile to raise some important considerations concerning the nature of the interaction between the blast wave and structures. The following two paragraphs are largely based on a discussion given by Kinney ([D6], p. 25ff).

Damage to a structure from blast comes from motion of the structure as imparted by forces of the blast wave. In principle, an analytic solution for structural motion can be obtained from the equation of motion expressing the relation between structural mass, structural acceleration, and the unbalance between the driving force of the blast wave and the resistance of the structure. The driving force is a transient one, given as the product of structure cross-section area and a blast-wave overpressure. The resistance of the structure depends on its mechanical features. However, for dynamic situations, this is seldom known precisely and indeed perhaps is not capable of being known. Furthermore, even if both the transient driving force of the blast wave and the dynamic resistance of the structure were known, the mathematical form of the equation of motion is not conducive to a simple solution, but rather calls for numerical or analogue methods. Hence, only in simpler situations is a precise solution for structural motion in response to blast to be obtained.

As an alternative to an exact solution for structural motion, various empirical estimates of the damage potential of blast have been used. The most common of these is based on the peak overpressure in the free-field blast wave. For example, it may be stated that a peak overpressure of such and such psi causes major structural damage. It should be recognized that such a statement even if correct, can at best be only a crude approximation. It ignores the fact that the damage potential of blast is a function of two individual items, the transient blast loading plus the dynamic response of the structure; two such aspects are always involved in assessment of damage potential.

Since the VM must treat a large number of disparate structures whose mechanical characteristics are probably unknown (possibly difficult or impossible to obtain), it seems prudent to use the less sophisticated approximation involving only a single parameter related to the blast wave. Although details of structural response could be considered eventually, especially for large or important buildings, for now the single level blast wave characterization given by reference [D1] is used.

The damage levels for structures are given in Table D-13. These data are for frame structures subject to a blast from an explosion equivalent to 500 tons of TNT. To obtain the probit equation for glass breakage it was assumed that the 1% level for structual damage corresponds to the 90% level for glass breakage. The probit equations for damage to structures from explosion are thereby obtained. For overall structural damage the probit equation, S1, is given by:

$$\text{Probit} = -23.8 + 2.92 \log_e Pp \qquad \text{(D-17)}$$

and for glass breakage alone the probit equation, S2, is given by:

$$\text{Probit} = -18.1 + 2.79 \log_e Pp \qquad \text{(D-18)}$$

where Pp is in N/m^2.

This concludes the treatment of explosion damage to vulnerable resources.

FIRE DAMAGE

Damage to personnel and damage to property from both flash fire and pool burning are similar enough to be treated together. For both personnel and property, the damage criteria consist of both a thermal radiation factor and a time factor. To cause a certain level of damage, say second-degree burns to bare skin, a thermal radiation level must be exceeded and the radiation must persist for a specified time. In general, as the radiation level becomes higher, the time required to cause a certain level of damage becomes smaller.

Both the flash fire and pool burning models were designed so that the ouput from Phase I is both a radiation level and a duration (time). For the flash fire, since radiation level changes rapidly with time, an effective radiat on level and time are given. Essentially, an equivalent square time pulse of radiation is substituted for the actual time-varying radiation pulse.

For damage to structures, the basic concern is whether ignition occurs. Since surface treatment, geometrical position, and other factors play such an important role in the determination of ignition, the problem is simplified by considering only the ignition of wood. In a classic paper [D7] Lawson and Simms developed two empirical relations for the ignition of wood.

These investigators experimentally determined the intensity of radiation required to ignite wood spontaneously both with and without a pilot flame one-half inch from the surface of the material. The expression relating time for ignition, t, to the critical ignition intensity, I, is the following:

[D7] Lawson, D.I., and D.L. Simms. The ignition of wood by radiation. Brit. J. Appl. Phys. 3:288-292, 1952.

Target	Damage Level	Peak Overpressure	
		psi	(N/m^2)
Frame Structure			
	Threshold Glass Breakage (1%)	0.25	1,700
	Threshold Structure Damage (1%)	0.90	6,200
	50% Structural Damage	3.00	20,700
	Total Damage (99%)	5.00	34,500

TABLE D13

DAMAGE LEVELS FOR SELECTED TARGETS

Relationship between structural damage and peak overpressure. Based on data [D1] for frame structures exposed to a blast from an explosion of 500 tons TNT equivalent yield.

$$(I - I_p)\, t^{2/3} = 0.025 \times 10^6\, (K\rho s + 68 \times 10^{-6}) \qquad \text{(D-19)}$$

where

I = thermal radiation intensity (cal/cm^2/sec)

I_p = critical intensity for pilot ignition (cal/cm^2/sec)

K = thermal conductivity (cal/cm^2/sec/°C)

ρ = density (g/cm^3)

s = specific heat of the material (cal/g/°C)

t = time to ignition (sec)

The corresponding expression for spontaneous ignition was found to be

$$(I - I_p)\, t^{4/5} = 0.05 \times 10^6\, (K\rho s + 35 \times 10^{-6}) \qquad \text{(D-20)}$$

where

I_s = critical intensity for spontaneous ignition (cal/cm^2/sec)

Values of I_p and I_s for various types of wood are given in reference [D7].

Pilot ignition implies the presence of an open flame near the irradiated wood, while spontaneous ignition implies the absence of a nearby flame. In the context of the VM, the flash fire provides a flame nearby the irradiated wood, while pool burning, as a general rule, does not. Thus equation (D-19) was chosen to provide a basis for an ignition criteria in the case of flash fire, while equation (D-20) was used for the case of pool burning. The product of constants $K\rho s$ was chosen to be the average of those materials tested by Lawson and Simms; likewise the critical intensities, I_s and I_p, were taken to be the average for those materials tested. These average values are given by:

$$I_p = 0.32 \text{ cal/cm}^2\text{/sec} = 13{,}400 \text{ Joules/m}^2\text{/sec} \qquad \text{(D-21)}$$

$$I_s = 0.61 \text{ cal/cm}^2\text{/sec} = 25{,}400 \text{ Joules/m}^2\text{/sec} \qquad \text{(D-22)}$$

$$K\rho s = 5 \times 10^{-6} \text{ cal}^2\text{/cm}^5\text{/(°C)}^2\text{/sec} \qquad \text{(D-23)}$$

For these average values, equation (D-19) and (D-20) become respectively,

$$(I - 1.34 \times 10^4 \text{ J/m}^2\text{/s})\, t^{2/3} = 8050 \text{ J/m}^2\text{/s}^{1/3} \qquad \text{(D-24)}$$

and

$$(I - 2.54 \times 10^4 \text{ J/m}^2\text{/s})\, t^{4/5} = 6730 \text{ J/m}^2\text{/s}^{4/5} \qquad \text{(D-25)}$$

From these equations the following criteria for ignition of structures are obtained.

For ignition from flash fire:

1. The vapor concentration at grid cell center must be between the limits of flammability for the spilled substance (this to assure the presence of a pilot flame).

2. The radiation intensity, I_r, must exceed the value

$$I_p = 1.34 \times 10^4 \frac{\text{Joules}}{m^2 - s}$$

3. The effective duration of the radiation, t_{eff}, must exceed the value given by:

$$t_p = \left[\frac{7.22 \times 10^5 \frac{J}{m^2 - s}}{(I_r - I_p)} \right]^{3/2} \qquad \text{(D-26)}$$

i.e.,

If $t_{eff} \geq t_p$ then there is ignition of structures

If $t_{eff} < t_p$ then there is no ignition of structures

For ignition from pool burning:

1. For every grid cell look up the radiation intensity, I_r, at the cell center.

2. The radiation intensity at the cell center must exceed the value,

$$I_s = 2.54 \times 10^4 \frac{\text{Joules}}{m^2 - s}$$

3. The duration of the pool burning, t_b, must exceed the time given by,

$$t_s = \left[\frac{6.10 \times 10}{(I_r - I_s)} \right]^{5/4} \qquad \text{(D-27)}$$

4. If $t_b \geq t_s$ then there is ignition of structures

If $t_b < t_s$ then there is no ignition of structures

where in both cases,

I_r = radiation intensity at the cell center

If these ignition criteria are satisfied at the cell center (flash fire or pool burning), one-fourth of the structures in the cell are assumed to ignite. This assumption was made to account for the fact that some structures will be shielded from thermal radiation by others.

As with inanimate objects, burn damage to people depends on a combination of radiation level and duration. The relation between level and duration has been the subject of considerable attention from the nuclear weapon effects community. In Table D-14, taken from reference [D3], the radiation level required to cause certain damage is given. The thermal radiation is the thermal radiation intensity integrated over time and is parameterized, not by pulse duration, but by weapon yield. For our purposes, we require a thermal radiation intensity level and an effective duration.

A standard reference [D8] provides a formula to calculate the effective duration of the thermal pulse of a nuclear weapon from a knowledge of the yield. By calculating the thermal pulse duration and dividing into the integrated radiation values displayed in Table D-14, the desired data are obtained. Table D-15 gives the critical radiation intensity levels required to cause various levels of damage, for various sizes of weapons. The effective time durations given at the bottom margin of the table are the calculated time durations of the thermal pulse for the weapon size indicated.

From the data in Table D-15, it may be deduced that the effects of thermal radiation are generally proportional to $tI^{4/3}$, where t is the time and I is the radiation intensity. For the 20KT, 1MT, and 20MT bomb data, the critical levels of radiation intensity were converted to MKS units and the dosage, in the quantity $tI^{4/3}$, was calculated. The results thus obtained for lethal levels are presented in Table D-16. From these data the probit equation, Fl, for death from burns in a flash fire is calculated:

$$\text{Probit} = -14.9 + 2.56 \times \log_e(tI^{4/3} \times 10^{-4}) \qquad \text{(D-28)}$$

where t is in seconds and I is in Joules/m^2/sec.

For nonlethal burns, we are interested only in the threshold. Averaging the three values given in Table D-15 for first-degree burns, the criterion obtained by a curve fit is:

$$tI^{1.15} = 550{,}000$$

where I is in Joules/m^2/sec and t is in seconds. A power law of 1.15 fits this data better than the 4/3 power found for the lethal levels. If the value $t_{eff}I^{1.15}$ exceeds 5.5×10^5 then first-degree burns are presumed to occur in those cells where the vapor concentration is within flammable limits at the cell center. Burn deaths from pool burning are assessed by probit equation (D-28) except that actual burning time and radiation level are used instead of effective values as in the case of flash fire.

[D8] Glasstone, S., ed. The effects of nuclear weapons, p. 357 ff., USAEC, April 1962.

Critical event	Thermal radiation in cal/cm^2 for indicated explosive yield				
	20 kt	100 kt	1 Mt	10 Mt	20 Mt
First degree burn	2.5		3		4
Second degree burn	4.5	5	6.5	9	10
Lightly clothed (summer)					
Few if any injuries	2.5		3		4
Significant injury threshold	4	4.5	6	8.5	9.5
Lethality					
Threshold	5	6.0	8	10.0	11
Near 50 per cent	9	11.0	14	18.0	20
Near 100 per cent	20	24	31	40	43
Burns due to hot debris and hot, dust-laden air.			No biological criteria available, but probably a serious problem for large-yield explosions.		

TABLE D14

TENTATIVE BIOMEDICAL CRITERIA FOR THERMAL RADIATION

Relationship between biological damage and thermal radiation. This data [D3] is for thermal pulses from nuclear weapons; thermal radiation the time integral of the radiation intensity.

	20 KT	100 KT	1 MT	10 MT	20 MT
1st degree burn	1.75		.297		.0886
2nd degree burn	3.14	1.56	.643	.281	.221
Slightly clothed (summer) few if any injuries	1.75		.297		.0886
Significant injury threshold	2.80	1.405	.594	.266	.210
Lethality					
Threshold	3.50	1.875	.792	.312	.243
Near 50%	6.30	3.44	1.385	.563	.442
Near 100%	14.0	7.5	3.07	1.25	.952
Effective Time Duration(s)	1.43	3.20	10.1	32.0	45.2

TABLE D15

CRITICAL RADIATION INTENSITY LEVELS AND DURATIONS REQUIRED FOR CERTAIN TYPES OF INJURY

[Thermal radiation intensity in $\frac{cal}{cm^2-s}$]

Relationship between thermal injury and the radiation intensity and duration. Based on the data given in Table D14.

Portion Killed (%)	Duration (sec)	Radiation Intensity		Dosage $tI^{4/3}$
		($cal/cm^2/sec$)	($Joules/m^2 sec$)	
1	1.43	3.50	146,000	1099×10^4
1	10.1	.792	33,100	1073×10^4
1	45.2	.243	10,200	1000×10^4
50	1.43	6.30	263,600	2417×10^4
50	10.1	1.385	57,950	2264×10^4
50	45.2	.442	18,500	2210×10^4
99	1.43	14.0	586,000	7008×10^4
99	10.1	3.07	128,000	6546×10^4
99	45.2	.952	39,800	6149×10^4

TABLE D16

RELATIONSHIP OF DEATH FROM RADIATION BURNS TO RADIATION LEVEL AND DURATION

Based on data in Table D15. The sequence of data is for 20KT, 1MT, and 20MT weapons. The dosage has been calculated for the radiation intensity in Joules/m^2/sec.

APPENDIX E

INHALATION TOXICOLOGY OF CHLORINE AND AMMONIA

Emphasis has been placed on human inhalation toxicology of chlorine and ammonia since these are clearly the most significant toxic hazards of the five substances of immediate concern in the VM. A full treatment would consider also:

- Human inhalation toxicology of LNG, methanol, gasoline, and combustion products
- Human ingestion toxicology of all five materials
- Effects on other land fauna, and on flora
- Effects on aquatic biota
- Impairment of beneficial water uses in general.

Some data and comments on these are summarized at the end of this section.

General

The Vulnerability Model translates concentration/time histories or cumulative doses into percent response of an exposed population in each grid cell. These are then converted into estimated numbers of casualties by using population numbers in each cell. The basic response data are for unprotected healthy adults in the open. The question of high risk populations - very young, very old, sick - is dealt with in a later section. Reduction of hazard by physical protection, e.g., in closed buildings with recirculated air, is not a toxicological problem but a matter of applying a proportionality factor to calculated open-air exposures.

Levels of Response

Response to increasing exposure ranges from threshold odor and irritation to death. Sublethal effects must be considered. The most drastic of these may involve permanent or long-term impairment, but transient effects are likely to be more important. They may cause temporary incapacitation and even if there is no actual harm, harm may be imagined. The number of people exposed to "threshold" effects is likely to be many more than those experiencing dangerous exposure.

Examination of the toxicological effects of chlorine and ammonia suggests three basic levels for consideration: (1) odor, (2) respiratory and eye irritation, and (3) death. These correspond to three levels of public receptor response: awareness of abnormal environment, possibly eliciting complaint; actual harassment and temporary incapacitation, leading to complaint and perhaps some real harm; and death. The toxicological properties of chlorine and ammonia are such that long-term impairment is likely to be

significant only in aggravation of pre-existing conditions such as chronic respiratory disease. This does not mean that there will be no long-term effects, but that they will be minor relative to the total consequences: see the following section.

Long-Term Effects

The question of permanent harm was considered, with particular reference to chlorine. Should we include this category of effect, between the categories of temporary hospitalization and death? A search of the literature relating particularly to World War I and to major accidental spills, and discussion with two eminently qualified toxicologists [E1, E2], substantiated the view that the relative importance of this category was low enough to justify ignoring it: i.e., the percentage of permanent casualties would be very small.

The most recent paper seen was Weill et al. [E3]. They say that their data for subjects seven years after an accidental exposure to chlorine "are consistent with the prevailing clinical view that significant permanent lung damage does not result from acute exposure to chlorine gas." Reports referenced in their paper support this finding: for example, "no evidence that chlorine intoxication produced residual pulmonary disease" in the 33 most severely affected victims of a major accident; a large survey of industrial exposures did not find "any evidence of permanent damage to the respiratory tract"; another study including war casualties found that "permanent pulmonary injury was rare." The common belief in extensive permanent disability is apparently based on World War I gas casualties, but Vedder, in The Medical Aspects of Chemical Warfare [E4], presents the view that a strong bias is introduced by the incentive of permanent pensionable status, and says that "very few individuals have any pathological basis for symptoms more than a year after even the most severe gassing" and most recoveries are very much earlier.

There are a few reports of effects other than pulmonary, more than a year after exposure: these include cardiac irregularity and anxiety reactions, but the percentage vs. total casualties is low.

Our conclusion is that the incidence of permanent effects is certainly low and probably negligible in the context of the VM study; this is more evidently true for pulmonary effects than for other effects which have received less attention. This conclusion applies here only to chlorine and to ammonia, the effects of which are essentially acute and short-term.

[E1] Kramer, C. G. Personal communication, 1974.
[E2] Wands, Ralph M. Personal communication, 1974.
[E3] Weill, H., G.M. Schwarz, and M. Ziskind. Late evaluation of pulmonary function after acute exposure to chlorine gas. Am. Rev. Resp. Dis. 99:374-379, 1969.
[E4] Vedder, E.B. The Medical Aspects of Chemical Warfare. Williams and Wilkins Co., Baltimore, 1925.

The Significance of Concentration and Dosage

In inhalation toxicology the following variables are important:

	Usual Units	Symbols
Concentration of toxic gas (a) Peak (b) Average	mg m^{-3} or ppm	C
Time of exposure	min	t
Breathing rate ("respiratory minute volume")	liter min^{-1}	
Retention of inhaled material	%	
Dosage	mg min m^{-3}	Ct
Dosage lethal for 50% of those exposed	"	LCt_{50}

Note the special usage of the term "dosage" for the product of concentration and time. It is not to be confused with "dose", which is the amount actually retained and depends on the breathing rate and percent retention. Dosage is the same for all subjects exposed to the same cloud, no matter whether they breathe fast or slow, or put on gas masks.

In the VM development we are concerned with both concentration and dosage. For example, men exposed to a concentration of 150 ppm of ammonia lacrimate immediately and continue to do so until removed to clean air, but do not risk other effects. Exposed to 15 ppm of chlorine they similarly experience immediate harassment, but in this case there is also a cumulative effect and after an hour or so at this concentration it is likely that some will die: i.e., we are concerned with the dosage (concentration times time) as well as the level of concentration. At a higher concentration, deaths occur after shorter exposure. Haber's law, $Ct = k$, is widely applicable to toxic gases but unfortunately not to chlorine over a wide range of concentration. The reason is that chlorine attacks by two mechanisms: immediate respiratory spasm from intense irritation, and delayed (ca. 24 hours) effects from oxidative and other destructive effects on lung tissue: the first effect is a function of concentration and the second of dosage. Hence, as concentration increases the acute effect becomes more important and progressively dominates the other: that is to say, the 50% lethal dosage (LCt_{50}) decreases.

High Risk Populations

There is no doubt that dose response estimates based on healthy adults will underestimate the sensitivity of certain sectors of the population,

notably the very young, old and sick. Kramer [E5] has commented on this in relation to chlorine, and it is interesting to note that the one death among 100 treated casualties in the 1961 Louisiana chlorine spill was an 11-month old infant [E6]. (Older siblings who were similarly exposed did not die.) The problem in attempting to assign appropriate factors is that there are virtually no sound data. Such indications as we have, come from accidents like the one just mentioned, in which there are of course no measurements of the degree of exposure. And extrapolation from animal experiments, always a questionable matter, is even less trustworthy in modeling groups such as human infants or advanced emphysema patients.

The problem was discussed with Kramer (see footnote [E1]) who confirmed the absence of data but said that in-plant experience was that subjects with well-established bronchitis/emphysema are "much more sensitive" to chlorine. He remarked that the 7-8 ppm region of chlorine concentration is a critical one in which exposure may be tolerated with lasting harm, especially in susceptible subjects: i.e., the concentration is not above the level of tolerance, but after some time the cumulative dosage (and the retained dose) may hospitalize the subjects with pulmonary edema, etc.

We suggest that high risk populations be defined as (a) infants, (b) those over 70 years, and (c) others with advanced pulmonary/cardiovascular disease (as defined by some acceptable medical criterion, not yet established). These groups should be aggregated. A proposed scaling, which we have applied to specific concentrations and exposure times for chlorine and ammonia, is:

	Deaths, %	
Level of Effect	General Population	High Risk Population
Severe harrassment with some risk	0	25
Lethal	3	50
Lethal	50	100

We recognize that these are guesses and probably on the high side, but it seems better to be pessimistic about the effects than to ignore an augmenting factor which certainly exists and may be substantial.

Estimating Dose Response Relationships for the VM

Most of the published work with toxic vapors is directed towards establishing response levels rather than dose response regression equations: e.g., odor and irritation thresholds, maximum acceptable concentrations, and exposures that are "dangerous" or "lethal". Experiments are often reported this way: e.g., in an ammonia inhalation experiment, volunteers were "all

---

[E5] Kramer, C.G. Chlorine. J. Occup. Med. 9:193-196, 1967.
[E6] Joyner, R.E., and E.G. Durel. Accidental liquid chlorine spill in a rural community. J. Occup. Med. 4:152-154, 1962.

of the opinion that no person would remain in such an atmosphere..." There are limited data on volunteers exposed to controlled concentrations to determine odor and irritation thresholds, but none, of course, on dangerous and lethal exposures. Available data for humans are therefore estimates, based on extrapolations and accidents, plus the few low-level laboratory data.

The need in the VM is for dose response models which can translate exposure into percent effects in the exposed population. Our approach to estimating data which are experimentally unavailable is as follows:

Dose response data for lethality of chlorine were taken from four experiments with mice [E7], two with rats [E8], and one with dogs [E9]. These are plotted on Figure E1. Dose response data for nose and throat irritation by ammonia in man are also plotted [E10]. It is the slopes that interest us, because we want to use these data to help us estimate percent response at various dosage levels from estimates at one particular level, and it will be seen that the chlorine dose-response lines have similar slopes and the ammonia slopes are not greatly different. (Dose units are not shown and the lines are arbitrarily placed with respect to the dose axis, because we are not interested in, for example, the actual dose which kills a mouse; it is the slope we are using.) Slopes were averaged and composite lines for chlorine lethality and ammonia irritation were drawn, passing for convenience through the intersect of 50% response and unit dose. The relative doses for 90% response, vs. unit dose and 50% response, are 1.54 for chlorine and 1.78 for ammonia. These figures differ by only 0.12 or 7% from their average of 1.66. The similarity of dose response for different subjects, concentrations and effects suggests that we may justifiably use the composite chlorine lethality line, for example, to estimate dosages for various lethality rates in man from a published estimate of the 50% lethal dosage.

This proves to be not inconsistent with the estimates of "dangerous" and "lethal" exposures to chlorine in the National Academy of Sciences Guide for Short-Term Exposure [E11]:

Dangerous exposure is given as 14 to 21 ppm, 1/2 to 1 hour.
The corresponding dosage = $\frac{14 + 21}{2} \times \frac{0.5 + 1}{2}$ = 13 ppm-hr

Lethal exposure is given as 34 to 51 ppm, 1 to 1-1/2 hour.
The corresponding dosage = $\frac{34 + 51}{2} \times \frac{1 + 1.5}{2}$ = 53 ppm-hr

---

[E7] Weedon, R. F., et al. Toxicity of ammonia, chlorine, hydrogen cyanide, hydrogen sulfide and sulfur dioxide. Contr. Boyce Thompson Inst. II, p. 365ff., 1940.

[E8] Silver, S.D., and F.P. McGrath. Chlorine median lethal concentration for mice. DATR 351, Edgewood Arsenal, Md., May 9, 1942.

[E9] Silver, S.D. et al. Chlorine median lethal concentration for mice. DATR 373, Edgewood Arsenal, Md., July 17, 1942.

[E10] American Conference of Governmental Industrial Hygienists. Documentation of threshold limit values for substances in workroom air, 3rd ed. ACGIH, Cincinnati, Ohio, 1971.

[E11] National Academy of Sciences - National Research Council, Committee on Toxicology. Guides for short-term exposures of the public to air pollutants. VIII: Guide for chlorine. NAS-NRC, Washington, March 1973.

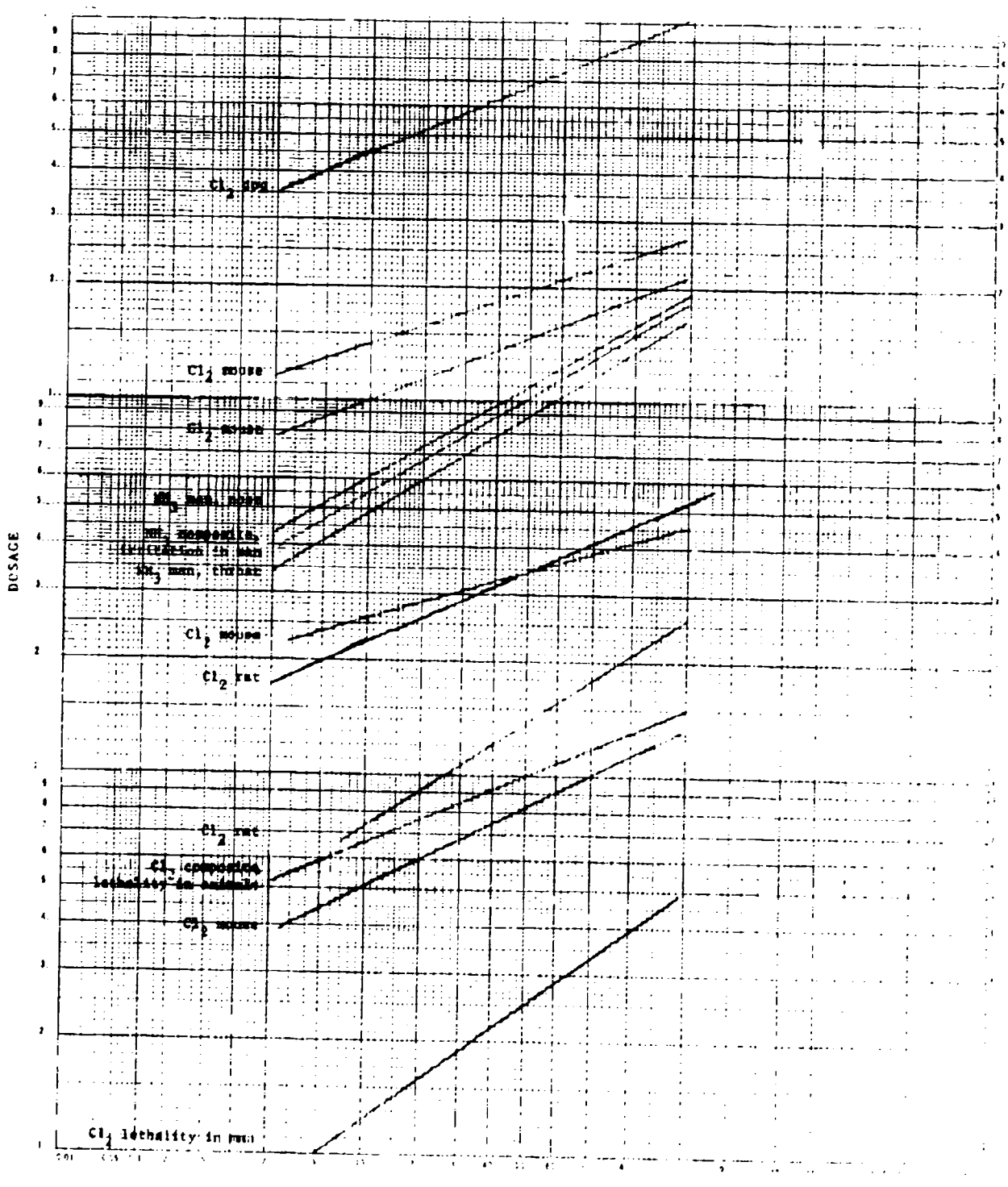

RESPONSE, %

FIGURE E-1. Dose Response Data

If we assume that "dangerous" means 5/100 dead and "lethal" means 90/100 dead, we get the chlorine lethality line of Figure E1 (the line at the extreme left) which agrees very tolerably with the animal data.

Notes on Toxicology

Some notes are collected here which are relevant to chlorine and ammonia in the context of the VM. Data are from the NAS-NRC reports (see footnote [E11] and) [E12].

Chlorine

TLV (Threshold Limit Value - this is the upper limit for regular and indefinitely continued occupational exposure established by the American Conference of Governmental Industrial Hygienists: ACGIH, 1971.)

1 ppm time-weighted average for 8-hr working day

3 ppm permissible excursion for 15 min.

STPL (Short Term Public Exposure Limit - mild odor, minimal irritation, no health hazard.)

1 ppm for 10 min.

0.5 ppm for 30 min.

0.5 ppm for 60 min.

PEL (Public Emergency Limit - strong odor, some irritation; these are ceilings, not averages.)

3 ppm for 10 min.

2 ppm for 30 min.

2 ppm for 60 min.

EEL (Emergency Exposure Limit - proposed by Zielhuis [E13], for chlorine in manufacturing areas, transport and storage.)

7 ppm for 5 min.

5 ppm for 15 min.

4 ppm for 30 min.

3 ppm for 60 min.

[E12] National Academy of Sciences - National Research Council, Committee on Toxicology. Guides for short-term exposure of the public to air pollutants. IV: Guide for ammonia. NAS-NRC, Washington, November 1972.

[E13] Zielhuis, R.L. Tentative emergency exposure limits for sulfur dioxide, sulfuric acid, chlorine, and phosgene. Ann. Occup. Hyg. 13:171-176, 1970.

Ammonia

TLV 25 ppm

Occupational ceiling (recommended) 50 ppm

Odor Reported threshold 5 ppm to 50 ppm: lower value is probably correct for near 100% detection, upper limit for 100% in all circumstances.

100-500 ppm Irritant but tolerable. 100 ppm for 8-hour working day causes irritation but no adverse effect. This is the generally accepted threshold of tolerance and in one experiment all agreed 140-200 ppm was not willingly tolerable; however, in another experiment volunteers inhaled 500 ppm/30 min.

400-700 ppm Strongly irritant, but infrequent brief (1 hour) exposure has no serious effect.

2000-3000 ppm Convulsive coughing, very irritant, may be fatal; no permissible minimal time.

Over 2500 ppm (2500-6500) Dangerous in 1/2 hour.

5000-10,000 ppm Rapidly fatal.

Long industrial experience indicates no permanent injury from lifetime working exposure below the level of intolerable acute effects.

STPL

20 ppm for 10 min.
10 ppm for 30 min.
10 ppm for 60 min.

(Note however that odor is objectionable to many, who may complain at <u>any</u> exposure, however brief, above their threshold of olfactory perception.)

PEL

100 ppm for 10 min.

75 ppm for 30 min.

50 ppm for 60 min.

Interpretation of Data and Selection of Levels of Exposure/Effect

There are two problems:

- Estimates of hazardous/lethal exposures for man are necessarily guesstimates, based on animal experiments, non-hazardous exposures on man, and non-quantitative accidents.

- With these highly irritant gases the immediate effect of concentration contributes largely and may dominate the cumulative effect of dosage. Hence one cannot, for example, use a constant value the 50% lethal dosage outside a limited time (or concentration) range.

The following dosage-response estimates were used.

Chlorine

Concentration	Time	Effect
3 ppm	Any	No risk, but public complaints with some harassment (NAS Public Exposure Limit for 10 min. is 3 ppm)
7 ppm	1 hour or more	Strong to intolerable irritation, with some risk to highly susceptible subjects only
20 ppm	Several hours	50% lethal (our estimate, based on the following 1 hour figure)
33 ppm	ca. 1 hour	50% lethal (based on the figures in the NAS-NRC report referred to in footnote [E11])
60 ppm	ca. 10 minutes	50% lethal (our estimate)

Ammonia

Concentration	Time	Effect
20 ppm	Any	Odor detected by majority of population
100 ppm	Any	Irritation and complaint
500 ppm	Any	Strong to intolerable irritation, with risk to high susceptible individuals
2500 ppm to 5000 ppm		Fatalities mostly from a few in the first 5 minutes to 90% to 100% after 1 hour, depending on concentration
Above 5000 ppm		100% fatal. Heavy casualties in 5-10 minutes, and shorter exposures are unlikely in practice (Neither short time of cloud passage nor effort to escape is likely to reduce casualties much below 100% at these concentrations)

Dose response figures for irritation in man are available but seem of doubtful value: (1) the levels for odor/irritation are for majority of exposed population and there is not much benefit in estimating 25%, 50% etc. intolerably irritated; (2) the estimated effect at 2500-5000 ppm in fact corresponds roughly with slope estimates; (3) the heavy casualty level is not subject to reduction, for reasons given above in the table.

A Note on Medical Treatment

It has been suggested that a complete VM could take account of medical treatment. This does not appear necessary for the particular cases of inhalation effects of chlorine and ammonia, though it certainly will be in other areas. The reason is that the consequences of exposure are largely determined during the exposure and not too much can be done except for shock, coma, and respiratory arrest. For other patients, rest (perhaps with sedation) and oxygen are helpful. For chlorine especially, intermittent positive pressure oxygen has been recommended; also, cough suppressants and bronchodilators. But it seems, on the whole, that if a patient is going to die or be hospitalized, his fate is pretty well settled at the termination of exposure. Medical treatment will do some good and medical ethics demand utmost effort -- but in terms of VM casualty estimates, the difference is likely to be insignificant.

Note incidentally that references here to lethality are not limited to death during the specified exposure but include later death, usually quite early (though there may be a small proportion after several weeks).

Notes on Other Topics

Human Toxicity by Inhalation of LNG, Methanol, and Gasoline

The American Conference of Governmental Industrial Hygienists (see footnote [E10]) classes methane and related aliphatic hydrocarbons among the "simple asphyxiant, non-toxic" gases. (Pentane is given a TLV of 500 ppm, being slightly narcotic; however, the fatal concentration is estimated as 130,000 ppm.) We conclude that LNG is non-toxic in the context of the VM. However, consideration should be given to the risk of asphyxiation in high concentrations of LNG vapor.

Methanol is given a TLV of 200 ppm by the ACGIH (see footnote [E10]), indicating a low level of toxic risk. It has been left aside for immediate purposes but should be reconsidered to determine the risk that high concentrations could result in (a) a toxic dose, based on known figures for toxicity by ingestion, or (b) in asphyxia.

Gasoline presents a problem, because its toxic properties depend mainly on the aromatic hydrocarbon content, which is widely variable. Since the toxicity is not high, and no sound way is apparent for estimating a representative value, it has been set aside for the present.

Combustion products of the above substances and of ammonia: it appears likely that a combustion source generating a large amount of a toxic product such as carbon monoxide would at the same time generate so much heat - and hence convective turbulence - as to dilute the product below hazard level outside the fire hazard zone. This intuitive conclusion might be reexamined in any future work.

Human Toxicity (Ingestion)

Some toxicity figures are available, but we have not considered this problem because it is unlikely in the VM context that a large number of people would be exposed to this danger. The circumstances in which a large number of persons would swallow the material, or water contaminated by it, are not easily imagined. Nevertheless some group of people, possibly uninvolved bystanders, might be exposed to a significant danger. Therefore further study is recommended to model the potential hazard of polluted waters, so that controls on water usage, both commercial and recreational, may be scientifically formulated.

Effects on Other Land Fauna

For large animals the lethality figures for men should be good enough if estimates of economic damage are to be developed later.

Effects on Land Flora

The level of "irritation" in man appears to approximate to the level of visible damage in more sensitive plants, with some risk of economic damage.

Effects on Aquatic Biota

The range is so wide, and the biota at risk in specific places so varied, that "damage" level is not treated at present in the VM.

Impairment of Beneficial Water Uses

These seem to fall outside the scope of the model. For a specific site the VM could be used to generate an "exposure history" for specific municipal/industrial intakes, from which a "damage" could be estimated: this might often be a simple economic estimate of the cost of shutting down while acceptable intake limits were exceeded.

APPENDIX E. INHALATION TOXICOLOGY OF CHLORINE AND AMMONIA

List of References

[E1] Kramer, C. G. Personal communication, 1974.

[E2] Wands, Ralph M. Personal communication, 1974.

[E3] Weill, H., G. M. Schwarz, and M. Ziskind, Late evaluation of pulmonary function after acute exposure to chlorine gas, Am. Rev. Resp. Dis. 99:374-379, 1969.

[E4] Vedder, E. G. The Medical Aspects of Chemical Warfare. Williams and Wilkins Co., Baltimore, 1925.

[E5] Kramer, C. G. Chlorine. J. Occup. Med. 9:193-196, 1967.

[E6] Joyner, R. E., and E. G. Durel. Accidental liquid chlorine spill in a rural community. J. Occup. Med. 4:152-154, 1962.

[E7] Weedon, R. F., et al. Toxicity of ammonia, chlorine, hydrogen cyanide, hydrogen sulfide and sulfur dioxide. Contr. Boyce Thompson Inst. II, p. 365ff., 1940.

[E8] Silver, S. D., and F. P. McGrath, Chlorine median lethal concentration for mice. DATR 351, Edgewood Arsenal, Md., May 9, 1942.

[E9] Silver, S. D., et al. Chlorine median lethal concentration for mice. DATR 373, Edgewood Arsenal, Md., July 17, 1942.

[E10] American Conference of Governmental Industrial Hygienists Documentation of threshold limit values for substances in workroom air, 3rd ed. ACGIH, Cincinnati, Ohio, 1971.

[E11] National Academy of Sciences-National Research Council, Committee on Toxicology. Guides for short-term exposures of the public to air pollutants. VIII: Guide for chlorine. NAS-NRC, Washington, March 1973.

[E12] National Academy of Sciences-National Research Council, Committee on Toxicology. Guides for short-term exposure of the public to air pollutants. IV: Guide for ammonia. NAS-NRC, Washington, November 1972.

[E13] Zielhuis, R. L. Tentative emergency exposure limits for sulfur dioxide, sulfuric acid, chlorine, and phosgene. Ann. Occup. Hyg. 13:171-176, 1970.

APPENDIX F

CASE STUDIES

This Appendix presents fourteen case studies of actual vapor cloud fires and explosions, to provide back-up detail for the generalization highlighted in Chapter 9. The cases illustrate three different kinds of events:

- Explosion of an open-air cloud.
- Explosive rupture of a pressurized tank, followed by a fireball.
- Fireballs without blasts.

Each kind of event poses its own special problems and hazards.

The fourteen cases are drawn from a larger pool of known and studied accidents, but they include all those which were reported in sufficient detail to be instructive. The cases which were excluded would add little to the picture.

Since this study was directed toward unpublished case studies, a large number of the sources are perforce private communications; but references to published reports are also given wherever possible. Some of the unpublished cases, notably Cases F.1 and F.3, will enter the literature when investigations still going on at this writing are completed.

F.1 CYCLOHEXANE CLOUD EXPLOSION
FLIXBOROUGH, ENGLAND - 1 June 1974

On 1 June 1974, the Nypro caprolactam plant near Flixborough, England, suffered a rupture of a 28-inch diameter pipe carrying cyclohexane at a temperature of 145°C and a pressure of 120 psi. The hot liquid poured out through both 28-inch diameter ends and flashed into a mixture of vapor and mist. 50 to 60 tons of cyclohexane were lost, and it is estimated that about 1/4 of that (15 tons) formed a white, vapor-mist cloud about 50 feet thick and many hundreds of feet in diameter. Another estimate indicated 30 tons in a cloud of about 100 meters in radius and occupying a volume of at least a million cubic feet.

The wind was about 18 knots from the southwest, and it distorted the cloud into the approximate shape shown in the following figures. The cloud boundaries shown were deduced from observed carbonization, melting and soot formation, and from the results of jet flow calculations.

Ignition occured after a delay of approximately 54 seconds, probably at the reformer furnace of the hydrogen plant; and a massive explosion resulted. Most of the explosion appeared to have been a deflagration, but it is felt that a kernel of gas about 7 meters in radius and containing about 1.4 tons of cyclohexane detonated with the force of about 15 tons of TNT. Both the fact of detonation and the size of the kernel are deduced from the degree of damage observed.

The blast was devastating. Processing units, main pipe racks, tanks and operating buildings in the cyclohexane caprolactam area were totally destroyed. Towers were blown down, twisted, crushed or bent over into piles of rubbish. Pipe racks were blown off their foundations for their full lengths and toppled over. Buildings, including two-story, reinforced concrete buildings, were crushed into piles of rubble. Exposed steel supports of the pipe racks were shifted five to ten feet off their foundations. Large vessels, towers, etc., appeared to be crushed from the top "as though some giant hand

had smashed them". There were also raging fires from liquid spillage on the northeast side of the area, but most of the damage appears to have been done by the blasts. Damage estimates exceed $100,000,000.

Twenty-nine people were killed, most of them in the plant control room which was completely demolished. Reports available at this writing do not specify what actually killed them, but it appears that either the blast or the fireball would have been sufficient. One early, private report said that there was no eardrum damage, which would imply overpressures of less than about 6 to 12 psi and suggest fire deaths; but such a low overpressure seems inconsistent with the observed structural damage in the area, and the report needs confirmation.

Damage to neighboring structures was much less severe, and less severe than early newspaper accounts indicated. An on-site observer reported that there was damage to tile roofs, and that windows were broken in the village of Flixborough, about 1/2 to 3/4 mile to the west atop a hill but out of the line of sight from the plant; but that "the damage was not what is normally called 'severe'". Five or six dwellings in a row about half way between Flixborough and the plant had heavy damage to windows, doors and tile roofs; but their walls were all intact. Window breakage was reported up to eight miles from the plant.

The overpressure in the center of the blast has been estimated at approximately 25 - 30 psi by scaling from the observed damage patterns. The overpressure gradient was also estimated from the same observations, and the corresponding circular isobars are shown on one of the following figures. The same damage patterns were used to locate the apparent epicenter of the blast, to conclude that part of it was a detonation, and for one estimate of the cloud size and shape.

This accident is still under intensive investigation at this writing (December 1974); and there will ultimately be a very detailed report. There even appears to be a movie of the initial pipe break, cloud formation and explosion - made by an amateur who just happened to be filming the scene. Pending the complete, documented report, all conclusions should be tentative.

Sources:

1. *Chemical & Engineering News*, 10 June 74, page 4.
2. Testimony of Professor Sir Fredrick Warner, of Cremer and Warner, Consulting Engineers, at the court inquiry into the accident.
3. Several private communications and confidential memos which were shared in the interests of safety but "not for attribution because still preliminary".

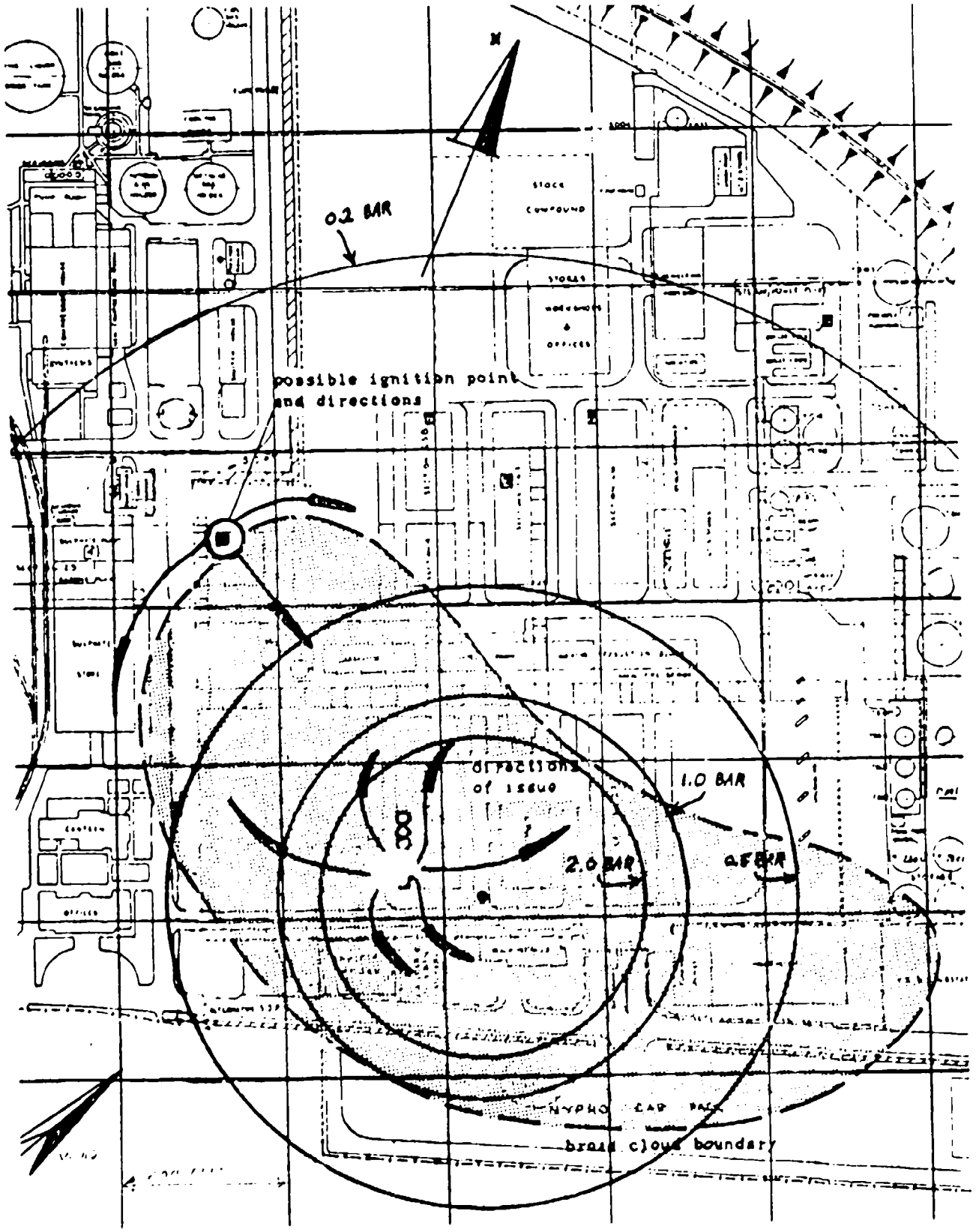
0.2 BAR
possible ignition point
and directions
directions
of issue
1.0 BAR
2.0 BAR
0.5 BAR
broad cloud boundary

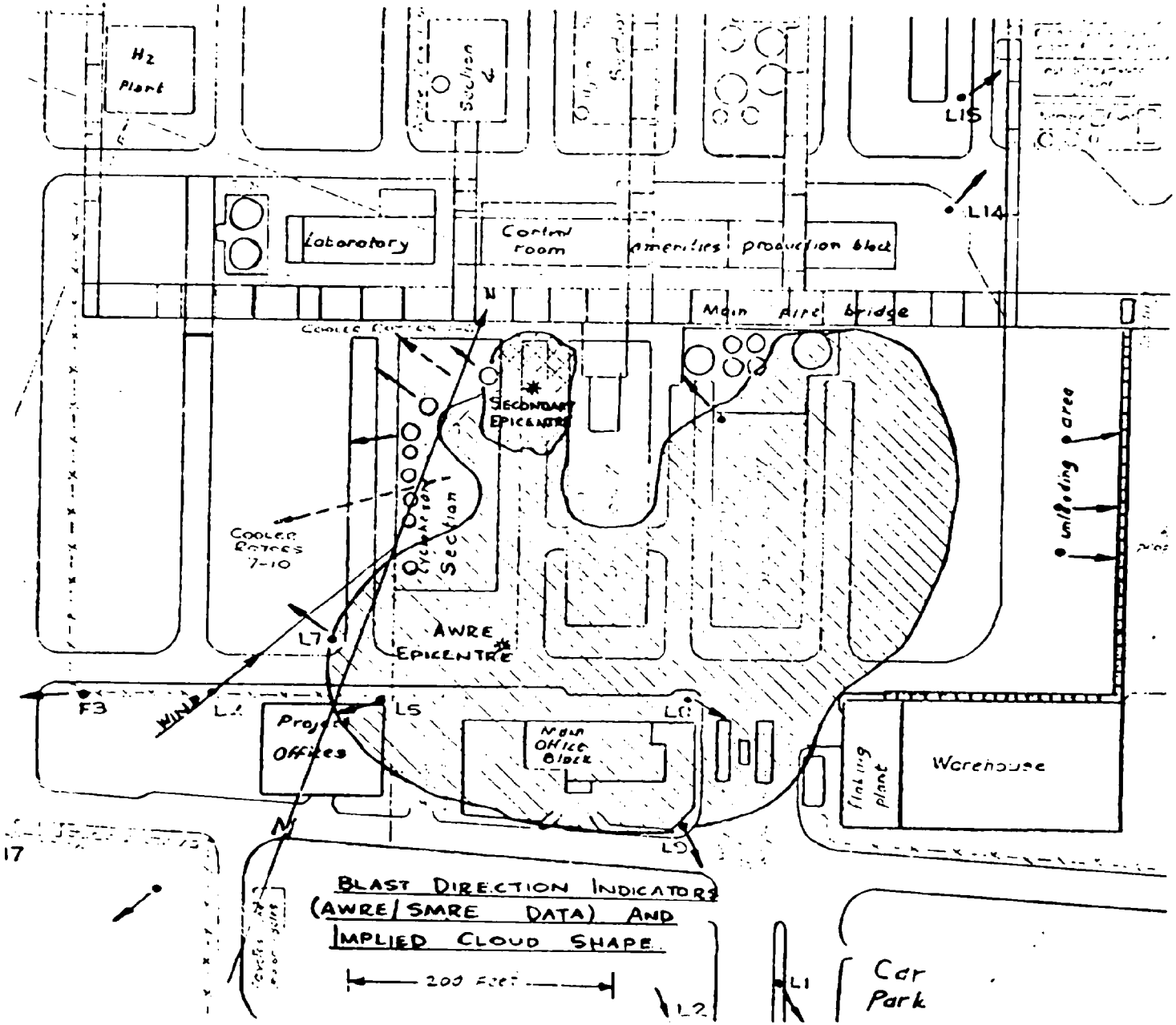
H2 Plant
Laboratory
Control room
amenities
production block
Main Fire bridge
L15
L14
Cooler Boxes
SECONDARY EPICENTRE
Cooler Boxes 7-10
AWRE EPICENTRE
L7
F3
WIND
L4
L5
L6
Project Offices
Main Office Block
Warehouse
Flashing plant
N
L3
17
BLAST DIRECTION INDICATORS (AWRE/SMRE DATA) AND IMPLIED CLOUD SHAPE
200 FEET
L2
L1
Car Park

A CYCLOHEXANE CLOUD WHICH DID NOT IGNITE

The Flixborough disaster is illuminated somewhat by a closely similar spill on 11 Sep 1971 at a caprolactam plant in Pensacola, Florida, which however did not ignite.

As at Flixborough, a pipe rupture released a massive amount of cyclohexane under pressure and above its boiling point in the midst of a large industrial complex. In this case, 74,000 pounds of cyclohexane were released; and "a sizeable amount" is thought to have flashed into vapor, with the rest mostly ending up as mist. It formed a dense, white cloud estimated at over 100 feet high by reference to taller equipment and approximately 2000 feet across at its maximum. The wind was "about at a dead calm" at the time of the rupture, and it "picked up to a very slight breeze from the southwest" during the event. The attached map shows a sketch of the size and shape of the cloud.

The cloud was rich enough that two trucks stalled in it from lack of oxygen. Some of it was drawn into a power house furnace, causing the stack to emit thick, black smoke. Amazingly, the cloud never did ignite; and eventually it dissipated harmlessly.

The attached sketch map shows the growth of the cloud. The area was a typical, densely built, chemical complex, with both open and closed operating areas, pipe racks, distillation towers, storage tanks, and the like very much like the complex at Flixborough, and with a gridwork of roads lacing it in both directions. Only a few of the buildings are shown on the map to give an idea of scale; there was essentially no unoccupied space in the area.

Source: Private communication from Walter B. Howard, Monsanto Company.

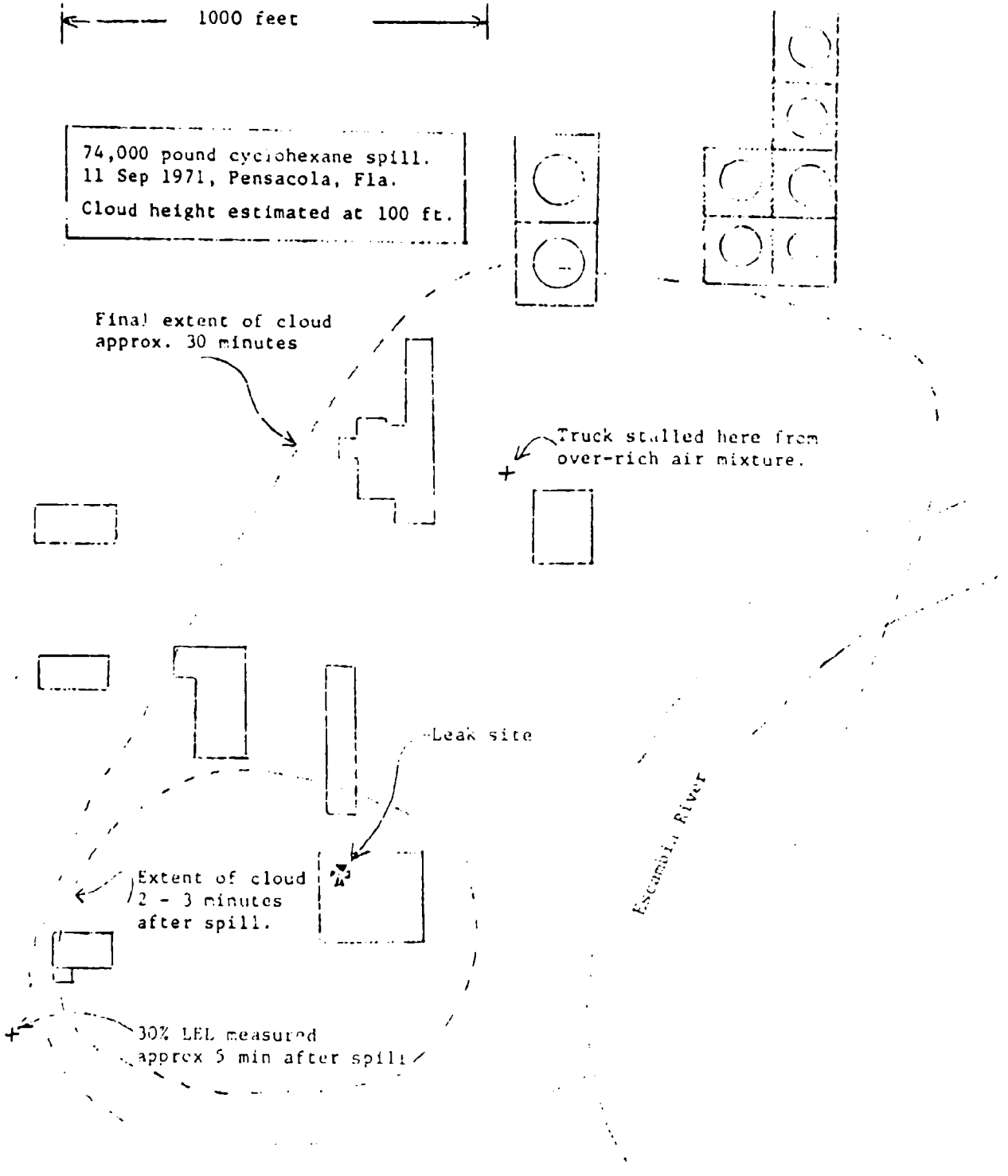
1000 feet
74,000 pound cyclohexane spill.
11 Sep 1971, Pensacola, Fla.
Cloud height estimated at 100 ft.
Final extent of cloud
approx. 30 minutes
Truck stalled here from
over-rich air mixture.
Leak site
Extent of cloud
2 - 3 minutes
after spill.
30% LEL measured
approx 5 min after spill
Escambia River

F.2 ETHYLENE CLOUD EXPLOSION
LONGVIEW, TEXAS - 25 February 1971

On 25 February 1971, a 1/2-inch pipe carrying high pressure ethylene gas broke in an industrial complex near Longview, Texas, releasing an estimated 1000 pounds of ethylene. The resulting cloud found an ignition source and exploded, breaking numerous other pipes and releasing many thousands of pounds of fresh ethylene which then formed a much larger cloud. The larger cloud apparently suffocated a gas-driven compressor and was itself ignited. The second explosion "shook the earth". It killed four people in the immediate area and hospitalized 60 others. Fires, mostly liquid fed, raged for two and a half hours; and the ultimate damage reached $14,000,000.

Damage was mostly confined to the industrial complex itself, and the majority of it was within 1800 feet of the blast center. A few windows were broken in the city of Longview, five miles away; but the pattern of window breakage was very erratic - a house 1-1/2 miles away was untouched. The documented damage is indicated on the following sketch map and explained in the accompanying detail notes.

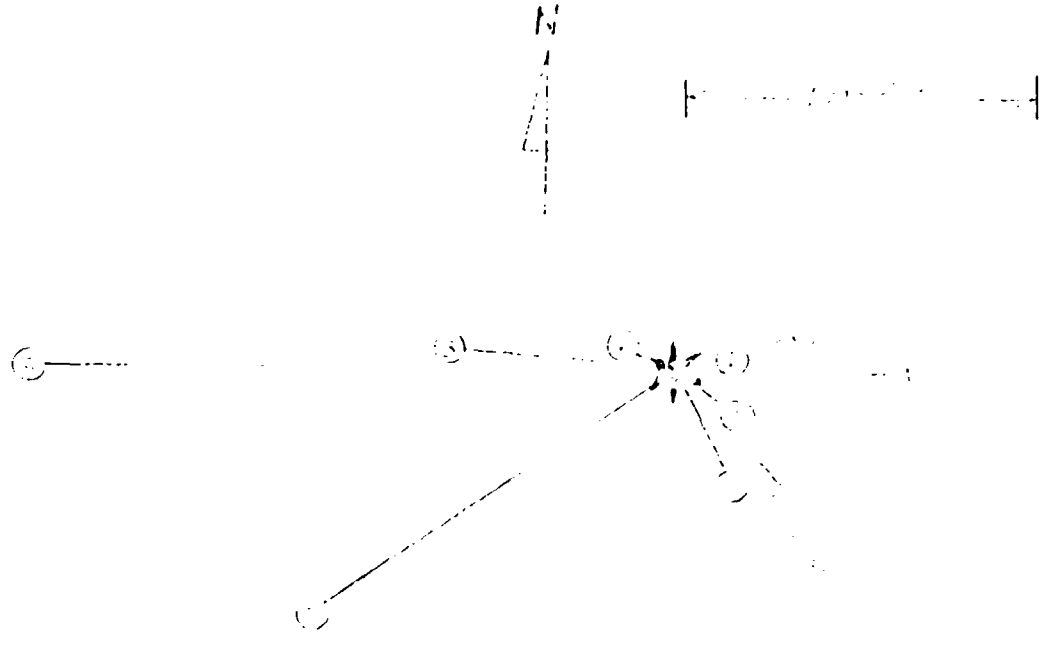

DAMAGE NOTES:

Blast site - Completely demolished, but personnel were found alive behind control panels and in other protected places. Overpressure estimated at 15 psi, based on observed damage to equipment.

A - Warehouse 600 feet east. Building was 150' wide by 500' long. The sheet metal roof was buckled inward but not fallen. The 14-guage sheet metal walls were buckled inward but not detached.

B - Processing building 600 feet west. Windows blown in. Brick wall standing but ruined and had to be pulled down. Sheet metal roof buckled inward but not fallen.

C - Brick administration building 1800 feet west. About half of the windows on the blast side were broken, none on the far side. There was no brick damage and no roof damage.

D - Shop building 1200 feet southwest. Wire glass windows broken but not torn from their frames. Brick wall undamaged.

E - Open structure alcohol plant 300 feet southeast. Open part undamaged; sheet metal wall stripped from adjacent weigh building.

F - Cooling tower 150 feet southeast. Transite siding ripped off.

G - Open sided compressor shed 600 feet southeast. Transite roof stripped off.

H - Brick building 400 feet southeast. Wall OK; transite roof gone.

I - Processing building 100 feet east. Brick wall smashed and all glass gone. Steel frame bent but standing.

J - Warehouse 300 feet east northeast. Sheet metal walls largely torn away. Sheet metal roof buckled and parts torn away. Steel frame largely intact.

K - Brick building 100 feet west. Roof gone. Brick wall badly broken but mostly standing.

Source: Private communication from Mr. William Lauderback, of Texas Eastman Company.

F.3 PROPANE CLOUD EXPLOSION
DECATUR, ILLINOIS - 19 July 1974

At 5:03 AM on 19 July 1974, a railroad tank car full of propane suffered a puncture in the yards of the Norfolk and Western Railroad in Decatur, Illinois. The escaping propane formed a greyish white ground fog reaching up to a height of 10 to 12 feet above the nearby boxcars and spreading toward the west, south and north. There was "very little" spread toward the west. The wind was generally from the north (020° at 10 knots); but local circulation patterns were more important. The temperature was 77°F, and the dewpoint was 68°F.

The cloud found an ignition source somewhere and exploded. A distant observer reported a fireball "100 to 150 yards in height and 200 to 300 yards in length" when he looked up at the sound of the blast. There were several more explosions during the next ten minutes, apparently as secondary pockets of vapor found ignition sources - which were plentiful by then.

There were seven fatalities, most of them very near the center of the blast; and there were 152 injuries, most of them minor glass cuts and burns.

General damage profiles are sketched on the accompanying map. Zone "A" is the area of "severe structural damage"; "B" is "scattered structural and severe glass damage"; "C" is "scattered light damage" and "D" is an anomalous area of "light structural and heavy glass damage" well outside the general area of such damage, apparently the result of atmospheric refraction and focusing of the blast waves, a not uncommon feature of blast damage maps. 700 residences had damage, most of it minor; but 67 residences were posted as unsafe. They were concentrated in the northwestern part of Zone "A", with a few of them in Zone "B" just to the west of Zone "A" and a few of them in the lower end of Zone "A". A school in the southeastern quadrant of Zone "A" near the edge had extensive window, ceiling and partition damage; and an unfinished gymnasium addition collapsed to the ground.

Damage was characteristically erratic and spotty. Even in the central blast area, intact railroad cars were left sitting beside completely destroyed cars. Cars were sometimes split open as if there had been an internal explosion, with the shattered pieces of wood inside bearing no scorch marks. The Norfolk and Western Annex, scene of several severe injuries, was devastated in some places and practically untouched in others, despite the fact that it was near the center of a large fire.

Nor was the damage anything like total even near the center of the blast. Aerial photos show intact freight cars all over the yard, as well as several areas of destroyed cars. The industrial buildings adjacent to the railroad yard look intact in the photos, although they doubtless had extensive window and perhaps partition damage. Trees, shrubs and automobiles all appear intact; and indeed a newspaper account noted that a row of trees alongside the railroad right-of-way all retained their leaves - except for one 25-foot swath. The photos are to some extent deceiving - after all there were 67 houses posted unsafe - but the point remains that non-detonative gas cloud blast damage is by no means similar to, say, tornado damage. No houses were leveled, and the aerial photos give little hint of any damage at all except in a few cases (for example the school) and under high magnification. People are indeed killed, and property damage is indeed widespread; but whole sections of cities are *not* wiped out, and repairs are made relatively quickly.

This explosion is still under active investigation at this writing (December 1974). It promises to be one of the most thoroughly investigated and documented events in the record, and it will reward additional browsing - especially in the NTSB files - after the investigations are completed.

Sources:

1. Private communications from personnel at NTSB.
2. Newspaper clippings reviewed at Calspan Corporation

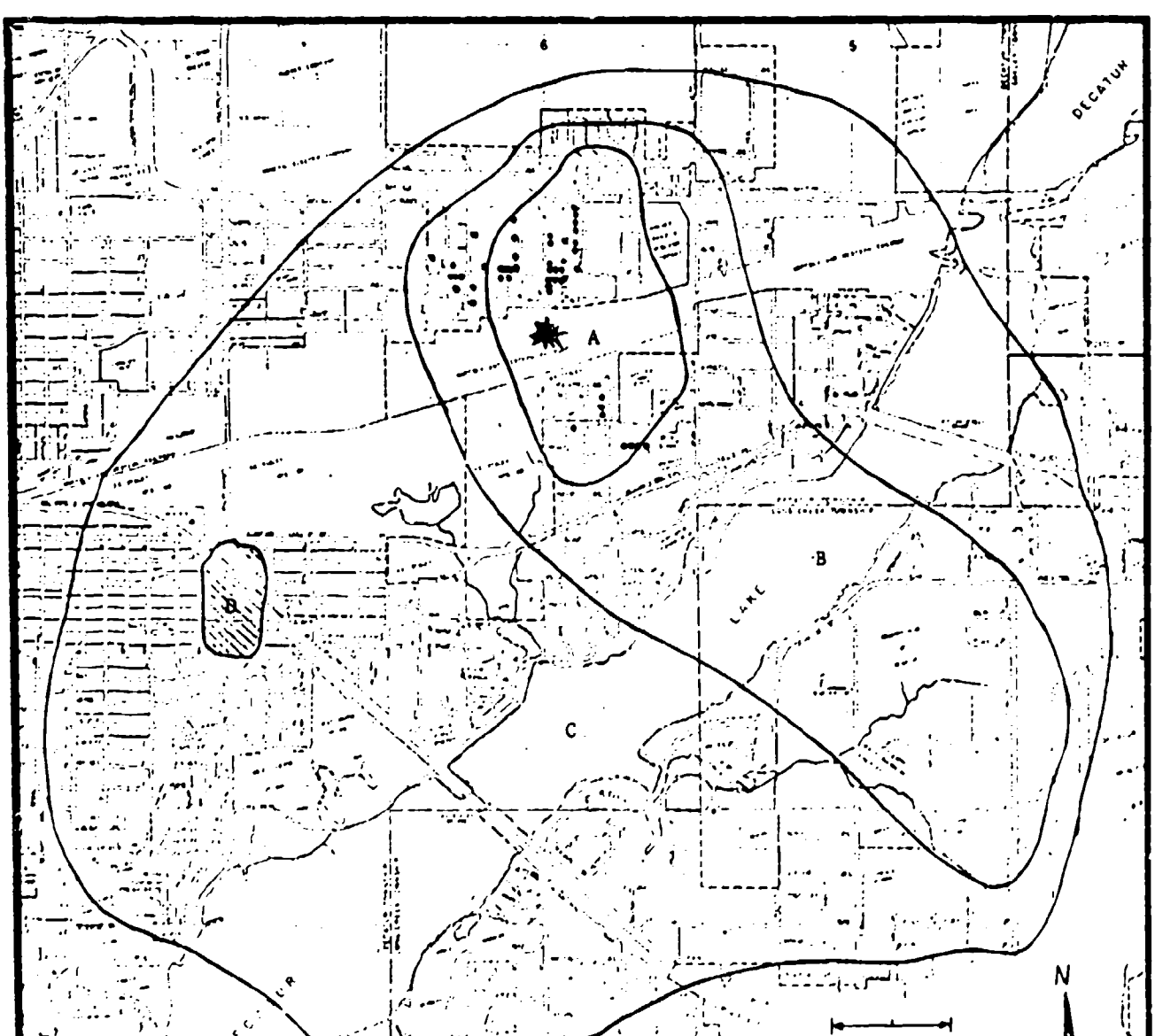

BLAST DAMAGE MAP - DECATUR EXPLOSION

A - Innermost zone - Severe structural damage.
B - Second zone - Scattered structural damage (cosmetic) and severe glass damage.
C - Third zone - Scattered light damage.
D - Hatched zone - Light structural damage and heavy glass damage.
- Dots - Residences so damaged as to be "unsafe".

F.4 VINYL CHLORIDE MONOMER CLOUD EXPLOSION CLIMAX, TEXAS - 29 June 1974

At 7:45 PM on 29 June 1974, a freight train derailed at Climax, Texas, about ten miles from the city of Nacogdoches. A 32,137 gallon tank car of vinyl chloride monomer was punctured in the derailment, tearing a hole about 4x4 feet in one end. The escaping vinyl chloride vapor traveled about 1600 feet with a slight southwest breeze to the derailed locomotive units where the vapor was ignited.

The resulting air blast appears to have been a true detonation, one of the few that have been observed in unconfined gas clouds. It wrecked the locomotive, destroyed several cars, pulled some trees from the ground and completely stripped the foliage from all vegetation in an area about 400 yards east and west of the blast area. Trees on the east side of the track were pulled toward the blast center, while trees on the opposite side of the track were flattened away from the blast center. Investigators at the scene theorized that the detonation was initiated by a strong shock wave from the exploding Diesel engine, whose cylinder head was blown off by an internal explosion thought to have due to ingesting vinyl chloride monomer through the air intake.

Windows were broken in Nacogdoches, about 6 to 7 miles away; but otherwise there was remarkably little damage to other than railroad property. There was no damage to numerous homes northeast of the site on the back side of a hill, and there was only spotty damage to the south. A home about three-quarters of a mile away on the crest of a hill and in sight of the wreck scene received only light damage, and a home directly behind it received none. In contrast however, a house 1/4 mile further away and down the slope received heavy damage. A man about a mile to a mile and a half away from the blast reported feeling the concussion, but there was no damage there.

The derailment and blast site was in a cut [illegible] feet wide at the bottom, about 300 feet long east to west, and 12 feet high on the north side and about 18 feet high on the south side. Hills rise further on both sides.

After the air blast, the punctured tank car continued to burn torch-fashion, with the flame impinging on a so-far undamaged car of vinyl chloride in front of it. About 20 minutes later, the second vinyl chloride car exploded from internal overpressure. When this car exploded, the center section of the shell, from about 9 feet from one end of the tank to about 30 inches beyond the manway cover plate, was flattened and left diagonally across the remainder of the truck structure. One end of the tank, approximately 12 feet in length, was found about 1/2 mile from the scene of the derailment and explosion. From damaged trees in the path of the tank head, it appeared that the head was rocketed to an altitude of over 60 feet, clearing trees of that height. The trajectory of the head is uncertain, but it appears that on descent it traveled at no more than about 40 feet above the ground for about 300 yards. It landed first about 250 feet from the final resting place. In the initial landing, the head dug a hole about 4 feet deep and 12 feet in diameter. The head bounced a total of four times before coming to rest in a grove of small trees. The other end of the car never was found.

Two 6,000 gallon tank cars of Motor Fuel Anti-Knock Compound were also ruptured by flame impingement and destroyed, but there is no report of rocketing parts from them. Two 20,000 gallon tank cars containing hexamethylene diamine solution were also "ruptured in the derailment with loss of all contents", but the report does not mention fire impingement or explosion.

The initial blast did ignite other ladings on the train, including raw rubber ingots which were blown out of cars near the explosion and thrown burning as much as a mile, starting spot fires where they fell. However, most of the thermal damage to vegetation was confined to about 100 to 150 yards to both sides of the derailment site. There was virtually no fire or blast damage beyond about 500 yards away.

There were no injuries reported as a result of the accident.

Source: Private communication [illegible], Federal Railroad Administration.

F.5 PROPYLENE CLOUD EXPLOSION
EAST ST. LOUIS, ILLINOIS - 22 January 1972.

At 6:20 AM on 22 January 1972, a large cloud of vaporized LPG (93-94% propylene and 5-6% propane) from a punctured tank car exploded in the Alton and Southern Railroad Company's Gateway Yard in East St. Louis, Illinois, injuring more than 230 persons and doing more then $7.5 million dollars worth of damage. There were no deaths, but 19 persons were hospitalized. The injuries were mostly from lacerations.

The spill occured when an LPG tank car containing 28,289 gallons of LPG was struck and punctured by the coupler of another car while rolling free in the railroad yard. The punctured car, with four other cars, rolled approximately 1300 feet at a speed of approximately 15 MPH, spewing liquid LPG as it went, until it finally came to rest as shown on the following map. The LPG vaporized into a visible cloud which traveled to the position shown and covered an area of about 5 acres when it was ignited by a source in an unoccupied caboose.

Flames first spread out horizontally, then an orange flame spread upward, and then a large fireball flared upward with explosive force. Almost immediately thereafter, a second, more severe, explosion occured. The force of the explosion damaged buildings and a number of freight cars in the area of the caboose. Some of the cars caught fire. Heat from the fires damaged some of the rails, and the force of the explosions wrapped some of the switch targets around switch stands. The office building of the yard and its roof tower were damaged and some manhole covers in the drainage system were dislodged. Approximately 870 to 1000 homes and buildings were damaged out in the city. The accompanying damage map shows the pattern of the damage in the surrounding community, ranging from broken glass in Area 5 to serious structural damage in Areas 1 and 5.

Prof. Roger Strehlow has analyzed the apparent yield of the explosion (from the given distance/damage data) and concluded that the explosive energy release was equivalent to that from about 2000 to 5000 pounds of TNT. This is about 0.1 to 0.3 percent of the potential energy available if all the propylene had mixed stoichiometrically with air and detonated. Prof. Strehlow has also concluded that one or more gas detonations probably occured inside empty boxcars where the confinement was apparently sufficient to permit a deflagration-to-detonation transition.

Sources:

1. Private communication from Prof. Strehlow.
2. NTSB Railroad Accident Report NTSB-RAR-73-1.
3. Roger A. Strehlow, *"Equivalent Yield of the Explosion in the Alton and Southern Gateway Yard, East St. Louis, Illinois, January 22, 1972."*, University of Illinois Report AAE TR 73-3, June 1973.

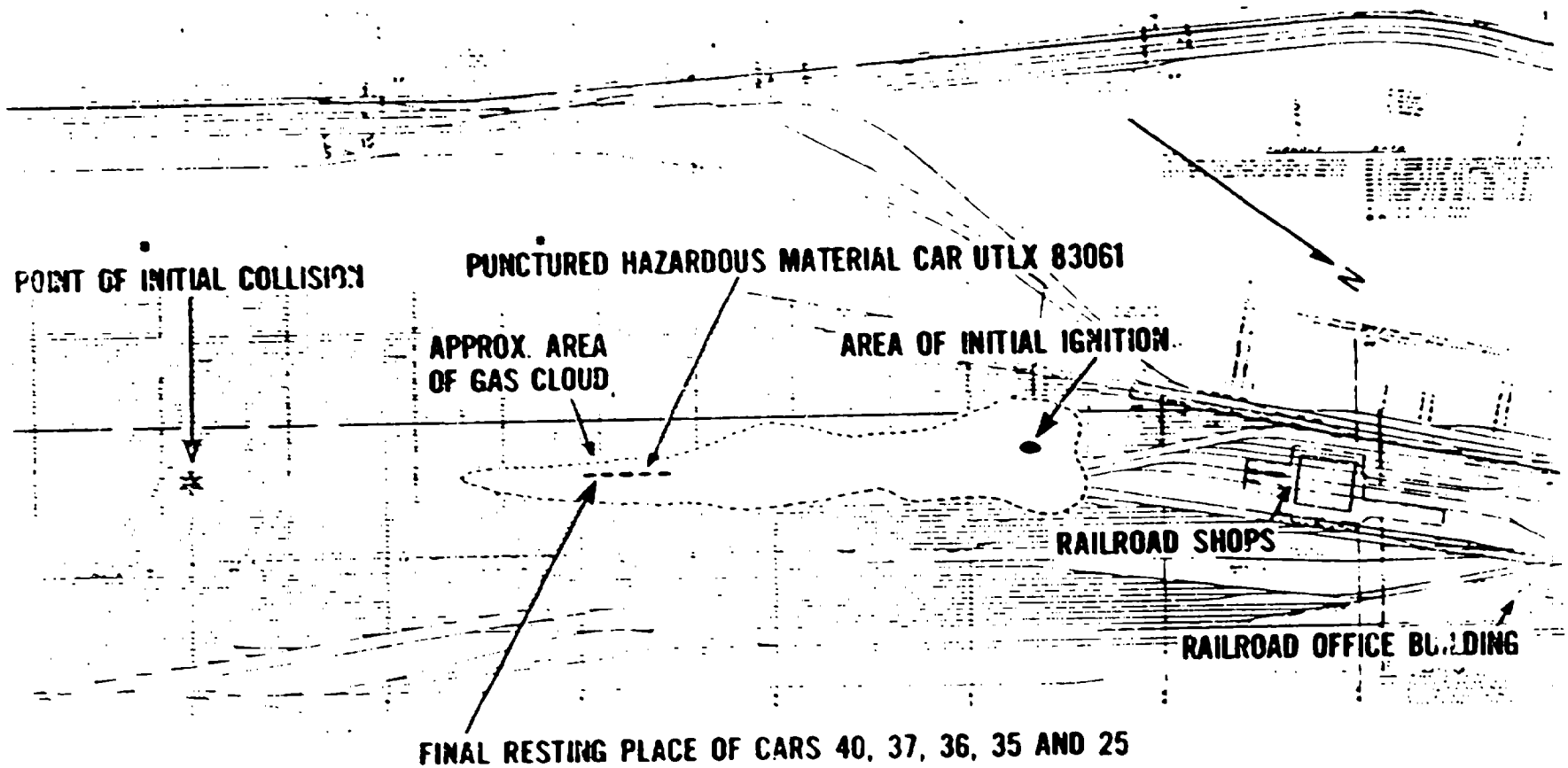

Plan of Alton & Southern Gateway Yard.

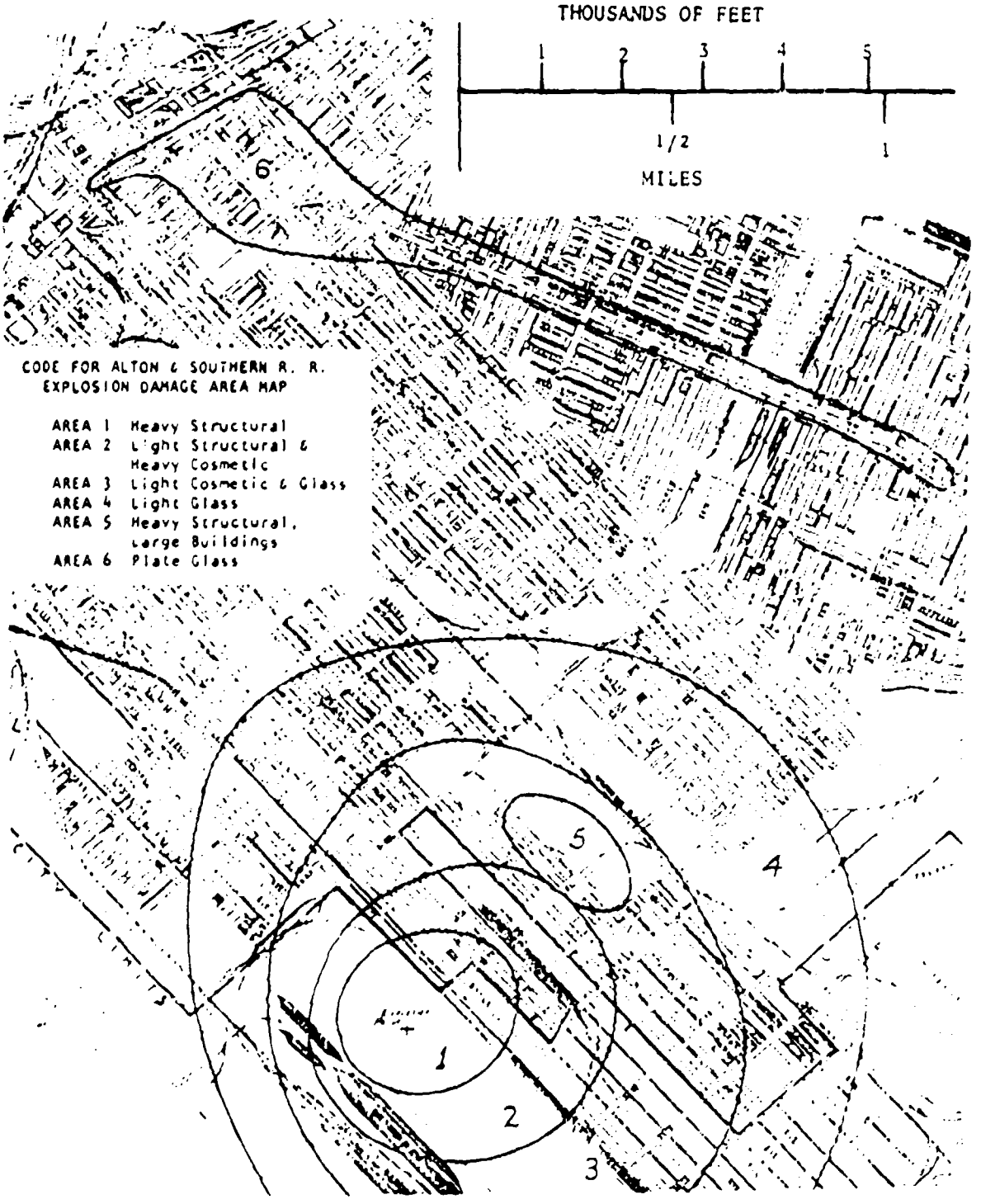

Map of Explosion Damage

F.6 PROPANE CLOUD DETONATION
FRANKLIN COUNTY, MISSOURI - 9 December 1970.

At 10:20 PM on 9 December 1970, an 8-inch pipeline carrying liquid propane under pressure ruptured and spilled propane in a rural area of Franklin County, Missouri, about seven miles south of the town of New Haven. Propane, escaping from a 6-foot split in the underside of the pipe, dug a 4-foot-deep, 10-foot-diameter crater and geysered 50 to 60 feet high, creating a heavy white fog which flowed downhill and slowly filled the entire shallow valley nearby. A breeze of 5 knots was blowing from the northeast, the temperature was 34°F, and there was a well-defined temperature inversion with a very stable air condition on the ground. Approximately 756 barrels of propane (31,752 gallons) of propane was released before ignition occured, for a calculated vapor volume of 1,143,072 cubic feet. This vapor, mixed with air to form a flammable mixture, covered an estimated 400,000 square feet of ground.

At 10:44 PM, 24 minutes after the rupture, the propane-air mixture detonated, generating a double boom. To the eye, the cloud "ignited simultaneously at all points in the valley." A huge ball of fire immediately followed the blast, mushroomed upward and enveloped the entire area, rolling from east to west across the valley bottom. The thermal column of fire was hundreds of feet high. The blast, the noise, and the pillar of fire passed over the area; and firebrands, broken boards, branches, rubble and debris fell on the countryside.

At the bottom of the valley, trees were snapped off like matchsticks, burned, blackened and strewn over the ground. In the open pastureland, many small evergreens were uprooted and large expanses of grass had been burned black. The uprooted trees and broken branches almost uniformly pointed toward the center of the blast. A ranch-type stone farmhouse was incinerated, and debris of all varieties was scattered over the landscape. A black, charred stream bank traced one path of the fire for more than 1,000 feet to the southeast. A concrete block, two-story warehouse, located near the ranch-type stone house was obliterated; this area was the origin of the blast. Another farmhouse,

one-half mile southeast of the detonation origin, was destroyed; the windows were smashed, doors were broken and debris littered the interior.

Higher up on the rim of the valley, several houses along the highway also took the full brunt of the explosion. Glass-riddled walls, broken exposed roof beams and blown-in windows were in evidence. Sections of exterior brick and stone walls were torn from their sidings, and other adjacent frame houses were partially blown down.

Within a two-mile radius of the blast, major structural damage occurred to 14 houses; minor structural damage affected an additional 14 houses; and windows were damaged in a total of 37 dwellings. Within a 7-mile radius, excluding the inner 2-mile section, some 17 houses sustained minor structural damage; and 124 houses and other buildings had window damage. Within a 12-mile radius, which included the city of Washington, Missouri, 12 commercial building had windows blown out, and 87 houses had broken windows. Two state policemen, on routine highway patrol about 25 miles from the scene, felt two separate concussions, heard what sounded like a sonic boom, and then saw the fireball. The City of St. Louis, Missouri, 55 miles away, felt the detonation; and a reading of 3.5* was recorded on a seismograph there. The small map immediately following this page shows the locations and distances of damaged homes in the immediate area, and the larger map shows the location of all damage claims resulting from the explosion. The graph relates window damage to distance from the blast center.

There were no fatalities in this event. The area was thinly settled, and the few residents there were amply warned by the roar of the escaping propane and the sight of the spreading cloud. They evacuated the valley and were all up on the valley rim when the blast and firestorm occurred. Ten persons were treated for injuries.

---

* The scale (Richter) was not specified in the sources consulted, but a vertical ground displacement of 2.2×10^{-2} m was mentioned.

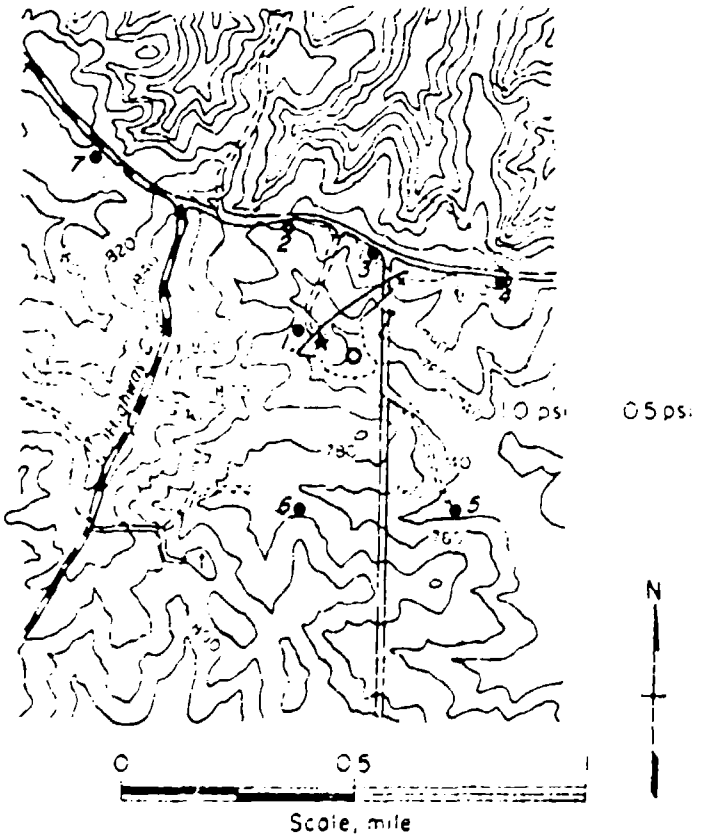

Map of accident area showing derived location of detonable cloud and locations of damaged homes.

× - Pipeline break
★ - Point of ignition
⊙ - Apparent center of blast

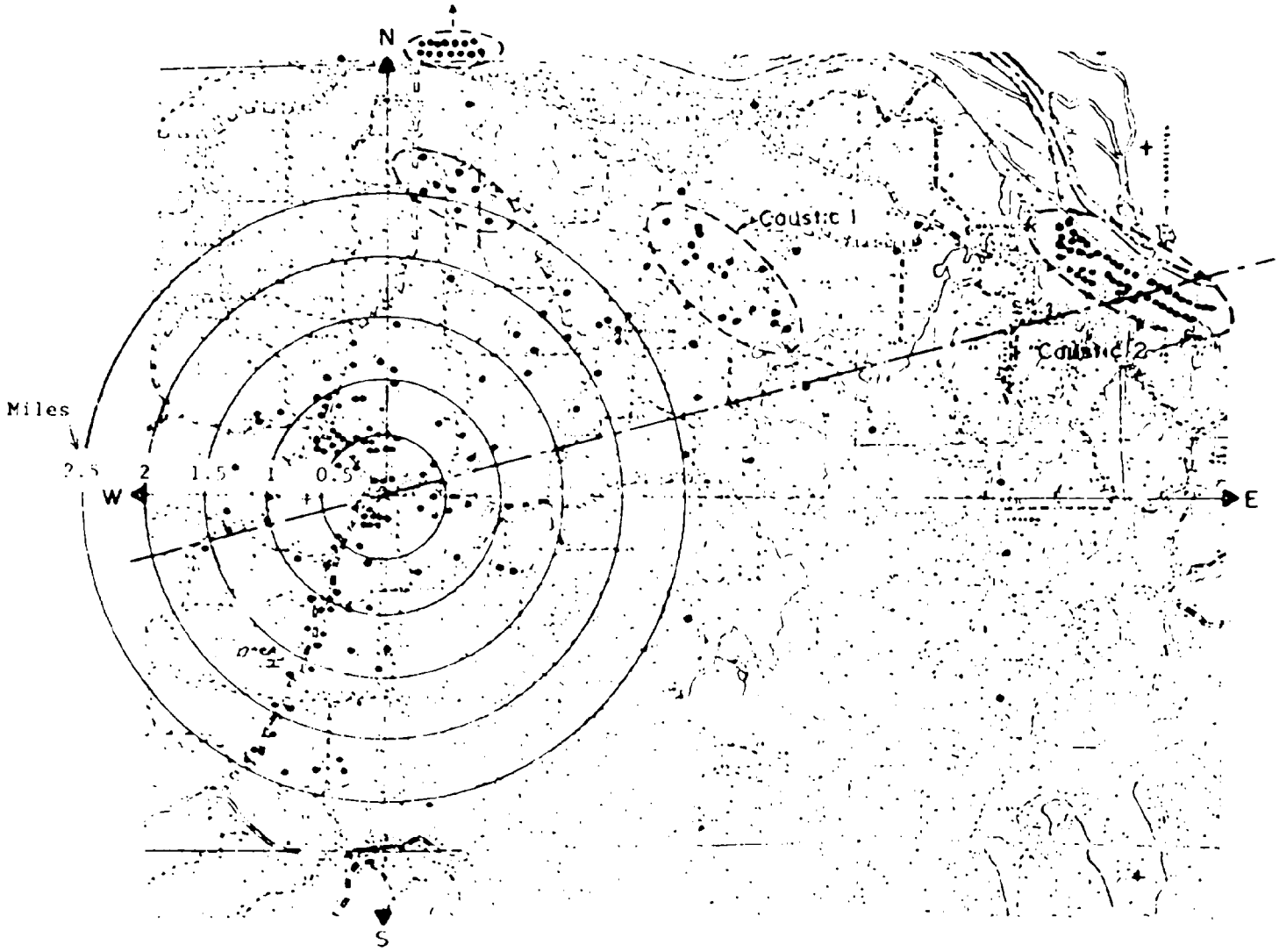

Map of area showing damage claims resulting from explosion.

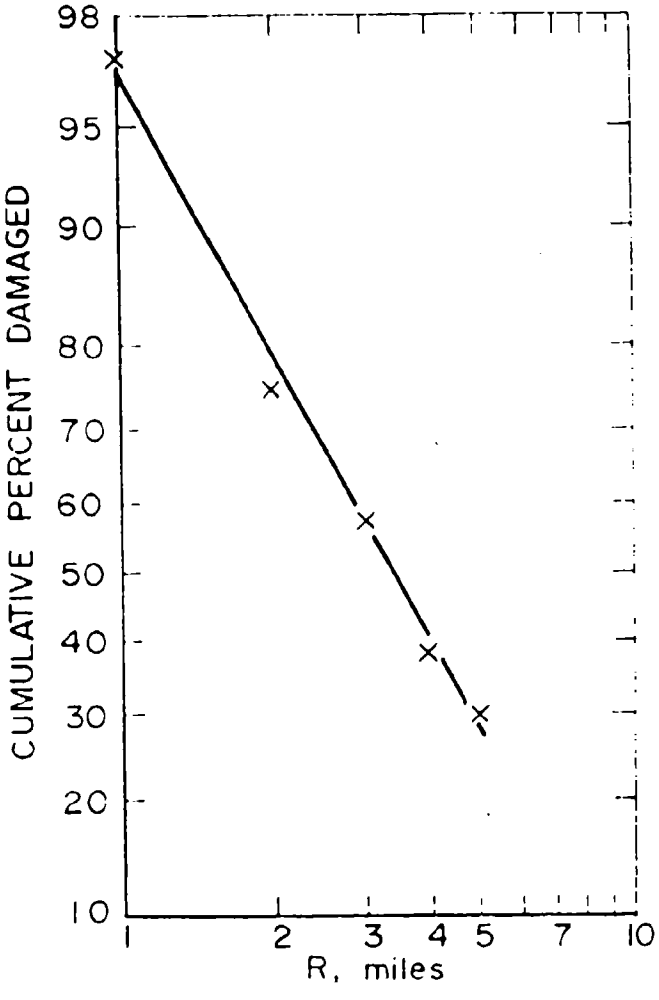

WINDOW DAMAGE - Percentage of structures with window damage within 5 miles of the blast site

This explosion is most unusual in that it is authoritatively thought to have been a detonation and not just the usual deflagrative explosion. Buildings were shattered and obliterated, rather than merely having roof and wall panels torn off. Trees were uprooted and stripped of all foliage, rather than being essentially unharmed as in the usual gas cloud blast. "The entire valley lit up at once" when the cloud ignited, rather than a flame rolling from one side of the cloud to the other as in the usual explosion report.

Not all of the propane detonated, of course. There was a rolling firestorm following the blast, and a billowing fireball continued to burn at the rupture site for the next twelve hours. Burgess and Zabetakis estimated (from the distance-vs-damage data) that approximately 7.5% of the propane released prior to the blast entered into the detonation with an energy equivalent to that from 50 tons of TNT. The balance burned.

The circumstances that led to detonation were a bit unusual too. The vapor cloud collected in a valley under a strong temperature inversion, where it was restrained from normal dispersion and where blast waves could be refracted back down into the flammable mixture. More importantly, the blast is thought to have grown to detonation *inside the confinement* of a concrete block warehouse where the reaction pressure was not readily relieved. It is the current general consensus that flammable clouds will not burn to detonation in the open but require some confinement; although the investigators of the Flixborough explosion - *cf.* Case Study F.1 - have recently challenged that view, and the Climax vinyl chloride cloud appears to have detonated (Case Study F.4). The latter may have been initiated by the shock wave from one of the Diesel engines, which apparently ingested VCM vapor and suffered an internal detonation which blew off the cylinder head. Roger Strehlow believes the East St. Louis railroad yard propylene explosion also involved a detonation inside the confinement of a boxcar (*cf.* Case Study F.5).

Sources:

1. Private discussions with Dr. David Burgess, BuMines, and Prof. Roger Strehlow, Univ. of Illinois.

2. BuMines RI-7752 "Detonation of a Flammable Cloud Following a Propane Pipeline Break" 1973.

3. NTSB Pipeline Accident Report, "Phillips Pipe Line Company Propane Gas Explosion, Franklin County, Missouri, December 9, 1970", NTSB-PAR-72-1.

F.7 CRUDE OIL VAPOR-MIST EXPLOSION
HEARNE, TEXAS - 14 May 1972

At 12:30 AM on 14 May 1972, an 8-inch crude oil pipeline ruptured near Hearne, Texas; and crude oil sprayed into the air from a 6-inch irregular split in the top of the pipe. The sparsely populated surrounding countryside was showered with crude oil vapors and liquid. The crude oil flowed along a stream, passed through culverts beneath a railroad and a highway, and finally pooled up on a stock pond 1,800 feet away from the rupture.

Two frame houses were located 600 feet west of the leak in a fenced area which bordered the stream on the north side. One of these houses was within 50 feet of the stream; the other was 100 feet farther north. A petroleum tank-truck operation was located within 600 feet of the stock pond on which the crude oil had dammed up.

At 5 AM, 4-1/2 hours after the pipe had split, crude oil vapors were ignited by an unknown source in or near the small, single-story frame house adjacent to the crude-filled stream. The resultant explosion and fire killed one man, seriously burned another man and a young boy, and destroyed the house. An intense petroleum fire was kindled along the stream, which burned over and under the highway and the railroad culverts and ignited the crude oil in the stock pond. A fire 1800 feet long and several hundred feet high scorched the entire area from the leak site to the stock pond and killed all vegetation within this zone. The highway and railroad bridges were heat-damaged, and all highway and railroad traffic was stopped by the fire. The telephone, railroad, and pipeline communication lines were melted, and the poles were burned. 7,913 barrels of crude oil escaped and burned.

This rather sketchy case study has been included in this report partly because it was a flammable spill on water and partly because crude oil is not ordinarily thought of as dangerously flammable. However, crude oil contains an appreciable percentage of volatile material, and this particular

crude was about 10% (by weight) lighter than hexane. Ten percent of 332,346 gallons (7,913 barrels) is 33,234 gallons of light hydrocarbons, or about one railroad tank car; and the spraying mode of the leak would strip it out into the air fairly efficiently to yield a flammable cloud much like that from a gas leak. A quiet spill onto the water of a harbor would give less efficient stripping of course, but even so the thin film of oil would yield up its light ends content fairly quickly and lead to a dangerously flammable vapor cloud.

Source: NTSB Pipeline Accident Report, "Exxon Pipe Line Company Crude Oil Explosion at Hearne, Texas, May 14, 1972", NTSB-PAR-73-2.

F.8 NATURAL GAS CLOUD EXPLOSION AND FIRE HOUSTON, TEXAS - 9 September 1969

At about 3:40 PM on 9 September 1969, a high pressure natural gas pipeline in a suburb north of Houston, Texas, burst from accidental over-pressuring and filled the neighborhood with a cloud of natural gas. The initial pressure burst produced a concussion that threw several people, within a radius of 250 feet, from their chairs, couches or beds. There was a noise as of jet engines so severe that it was difficult to hear anything else, and the blowing gas created a duststorm-like condition that obscured visibility in the area.

Approximately 8 to 10 minutes later, a resident about 200 feet from the point of rupture heard a "crackling or sparking-type noise", followed by an explosion and fire. He was knocked down and suffered burns on his arm and face. Five houses in a row exploded at this time, indicating that the escaping gas had entered into these buildings. Fires broke out and raged to a height of 125 feet at the rupture point. The heat of the fires was so intense that buildings up to 250 feet away were completely destroyed. In all, thirteen houses were completely destroyed, and 106 others were damaged. The total damage was estimated to be $500,000.00. All of the destroyed houses and those heavily damaged were within 300 feet of the rupture point; they are located on the following sketch map. Between 300 and 600 feet from the rupture point, damage consisted mainly of cracked walls, blistered paint and broken windows. From 600 to 900 feet, damage was due to objects falling from shelves or walls. The destruction and heavy damage was concentrated to the north of the rupture site, apparently due to some protecting earth mounds to the south; but the lesser damage was consistent in all directions.

There were no deaths, partly due to swift evacuation efforts before the explosion-fire; but nine persons were injured, two seriously.

Source: National Transportation Safety Board Pipeline Accident Report, "Mobil Oil Corporation High-Pressure Natural Gas Pipeline, Near Houston, Texas September 9, 1969". NTSB-PAR-71-1.

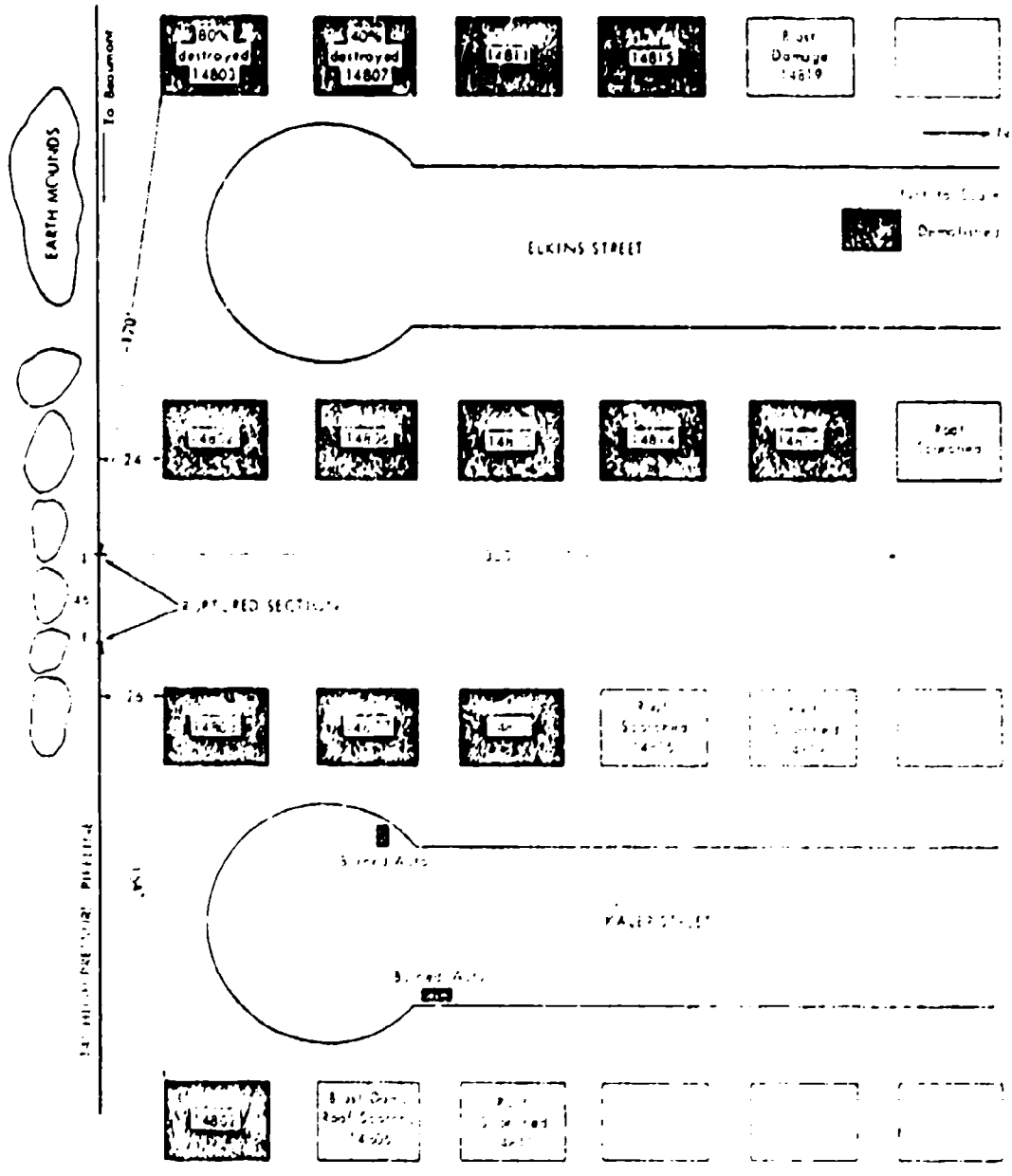

SKETCH MAP OF SEVERE DAMAGE FROM BLAST AND FIRE
NORTH OF HOUSTON, TEXAS, 9 SEPTEMBER 1969

F.9 LPG TANK CAR EXPLOSIONS
CRESCENT CITY, ILLINOIS - 21 June 1970

At 6:30 AM on 21 June 1970, 15 railroad cars including nine tank cars loaded with liquefied petroleum gas derailed in the town of Crescent City, Illinois. The force of the derailment propelled the 27th car in the train over the derailed cars ahead, and its coupler struck the tank of the 26th car in passing, puncturing that tank. The released propane was ignited immediately by some unidentified source, possibly by sparks produced by the the derailing cars or by the overheated journal that caused the derailment in the first place. The initial ignition of the gas produced a fireball that reached a height of several hundred feet and extended into that part of the town surrounding the tracks. Several buildings were set on fire.

The safety valves of other tank cars near the fire operated, releasing more propane which provided more fuel for the fire. More heat was directed against the elevated portion of the 27th car, which increased the pressures within that car until it ruptured with explosive force at about 7:33 AM. The east end of the car, which included the manway, dug a crater in the track structure and then was hurled about 600 feet eastward, where it stopped at an incersection in town. Fire in this section continued there after it came to rest. The west end of the car was hurled in a southwesterly direction for a total distance of about 300 feet. This section struck and collapsed the roof of a gasoline service station. Two other sizeable portions of the tank were hurled in a southwesterly direction and came to rest at points 600 feet and 750 feet from the tank.

At about 9:40 AM, the 28 car in the train ruptured. The south end of the car was hurled about 200 feet southward across the street where it entered a brick apartment building. The north end of the car was hurled through the air in a northwesterly direction over the roofs of several houses and landed in an open field. It continued to roll and finally stopped after traveling about 1600 feet.

About five minutes later, at approximately 9:45 AM, the 30th car in the train ruptured. This car had been lying in a generally north-south position. The north end of the car, which included about one half of the tank, was propelled along the ground in a northeasterly direction for about 600 feet. This portion of the tank passed through and completely destroyed two buildings and came to rest within a third. The other end of the tank stayed in the vicinity of the general derailment site.

At about 10:55 AM, the 32nd car in the train and the following car ruptured almost simultaneously. One of them split longitudinally and did not separate into hurtling pieces. The west end of the other was hurled westward where it struck and punctured the head of the 34th car. Propane released from the puncture ignited immediately. The other end of the 33rd car was hurled through the air. It struck the 34th car, ricocheted, and then struck the protective housing of the 35th car. The housing and valves of the 35th car broke off, permitting still more propane to escape and ignite. Fires continued to burn at the punctured cars for a total of 56 hours.

In all, 16 business establishments were destroyed and seven were damaged. Twenty-five residences were destroyed and a number of others were damaged extensively. Total injury and property damage costs amounted to approximately two million dollars. Sixty-six persons were injured; there were no deaths.

The key damage mechanism in this accident was the rocketing of burning tank cars which spread massive missiles of steel and new fireballs up to 850 feet from the derailment site. This is a characteristic result of all accidents wherein pressure vessels are exposed to massive fires, and it should be included in all disaster scenarios. The following map shows the paths of the major tank fragments in this accident.

Source: National Transportation Safety Board Railroad Accident Report, "Derailment of Toledo, Peoria and Western Railroad Company's Train No. 20 with Resultant Fire and Tank Car Ruptures, Crescent City, Illinois, June 21, 1970". NTSB-RAR-72-2.

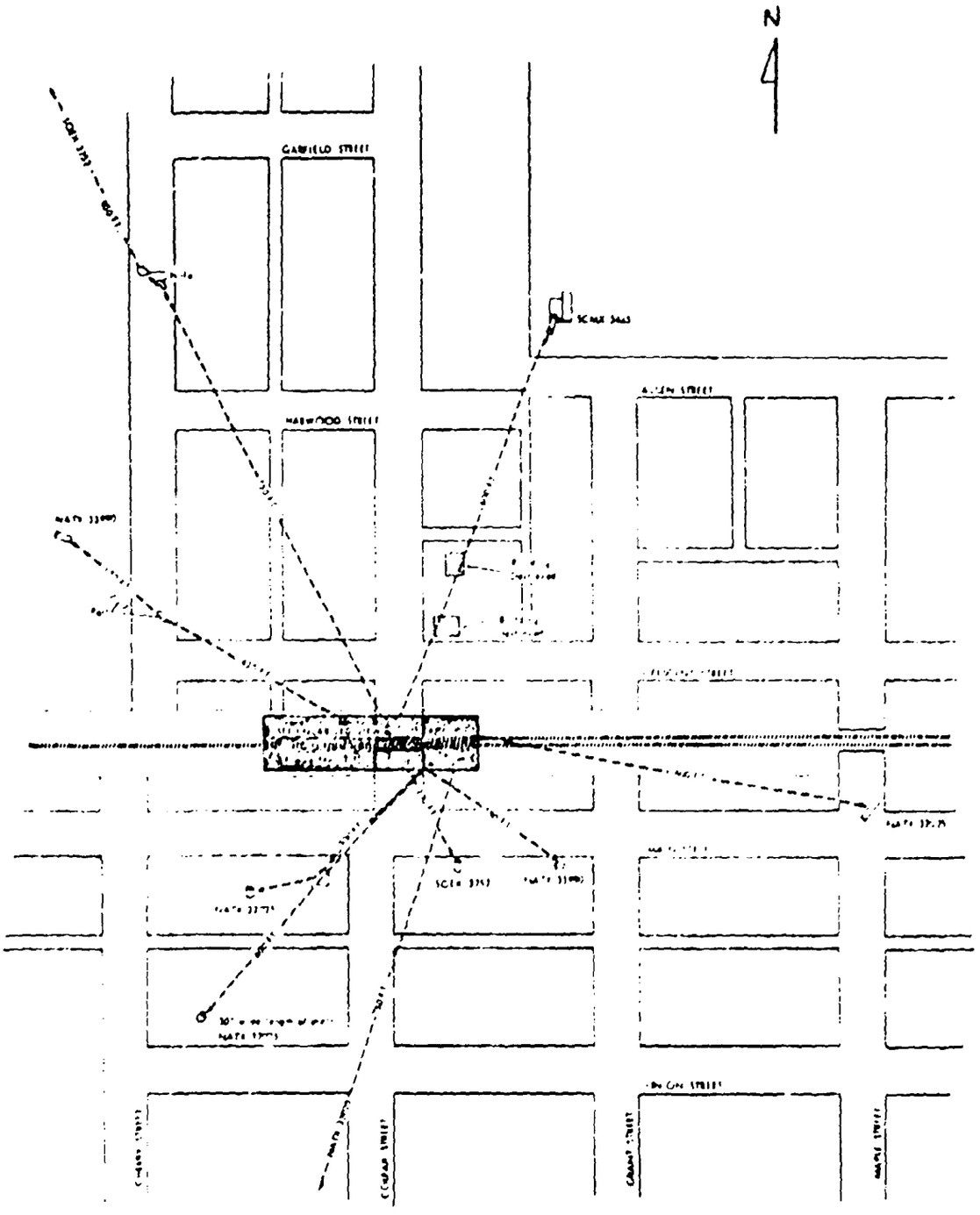

TRAJECTORIES OF TANK CAR FRAGMENTS

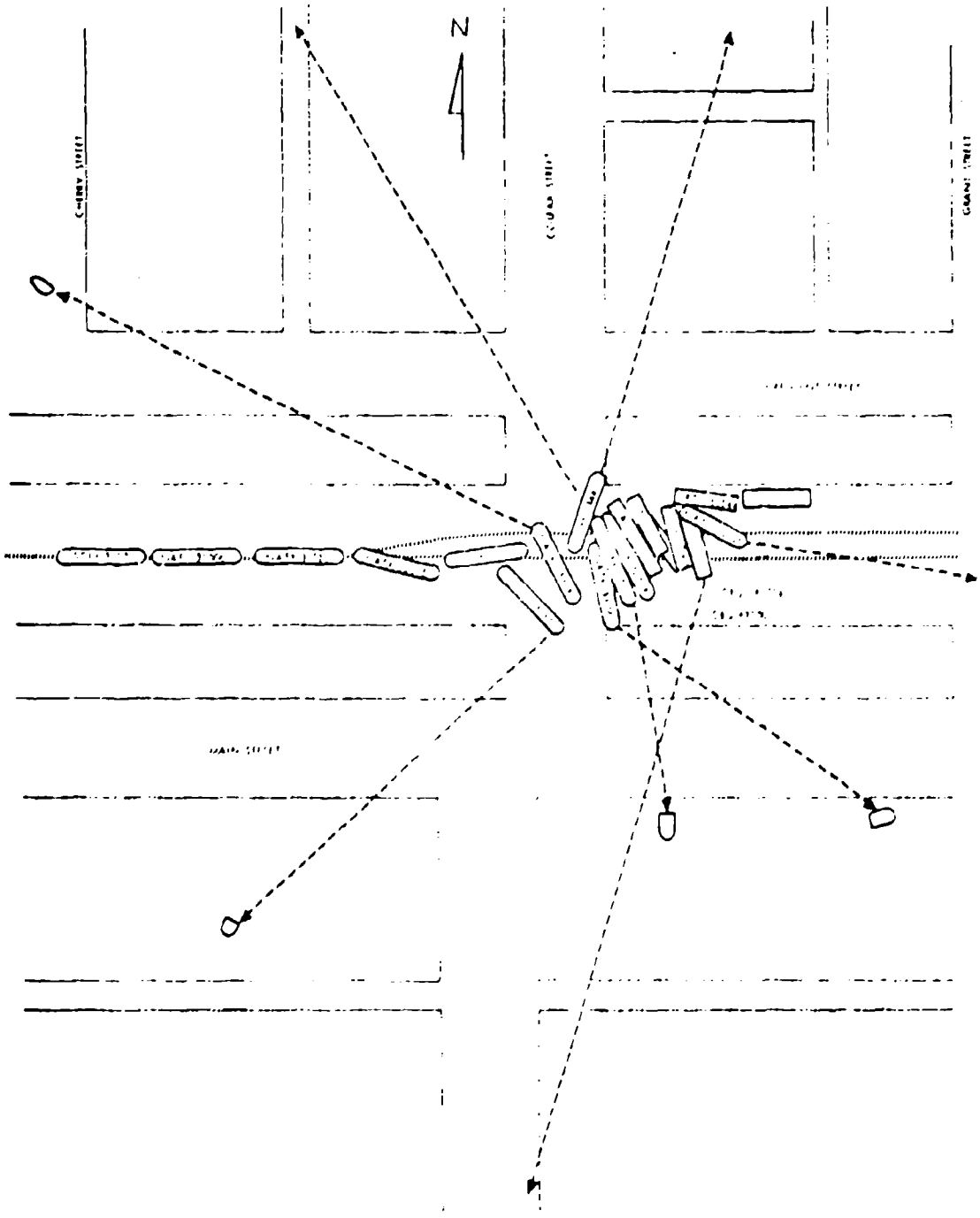

DERAILMENT CONFIGURATION

F.10 LPG TANK CAR EXPLOSIONS
LAUREL, MISSISSIPI - 25 January 1969

At 4:15 AM on 25 January 1969, a train carrying 15 tank cars of liquefied petroleum gas (primarily propane) derailed in the middle of the town of Laurel, Mississippi. The derailment was followed by an immediate, violent fire and explosion; and other explosions followed at intervals for the next 40 minutes as the fire caused one tank car after another to over-pressure and burst.

The initial fireball immediately set fire to buildings 200 to 400 feet away, primarily residences, between the wreck and Meridian Avenue (see map) and to industrial buildings about 200 feet away on the opposite side of the tracks. Smaller, spot fires were set by burning fragments up to about 10 city blocks away.

The concussion from the explosions caused structural damage to both private and industrial buildings within about 400 feet. Broken windows were reported as far as three miles west of Laurel, but the majority of the broken glass was in the downtown area about 8 blocks away. One witness put it, "Very little glass survived within about half a mile to a mile". Damage claims were filed - and paid - from up to five miles away; but they were distributed in scattered bunches and not generally distributed. Cracked and broken plumbing was widespread in the concussion area; but such damage was thought to be a special case due to the prevalence of light-construction, frame buildings, simple-construction foundations and uncompacted soil which had already seen some creep and shifting due to heavy rains.

The major damage mechanism was impact and fire from rocketing tank car fragments and burning propane. Building and automobiles in the immediate vicinity were destroyed by direct flames or by heat radiation from the fireballs. Parts of the tank cars which were hurled through the area set fire to buildings as far as 1500 feet away as well as inflicting impact damage. A 37-foot section of PDTX car 261 (see map) was propelled through the air in a southeasterly direction, striking the ground three times before it came to rest. It struck

the ground first about 1,000 feet from the wreck. After the first bounce, it carried another 300 feet over some residences without striking them; bounced again for 200 feet, and again for 100 feet, coming to rest atop a dwelling 1,600 feet from the wreck center. The resulting fire where the tank came to rest destroyed three houses. A 37-foot section of PDTX car 269 was propelled through the air in a northwesterly direction striking the peak of the roof of a mill 800 feet from the track. This section then struck in the parking area and bounced end over end successively 100 feet, 200 feet and 50 feet before coming to rest in a reversed position on the rear of a dwelling 1,100 feet from the wreck. Other fragments took other trajectories, as shown on the map.

In all, some 2930 buildings suffered damage. Fifty four residences were destroyed, mostly by fire. A large transfer and storage company warehouse about 200 feet away and its contents were almost totally destroyed by fire, and a wash-and-dry laundry was totally destroyed. The structures of four other industries and businesses were heavily damaged: a hardboard fabricating plant and the Mississippi Power Company, west of the tracks; a machine shop and a wholesale grocer, east of the tracks (see map). Six public schools and five churches were damaged, all in the downtown area. Total property damage settlements amounted to $6,615,195.

Two fatalities resulted from the wreck. A 65-year old minister died as a result of burns, and a 17-year old girl died about a month after the wreck. There were 976 other personal injuries, most of them burns and cuts from flying glass. Seventeen persons were hospitalized for more than a month.

The large number of personal injuries was the result of another special case which is instructive in itself. At the sound of the first explosion, people poured out into the streets instead of seeking shelter; and the streets were filled with people when the second explosion and fireball occurred. They were then trapped between the fire and the many fences that paralleled the tracks

and could not get back to shelter. There were many purely panic injuries as people were trampled in the rush and injured attempting to scale the fences. They were of course only 200 to 400 feet from the towering fireballs, and many burn injuries occurred.

There was still another unusual aspect to this accident. A National Guard explosive ordnance team punched holes in two unruptured tank cars, using shaped demolition charges, to prevent them from exploding. The wisdom of such action is still controversial, but in this case it worked. The gas ignited immediately with a sound described as "like a jet plane taking off", and about two hours later the area was declared safe for the people to return.

Sources:

1. Private communication, Mr. W. L. Millwood and his staff at Southern Railway System, Washington, DC.

2. National Transportation Safety Board Railroad Accident Report, "Southern Railway Company Train 154 Derailment with Fire and Explosion, Laurel, Mississippi, January 25, 1969". October 6, 1969. (No NTSB number assigned)

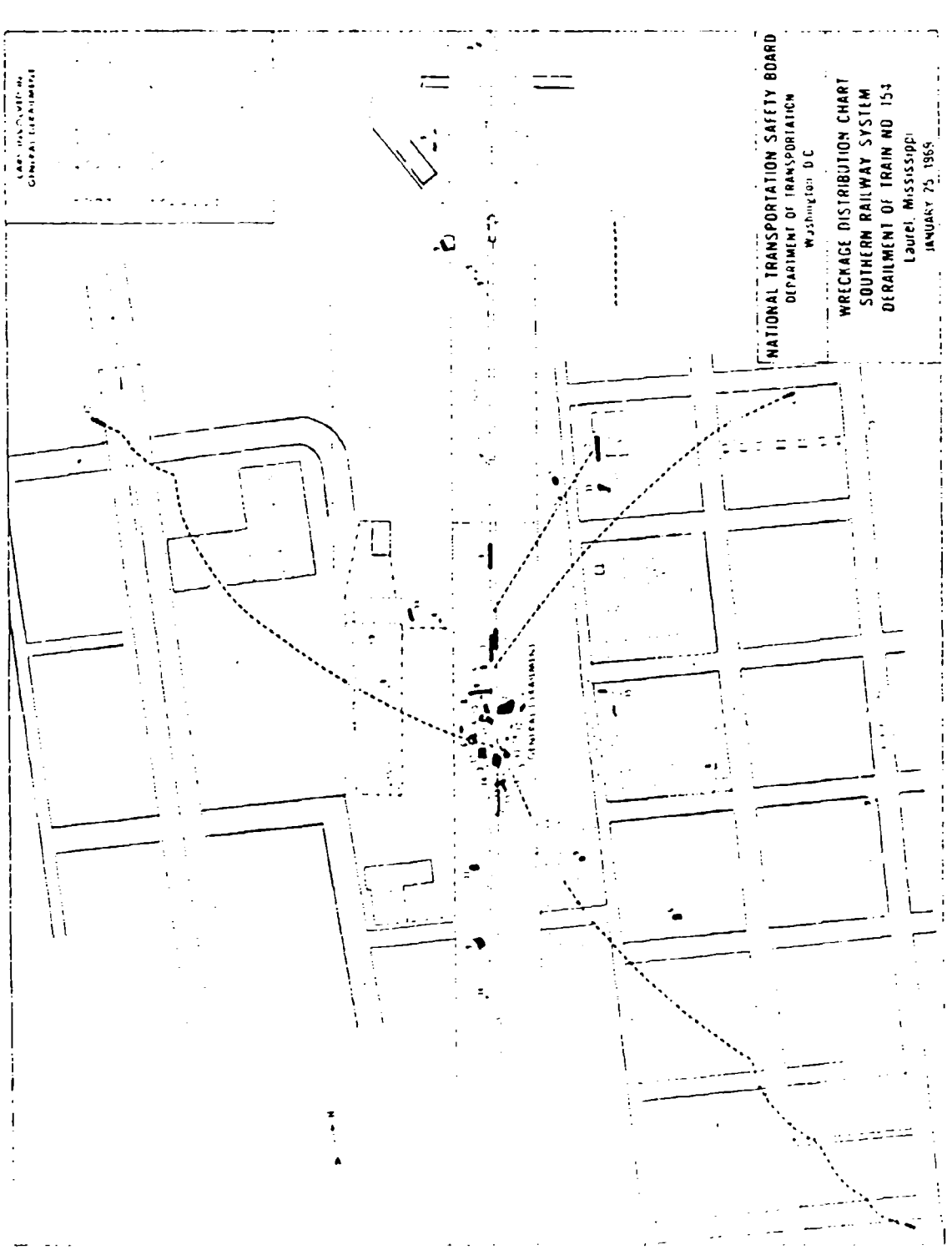
NATIONAL TRANSPORTATION SAFETY BOARD
DEPARTMENT OF TRANSPORTATION
WRECKAGE DISTRIBUTION CHART
SOUTHERN RAILWAY SYSTEM
DERAILMENT OF TRAIN NO 154
Laurel, Mississippi
JANUARY 25, 1969

F.11 VINYL CHLORIDE MONOMER TANK CAR EXPLOSIONS HOUSTON, TEXAS - 19 October 1971

At 1:44 PM on 19 October 1971, 20 freight cars were derailed at Mykawa Station, approximately 2 miles inside the southern city limits of Houston and 10 miles south of the city center. Six of the cars contained flammable vinyl chloride monomer, a liquefied gas under a pressure of approximately 40 psi at the existing temperature; and two others contained butadiene (also a flammable, compressed gas) and acetone. The cars jackknifed in the derailment, and two vinyl chloride cars were punctured.

There was an explosion and a billowing fire before the wrecked cars had ceased to move. The two punctured cars came to rest in the burning area, and the fire enveloped large areas of the tank cars. The heat increased the internal pressure until at approximately 2:30 PM a violent rupture and massive energy release occurred when the tank of one car suddenly failed. The sudden release of approximately 100,000 pounds of vinyl chloride monomer produced a large fireball and rocketing tank fragments. Residual vinyl chloride in the other tank car ignited inside the car at that point; and the car rocketed in one piece to a point approximately 300 feet away, spewing burning, liquefied vinyl chloride from its punctures. The acetone car, which had been struck and damaged by the rocketing car, caught fire; and a house and several vehicles were ignited by the stream of burning vinyl chloride. The secondary fires burned for approximately five hours before the last one was extinguished.

Other than the train and railroad roadbed, damage was very light. A nearby residence, a fire truck, an automobile and a railroad motor truck were destroyed by fire; and several buildings in the area incurred such damages as paint blisters or broken windows. Fortunately, the area was very sparsely built and populated.

One fireman was killed; and 50 people, most of them firemen, were injured. Their approximate locations are plotted on the map. Twenty of the injured were hospitalized, mostly for burns. An autopsy was not performed on

the fireman who was killed, but he had suffered severe head injuries as well as burns. Most of the injuries appear to have been burns from fireball radiation, an observation that is consistent with the firefighters' rule of thumb that firemen have succumbed to radiation burns incurred when they were as far away as 250 feet from very large fireballs.

The following map shows the location of the burning tank cars, the injured persons and the approximate outline of the area which contained scorch marks and debris.

Source: National Transportation Safety Board Railroad Accident Report, "Derailment of Missouri Pacific Railroad Company's Train 94 at Houston, Texas, October 19, 1971". NTSB-RAR-72-6.

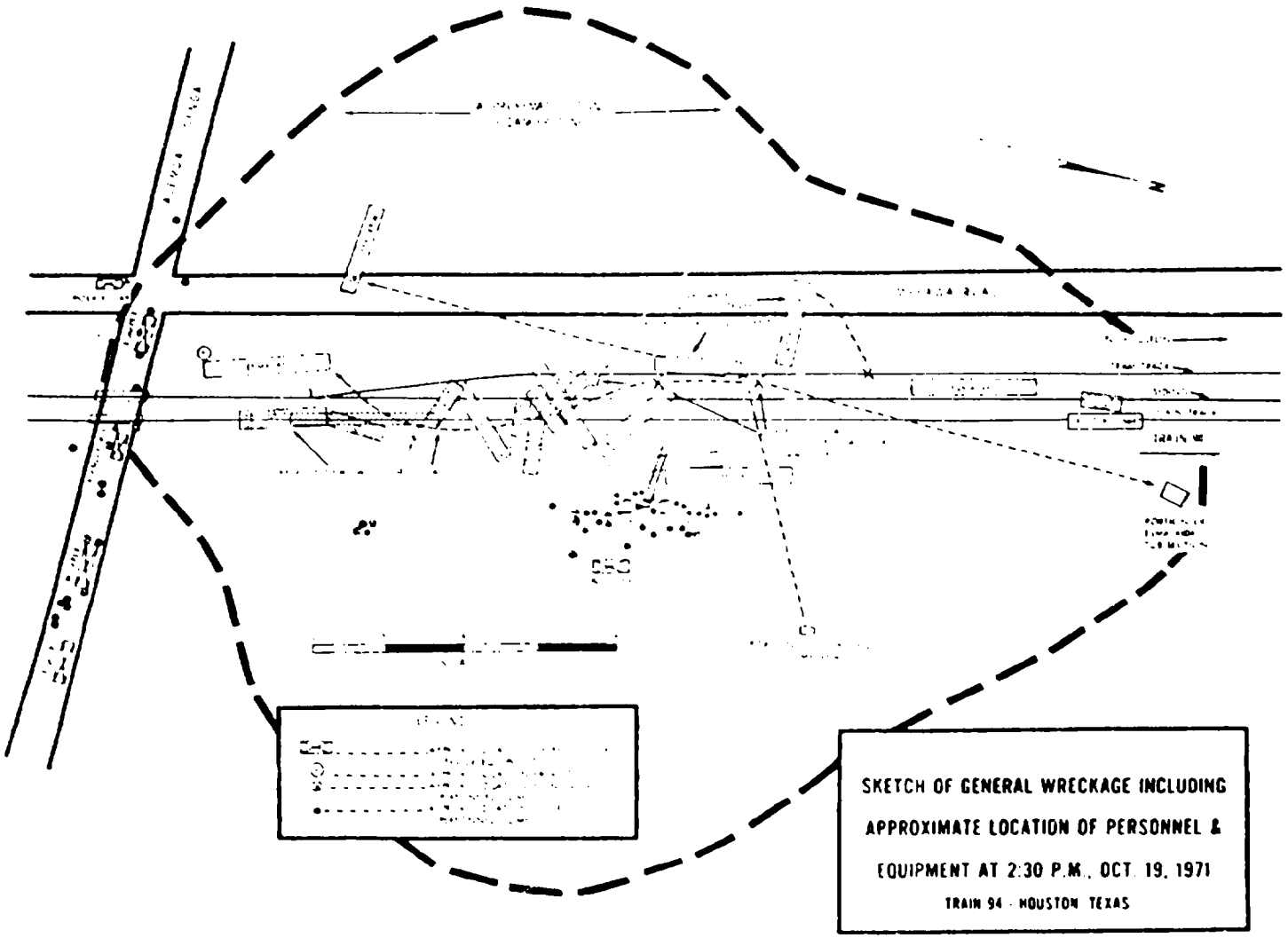

SKETCH OF GENERAL WRECKAGE INCLUDING
APPROXIMATE LOCATION OF PERSONNEL &
EQUIPMENT AT 2:30 P.M., OCT. 19, 1971
TRAIN 94 - HOUSTON TEXAS

F.12 PROPYLENE TANK TRUCK EXPLOSION
NEW JERSEY TURNPIKE - 21 September 1972

At 8:25 PM on 21 September 1972, a tractor-semitrailer (tank) carrying propylene liquid petroleum gas sideswiped a Greyhound bus (carrying no passengers) in the southbound lanes of the New Jersey Turnpike about one mile south of Exit 8. Fire, caused by friction sparks when the tractor-trailor scraped the median guardrail, ignited fuel escaping from the tractor's left-side fuel tank and spread to propylene which was leaking from the cargo tank's damaged plumbing, enveloping a large part of the cargo tank in flame.

About 20 or 25 minutes after the crash, the cargo tank exploded in a huge ball of fire which inflicted burns and other injuries to 28 persons, including 7 police officers and at least one bystander who was 600 feet south of the explosion. None of these injuries was serious. Two people trapped in an automobile wedged between the tank truck and the guardrail were killed, but it is not clear whether they were alive at the time of the explosion. Their bodies were extensively charred. A water-tank fire truck parked about 100 to 150 yards south of the explosion suffered scorched paint and warped plastic light components; an occupant said that a flaming mass came directly over the vehicle. At the time of the explosion, there were about 200 onlookers dispersed along the east and west property lines at distances ranging from 150 to 1000 feet. The locations of all 28 injured persons could not be established, but the known positions of eight of them are shown on the map following.

Pieces of the exploded tank shell rocketed. The front section, about 27 feet long or three-quarters the length of the tank was found 1,307 feet northeast of the explosion point and 402 feet east of the highway center. The rear head was 549 feet southwest, and the rear one-quarter of the cylindrical section was 229 feet southwest of the explosion point. Other tank components were found at various points along an 850-foot line generally

southeast of the explosion point. Parts of the trailer suspension and the two axles, with the tires burned off, were found along the eastern embankment of the turnpike. When first seen, the axles and wheels were glowing.

There was no air blast; the explosion was that of the bursting tank shell. Most of the fireball was produced when the expelled vapor burned in air after rupture of the tank. The tank had originally contained 7,209 gallons of propylene.

Source: National Transportation Safety Board Highway Accident Report, "Multiple-Vehicle Collision Followed by Propylene Cargo-Tank Explosion, New Jersey Turnpike, Exit 8, September 21, 1972". NTSB-HAR-73-4.

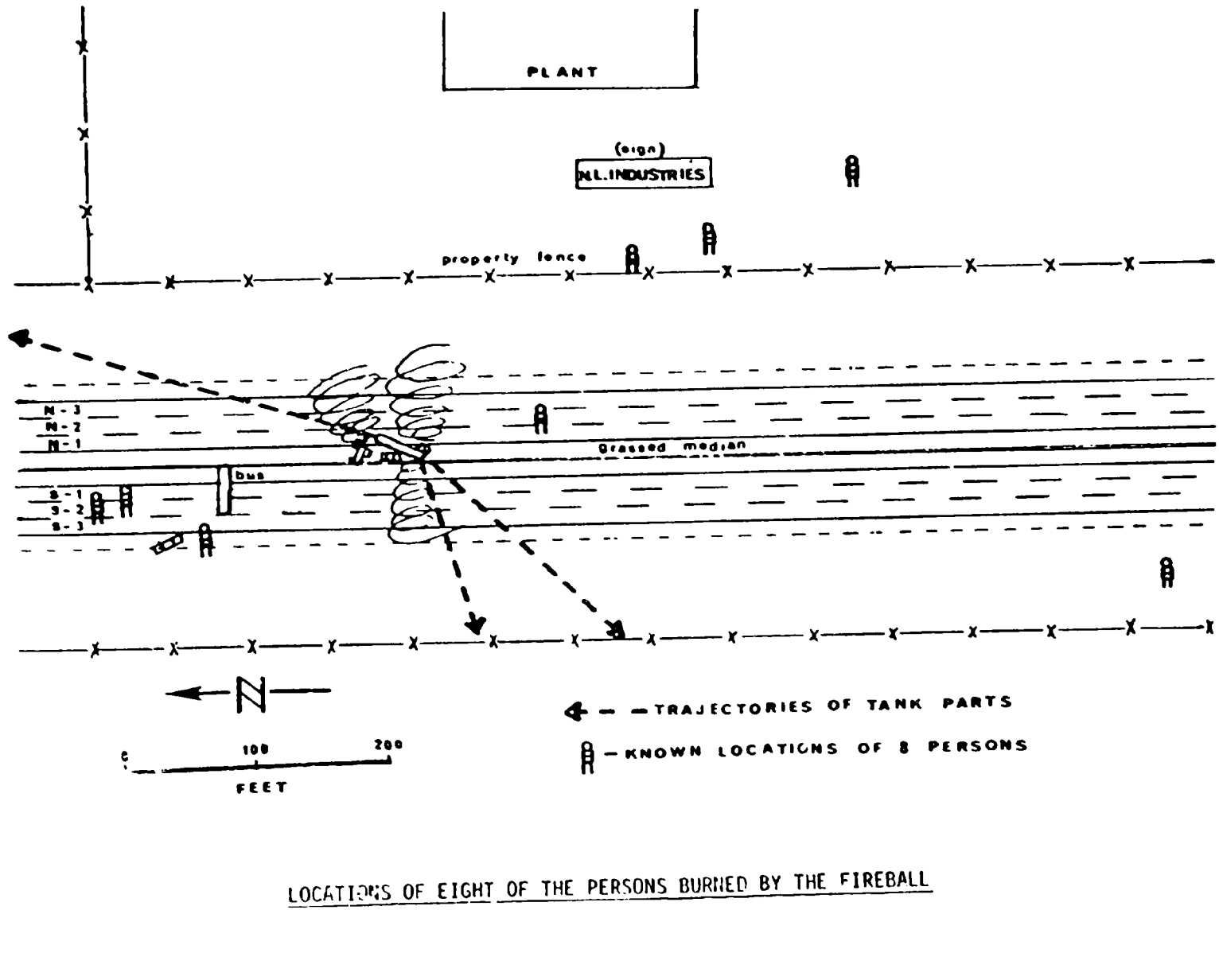

LOCATIONS OF EIGHT OF THE PERSONS BURNED BY THE FIREBALL

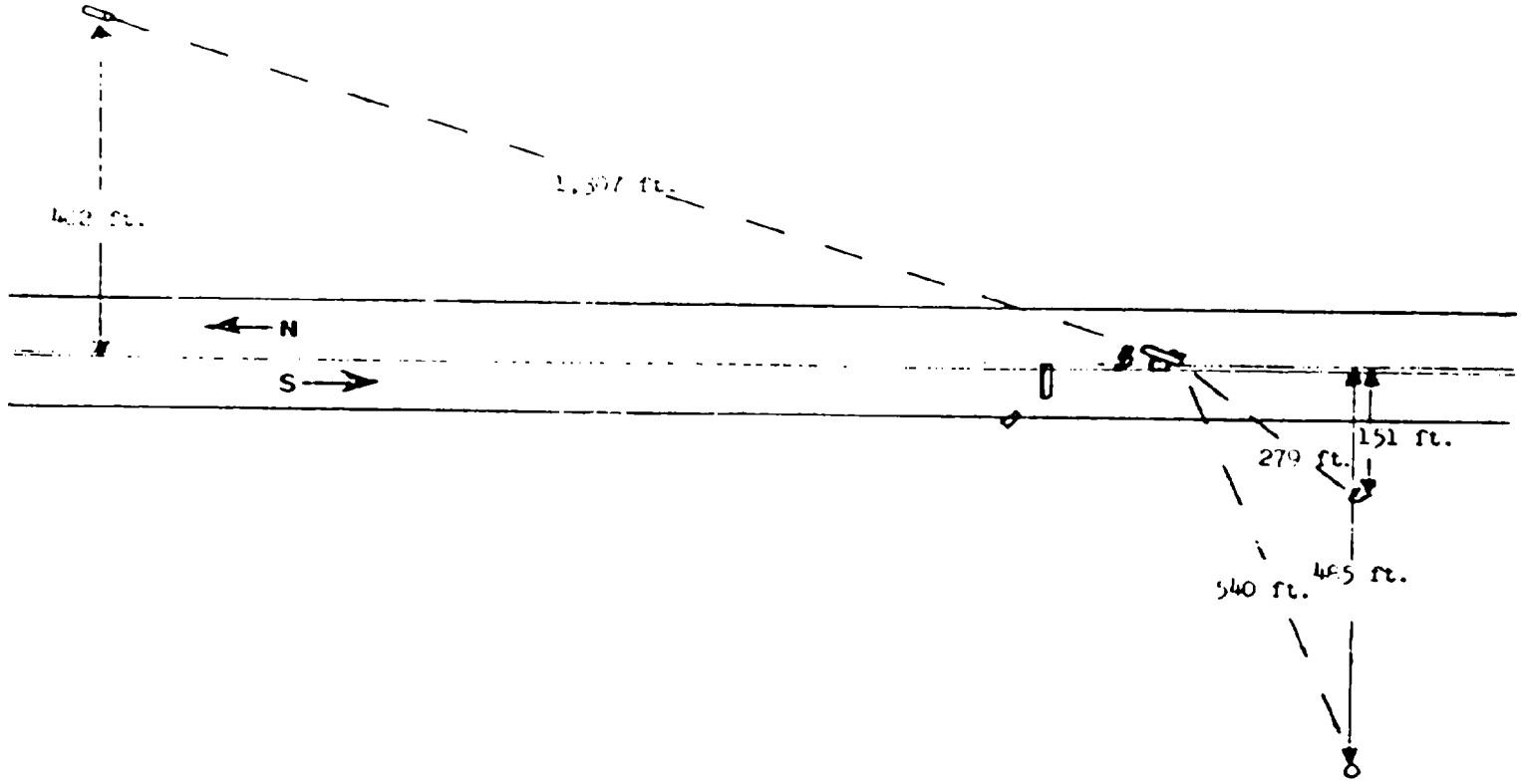

LOCATION OF CARGO-TANK SEGMENTS AFTER THE EXPLOSION

F.13 PROPANE CLOUD FIREBALL
LYNCHBURG, VIRGINIA - 9 March 1972

At 2:30 PM on 9 March 1972, a tractor-semitrailer tank truck carrying 9,208 gallons (38,854 pounds) of LPG (mostly propane) overturned and was punctured. As the truck fell onto its right side, a 32-inch hole was torn in the LPG tank; and liquid LPG poured out and began to vaporize. It is estimated that approximately 4000 gallons of liquid were discharged before the level dropped below the opening and the flow of liquid stopped.

As the propane escaped, a visible vapor cloud containing a mixture of propane and air immediately began to form at the trailer and spread rapidly throughout the area. At the site, an embankment east of the highway rose steeply, while an embankment west of the highway consisted of a steep dropoff. A house and some outbuildings were located 200 feet west of and about 60 feet below the accident site. A fringe of trees and underbrush jutted above the level of the road.

The driver climbed out of the truck, attempted to wave oncoming motorists away and then began to run downhill away from the truck and the expanding cloud. When he had run approximately 270 feet, the vapor cloud, which had continued to expand, ignited into a fireball with an estimated radius of at least 400 feet, enveloping him and killing him. Three witnesses standing beside their automobiles approximately 450 feet away were severly burned by radiation but were not touched by the flames. The occupants of the house, hearing the crash and seeing the cloud, fled from the house and were about 420 feet from the truck when the cloud ignited. They were severly burned, and one later died; it is not clear whether they were just inside or just outside the fireball. The house, 200 feet from the wreck, was enveloped in the flames and destroyed.

There appears to have been no blast. Two motorists 600 feet or so to the north (uphill, around a curve and out of the line of sight) heard only a muffled roar and saw an orange-red fireball. No concussion was felt, and

they were not injured. The actual fireball appears to have been approximately 400 feet in radius (that is, in the downhill direction; it is not thought to have been symmetrical); and there was incendiary radiation beyond that. Five people slightly more than 400 feet from the wreck site were severely burned, and an ensuing conflagration destroyed the house and outbuilding and 12 acres of woodland.

No mention is made of wind or weather in the report, and that would seem to indicate the absence of any high winds or of rain.

Source: National Safety Transportation Board Highway Accident Report, "Propane Tractor-Semitrailer Overturn and Fire, U.S. Route 501, Lynchburg, Virginia, March 9, 1972". NTSB-HAR-73-3.

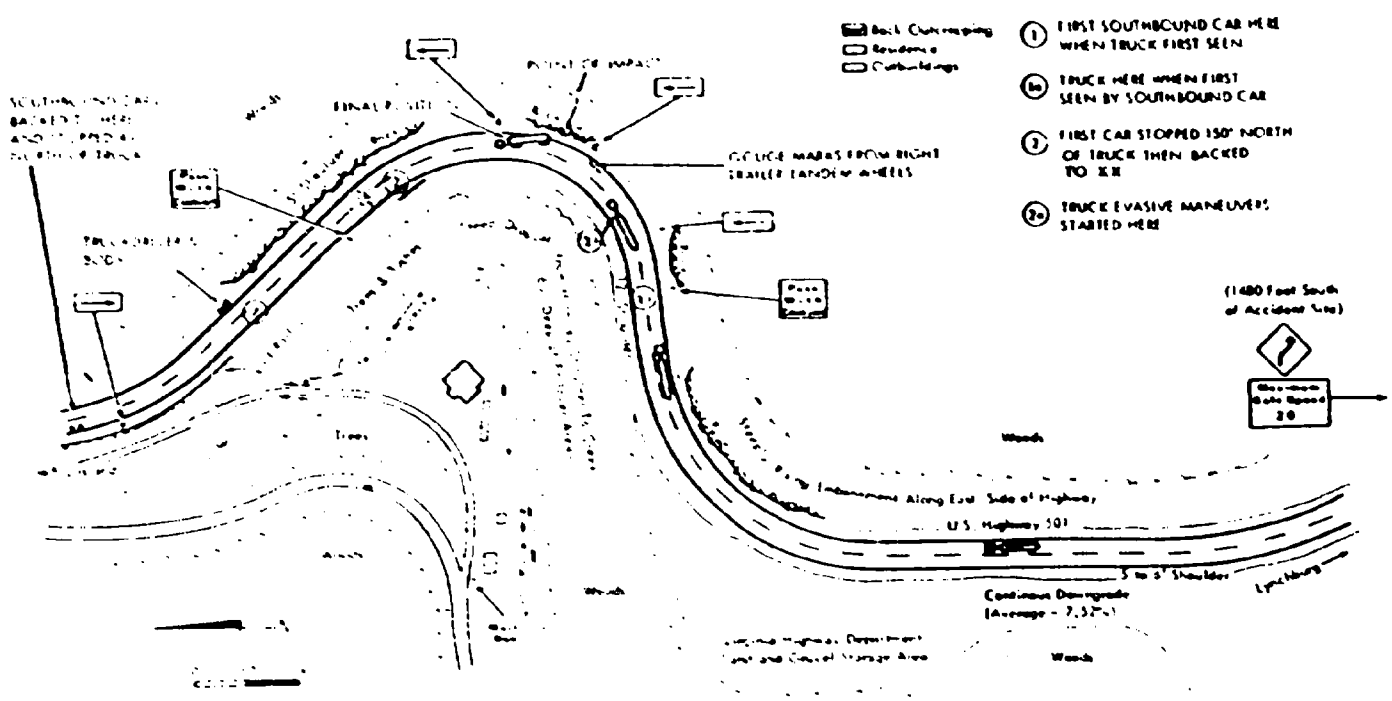

MAP OF ACCIDENT SITE

F.14 NATURAL GAS LIQUIDS VAPOR CLOUD FIRE
AUSTIN, TEXAS - 22 February 1973

At 10:53 PM on 22 February 1973, a 10-inch pipeline carrying natural gas liquids (NGL) at a pressure of 525 psig failed at the Austin pump station, releasing a total of 6,640 barrels (278,880 gallons) of NGL. The NGL blew a 10-foot diameter hole in the ground, sprayed into the air, flowed into ditches on both sides of a road adjacent to the station, and formed a white, fog-like vapor which enveloped the area.

Shortly after 11 PM, two cars traveling eastbound entered the vapor-rich zone and stalled. Both drivers got out of their cars, heard the roar of the escaping NGL, and smelled what they thought to be natural gas. Neither driver attempted to restart his car. Both ran eastward along the road through the two-foot-deep NGL vapor. Shortly after the two cars stalled, a Dodge van carrying six adults and two small children entered the vapor-rich zone and also stalled. The passengers got out and started to walk eastward toward the two other stalled vehicles, and the driver attempted to restart his engine.

A large spark emerged from underneath the van, and flames leaped hundreds of feet into the air. The fire burned 2,400 feet east from the stalled vehicle, over and along both sides of the road, and back to the pipe rupture. The eight persons still in the vapor-rich zone and the three vehicles were completely engulfed by flames.

Four of the occupants of the van died immediately. The four other occupants were hospitalized; two of them subsequently died, and the other two suffered severe burns. The van and the two stalled automobiles were completely destroyed by the fire, and the power and communications lines on the poles next to the road were melted. The asphaltic pavement of the road had been charred; fenceposts and pasture on both sides of the road were burned black in a 2,400-foot long line.

There was no blast. Two police officers in a radio patrol car saw the fire ignite, but they neither heard any explosion nor felt any shock wave.

The weather at the time of the pipe failure was cloudy, and a light wind was blowing from the southeast at 6 mph. The temperature was 44°F, and the humidity was 86 percent. By 11:30, the wind velocity had dropped to zero.

NGL is a member of the liquefied petroleum gas family. It is liquid stripped out of natural gas by pressure condensation, and contains about 85% butane and lighter, predominately propane. It is liquid only under greater than atmospheric pressure (or refrigeration). When released to the atmosphere at normal temperatures, it will vaporize, cool the surrounding air, and cause any moisture contained therein to appear as a white fog.

Source: National Transportation Safety Board Pipeline Accident Report. "Phillips Pipe Line Company Natural Gas Liquids Fire, Austin, Texas, February 22, 1973". NTSB-PAR-73-4.

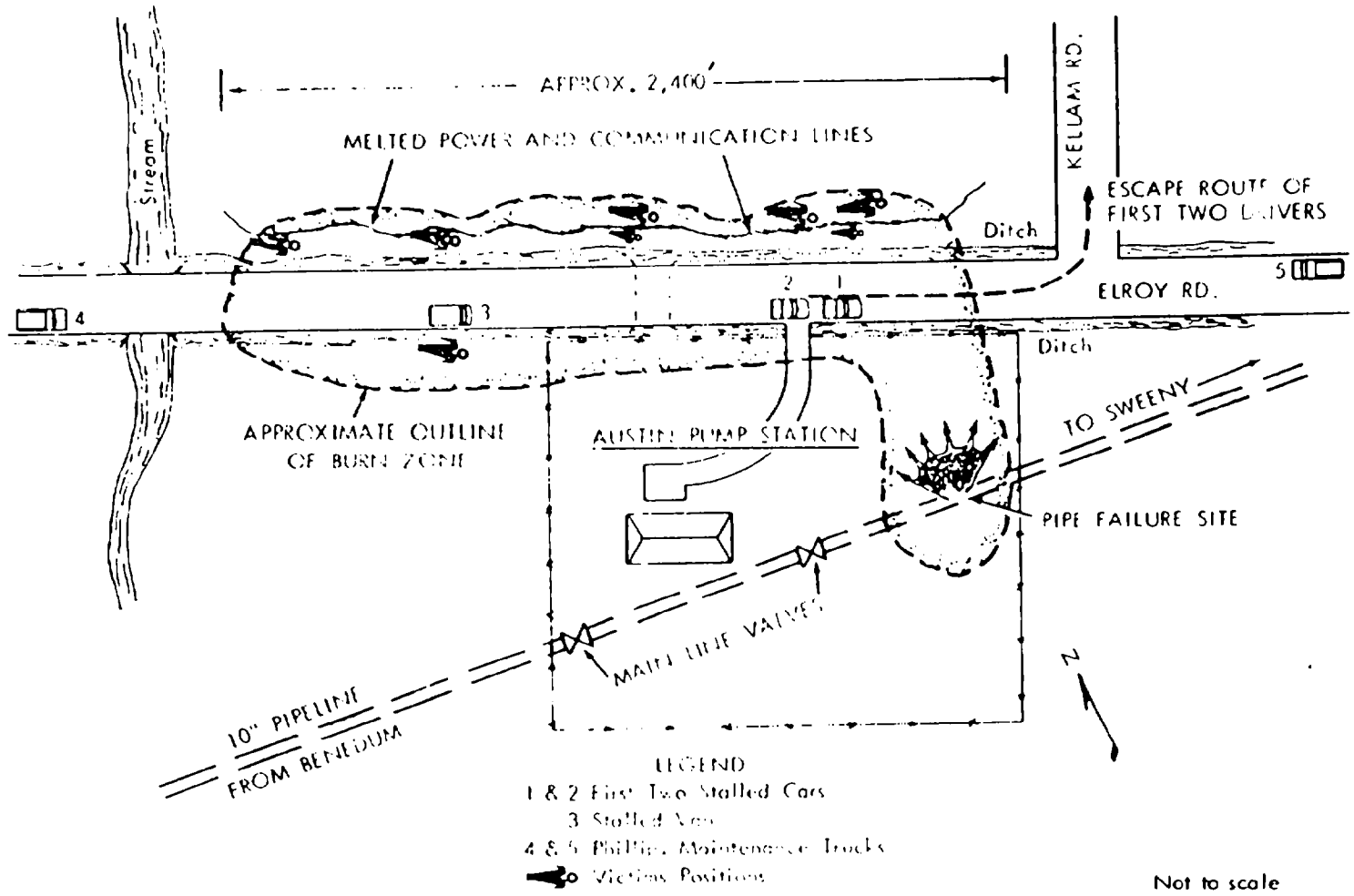
APPROX. 2,400'
MELTED POWER AND COMMUNICATION LINES
Stream
KELLAM RD.
ESCAPE ROUTE OF FIRST TWO DRIVERS
Ditch
ELROY RD.
Ditch
APPROXIMATE OUTLINE OF BURN ZONE
AUSTIN PUMP STATION
TO SWEENY
PIPE FAILURE SITE
MAIN LINE VALVES
10" PIPELINE FROM BENEDUM
N
LEGEND
1 & 2 First Two Stalled Cars
3 Stalled Van
4 & 5 Phillips Maintenance Trucks
Victims Positions
Not to scale

APPENDIX G

ADJUSTMENTS TO PREVENT DOUBLE COUNTING

Provisions have been made in the VM to prevent double counting in three different situations. Double counting is used in this context to mean the inclusion of an element of some vulnerable resource (e.g. a person or a building) in more than one category of damage or injury. Three situations arise in which double counting will occur unless provisions are made to prevent it. The situations are:

(1) A single damage mechanism from one event simultaneously causes injuries of differing severity (e.g. inhalation of toxic gas may cause death, non-lethal injury, or irritation).

(2) Two or more damage mechanisms from one event simultaneously cause injuries of the same severity (e.g. an explosion can kill people either by direct blast effects or by impact).

(3) Different events at different times both cause damage to the same resource, and the first event so severely damages some portion of the resource that further damage is irrelevant (e.g. persons killed by toxic gas cannot be further injured by a subsequent explosion).

The problem of double counting encountered in situation (1) arises from the way the probit equations, described above, are obtained. A probit equation assesses the fraction of the vulnerable resource in a given category of damage or injury without regard to other categories of damage. For events that cause an escalating sequence of damage categories, the results of the unmodified probit equations are misleading, because that portion of the subject resource in a given damage category is also counted in all more serious damage categories. As an example, consider the case of a toxic vapor: those people counted as irritated include those people with non-lethal injuries and those killed by the vapors, since the threshold for irritation is lower than the threshold for injury or death; i.e. to be injured or killed, one has to have passed through the stage of irritation.

An unattractive feature of using the unmodified results of the probit equations is that the sum of the percentages of resource in the various damage categories may exceed 100%.

To correct for this type of double counting, the fraction of the total resource in a given damage category is reduced by the sum of the fractions of total resource in all damage categories more serious than the given category; of course, the adjusted fraction must not fall below zero. To state this in mathematical terms let,

P_i = the probit equation for damage category i, where the damage becomes more serious as i increases

and $F(P_i)$ = the fraction of the total resource calculated to be in category i from the probit equation, P_i

$$\text{then} \quad F'(P_i) = F(P_i) - \sum_{j=i+1}^{M} F'(P_j) \qquad \text{(G-1)}$$

where $F'(P_i)$ = the adjusted value for the fraction of the total resource in category i (a single prime(') indicates adjustment for category (1) situations); if $F'(P_i) < 0$, then set $F'(P_i) = 0$.

M = the total number of damage categories.

As an example consider the following case where the concentration history resulted in 4% of the population of a given cell dying:

Type of Injury	Initial Percent	Adjusted Percent
Lethal	4	4
Non-lethal	12	12 - 4 = 8
Irritation	100	100 - (4+8) = 88

In the first column is the percentage affected when more serious effects are included at each level, while the more easily interpreted figures are in the final column. Using the initial figures, one might conclude that 116% of the population was affected. This type of correction procedure is applied to injuries from direct blast effects:

$$F'(E3) = F(E3) - F(E1) \qquad \text{(G-2a)}$$

to injuries from impact:

$$F'(E4) = F(E4) - (F(E2) \qquad \text{(G-2b)}$$

to glass breakage:

$$F'(S2) = F(S2) - F(S1) \qquad \text{(G-2c)}$$

and to sublethal toxic effects:

$$F'(T2) = F(T2) - F(T1) \qquad \text{(G-2d)}$$

$$F'(T3) = F(T3) - \big(F(T1) + F'(T2)\big) \qquad \text{(G-2e)}$$

The problem of double counting encountered in the situations (2) arises because the probit equations assess injury without regard to other injuries occurring simultaneously from different causes. Thus some fraction of the vulnerable resource may be subject to two or more causes of damage. This may be visualized by means of a diagram in which geometrical area represents resources in a particular state. By allowing overlap, the effects of multiple mechanisms may be considered. These diagrams, known as Venn diagrams, are shown in Figure 6-1 for the cases of two and three competing mechanisms. For two damage mechanisms, Figure 6-1a shows that the resource is partitioned into four categories. For three mechanisms, Figure 6-1b shows that eight categories result. In general, for n competing simultaneous mechanisms, 2^n categories will result.

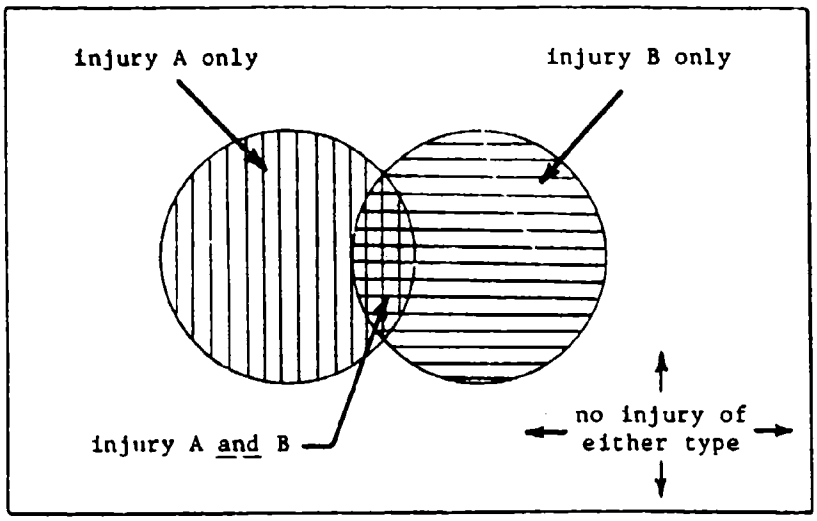

FIGURE G-1a

A Venn diagram for two simultaneous injury mechanisms; the four resulting categories of injury are:

(1) injury A only
(2) injury B only
(3) injury A and B
(4) no injury of either type

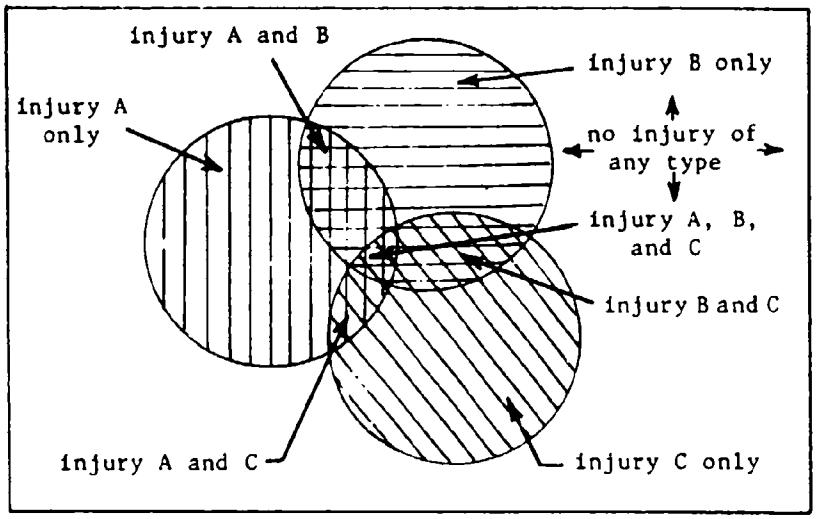

FIGURE G-1b

A Venn diagram for three simultaneous injury mechanisms; the eight resulting categories of injury are:

(1) injury A only
(2) injury B only
(3) injury C only
(4) injury A and B
(5) injury A and C
(6) injury B and C
(7) injury A, B, and C
(8) no injury of any type

Since the probit equations give the fraction of the vulnerable resource in any independent damage category, the fraction of the vulnerable resource in those categories arising from the simultaneous occurrence of damages may be calculated using the techniques of mathematical probability[G1] (particularly the complementation rule and the multiplication rule).

To illustrate these techniques consider the following example. Two injury mechanisms, A and B, occur simultaneously. Let

F(A) = fraction of vulnerable resources injured by mechanism A.

F(B) = fraction of vulnerable resources injured by mechanism B.

Then by the complementation rule the fraction not injured by mechanism A is given by the quantity 1-F(A) and the fraction not injured by mechanism B, is given by the quantity 1-F(B).

By use of these results and the multiplication rule the fraction of vulnerable resource in each of the four categories of injury may then be calculated; thus:

fraction injured by A only = $F(A)\ [1-F(B)]$

fraction injured by B only = $F(B)\ [1-F(A)]$

fraction injured by both A and B = $F(A)\ F(B)$

fraction uninjured = $[1-F(A)]\ [1-F(B)]$

This procedure is illustrated by a specific numerical example shown in Figure 6-2.

At the present time the VM only treats explosions as causing damage by several simultaneous damage mechanisms. Death may be caused by either direct blast or by impact effects. Non-lethal injuries may be caused by direct blast, by impact, or by fragments.

In the case of deaths it is not of particular relevance that part of the population killed may have received two types of injury each sufficient alone to cause lethality. For this reason a separate category of deaths by multiple cause was not established for reporting out the results of Phase II. Instead the fraction of deaths from multiple cause was added to the fraction of deaths from each cause alone in proportion to the deaths caused by each effect alone. That is, the fraction of deaths due to multiple causes is given by

$$F(EM) = F(E1)\ F(E2)$$

[G1] Kreyszig, E. Advanced Engineering Mathematics. John Wiley and Sons, Inc., N.Y., 1967. Section 18.5.

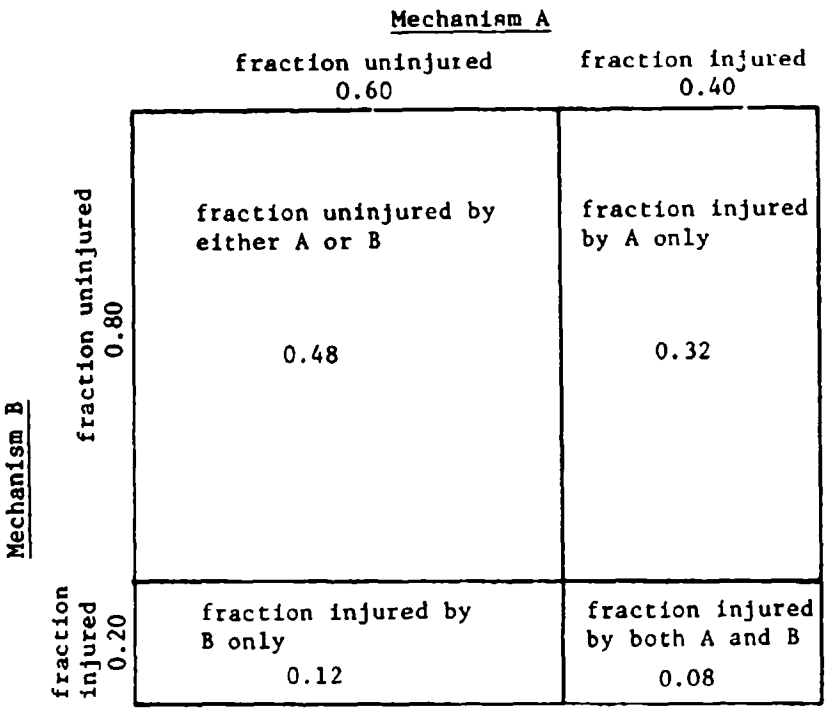

In this example it is assumed that two mechanisms simultaneously cause damage to a resource or population. Let F(A) = 0.40 and F(B) = 0.20. Let the entire area of the square above represent the number of elements of the vulnerable resource.

If two adjoining sides of the square are segmented proportional to the fraction of vulnerable resource injured respectively by the two mechanisms, then the areas of the regions formed within the square are proportional to the fraction of the resource in each of the four damage categories shown.

FIGURE G-2

DAMAGE APPORTIONMENT DIAGRAM

where

F(EM) = fraction of deaths due to multiple causes

F(E1) = fraction of deaths caused by direct blast effects

F(E2) = fraction of deaths caused by impact.

The fraction of deaths due solely to one cause is given by

$$F(EB) = F(E1)\ [1-F(E2)] \qquad \text{(G-3a)}$$

$$F(EI) = F(E2)\ [1-F(E1)] \qquad \text{(G-3b)}$$

where

F(EB) = fraction of deaths due solely to direct blast

F(EI) = fraction of deaths due solely to impact.

Now the fraction of deaths due to multiple causes, F(EM), is added to the deaths due to each cause alone in proportion to their relative magnitude; i.e.

$$F''(E1) = F(EB) + F(EM)\left[\frac{F(EB)}{[F(EB) + F(EI)]}\right] \qquad \text{(G-4a)}$$

and

$$F''(E2) = F(EI) + F(EM)\left[\frac{F(EI)}{[F(EB) + F(EI)]}\right] \qquad \text{(G-4b)}$$

where F''(E1) and F''(E2) are taken to be the adjusted fractional values for deaths from direct blast and impact respectively.

In the case of injury from explosions the fact that part of the population is wounded by several mechanisms is considered important. Therefore, the fraction of the population in this category is determined and reported out in Phase II of the VM; however, no distinction is made between the different categories of multiple injury (there are four categories: (1) direct blast and impact, (2) direct blast and fragments, (3) impact and fragments, (4) direct blast and impact and fragments).

The adjusted fractional values for various types of explosion injury are calculated using the techniques of mathematical probability. The adjusted fractional values reported out by the VM are calculated by the following formulas:

$$F''(E3) = F'(E3)\ [1-F(E4)]\ [1-F(E5)] \qquad \text{(G-5a)}$$

$$F''(E4) = F'(E4)\ [1-F(E3)]\ [1-F(E5)] \qquad \text{(G-5b)}$$

$$F''(E5) = F(E5)\ [1-F(E3)]\ [1-F(E4)] \qquad \text{(G-5c)}$$

$$F''(EM) = F(E5)\ F'(E4)\ [1-F(E3)] + F(E5)\ F'(E3)\ [1-F(E4)] + F'(E3)\ F'(E4)\ [1-F(E5)] + F(E5)\ F'(E3)\ F'(E4) \qquad \text{(G-5d)}$$

where,

$F''(E3)$, $F''(E4)$, $F''(E5)$, $F''(EM)$ =

the adjusted values for fraction of deaths due to direct blast only, impulse only, fragments only, and multiple injury respectively.

and

$F'(E3)$, $F'(E4)$ are given respectively by equations (G-2a), (G-2b).

The problem of double counting encountered in situation (3) arises because the probit equations for a given damage mechanism do not consider the reduction in the population of a vulnerable resource caused by a prior damage mechamism. In situation (3) the temporal order of the damage mechanism affecting a given vulnerable resource is crucial Figure G-3 is useful for visualizing the temporal order of various damage mechanisms. As indicated in figure G-3 diffusion of toxic gases may be followed by either flash fire or explosion; either of these events may then be followed by pool burning.

The VM models pool burning as causing no damage to people; therefore, this type of double counting may arise for the vulnerable resource "people" only when explosion or flash fire follow a significant toxic dose. The VM models toxicity as causing no damage to structures; therefore, this type of double counting may arise for the vulnerable resource "structures" only when pool burning follows explosion or flash fire.

A correct assessment of damage from a sequence of events requires the double counting correction for situation (3). However, the degree of threat imposed by each event is also of interest. For example, even though an explosion may destroy all the structures in a given region, the fact that a subsequent pool burning would also destroy these structures is of some interest to the users of the VM. Therefore, this correction is not made as each damage-causing event is simulated. Instead the uncorrected percent damage is reported out by the VM. Then after the simulation is complete, a summary damage report is generated; it is for the summary damage report that this correction for double counting is made.

For structures the correction made for the summary is given by,

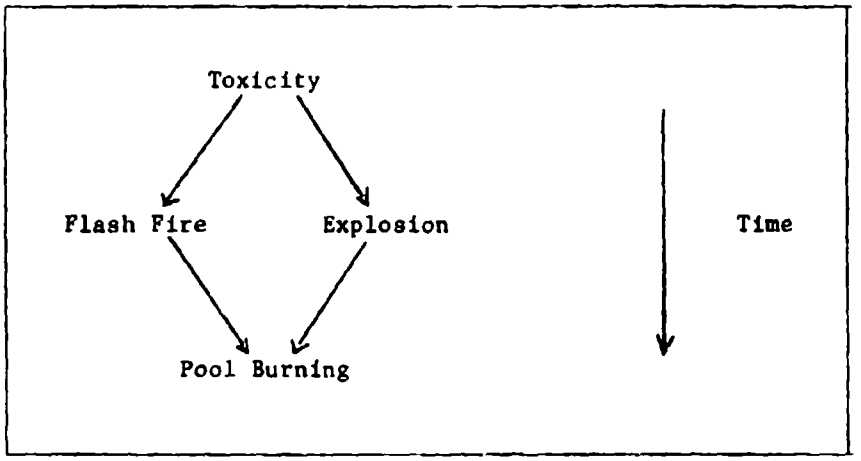

FIGURE G-3. Diagrammatic representation of the sequence of events that can threaten vulnerable resources.

$$F'''(PB) = F(PB) \cdot [1-G] \qquad \text{(G-6a)}$$

where

$$G = \begin{cases} F(FF) & \text{if flash fire} \\ F(S1) & \text{if explosion} \end{cases} \text{ precedes pool burning} \qquad \text{(G-6b)}$$

and where

$F'''(PB)$ = the corrected fractional structural damage for pool burning

$F(PB)$ = the original fractional structural damage for pool burning

$F(FF)$ = the fractional structural damage for flash fire

$F(S1)$ = the fractional structural damage for explosion

For people the correction made for the summary is given by the following:

for explosion:

$$F'''(E1) = F''(E1)\,[1-F(T1)] \qquad \text{(G-7a)}$$

$$F'''(E2) = F''(E2)\,[1-F(T1)] \qquad \text{(G-7b)}$$

$$F'''(E3) = F''(E3)\,[1-F(T1)] \qquad \text{(G-7c)}$$

$$F'''(E4) = F''(E4)\,[1-F(T1)] \qquad \text{(G-7d)}$$

$$F'''(E5) = F''(E5)\,[1-F(T1)] \qquad \text{(G-7e)}$$

$$F'''(EM) = F''(EM)\,[1-F(T1)] \qquad \text{(G-7f)}$$

for flash fire:

$$F'''(F1) = F(F1)\,[1-F(T1)] \qquad \text{(G-7h)}$$

where the triple-primed variables are the frational damage corrected for the summary and the other symbols have been previously defined.

U S GOVERNMENT PRINTING OFFICE 1979